Targeted Delivery of Nanotherapeutics to the Placenta

A thesis submitted to The University of Manchester for the degree of Doctor of Philosophy (PhD) in the Faculty of Medical and Human Sciences.

2016

Anna King

School of Medicine

Final word count = 53, 410

List of Figures

Chapter 1: Introduction

List of Tables

Abbreviations

^{51}Cr-EDTA	^{51}Chromium-ethylenediaminetetraacetic acid
ACon	Antibody conjugate
ADA	Adenosine deaminase
AMPh	Amphotericin
ARA	ARALPSQRSRC
ATP	Adenosine-5'-triphosphate
BM	Basal membrane
BMI	Body mass index
bp	Base pair
C57	C57BL/6J wild type mouse
CendR	C-end Rule
CFS	Carboxyfluorescein
CGKRK	CGGGCGKRK
COMT$^{-/-}$	Catechol-O-methyl transferase knock out mouse model
CT	Cytotrophoblast
DAPI	4',6-diamidino-2-phenylindole
DLS	Dynamic light scattering
DMEM	Dulbecco's modified eagle medium
DMSO	Dimethyl Sulfoxide
DOTAP	1,2-doleoyl-3-trimethylammoniumpropane
DOXIL	Liposomally encapsulated doxorubicin
DSPC	Distearoyl phosphatidylcholine
DSPE-PEG	Distearoyl phosphoethanolamine-poly(ethylene glycol)
DSPE-PEG-maleimide	Distearoyl phosphoethanolamine-maleimide poly(ethylene glycol)
DTNB	5,5’ dithiobis-(2-nitrobezoic) acid, Ellman's reagent
DVT	Deep vein thrombosis
E	Embryonic day
EC	Ezyme conjugate
ECP	Ectoplacental cone
EET	Extra-embryonic tissues
EGF	Epidermal growth factor
EGFR	Epidermal growth factor receptor
ELISA	Enzyme-linked immunosorbent assay
eNOS$^{-/-}$	Endothelial nitric oxide synthase knock out mouse model
EPR	Enhanced permeability and retention
EVT	Extravillous trophoblast
FBS	Fetal bovine serum
FDA	Food and drug administration
FGF	Fibroblast growth factor
FGR	Fetal growth restriction

FITC	Fluorescein
GCSF	Granulocyte colony-stimulating factor
GH	Growth hormone
GSH	Glutathione
GSP	Glutamine, Streptomycin, Penicillin
hCG	Human chorionic gonadotrophin
HGF	Hepatocyte growth factor
HIV	Human immunodeficiency virus
hPL	Human placental lactogen
HPLC	High performance liquid chromatography
HUVECs	Human umbilical vein endothelial cells
I.M	Intramuscular
I.R	Intravitreous
I.T	Intratrathecal
I.V	Intravenous
ICM	Inner cell mass
IFN-γ	Interferon-γ
IGF-1R	Type-I IGF receptor
IGF-2R	Type-2 IGF receptor
IGFBP1-6	Insulin-like growth factor binding proteins 1-6
IGF-I	Insulin-like growth factor I
IGF-II	Insulin-like growth factor II
IL-2/4/10	Interleukin-2, 4 or 10
InsR	Insulin receptor
iRGD	CRGDKGPDC
IRIV	Immunopotentiating reconstituted influenza virosome
Jz	Junctional zone
K	Kidney
Lab	Labyrinth
LDA	Low dose aspirin
LDE	Laser Doppler micro-electrophoresis
Leu^{27}IGF-II	Human IGF-II analogue
LMWH	Low molecular weight heparin
mPL	Mouse placental lactogen
MPS	Mononuclear phagocyte system
MR	Molar ratio
MRI	Magnetic resonance imaging
MVM	Microvillous membrane
NBD-DSPE	Distearoyl phosphoethanolamine-nitrobenzoxadiazol
NBF	Neutral buffered formalin
NGF	Nerve growth factor
NO	Nitric oxide
OCT	Optimal cutting temperature
$ONOO^-$	Peroxynitrite

Ov	Ovarian artery
P32	p32/gC1qR/HABP protein
P0/ $P0^{-/+}$	IGF-II transcript knock out mouse model/ mutant fetuses
$P0^{+/+}$	P0 wild type fetuses
PBS	Phosphate buffered saline
PCR	Polymerase chain reaction
PDI	Polydispersity index
PE	Pre-eclampsia
PEG	Poly(ethylene glycol)
PET	Positron emission tomography
PFA	Paraformaldehyde
PlGF	Placental growth factor
PlGH	Placental growth hormone
QD	Quantum dots
Rh	Rhodamine
RNA	Ribonucleic acid
ROS	Reactive oxygen species
S.C	Subcutaneous
SA	Spiral artery
SD	Size distribution
SDil	Sample diluent
sFlt-1	Soluble fms-like tyronsine kinase 1
siRNA	Small interfering ribonucleic acid
SM	Sphingomyelin
SOD	Superoxide dismutase
SoyHPC	Hydrogenated soyaphosphatidylcholine
SoyPC	Soya phosphatidylcholine
Sp	Spongiotrophoblast
SS	Stop solution
ST	Syncytiotrophoblast
STRIDER	Sildenafil therapy in dismal prognosis early-onset intrauterine growth restriction trial
Sub	Substrate solution
T_4	Thyroxine
TB	Tissue bank
TBS	Tris-buffered saline
TEM	Transmission electron microscopy
TGC	Trophoblast giant cells
Th-1/2	T helper cells 1 or 2
tLyP-1	Neuropilin-1 receptor
TNF-α	Tumor necrosis factor alpha
Tr	Trophectoderm
Ut	Uterine artery
UV	Ultra violet

VEGF	Vascular endothelial growth factor
VEGFR	Vascular endothelial growth factor receptor
VIP	Vitamins in pre-eclampsia trial
VS	Villous stroma
VT	Villous trophoblast
WB	Wash buffer
WT	Wild type
ZP	Zona pellucida
ZP	Zeta potential

Abstract

The University of Manchester
Anna King
Doctor of Philosophy (PhD)
Targeted Delivery of Nanotherapeutics to the Placenta
March 2016

During pregnancy the placenta is responsible for ensuring sufficient nutrient transfer and gaseous exchange between the maternal and fetal circulations. Fetal growth restriction (FGR), defined as the inability of the fetus to grow to its genetically determined potential, is often the result of a poorly functioning placenta. Unfortunately there is currently no treatment for FGR except to deliver the fetus early, which has a high risk of morbidity and mortality. Several drugs have previously been shown to enhance placental function and in doing so have improved fetal growth and viability in both human and animal studies. However, the risk of teratogenesis prevents these drugs from reaching the clinic. We have developed a way of targeting drugs specifically to the placenta with the aim of enhancing placental function, increasing fetal growth and improving fetal outcome, whilst minimising off target side effects. Biocompatible nanoparticles called liposomes were prepared to display the homing peptide sequences iRGD and CGKRK, both of which bind to the human and mouse placental exchange regions, to created targeted liposomes. We report that these peptide-decorated liposomes bound to the mouse and human placenta and were able to deliver a fluorescent cargo to the area. Insulin-like growth factors-I and -II (IGF-I and IGF-II) were separately incorporated inside of the targeted liposomes and administered as a biological cargo to pregnant mice. IGFs are particularly important for placental and fetal growth and can improve fetal growth and viability. Treatment in healthy pregnant C57/BL6J mice increased placental weight, but not fetal weight. Treatment in mice displaying an FGR phenotype ($P0^{+/-}$) increased the weight of the lightest fetuses, but did not affect normally grown fetuses. Treatment was well tolerated and did not cause any gross pathology in mothers or fetuses. These data provide proof of principle for targeted delivery of drugs to the placenta and are a novel platform for the development of placental-specific therapeutics to treat conditions such as FGR.

Declaration

No portion of the work referred to in this thesis has been submitted in support of an application for another degree or qualification of this or any other university or other institute of learning.

Copyright Statement

Acknowledgements

I would like to thank my three supervisors Dr Lynda Harris, Professor John Aplin and Professor Nicola Tirelli for their continuous support and guidance over the past four years. I would like to give particular thanks to Lynda for being an amazing supervisor and friend. Thanks for always being there for me with an encouraging word and unwavering enthusiasm; I couldn't have asked for a better supervisor! I would also like to thank everyone who has helped me in the MFHRC, the School of Pharmacy and the BSU.

Special thanks go to my family and friends in particular to my mum, my brother, my grandparents, my amazing boyfriend Billy and my best friend Lisa. Thank you for your unconditional love and support in helping me get to where I am today.

Chapter 1: Introduction

1.1 Overview

Fetal growth restriction (FGR) is defined as the inability of the fetus to reach its maximum growth potential in utero (Chiswick 1985). Apart from the 5-15% of cases that are caused by genetic abnormalities, the major cause of FGR is a poorly functioning placenta (Chiswick 1985). Reduced placental weight, volume, diameter (Biswas & Ghosh 2008) and villous surface area (Biswas et al. 2008) are associated with FGR, as is altered placental cell turnover including an increase in syncytiotrophoblast apoptosis (Ishihara et al., 2002; Smith, Baker, & Symonds, 1997) and syncytial knot formation (Calvert et al. 2013). FGR is also caused by impaired placental blood perfusion which is usually observed with increased vascular resistance (Chiswick 1985; Brosens et al. 1972) and placental hypoxia (Hung et al. 2001). Reduced placental nutrient and/or gaseous transport capacity (Desforges & Sibley, 2010) caused by altered nutrient transporter activity (Jansson 2001; Sibley et al. 1997) is also a leading cause of FGR.

Unfortunately, there is no adequate treatment for FGR, which affects 5-10% of pregnancies world-wide (Chiswick 1985). The only medical intervention available is to increase fetal monitoring and to deliver the baby prematurely if the condition worsens (Fisk & Atun 2008). Small or prematurely delivered babies often need expensive neonatal intensive care and are at an increased risk of developing conditions such as respiratory distress syndrome, retinopathy, cerebral palsy, and have a higher risk of contracting infections that can result in neonatal death (McIntyre et al. 1999). These FGR babies are also predisposed to developing numerous diseases in adulthood, including obesity, type-2 diabetes (Barker, Hales, et al. 1993), hypertension (Barker et al. 1989), cardiovascular diseases (Barker et al. 1989; Barker, Godfrey, et al. 1993),

stroke, chronic renal failure, chronic obstructive lung disease, osteoporosis, schizophrenia, depression, certain cancers, and polycystic ovary syndrome (Ozanne et al. 2004).

Recently, several potential therapeutics for FGR have been identified, which have increased fetal growth by enhancing various aspects of placental function in animals models and have shown promise in several human trials. The vasodilator sildenafil citrate (Viagra®) reduced vascular resistance and improved fetal growth in several rodent models of FGR (Dilworth et al. 2013; Stanley, Andersson, Poudel, et al. 2012) and had great success in improving fetal viability in a small pilot study conducted in pregnant women (von Dadelszen et al. 2011). It is now under examination in a large cohort clinical trial called STRIDER (Sildenafil Therapy In Dismal prognosis Early-onset intrauterine growth Restriction) (Ganzevoort et al. 2014). The potent antioxidant melatonin has also been tested in several animal models of FGR. It decreased fetal hypoxia, improved neurodevelopment and decreased brain injury and oxidative stress in new born lambs, when administered to their mothers throughout gestation (Miller et al. 2012). It also increased birth weight and improved placental efficiency, whilst decreasing placental antioxidant expression in an rat model of oxidative stress (Richter et al. 2009). It has since moved into two clinical trials, where it is being examined as a potential treatment for FGR (Alers et al. 2013) and pre-eclampsia (PE) (Hobson et al. 2013), a life threatening condition which often accompanies FGR. Finally, the insulin-like growth factors -I and -II (IGF-I and IGF-II) are also being considered as a potential treatment for FGR as they have been shown to be important in regulating placental and fetal growth in humans, rodents and several other species (Sferruzzi-Perri et al. 2011).

Despite the obvious need for a treatment for FGR and the emergence of potential therapeutic interventions, there is reluctance by the pharmaceutical industry to develop drugs for use in pregnant women due to the fear of teratogenesis. Only three new obstetric drugs have been licenced in the UK in the past twenty years, two of which are for use after delivery (Fisk & Atun 2008) and in recent years, no new class of drugs has been developed in the EU or US to treat PE, FGR, pre-term labour or miscarriage (Jones et al. 2004). There is justified concern that systemic administration of any substance during pregnancy could cause detrimental off target side effects to mother or fetus. There is already evidence that the systemic administration of sildenafil citrate to pregnant mice displaying an FGR phenotype causes long-term cardiovascular and metabolic abnormalities in offspring (Renshall et al. 2014). For this reason, pregnant women are perceived as a high-risk low return cohort, and pharmaceutical companies are averse to investing in this area despite the clinical need. To circumvent this risk, developing a method of selectively targeting drugs to the placenta is desirable as it could limit teratogenic side effects and make treating FGR and other pregnancy complications safer.

In recent years, research has focused on developing targeted drug delivery systems for a variety of applications, mainly in the field of cancer therapy and several methods of passive and active drug targeting have been explored. It is beneficial for therapeutics to be delivered selectively to their target site, allowing a greater dose to be delivered to diseased tissue, whilst minimizing the exposure of healthy tissues, improving the efficacy of the drug and reducing the harmful side effects (Gabizon et al. 2002; Ruoslahti 2004). Work conducted in the Ruoslahti lab has shown that the vascular endothelium of all tissues express unique surface markers, which can be selectively

targeted by tissue-specific ‘homing peptides’ (Erkki Ruoslahti, 2002). The group have identified a catalogue of homing peptides that target specific surface markers expressed by tumour vasculature and are currently using them to develop targeted nanoparticles, capable of delivering chemotherapeutics directly to tumours (Ruoslahti et al. 2010).

Given the similarities of the developing placenta to a solid tumour (Holtan et al. 2009), it was hypothesized that existing tumour homing sequences may bind to markers selectively expressed on the placental surface. By in vivo phage screening, Harris et al. (Harris et al. 2012) showed that several tumour homing peptide sequences target and bind to the mouse placenta; a property which has since been validated in human placental explants. The main objective of this PhD project was to harness the targeting abilities of two of these homing peptides, iRGD (CRGDKGPDC) and CGKRK (CGGGCGKRK), to develop a novel biocompatible nanoparticle that can selectively deliver a range of drugs to the placenta, and to then test this targeted nanotherapeutic in animal models as a potential treatment for FGR.

1.2 The placenta

The placenta is responsible for maintaining the growth and development of the fetus throughout pregnancy. It does this by facilitating gaseous exchange between the maternal and fetal circulation, whilst absorbing and transporting nutrients needed for the developing fetus. Throughout pregnancy the placenta develops so that its structure meets the needs of the growing fetus, allowing for increased blood perfusion with a larger surface area for gaseous exchange and nutrient transport. As well as this, it produces hormones and placental-specific growth factors that support the pregnancy. It

also acts as a barrier, preventing harmful substances from entering fetal circulation, whilst suppressing a maternal immune attack. (Wang 2010).

1.2.1 Human placentation

Pregnancy begins with the fertilization of an oocyte by a spermatozoon to create a zygote (Figure 1.1A). The cells within the zygote rapidly proliferate (Figure 1.1B) and after five days become known as the blastocyst (Figure 1.1C), consisting of an inner cell mass (ICM) which eventually develops into the fetal embryo, surrounded by a layer of trophectoderm (Tr), which become the extra-embryonic tissues (EET), including the placenta. Once within the uterus, the blastocyst hatches from its protective zona pellucida (ZP) (Figure 1.1D), rotates so that the ICM is nearest to the decidua, and begins implantation (Figure 1.1E). The trophoblast lineage then differentiates into syncytiotrophoblast (ST) and cytotrophoblast (CT). The STs invade the uterine epithelium until the embryo is fully incorporated and covered by a continuous layer of multinucleated syncytiotrophoblast. Underlying CT act as progenitor cells, proliferating and fusing to expand the syncytiotrophoblast, forming the placenta. (Norwitz et al. 2001).

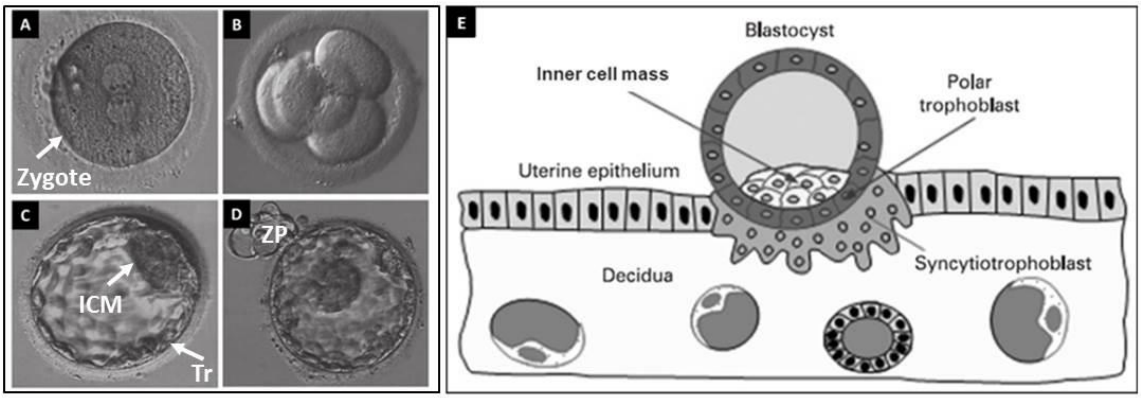

Figure 1.1: Blastocyst development and implantation. (A) Newly fertilized zygote, (B) zygote undergoes a series of cell divisions, (C) zygote reaches blastocyst stage, consisting of inner cell mass (ICM) and outer trophectoderm (Tr), (D) blastocyst hatches, shedding its zona pellucida (ZP) prior to implantation, (E) implantation of the blastocyst occurs with syncytiotrophoblast (ST) invading the uterine epithelium and primed decidua. Adapted from (Huppertz 2008) and (Farquharson & Stephenson 2010).

Over time, the placenta develops into the basal maternal surface, the chorionic fetal surface and a central exchange region (Figure 1.2A). The fetal surface is connected to the fetus by the umbilical cord and consists of several villous tree-like structures branching from the umbilical cord, grouped into cotyledons, surrounded by intervillous blood spaces. (Wang 2010). Placental villi provide a large surface area for efficient nutrient transfer without the maternal and fetal blood ever coming into direct contact (Figure 1.2B).

There are several types of villi in the placenta (Figure 1.3); stem (Figure 1.3C), immature (Figure 1.3B) and mature intermediate (Figure 1.3D), mesenchymal (Figure 1.3A) and terminal (Figure 1.3E). Stem villi (Figure 1.3C) are the largest villi and branch out from the umbilical cord insertion and contain the major fetal blood vessels. Terminal villi (Figure 1.3E) are at the end of the villous branches and are where exchange takes place. (Huppertz 2008). Villi consist of an outer layer of ST in contact with maternal blood, an underlying layer of proliferative CT and a villous stromal core

(VS) that contains fetal blood vessels. Collectively, the cellular layers that separate the maternal and fetal blood (ST, CT and the fetal capillary epithelium) are called the placental barrier (Figure 1.4) (Sibley et al. 1997).

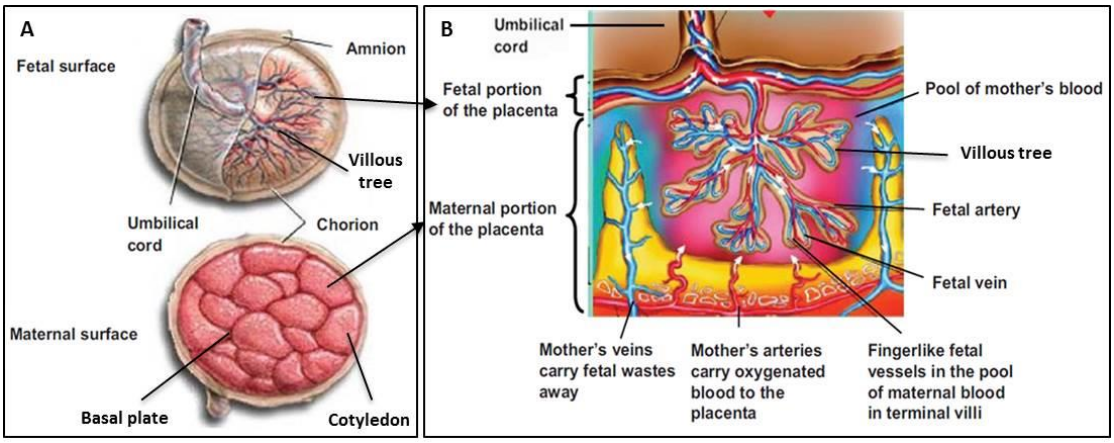

Figure 1.2: Schematic of human term placenta. (A) The maternal surface is composed of villi grouped into cotyledons and the fetal surface is connected to the fetus by the umbilical cord, (B) placental villous tree containing fetal blood vessels and surrounded by maternal blood (arrows show direction of blood flow). Adapted from (Wang 2010).

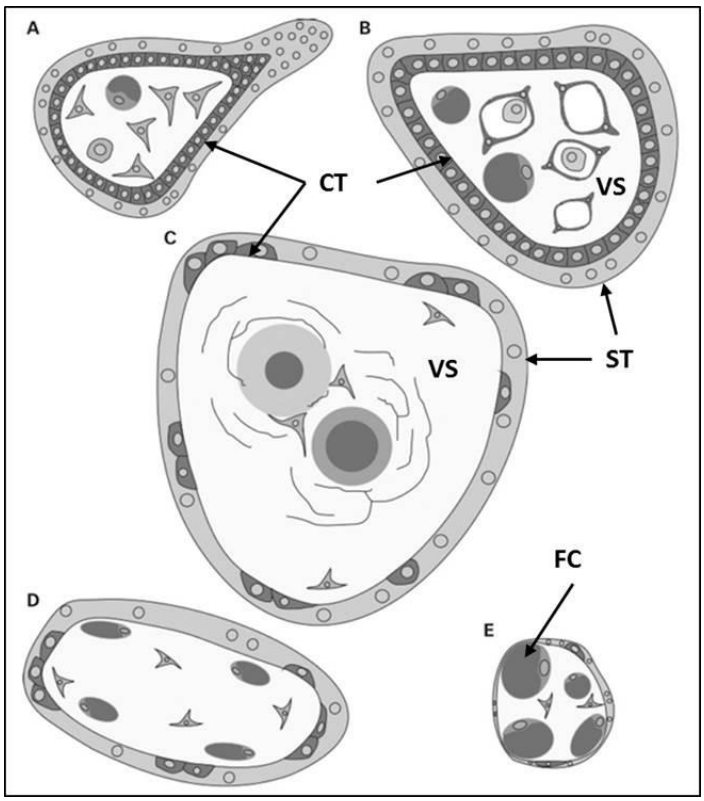

Figure 1.3: Types of placental villi. Cross section of (A) a mesenchymal villus, (B) an immature intermediate villus, (C) a stem villus, (D) a mature intermediate villus, and (E) a terminal villus. The light grey structure around the outside of the villi is the multinucleated ST with underlying dark grey proliferative CT. The white centre of the villi is composed of VS, which contains dark grey fetal capillaries; (C) shows the central fetal artery and vein coming from the umbilical cord. Adapted from (Huppertz 2008)**.**

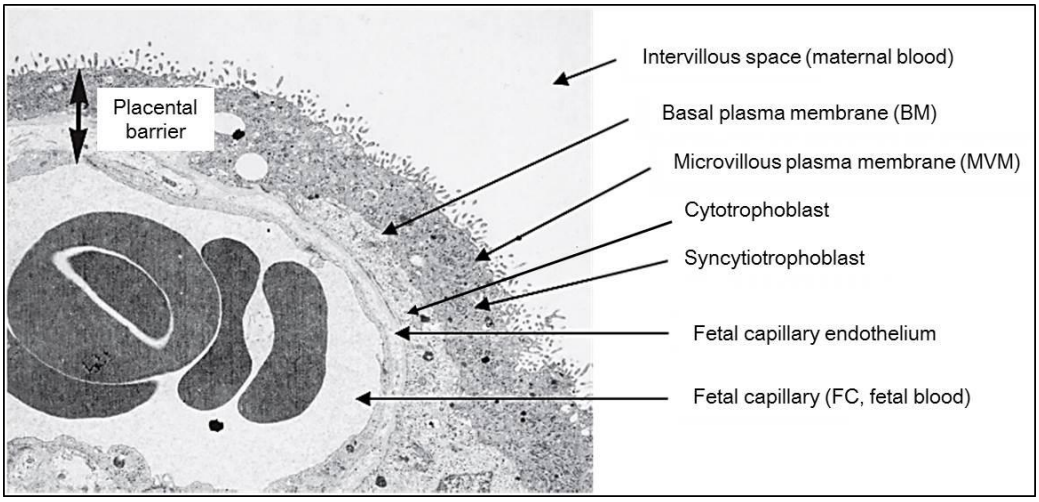

Figure 1.4: Electron micrograph image of the placental exchange barrier. Nutrients and amino acids are transported across the placental barrier (double headed arrow) between maternal and fetal blood. Adapted from (Desforges & Sibley 2010)**.**

1.2.2 Placental perfusion

Maternal decidual spiral arteries are responsible for maternal- placental blood flow. They are initially plugged by trophoblast aggregates, thus maternal blood does not circulate through the intervillous space until the end of the first trimester (Wang 2010). This is thought to protect the placenta from the potentially damaging force of maternal blood pressure (Aplin 2000). During this time the fetus is supported by glycoprotein-rich histotroph, secreted by uterine glands, and plasma filtrate (Filant & Spencer 2014; Jones et al. 2015). Towards the end of the first trimester, the plugs are dislodged and maternal blood flow is initiated from the openings of spiral arteries, perfusing the intervillous space before returning via the uterine veins. Deoxygenated blood flows from the fetus, along the umbilical artery and into the villi to be oxygenated and accumulate nutrients transported from the maternal blood. Blood rich in oxygen and nutrients then returns to the fetus along the fetal umbilical vein (Wang 2010).

Throughout gestation placental blood flow increases in volume to provide the growing fetus with a greater access to nutrient rich blood. To facilitate this increase, the decidual spiral arteries are remodelled to become wide bore, low resistance vessels, allowing a larger volume of maternal blood to flow into the intervillous space at a decreased pressure (Wang 2010). Figure 1.5 shows the process of spiral artery remodelling. Extravillous trophoblasts (EVT) differentiate from the tips of placental villi to become interstitial and endovascular EVTs. They invade the maternal decidua and inner third of the myometrium, instigating spiral artery remodelling and replacing the vessel walls (Wallace et al. 2012). This remodelling is usually complete by 20 weeks gestation (Harris & Aplin 2007).

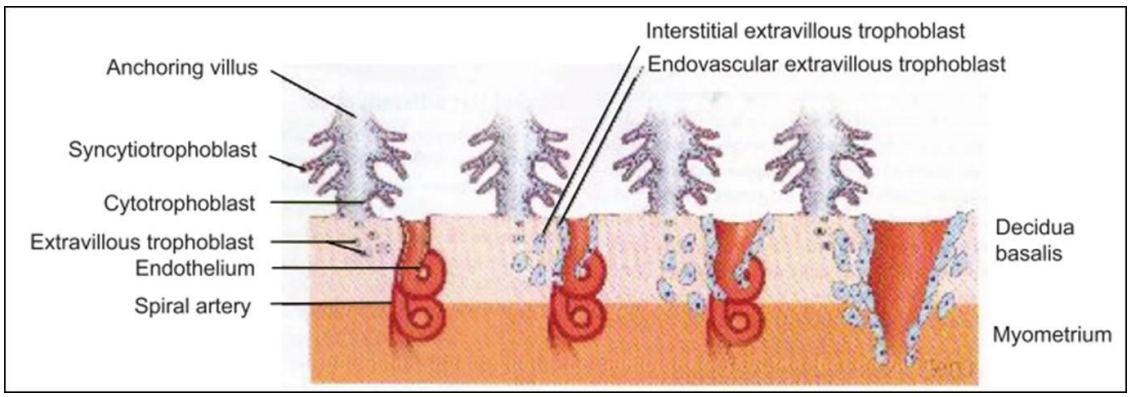

Figure 1.5: Uterine spiral artery remodelling during pregnancy. Interstitial trophoblasts invade the decidua and surround the spiral arteries, whilst endovascular trophoblasts invade via the lumen of the spiral arteries. EVT-mediated remodelling involves replacement of the endothelial lining and most of the musculoelastic tissue in the arterial walls, transforming the vessels into low resistance, high flow conduits. Reproduced from (Wang 2010).

1.2.3 Placental transport

Figure 1.6 shows a schematic of the ST layer, comprising the microvillous membrane (MVM) and the basal membrane (BM). This barrier permits the transfer of molecules between maternal and fetal circulation via several routes, with diffusion being the most common mechanism (Desforges & Sibley 2010). Glucose is the main energy source for the growing fetus and moves into fetal circulation by facilitated diffusion (Figure 1.6C) (Desforges & Sibley 2010). Small lipophilic molecules such as oxygen diffuse rapidly across the lipid bilayers of the cells making up the placental barrier (Figure 1.6A); whereas hydrophilic molecules cannot easily pass the lipid bilayers so may diffuse transcellularly (Figure 1.6B) at a slower rate. Diffusion of these molecules can be aided by the presence of transcellular channels and carriers. Channels allow for selective facilitated diffusion or active transport of ions such as Cl^- and K^+ (Figure 1.6G). Carriers combine selectively with the molecules and move with them across the membrane using energy harvested from facilitated diffusion and active transport (Figure 1.6F). Carriers can co-transport more than one molecule in the same direction (Figure 1.6D), or can

exchange two molecules in opposite directions across the barrier (Figure 1.6E) (Desforges & Sibley 2010). Finally, endocytosis (Figure 1.6H) is another way that molecules are transported across the placental barrier; the cell membrane invaginates to form an intracellular membrane-bound vesicle, the contents of which are then released on the other side of the cell. The exchange barrier gets thinner later in gestation, which increases the diffusion rate to meet the needs of the growing fetus (Jones & Fox 1991).

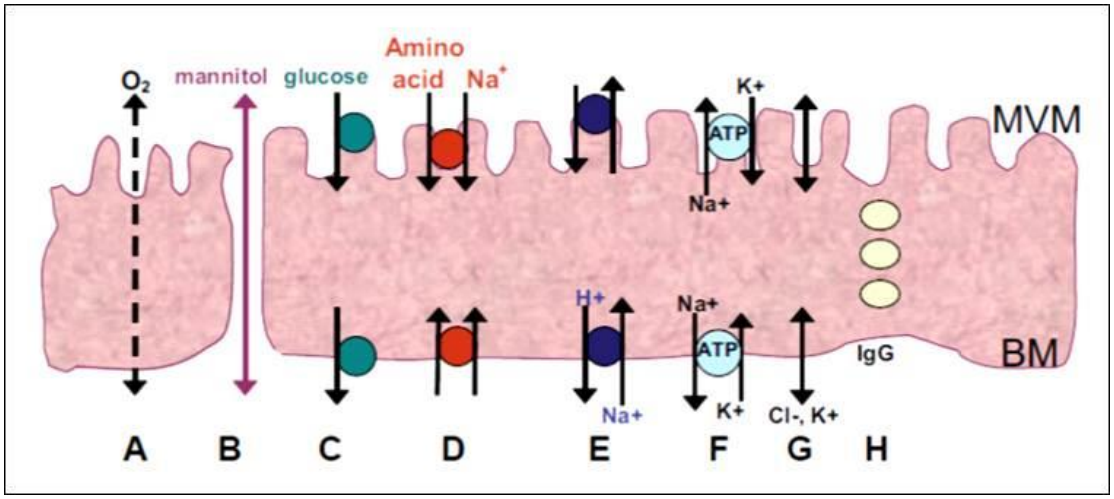

Figure 1.6: Cross section of the placental syncytiotrophoblast layer showing the main transfer mechanisms across it. Molecules cross the maternal facing MVM and the fetal facing BM via (A) diffusion of lipophilic substances, (B) paracellular transport of hydrophilic substances, (C) facilitated diffusion, (D) co-transport of amino acid with Na^+, (E) exchange of H^+ with Na^+, (F) active transport, using energy gained from the hydrolysis of adenosine-5'-triphosphate (ATP), (G) ion channels in the MVM and BM; (H) endo/exocytosis. Reproduced from (Desforges & Sibley 2010).

In general, the concentrations of amino acids in the fetal blood are higher than in the maternal blood (Philipps et al. 1978); thus amino acids are usually transferred or exchanged against a concentration gradient, via active transport mechanisms. To date, 15 transport systems have been identified in the human placental exchange barrier (Jansson 2001). Na^+-dependent systems, such as system A, ASC, Bº and β, co-transport amino acids using the Na+ electrochemical potential gradient (Jansson 2001). For Na^+-

independent systems, such as system L, it is believed that amino acid uptake is stimulated by high intracellular concentrations of the amino acids transported via the Na^+-dependent systems (Jansson 2001).

1.2.4 Placental endocrinology

The placenta produces many hormones and growth factors that support the pregnancy. Many of these hormones are either not present in the circulation of non-pregnant women, or are present in much higher concentrations in pregnancy (Linzer & Fisher 1999).

Human chorionic gonadotropin (hCG), initially synthesized by the developing blastocyst, stimulates the corpus luteum to produce estrogen and progesterone (Wang 2010). These hormones primarily act to decidualize the endometrium, aiding blastocyst implantation and preventing menstruation (Tortora & Derrickson 2009). Later in pregnancy, the placenta takes over production of estrogen and progesterone (Wang 2010), which increase gradually throughout gestation (Newbern & Freemark 2011) to maintain vascularisation of the placenta and prevent uterine contraction (Tortora & Derrickson 2009).

Human placental lactogen (hPL) and human placental growth hormone (PlGH) are produced by the placenta and their concentrations increase as the placenta grows (Newbern & Freemark 2011). They work together to initiate mammary gland lactation (Wang 2010) and help to control the concentration of glucose, lipids and amino acids that the fetus is exposed to (Newbern & Freemark 2011).

Growth factors, such as the insulin-like growth factors -I and -II (IGF-I and IGF-II), vascular endothelial growth factor (VEGF), epidermal growth factor (EGF) and fibroblast growth factor (FGF), are also produced by the placenta to promote and maintain trophoblast turnover and placental vascularisation. In combination, these factors are necessary for successful trophoblast invasion, differentiation and proliferation. (Wang 2010). They promote angiogenesis and the formation of mature and stable vessels (Wang 2010), and act as survival factors to reduce trophoblast apoptosis (Forbes et al. 2008; Moll et al. 2007). IGF-I and IGF-II have been found to be particularly important for fetal growth and development in several species. In combination with their receptors and binding proteins, IGFs increase maternal tissue growth, increase placental blood flow (Newbern & Freemark 2011; Sferruzzi-Perri et al. 2011), influence placental cell metabolism, mitogenesis and differentiation (Forbes et al., 2008; Fowden, 2003), and regulate fetal growth in response to maternal nutrient availability (Fowden 2003).

1.3 Fetal growth restriction (FGR)

In developed countries, FGR is responsible for the majority of stillbirths (Gardosi et al. 2005) and may occur due to poor maternal health, infection, or a fetal chromosomal abnormality. However, often it occurs in the absence of any triggers and is usually ascribed to placental insufficiency; abnormalities with placental development, function, or structure that impact on fetal growth (Chiswick 1985). FGR is often accompanied by PE, a life-threatening complication that also has its roots in placental insufficiency, and is characterised by maternal hypertension (>140/90mmHg), proteinuria (>300 mg in a

24-hour urine sample), maternal oedema and if severe, maternal seizures (eclampsia) and death (Garovic et al. 2007).

In clinical practice, FGR is generally defined as a fetal weight at any gestation falling below the customised 10th centile of the population, adjusted for fetal sex and maternal characteristics, such as height, weight and ethnicity (Gardosi et al. 2005). This customised birth weight adjustment aims to detect the difference between a physiologically small, but healthy baby, and a pathologically small baby (Gardosi et al. 2005; RCOG contributors 2013) where growth is limited for a medical reason (Sibley et al. 1997; Gardosi et al. 2005). As well as an immediate mortality risk, FGR babies have an increased risk of developing obesity, type-2 diabetes (Barker, Hales, et al. 1993), hypertension (Barker et al. 1989), cardiovascular diseases (Barker et al. 1989; Barker, Godfrey, et al. 1993), stroke, chronic renal failure, chronic obstructive lung disease, osteoporoporis, schizophrenia, depression, certain cancers, and polycystic ovary syndrome (Ozanne et al. 2004) as adults. The international society for Developmental Origins of Health and Disease (DOHaD 2015) has now termed this effect "fetal programming" and report that many of the conditions are due to epigenetic effects occurring in utero, which cause alterations in gene expression throughout life and can even propagate onto future generations (Aiken et al. 2015).

1.3.1 Aetiology of FGR

Fetal growth is directly correlated to the ability of the placenta to transport oxygen, nutrients and amino acids between the mother and the fetus (Sibley et al. 1997). It therefore follows that a placenta that cannot transport molecules effectively often

produces a growth-restricted fetus. A growth restricted fetus usually develops from a placenta of reduced weight, volume, diameter (Biswas & Ghosh 2008) and villous surface area (Biswas et al. 2008) when compared to adequately grown fetuses. Overall, there is a reduced placental surface area for nutrient exchange. Alterations in placental cell turnover have also been associated with FGR and PE, with an increase in syncytiotrophoblast apoptosis (Ishihara et al., 2002; Smith, Baker, & Symonds, 1997) and syncytial knot formation observed (Calvert et al. 2013).

To increase blood flow into the placenta over gestation, the uterine spiral arteries are remodelled. Brosens et al. (Brosens et al. 1972) first recognised a link between shallow trophoblast invasion, poor maternal uterine spiral artery remodelling and FGR/PE. Insufficient spiral artery remodelling results in an increased resistance to blood flow through the placenta, and reduced gaseous and nutrient transport to the fetus due to delivery of a reduced volume of blood. As well as this, unremodelled, high resistance spiral arteries cause pulsatile, high pressure 'jets' of blood to enter the intervillous space, which can also cause damage to the developing placenta (Burton et al. 2009).

Insufficient vascularisation and a reduced surface area for exchange are not the only contributors to FGR. It has also been found that the transport of amino acids, particularly via system A, is significantly reduced in FGR babies. This is due to an alteration in the activity of the transporter proteins present on the placental exchange surfaces (Sibley et al. 2005; Glazier et al. 1997). The FGR placenta transports amino acids less efficiently, meaning that there are a lower concentrations of some amino acids in the cord blood of FGR babies (Cetin et al. 1988).

1.3.2 Detection of FGR

For a potential treatment to be administered in a timely manner, it is necessary to be able to detect FGR early. At several points throughout pregnancy the expectant mother is seen by a clinician who measures parameters such as blood pressure, proteinuria and fetal growth via an ultrasound scan. If the growth trajectory of the fetus arouses concern, a Doppler ultrasound scan is often used to examine utero-placental and feto-placental blood flow. This functions by sending out ultrasound pulses and measuring the frequency shift of this pulse from the blood as it moves through a vessel, giving information about the speed and direction of blood flow. As pregnancy progresses, there is a decrease in impedance to flow through the uterine artery which can be detected by this device (Papageorghiou et al. 2004). In pregnancies complicated by FGR, often this decrease in impedance is not observed and in severe cases there is actually an increase in impedance, indicating that there is a high resistance to blood flow into the placenta (Papageorghiou et al. 2004). If implemented as a routine antenatal screen at 23 weeks gestation, it is estimated that this technique would identify around 40% of pregnancies that would go on to develop PE, and 20% of pregnancies that would go on to develop FGR (Papageorghiou et al. 2004).

Maternal circulating factors such as hCG, hPL (Reis et al. 2002), PlGF, VEGF, soluble fms-like tyrosine kinase (sFlt-1) (Levine et al. 2004), growth hormones (GH) (Reis et al. 2002), and IGFs with their binding proteins (Christians & Gruslin 2010) have all been examined as early predictors of FGR and PE. However due to inter-patient variability and the fact that FGR/PE have multifactorial pathologies, it is difficult to predict whether a patient will develop FGR/PE, especially without taking repeated

measurements throughout gestation. Unfortunately, current studies often produce conflicting results (Reis et al. 2002), making this an unreliable detection method.

Current techniques aren't robust enough to confidently predict FGR and/or PE before the clinical presentation of the disease, meaning that preventative treatments are not currently an option. If detected early, treatment could be administered earlier, giving the possibility of correcting placental insufficiency before the onset of growth restriction or PE.

1.3.3 Potential therapeutics for FGR

There is no satisfactory treatment for FGR. Currently clinicians identify high-risk patients and increase the frequency of monitoring. If the condition worsens then the baby may be delivered, usually prematurely, and will often need neonatal intensive care (Fisk & Atun 2008). Several drugs outlined below have been investigated as potential treatments in animal models and clinical trials; some are already in use in the clinic, but as yet nothing has come to fruition as a truly effective treatment for FGR.

1.3.3.1 Low Dose Aspirin (LDA)

Aspirin (acetylsalicylic acid) is a commonly used painkiller that also prevents platelet aggregation. In low doses it is an effective preventative treatment for heart attacks and strokes. LDA is readily prescribed to pregnant women at risk of FGR/PE, however there is conflicting evidence as to whether it improves pregnancy outcome.

Leitich et al. (Leitich et al. 1997) performed a meta-analysis of 13 studies, comprising 13,234 pregnant women and reported that early LDA treatment increased fetal growth when administered to women with FGR. However, Yu et al. (Yu et al. 2003) found that administration of LDA to pregnant women with impaired placental blood flow confirmed by uterine artery Doppler ultrasound, did not decrease the incidence of PE development, but the group did not assess FGR risk. Newnham et al. (Newnham et al. 1995) also report that LDA administered to women with pregnancies complicated by FGR did not increase gestation length, fetal growth or viability. More recently, a second meta-analysis stated that LDA treatment reduced the risk of PE, FGR and pre-term birth, but only when taken before 16 weeks gestation (Bujold et al. 2014), highlighting the need for early detection of these conditions.

PE/FGR are associated with placental hypoxia, which causes damage to endothelial cells and deregulation of the vasodilator prostacyclin and the vasoconstrictor thromboxane. It is believed that LDA can improve PE/FGR symptoms by acting on the enzyme cyclo-oxygenase to alter the ratio of prostacyclin and thromboxane. (Yu et al. 2003).

1.3.3.2 Low molecular weight heparin (LMWH)

LMWH has antithrombotic properties and is administered to patients who have had heart valve replacement, and those at an increased risk of myocardial infarction and stroke. It is prescribed extensively throughout pregnancy to treat vascular diseases, such as thrombophilia (an increased risk of forming blood clots) and deep vein thrombosis (DVT) (Ghidini 2014). It has also been found that LMWH is unable to cross the

placenta and is not found in fetal circulation so is considered more safe than other alternatives (Chan & Ray 1999).

Women with thrombophilia are more likely to have pregnancies complicated by FGR and PE (Many et al. 2001). In treating thrombophilia and DVT during pregnancy, it was observed that LMWH also reduced the occurrence of FGR/PE and improved fetal outcome (Many et al. 2001). As such, in a further study, LMWH and aspirin were prescribed in combination to 276 pregnant women with thrombophilia and PE/FGR in a small non-randomised trial. It was found that there was an increase in successful pregnancy outcome with the treatment (Riyazi et al. 1998). However, since this study, a further study has been conducted (Abheiden et al. 2015) which reported that administering LMWH and aspirin to pregnant women with hypertension and/or FGR and a previous history of thrombophilia did not increase fetal growth or improve umbilical or uterine artery flow velocity when compared with aspirin alone.

1.3.3.3 Vasodilators

Several pregnancy pathologies, including FGR, occur due to insufficient placental perfusion and/or insufficient vasorelaxation of both myometrial and placental vessels. Sildenafil citrate (Viagra®) is a vasodilator that has been investigated with the intention of increasing blood flow through the uterus and placenta by increasing vasodilation and reducing arterial resistance (Daraghmeh et al. 2001). Myometrial small arteries collected from human FGR pregnancies showed increased vasoconstriction when exposed to the thromboxane-mimetic U46619, and reduced endothelium-dependent relaxation when exposed to bradykinin, compared with those from uncomplicated

pregnancies (Wareing et al. 2005). When these arteries were incubated with sildenafil citrate, vasoconstriction was significantly reduced and endothelium-dependent relaxation was increased. This was not recapitulated in vessels collected from normal pregnancies when exposed to sildenafil citrate. Following this, sildenafil citrate was offered to women whose pregnancies were severely compromised by FGR (von Dadelszen et al. 2011). This pilot trial reported significantly improved fetal survival rates, but the study was underpowered so proper comparisons could not be made. There was, however, an increase in the abdominal circumference growth velocity of the fetuses in 9/10 women treated with sildenafil citrate, compared with an increase in only 7/17 in the untreated group. Sildenafil citrate is now undergoing a large cohort clinical trial (STRIDER) to further examine its effects on fetal growth further and to highlight any problematic side effects (Ganzevoort et al. 2014).

1.3.3.4 Antioxidants

Many placental pathologies are caused by an imbalance between pro- and antioxidants (Matsubara et al. 2015) and in pregnancies complicated by pre-eclampsia there is a significant decrease in the serum concentrations of certain antioxidants when compared with uncomplicated pregnancies, including superoxide dismutase (SOD) (Davidge et al. 1992). When there is insufficient placental perfusion, placental hypoxia occurs, resulting in the formation of reactive oxygen species (ROS), which limit the amount of free nitric oxide (NO; a vasodilator) present and can lead to the formation of peroxynitrite ($ONOO^-$; a free radical) (Roggensack et al. 1999), causing excessive vasoconstriction of the placental arteries.

Several antioxidants have been examined as potential treatments for pregnancy complications, with varying levels of success. In 2006, the results of a randomised placebo-controlled trial were published called the Vitamins in Pre-eclampsia (VIP) trial (Poston et al. 2006). Over 1000 high risk women were administered Vitamin C and E daily from the second trimester of pregnancy until delivery, at a dose lower than the maximum dose recommended for pregnant women by the Institute of Medicine's Food and Nutrition Board, USA. When compared with the control group, these vitamins did not reduce the risk of developing PE, but did significantly reduce the birth weight of treated infants. This study shows that antioxidant administration can be harmful in pregnancy and could increase the risk or the severity of FGR. The potential reasons for this were examined in vitro and it was found that incubating human CT with corresponding concentrations of Vitamin C and E decreased hCG and increased tumor necrosis factor- α (TNF-α) (Aris et al. 2008). Alterations in expression of these factors are known to be associated with endothelial dysfunction and adverse pregnancy outcomes.

The synthetic antioxidant compound, tempol has been tested in mouse models of FGR and PE to examine its role as a possible treatment. Hoffmann, et al. (Hoffmann et al. 2008) administered tempol to the BPH/5 mouse which exhibits impaired placentation, maternal hypertension, proteinuria and an increase in placental ROS. Treatment improved fetal growth and fetal survival, and also alleviated the maternal symptoms, such as hypertension and proteinuria. Stanley et al. (Stanley, Andersson, Hirt, et al. 2012) administered tempol in a mouse model of FGR; endothelial nitric oxide synthase knock out ($eNOS^{-/-}$) mice have elevated blood pressure before and during pregnancy, increased uterine artery resistance caused by abnormal spiral artery remodelling and

altered maternal vasodilatory responses. Ex vivo experiments have also shown that eNOS$^{-/-}$ mouse placentas contain an increased concentration of superoxide anions. Tempol treatment increased fetal weight and crown-rump length, which was hypothesised to be due to an increase in uterine artery perfusion. However, treatment also resulted in a limited decrease in superoxide anion production, no improvement in amino acid transport and a significant reduction in the vascular density of the placenta, showing that treatment may be detrimental for placental function.

More recently, the antioxidant melatonin has been found to improve fetal growth in a rat model (Richter et al. 2009) and an ovine model (Lemley et al. 2012) of FGR, with limited adverse side effects. It is now being tested in two phase-I clinical trials; one to assess whether melatonin treatment can prolong pregnancy in women with PE (Hobson et al. 2013) and a second to assess whether melatonin can reduce oxidative stress in the placenta in cases of severe early-onset FGR, confirmed by estimated fetal growth measurements and Doppler ultrasound (Alers et al. 2013). Melatonin has a good biosafety profile in adults, but it is known to cross the placenta so may have undesirable fetal effects which will need to be monitored closely.

1.3.3.5 Insulin-like growth factors (IGFs)

IGFs are mitogenic hormones that play a key role in growth in both humans and animals. They are key mediators of fetal and placental growth and function, and are also important for appropriate infant and pre-adolescent growth (O'Dell & Day 1998).

Throughout human pregnancy, IGF-I expression gradually increases (Figure 1.7), whereas IGF-II expression increases initially and then its levels are maintained. However, in other species this expression pattern is different (Sferruzzi-Perri et al. 2011). It is proposed that the maternal serum concentration of IGF-I increases in concentration during human pregnancy due to an increase in maternal tissue mass (Lof et al. 2005), whereas the concentration of IGF-II increases initially due to the development of the placenta, but then remains reasonably constant (Han & Carter 2000). IGF-I and -II are expressed by the CTs, EVTs and the mesodermal villous core during the first trimester, with IGF-II being more abundantly expressed throughout gestation (Nayak & Giudice 2003).

As shown in Figure 1.8, IGF-I and -II bind to three transmembrane receptors; type-I IGF receptor (IGF-1R), type-II IGF receptor (IGF-2R) and the insulin receptor (InsR) with varying affinities. Their actions are modulated by six binding proteins (IGFBP1-6) (Sferruzzi-Perri et al. 2011), which have been proposed to modulate IGF binding to their receptors (Nayak & Giudice 2003). Most of the mitogenic action of IGF-I and -II is mediated by binding with IGF-1R, with IGF-2R being responsible for clearance and degradation within lysosomes. IGF-II binds with a high affinity to IGF-1R and with a lower affinity to IGF-2R and IsnR; IGF-I binds to IGF-1R with a lower affinity than IGF-II, and has a very low affinity for IGF-2R (Denley et al. 2005)

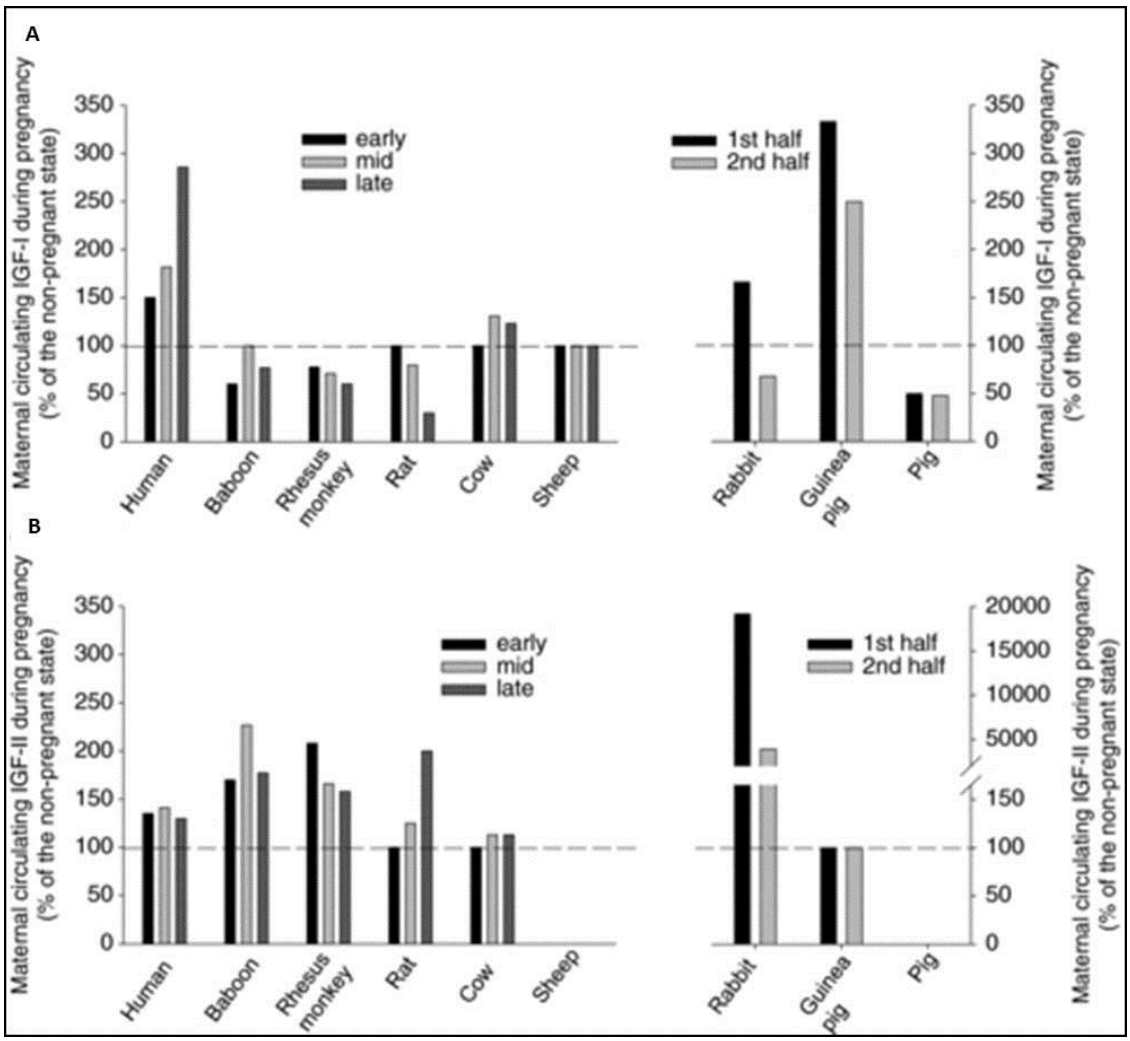

Figure 1.7: Maternal serum concentration of (A) IGF-I and (B) IGF-II during pregnancy. The concentration of IGFs were measured in human, baboon, rhesus monkey, rat, cow, sheep, rabbit, guinea pig and pig at different stages of gestation expressed as a percentage of the non-pregnant state. Dotted line is the concentration in serum from non-pregnant females. Reproduced from (Sferruzzi-Perri et al. 2011).

.

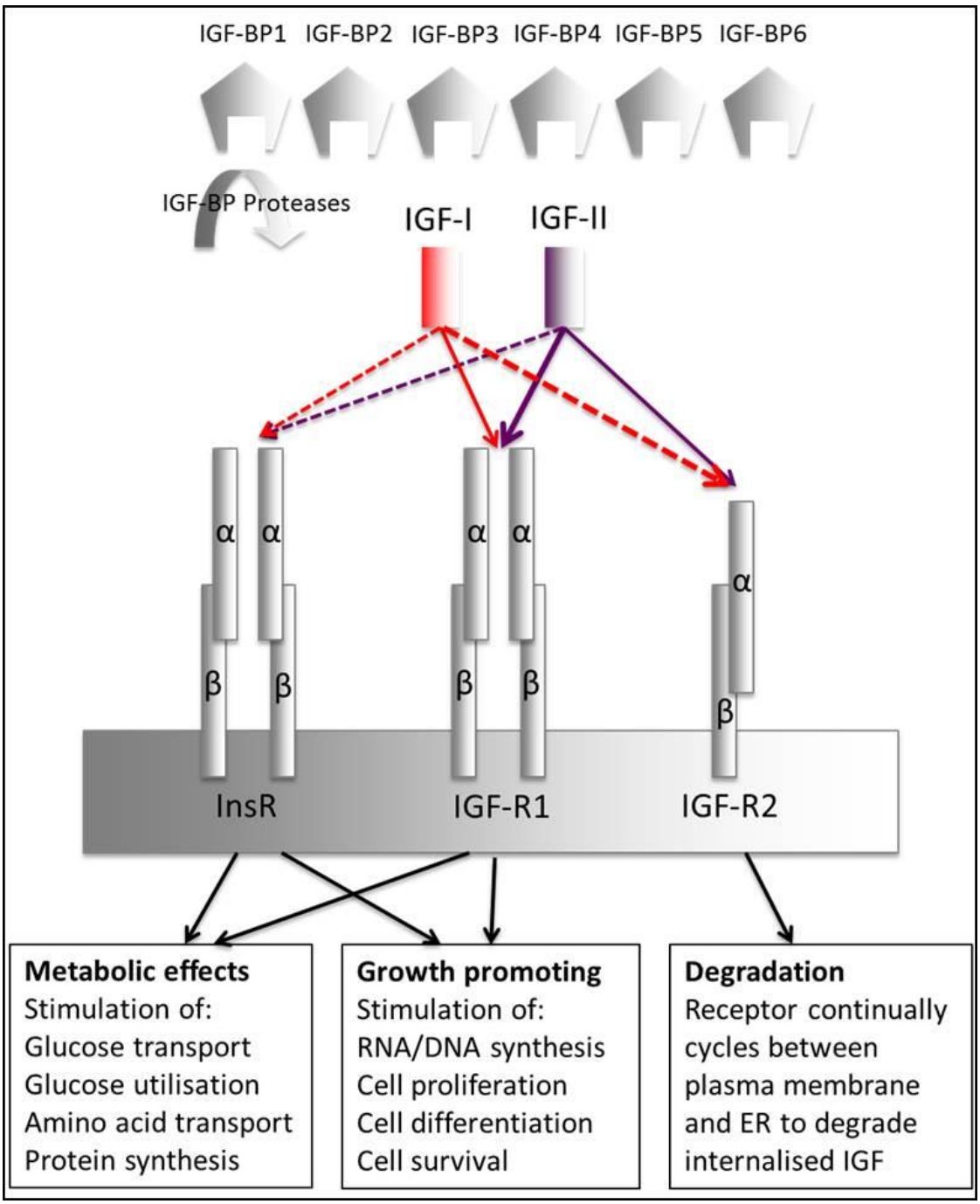

Figure 1.8: Schematic diagram illustrating the IGF axis. IGF-I and IGF-II are liberated by proteases from the six IGF-binding proteins (IGF-BP1-6) and interact with the IGF receptors (IGF-R1, IGF-R2) or the insulin receptor (InsR), leading to metabolic effects, growth promotion or degradation. Solid line shows high affinity binding, whereas dotted line shows lower affinity binding. Adapted from (Nayak & Giudice 2003; O'Dell & Day 1998).

In a review by Sferruzzi-Perri et al. (Sferruzzi-Perri et al. 2011), the effect of IGF administration to different animals during pregnancy was compiled (Table 1.1).

Treatment with IGF-I or IGF-II enhanced placental function in all species studied, affecting one or several of the following parameters depending on the species: placental weight; placental cell proliferation, migration and invasion; amino acid and glucose transport; volume or surface area for exchange and/or exchange barrier thickness.

A) Treatment	Species	Treatment regime	Analysis Day	Placental outcome
IGF-I	Mouse	In vivo: Daily E0.5-18.5 In vitro: primary EPC trophoblast	E19 1st trimester	←→ Weight ↑ Proliferation, ↑ Migration
	Rat	In vivo: Daily E9.5-20.5	E20.5	←→ Weight
	Guinea Pig	In vivo: Daily E19.5-36.5 In vivo: Daily E19.5-37.5	E39.5 E34.5 & E61.5	↑ Weight by 10% ←→ Weight and structure ↑ Glucose and AIB transfer
	Sheep	In vivo: 4h on ~E131.5	E131.5	↑ Lactate production
	Human	In vitro: Villous explants Villous explants Primary trophoblast Primary villous trophoblast Villous explants Primary villous and syncytialised trophoblast	 1st trimester 1st trimester 1st trimester 1st trimester Term Term	 ↑ Trophoblast proliferation ↑ Extravillous trophoblast migration ↓ Trophoblast apoptosis ↑ Secretion of hCG and hPL ↑ Proliferation ↑ Migration ↑ Invasion ↑ Glucose and amino acid uptake ↓ Release of vasoconstrictors ↓ TFN-α and INF-γ-induced apoptosis

B) Treatment	Species	Treatment regime	Analysis Day	Placental outcome
IGF-II	Mouse	In vitro: primary EPC trophoblast	1st trimester	↑ Differentiation into giant cells
	Rat	In vivo: Daily E15.5-21.5	E21.5	↑ 29% volume of junctional zone
	Sheep	In vitro: primary mononuclear trophoblast	1st trimester	↑ Migration
	Guinea Pig	In vivo: Daily E19.5-36.5 In vivo: Daily E19.5-37.5	E39.5 E34.5 & E61.5	↑ Weight by 9% ←→ Weight ↓ Area and proportion of interlobium ↑ Labyrinthine area, proportion and volume ↑ Surface area for exchange ←→ Placental barrier thickness ↑ Transfer of glucose
	Human	In vitro: Villous explants Primary trophoblast Primary villous trophoblast	 1st trimester 1st trimester 1st trimester Term	 ↑ Trophoblast proliferation ↑ Syncytial regeneration ↑ Extravillous trophoblast migration ↓ Trophoblast apoptosis ↑ Proliferation ↑ Migration ↑ Invasion ↑ Glucose and amino acid uptake ↑ Glucose and amino acid uptake

Table 1.1: The impact of IGFs on placental growth and function in vitro and in vivo. (A) IGF-I and (B) IGF-II administration to pregnant animals or incubation with human 1st trimester and term placental tissue. ECP; ectoplacental cone. Adapted from (Sferruzzi-Perri et al. 2011)**.**

It is hypothesized that IGF-I is important for fetal growth by initiating maternal metabolic adaptions that are necessary to produce an adequately grown fetus (Figure 1.9). Ablation of the IGF-I gene in mice reduced fetal weight to approximately 60% of wild type weight by the end of gestation, but placental weight was unaffected (Baker et al. 1993). Exogenous administration of IGF-I to guinea pigs did not alter placental weight, but increased fetal growth purportedly by diverting nutrients from the mother to the fetus and reducing maternal adipose tissue (Sferruzzi-perri et al. 2007). Similarly, exogenous administration of IGF-I to pregnant rodents did not alter fetal or placental, but did affect maternal weight gain (Gluckman et al. 1992; Gargosky et al. 1991). Elevated IGF-I levels in the pregnant ewe induced by maternal food restriction, increased maternal tissue mass in favour of fetal or placental weight gain (Wallace et al. 1996; Wallace et al. 1997).

Conversely, IGF-II is thought to be responsible for regulating fetal growth via its actions on the placenta (Figure 1.9). Knocking out the placental-specific IGF-II transcript, which abolishes IGF-II production in the placental labyrinth, affected both fetal and placental growth; fetuses weighed 69% of their wild type counterparts, and placental weights were 68% of wild type at term (Constância et al. 2002; Baker et al. 1993). IGF-II administration to the rat increased the junctional zone volume by 29% (Van Mieghem et al. 2009), but did not affect fetal weight. Whereas administration to the guinea pig increased the placental weight by 9% (Sohlström et al. 2001) and increased fetal weight by 7-11%, improving fetal viability (Sferruzzi-perri et al. 2007; Sferruzzi-Perri et al. 2006; Sferruzzi-Perri et al. 2008).

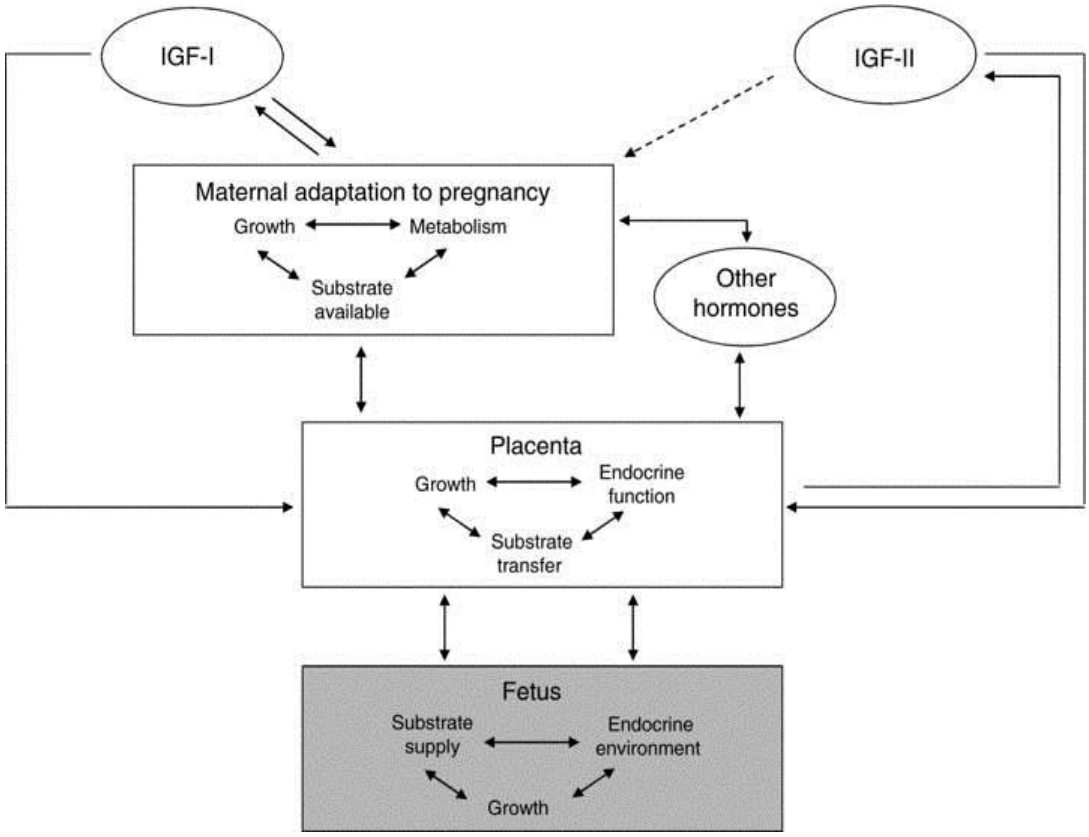

Figure 1.9: The proposed actions of maternal circulating IGFs on the mother and placenta that influence fetal growth. Adapted from (Sferruzzi-Perri et al. 2011)**.**

IGFs also play an important role in human placental development. In a human explant model, IGF-I and -II increased CT proliferation and decreased apoptosis (Forbes et al. 2008). They also improved human placental fibroblast function when virally transfected in vitro (Miller et al. 2005). IGFs reportedly stimulate amino acid and glucose uptake in human term placental explants (Kniss et al. 1994; Karl 1995; Roos et al. 2009), with IGF-I in particular stimulating glucose and amino acid uptake in isolated human trophoblasts (Karl 1995; Kniss et al. 1994) as well as inhibiting the release of the vasoconstrictors thromboxane and prostaglandin in human term placental explants (Siler-Khodr et al. 1995).

There is an association between FGR and alterations in IGF axis in human pregnancies, demonstrating the potential for clinical translation of IGF treatment. There are alterations in the concentration of IGFs and their associated binding proteins in maternal plasma and fetal cord blood collected from FGR pregnancies (Lassarre et al. 1991; Giudice et al. 2013; Holmes et al. 1997). There is a positive correlation between the maternal plasma concentration of IGF-I (Vatten et al. 2008) and IGF-II (Cooley et al. 2010) and the risk of developing PE. Finally, the expression of IGF-I and IGFBP1 is also reduced (Koutsaki et al. 2011), with a 33% reduction in the protein content of the IGF-I receptors (Laviola et al. 2005) in placentas collected from FGR pregnancies.

As yet, IGFs have not been administered to animals displaying an FGR phenotype or to humans with pregnancies complicated by FGR. However, there is an increasing body of evidence that suggests that IGFs are extremely important for fetal growth and that by increasing the concentration of IGFs, it is possible to enhance placental function in all animals studied; in turn it may be possible to increase fetal growth and viability.

1.3.4 The future of therapeutics for FGR

The majority of drugs in use currently are systemically administered and circulate throughout the entire body. As such, many cannot be given to pregnant woman due to the fear of teratogenicity and off-target maternal and fetal effects. Targeted therapeutic delivery may allow the treatment of placental abnormalities directly and specifically, without causing systemic side effects to the mother or baby. Targeted delivery also allows a lower dose of the drug to be administered to achieve the equivalent therapeutic concentration locally within the placenta, potentially making any candidate drug safer

and cheaper to administer. Nanoparticles are increasingly being used to facilitate the targeting of drugs to particular sites in the body and to enhance the pharmacokinetics and bioavailability of the drug administered.

1.4 Nanoparticles for drug delivery

Nanoparticles are defined as synthetic or natural materials with one or more dimension being less than 100 nm. Because of their size, nanoparticles possess properties different from their bulk counterparts, such as a large surface area to volume ratio, making them particularly useful for drug delivery. Using nanoparticles allows for the modification of existing drug characteristics such as solubility, blood circulation half-life, drug release profiles and tissue specificity. (Zhang et al. 2008).

There are several nanoparticle-drug compounds that are clinically available or are undergoing clinical trials (Table 1.2) (Zhang et al. 2008). Currently, these nanoparticle formulations rely on passive targeting utilising a phenomenon called the enhanced permeability and retention effect (EPR). Drugs conjugated to nanoparticles are protected from degradation and therefore become long-circulating therapeutics. Certain tumours display the EPR effect which permits the accumulation of long circulating nanoparticles in the leaky, immature vasculature that surrounds them (Maeda et al. 2000).

Composition	Trade name	Company	Indication	Route
Liposome amphotericin B	Abeket	Enzon	Fungal infections	I.V
Liposome amphotericin B	AmBisome	Gilead Sciences	Fungal and protozoal infections	I.V
Liposomal cytarabine	DepoCyt	SkyePharma	Malignant lymphomatous meningitis	I.T
Liposomal daunorubicin	DaunoXome	Gilead Sciences	HIV-related Kaposi's sarcoma	I.V
Liposomal doxorubicin	Myocet	Zeneus	Combination therapy with cyclophosphamide in metastatic breast cancer	I.V
Liposomal IRIV Vacicne	Epaxal	Berna Biotech	Hepatitis A	I.M
Liposomes IRIV Vaccine	Inflexal V	Berna Biotech	Influenza	I.M
Liposomal morphine	DepoDur	SkyePharma, Endo	Postsurgical analgesia	Epidural
Liposomal verteporfin	Visudyne	QLT, Novartis	Age-related macular degeneration, pathological myopia, ocular histoplasmosis	I.V
Liposome-PEG doxorubicin	Doxil/Caelyx	Ortho Biotech, Schering-Plough	HIV-related Kaposi's sarcoma, metastatic breast cancer, metastatic ovarian cancer	I.M
Micellular estradiol	Estrasorb	Novavax	Menopausal therapy	Topical
ι-Glutamic-acid, ι-alanine, ι-Lysine and ι-tyrosine copolymer	Copaxone	TEVA Pharmaceuticals	Multiple sclerosis	S.C
Methoxy-PEG-poly(D,L-lactide taxol	Genexol-PM	Samyang	Metastatic breast cancer	I.V
PEG-adenosine deaminase	Adagen	Enson	Severe combined immunodeficiency disease associated with ADA deficiency	I.M
PEG-anti-VEGF aptamer	Macugen	OSI Pharmaceuticals	Age-related macular degeneration	I.R
PEG-α-interferon 2a	Pegasys	Nektar, Hoffmann-La Roche	Hepatitis B, Hepatitis C	S.C
PEG-GCSF	Neulasta	Amgen	Neutropenia associated with cancer chemotherapy	S.C
PEG-HGF	Somavert	Nektar, Pfizer	Acromegaly	S.C
PEG-ι-asparaginase	Oncaspar	Enzon	Acute lymphoblastic leukemia	I.V, I.M
Poly(allylamine hydrochloride)	Renagel	Genzyme	End-stage renal disease	Oral
Albumin-bound paclitaxel	Abraxane	Abraxis BioScience, AstraZeneca	Metastatic breast cancer	I.V
Nanocrystalline aprepitant	Emend	Elan, Merck	Antiemetic	Oral
Nanocrystalline fenofibrate	Tricor	Elan, Abbott	Anti-hyperlipidemic	Oral
Nanocrystalline sirolimus	Rapamune	Elan, Wyeth Pharmaceuticals	Immunosuppressant	Oral

Table 1.2: Clinically approved nanoparticle based therapeutics. ADA; adenosine deaminase, GCSF; granulocyte colony-stimulating factor, HGF; hepatocyte growth factor, HIV; human immunodeficiency virus, I.M; intramuscular, I.R; intravitreous, IRIV; immunopotentiating reconstituted influenza virosome, I.T; intratrathecal, I.V; intravenous, PEG; poly(ethylene glycol), S.C; subcutaneous, VEGF; vascular endothelial growth factor. Adapted from (Zhang et al. 2008).

Liposomes are spherical nanoparticles composed from a phospholipid bilayer (Immordino et al. 2006). They are one of the most extensively used and well-characterised drug delivery systems available. Arguably, the most successful liposome formulation currently in clinical use is DOXIL®, also trading under the names Caelyx® or Myocet®. DOXIL® is liposomally encapsulated doxorubicin, a widely used chemotherapeutic, which works by passively targeting solid tumours. It was the first Food and Drug Administration (FDA) approved nanoparticle formulation and is licenced to treat Kaposi sarcoma, ovarian cancer and breast cancer. It is reported that DOXIL® is significantly more effective at reducing tumour growth than free doxorubicin, with significantly reduced cardiotoxicity (Working & Dayan 1996; Gabizon & Martin 1997).

Other examples of liposomally encapsulated drugs that function by passive targeting include: AmBisome (amphotericin B liposomes) used for fungal infections; DaunoXome (daunorubicin liposomes) used to treat Karposi sarcoma; DepoCyt (cytarabine liposomes) used to treat malignant lymphomatous meningitis; and Visudyne (verteporfin liposomes) used to treat age-related macular degeneration (Zhang et al. 2008). Encapsulating these drugs ameliorates many of the undesirable side effects associated with them, and improves their efficacy at the target tissue.

Several other nanomaterials being investigated as potential drug delivery systems include poly-drug conjugates, metallic nanoparticles (Jordan et al. 2006), carbon fullerenes (Dou et al. 2012), carbon nanotubes (Hadidi et al. 2013) and more recently graphene (Wang et al. 2013).

1.4.1 Active nanoparticle drug targeting

There are inherent limitations of passive targeting as only some organs and certain tumour types can be targeted. Active targeting allows for tumours to be selectively targeted, and means that tissues where the EPR effect isn't observed can benefit from drug targeting. Active targeting is a more recent concept, so these systems are still undergoing clinical and pre-clinical trials (Table 1.3).

Targeted with	Encapsulated drug	Disease
Anti-HER2	Doxorubicin	Breast, ovarian cancer
Anti-EGF	Doxorubicin, vinorelbine, methotrexate, DNA	Solid tumours
Anti CD19	Vincristine	Lymphoma
Anti CD 22	Doxorubicin	Anti-B-cell lymphoma
Anti CD 19	Imatinib	All
Anti-β1 integrin	Doxorubicin	Several cancers
Anti GD2	Doxorubicin	Neuroblastoma
GAH MAb	Doxorubicin	Gastric, colon and breast cancer
Anti-EGF receptor	RNA	Brain cancer

Table 1.3: Targeted liposomes undergoing advanced clinical trials for cancer treatment. Adapted from (Immordino et al. 2006).

The body has its own way of recognizing and targeting cells and tissues by selectively pairing antibodies with antigens; a method that scientists have exploited for processes such as immunohistochemistry. Several liposome formulations shown in Table 1.3 have been modified with antibody surface conjugates to produce targeted drug delivery systems that actively target tissues. In doing this, nanoparticles can, in theory, be made to target any matching antigen, as long as they come into contact.

There are several examples of targeted liposomes being used to improve cancer treatment in vitro and in animal models. Gupta et al. (Gupta & Torchilin 2007) demonstrated that DOXIL® coated with the tumour specific 2C5-antibody showed increased uptake in U-87 MG brain tumour cells both in vitro and in an intracranial mouse model. Treatment increased the efficacy of the chemotherapeutic compared to non-targeted DOXIL®, significantly reducing the tumour size and almost doubling the survival time of the mice, highlighting the benefits of targeted delivery

1.4.2 Nanoparticles for use in pregnancy

Nanoparticle encapsulation might be particularly beneficial when administering drugs to pregnant woman as it is unknown which drugs will cross the placenta and accumulate in the fetus, and which drugs will remain only in maternal circulation; nanoparticles can be engineered to control this transfer.

A number of drugs commonly used during pregnancy have been investigated for liposome encapsulation. Indomethacin is given to women in premature labour as it inhibits prostaglandin production and prevents uterine contractions. However, it readily crosses the placenta and has detrimental side effects on the fetus so cannot be given longer term. Refuerzo et al. (Refuerzo et al., 2015) demonstrated that when indomethacin was encapsulated inside liposomes and administered to pregnant mice, its action was limited to the uterus and it did not cross the placenta to the same extent as free indomethacin, but still maintained its pharmacological effects. In the future, this may allow for the safer treatment of premature labour.

Valproic acid is administered to pregnant women with epilepsy, but can cause serious fetal malformations. As such, Barzago et al. (Barzago, Bortoloiri, Efrati, Salmona, & Bonati, 1996) examined whether encapsulating valproic acid inside liposomes limited its placental transfer using the dual perfused human placental lobule model. They found that liposome encapsulation significantly reduced placental uptake and transfer, potentially reducing fetal exposure. Again, this strategy could make treating epilepsy during pregnancy safer.

There is a targeted nanoparticle that has been developed for use during pregnancy, targeting the trophoblast to treat disorders, such as ectopic pregnancy, placental accreta (where the placenta is pathologically adherent to the myometrium) and choriocarcinoma. Kaitu'u-Lino et al. (Kaitu'u-Lino et al. 2013) used bacterially-derived nanoparticles (400 nm) coated with antibodies specific to the epidermal growth factor receptor (EGFR) in order to target placental tissues with doxorubicin. When administered to mice bearing the JEG3 choriocarcinoma in the hind flank, it was found that treatment significantly increased the concentration of doxorubicin at the tumour site and reduced the tumour volume compared to free doxorubicin. Although EGFR is highly expressed on the surface of the placenta, many other tissues also express it, so strategies that target antigens that are highly expressed on the placental surface are not always truly selective. For this reason a new group of specific targeting moieties called homing peptides may be a better option for placental targeting.

1.5 Tissue-specific homing peptides

Pasqualini et al. (Pasqualini & Ruoslahti 1996) identified a novel group of targeting molecules called homing peptides using in vivo unbiased screening of random peptide sequences displayed on bacteriophage. A bacteriophage library was engineered so that each phage displayed several copies of one of 10^9 individual, random, short peptide sequences. The library was then injected I.V. into mice and allowed to circulate for several hours. The mice were culled and organs or tissues of interest were collected and the phage displaying peptide sequences that had accumulated there were amplified and were then re-injected. The process was repeated several times to ensure tissue specificity. The group reported that homing peptide sequences targeted vascular endothelial cell-specific surface markers such as peptidases, proteases, cell adhesion molecules and integrins that are selectively expressed in distinct vascular beds. The group are now developing homing peptide-decorated nanoparticles that are able to specifically target certain cancer cells with chemotherapeutics to improve the efficacy of treatment (Agemy et al. 2011).

Short peptides make ideal targeting elements as they are easier to screen for and are potentially more specific than antibodies (Friedman et al. 2013). They are also smaller than antibodies, so can be displayed on the surface of nanoparticles in a multivalent fashion, which can significantly improve binding avidity (Montet et al. 2006).

1.5.1 Active targeting of tumours using homing peptides

The tumour homing peptide CGKRK (Cys–Gly–Lys–Arg–Lys), identified by the Ruoslahti group (Hoffman et al. 2003), has been used to develop targeted nanoparticle-drug conjugates and trialled in several tumour-bearing animal models with a large amount of success. The group showed that when delivered to mice bearing a squamous cell carcinoma, CGKRK targeted the vasculature surrounding the tumour with an 80-1000-fold preference compared with non-targeting peptide sequences and other tissues (Hoffman et al. 2003). They report that CGKRK-decorated iron oxide nanoparticles accumulated rapidly in the vasculature surrounding a brain tumour induced in mice when intravenously delivered (Agemy et al. 2011). Once tumour targeting was confirmed, the nanoparticles were also coated in the proapoptotic peptide $_{D}[KLAKLAK]^{2}$. Systemic administration of the targeted nanotherapeutic reduced tumour growth and eradicated the tumours in a number of mice and was far more effective than non-targeted treatment. In a further study using the same nanotherapeutic, Agemy et al. (Agemy et al. 2013) report similar results in a mouse model of breast cancer. They state that one receptor for CGKRK is the protein p32, a ubiquitously expressed intracellular protein that is highly expressed on the surface of angiogenic endothelial cells and tumor cells (Agemy et al. 2013).

The homing peptide iRGD (CRGDKGPDC, Cys–Arg–Gly–Asp–Lys–Gly–Pro–Asp–Cys; internalising RGD) is a cyclic peptide that was first identified by Sugahara et al. (Sugahara et al. 2009) in the Ruoslahti group. Peptides that include the RGD sequence bind to the integrins $\alpha_v\beta_3$ and $\alpha_v\beta_5$, which are upregulated on the surface of angiogenic endothelial cells and on certain tumours. If the peptide also contains the sequence

R/KXXR/K (where R/K means R or K) at the C-terminus of the peptide (e.g. iRGD C**RGDK**GPDC) then the peptide is proteolytically cleaved by cell surface proteases to expose the fragment CRGDK/R (Figure 1.10). The peptide fragment loses its integrin-binding affinity, but the new sequence has an affinity for neuropilin-1 which mediates internalization and tissue penetration (Sugahara et al. 2010). Neuropilin-1 is a cell surface receptor with multiple ligands including several VEGF isoforms (Ellis 2006) and semaphorin 3A (Kolodkin et al. 1997), all of which increase vascular permeability to macromolecules when ligated to neuropilin-1 (Bates & Harper 2003; Becker et al. 2005).

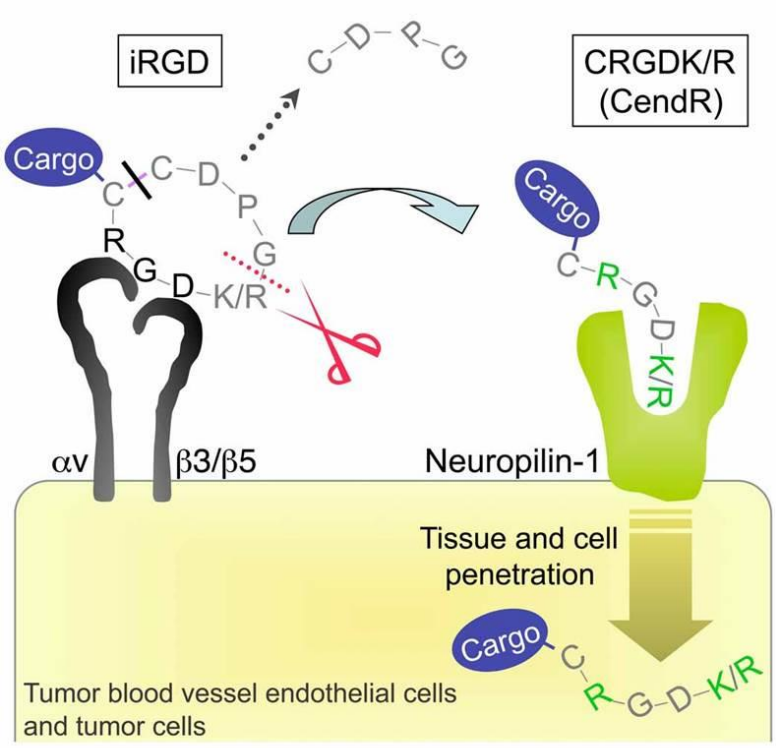

Figure 1.10: Binding and penetration mechanism of iRGD peptide. Homing peptides displaying an RGD sequence interact with integrin $\alpha_v\beta_{3/5}$ present on the surface of endothelial cells lining tumour vasculature and tumour cells. Peptides with the motif R/KXXK/R at the C-terminus of the peptide (CendR motif) will then be proteolytically cleaved to release CRGDK/R, which is then internalized into the cell via neuropilin-1 along with conjugated cargo. Reproduced from (Sugahara et al. 2009).

The cyclic iRGD sequence is a cell penetrating peptide, as it in internalised into cells via binding to neuropilin-1. It has been reported that molecules conjugated to iRGD are also endocytosed into cells due to the peptide's interaction with this receptor, and often appear in endocytotic vesicles inside the cells (Teesalu et al. 2009). However, the endocytotic mechanism responsible for this internalisation, whether clathrin mediated, caveolae-mediated or by micropinocytosis endocytosis, is disputed (Pang et al. 2014). Pang et al. report that iRGD is internalised by a distinct endocytotic pathway, that resembled micropinocytosis, but is mechanistically different and its activity is inversely correlated by the nutrient availability of the surrounding environment (Pang et al. 2014).

Co-administering free iRGD peptide improves the penetration and efficacy of intravenously injected nanotherapeutics into the extravascular tumour tissue, without actually being present on the nanoparticle's surface (Sugahara et al. 2010). However, iRGD, and variants of this sequence, have been used to create targeted nanoparticles which show increased accumulation in several xenograft mouse models including prostate, pancreatic, breast, bone, brain and cervical cancers (Sugahara et al. 2009).

Zhang et al. (Zhang et al. 2010) developed liposomes encapsulating both combretastatin A-4 (a vascular disrupting agent) and doxorubicin (a cytotoxic agent), coated in RGD (Arg–Gly–Asp). It is widely reported that administering these drugs separately to the same patient works for a short amount of time, but as the vascular beds respond to combretastatin A-4 they begin to collapse, thus doxorubicin can no longer access the tumour cells. The RGD peptide sequence targets integrins over-expressed by melanoma tumor cells and tumor endothelial cells, and the group hypothesized that delivering these drugs together using a targeted liposome would increase the tumour-destroying

efficacy of the treatment and prolong the time that doxorubicin has access to the tumour cells. The group then examined its anti-tumour activity in mice bearing a B16F10 melanoma and found that treatment dramatically decreased tumour size compared with control groups.

Du. et al. (Du et al. 2011) decorated liposomes encapsulating doxorubicin with the homing peptide sequence RGDF (Arg-Gly-Asp-Phe) to target integrins over-expressed by tumour cells. Active targeting of doxorubicin to tumours was observed in mice carrying the S-180 sarcoma and there was a 1.7-4.5 fold increase in the concentration of the cancer drug at the tumour site compared to controls. As a result, there was a significant decrease in tumour weight with treatment of RGDF liposomes encapsulating doxorubicin compared with all controls. This supports the use of homing peptides to improve nanoparticle accumulation and drug release in specific tissues.

1.5.2 Active targeting of the placenta using homing peptides

As the placenta behaves rather like a well-controlled tumour (Holtan et al. 2009), it was hypothesized that certain tumour homing peptides may accumulate in the vascular beds of the placenta. Using unbiased in vivo phage screening, Harris et al. (Harris et al. 2012) independently demonstrated that phage bearing the peptide sequences iRGD and CGKRK (Figure 1.11) selectively accumulated in the mouse placenta. In a further study (King et al. 2016) the group showed that when injected I.V into pregnant mice, the same peptide sequences selectively bound to the mouse placental labyrinth (Figures 1.12B, D & F) and decidual spiral arteries (Figures 1.12A, C & E) throughout pregnancy, but not to the junctional zone of the mouse placenta or the vascular beds of any other maternal

or fetal organs. Furthermore, when incubated with human first trimester and term placental explants, both homing peptides accumulated in the syncytiotrophoblast layer within 30 min and persisted for the 24 h examined (Figure 1.13A-D).

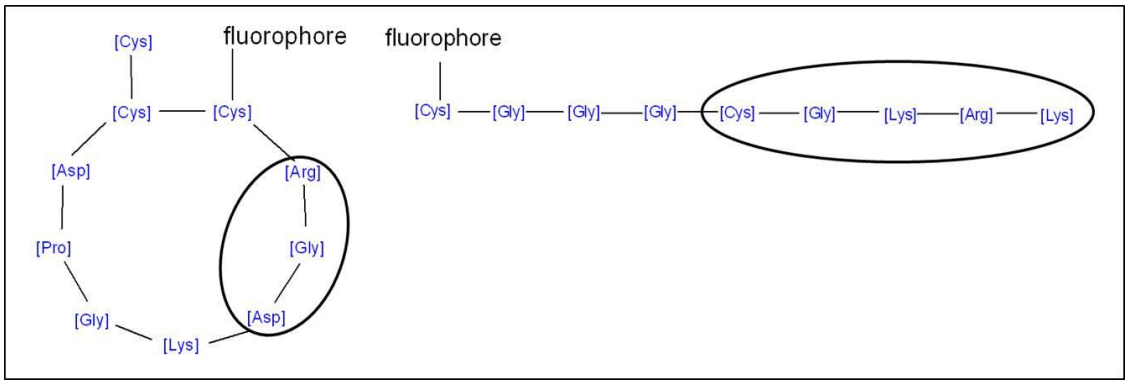

Figure 1.11: Amino acid structure of the homing peptides iRGD (left) and CGGGCGKRK (right). Circled are sequences that are thought to be important for placental targeting. MW (Rh-iRGD) = 1519.81 Da, MW (TAMRA-CGGGCGKRK) = 1277.48 Da.

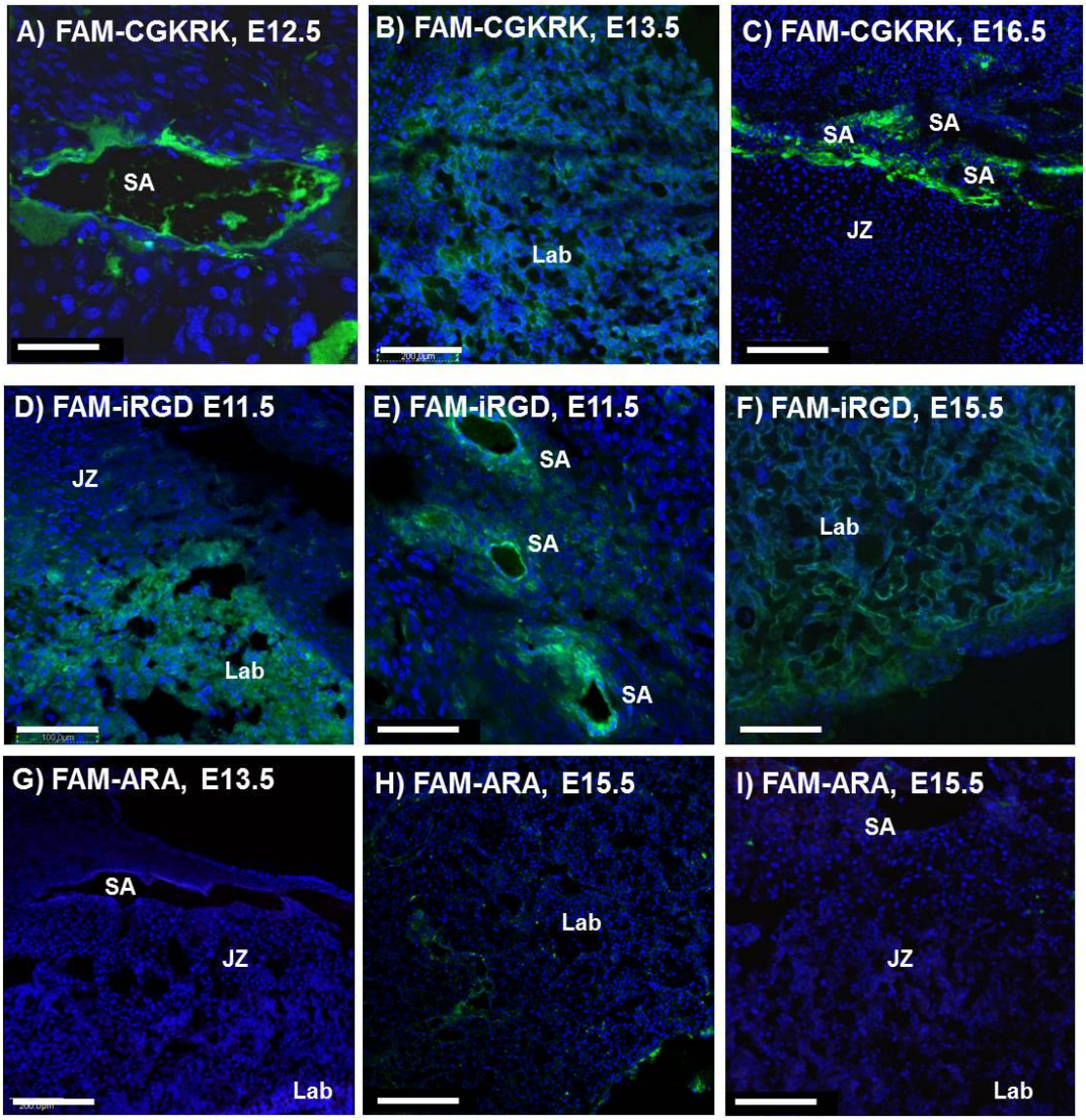

Figure 1.12: Tumour homing peptide accumulation in mouse placentas at several gestational time points. Peptides were injected into the tail vein of pregnant mice and after 3 h the placentas were collected and fluorescently imaged. (A–C) FAM–CGKRK; (D–F) FAM–iRGD; (G-I) FAM–ARA (control peptide) (n = 3). FAM–labeled peptides, green; DAPI (nuclei), blue. JZ; junctional zone; Lab; labyrinth; SA; spiral artery; Scale bar = 50 µm. Reproduced from (King et al. 2016).

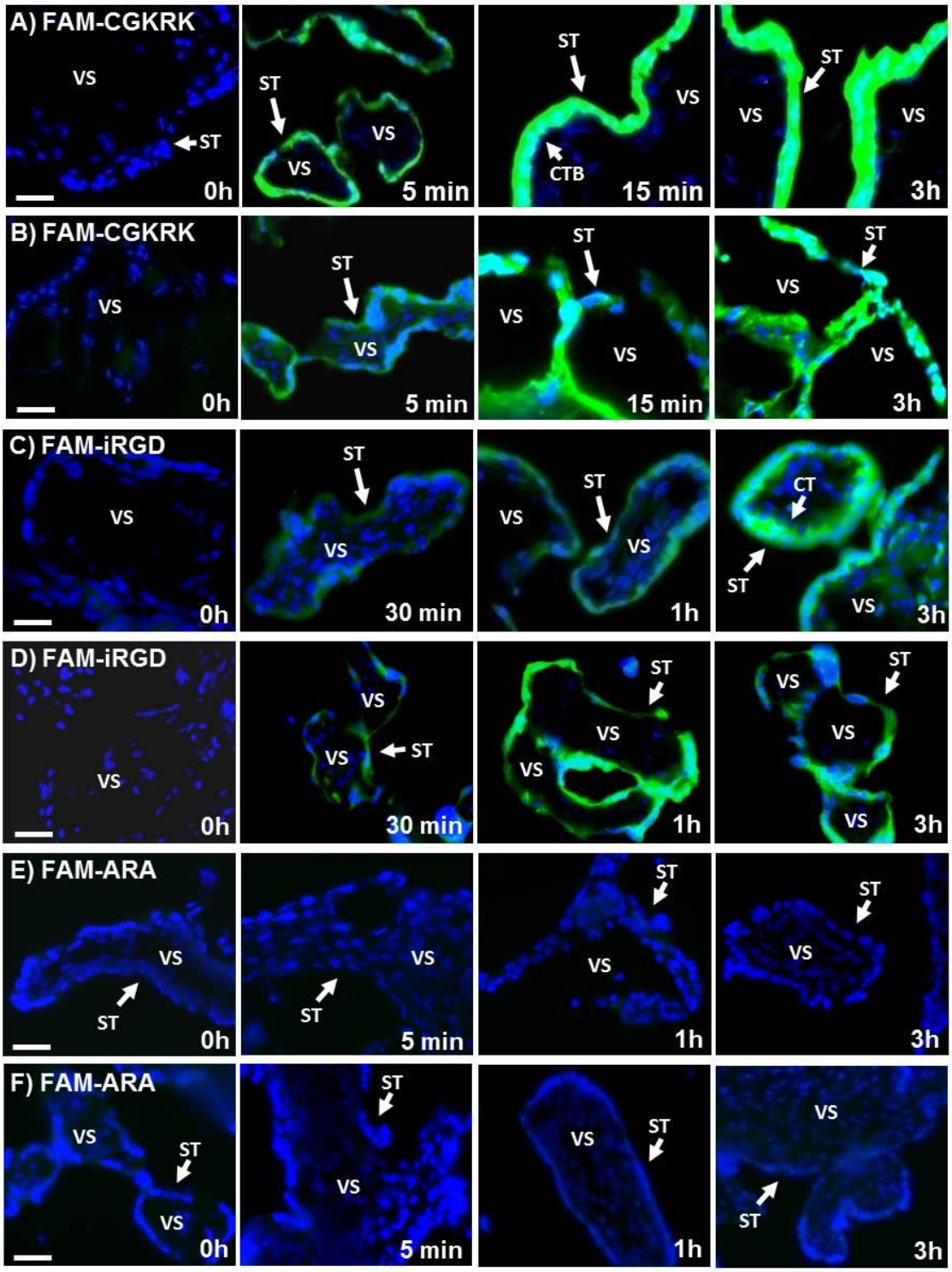

Figure 1.13: Tumour homing peptide accumulation in human placental explants. First trimester (A, C, E) or term (B, D, F) placental explants were incubated with iRGD, CGKRK or ARA peptides for 0-3 h. Binding and uptake was assessed by fluorescence microscopy (n = 3). FAM–labeled peptides, green; Scale bar = 50 µm. Reproduced from (King et al. 2016).

These targeted areas represent ideal tissues to deliver therapeutics to with the ultimate aim of treating placental pathologies that cause FGR. The syncytiotrophoblast is the outer surface of the placental barrier and controls nutrient and amino acid transfer. Altered cell turnover at the syncytiotrophoblast is associated with FGR and PE (Ishihara et al. 2002). Delivering therapeutics such as IGFs that increase trophoblast proliferation in human placental explants (Forbes et al. 2008) and improve placental nutrient transport in animal models (Sferruzzi-perri et al. 2007), may rescue a poorly functioning placenta.

1.5.2.1 Possible placental receptors for homing peptide binding

Sugahara et al. (Sugahara et al., 2009) report that iRGD binds to the integrin α_v subunit expressed on the endothelium of tumour vasculature. Supporting this, King et al. (King et al. 2016) report co-localisation of iRGD with integrin α_v expressed at the mouse placental materno-fetal interface. This integrin subunit is reportedly expressed on the mouse placenta throughout gestation (Sutherland et al. 1993). However, it is mostly limited to the spongiotrophoblast found in the junctional zone (Bowen & Hunt 1999), whereas King et al. observed peptide accumulation mostly in the labyrinth (King et al. 2016). Integrin $\alpha_v\beta_3$ is also expressed on the human placental surface (Vanderpuye et al. 1991) explaining the recapitulation of results when examining human placental explants.

King et al. (King et al. 2016) also examined the receptor responsible for the placental binding of the CGKRK peptide and found that rather than p32 as previously reported (Agemy et al. 2013), its placental receptor was more likely to be membrane-associated

calrecticulin. Calrecticulin is a highly expressed, intracellular protein observed in many tissues in the body, including the placenta (Protein Atlas 2016). It is highly expressed on the surface of cells in the labyrinth, junctional zone and spiral arteries of the mouse placenta and on the syncytiotrophoblast of human first trimester and term placenta (King et al. 2016), where it is available to bind to systemically administered peptide.

Many short peptide sequences mediate cell-cell adhesion by binding to cell surface receptors such as integrins. Ruoslahti states that some naturally occurring RGD sequences actually influence the activity of other naturally occurring peptides, by acting as a competitive inhibitors (Ruoslahti 1996). However, King et al. (King et al. 2016) showed that repeated administration of iRGD and CGKRK peptides throughout pregnancy did not adversely affect outcome; treatment did not alter litter size, number of resorptions, fetal weight, placental weight or maternal weight gain in mice, suggesting that they are safe for use as targeting ligands in pregnancy and do not interfere with normal ligand binding.

1.5.3 Active targeting of the placenta using homing peptide decorated nanoparticles

After demonstrating that the tumour homing peptides iRGD and CGKRK targeted human and mouse placental tissue, King et al. (King et al. 2016) attached the peptides to iron oxide nanoworms to ensure that their targeting ability was retained when attached to a nanoparticle that could be used to aid drug delivery. The peptide-nanoworm conjugates accumulated in the mouse placenta after tail vein I.V injection in a similar manner to the free homing peptides, confirming that even when the homing peptides

were held in a static orientation due to attachment to the nanoparticles, they were still able to bind to epitopes expressed by the placenta. Whilst appropriate for delivery of chemotherapeutics, it is unlikely that iron oxide nanoworms are compatible with optimal placental function. Biocompatible liposomes may be a better choice for administration of placental therapies as our ultimate aim is to enhance placenta growth and/or function.

It is important to understand how the placenta processes liposomes. In particular, it is important to try to limit the transfer of potentially harmful drugs to the fetal circulation. As the fetal blood-brain barrier is permeable and the fetus has a poor liver enzyme activity due to its immaturity, drug exposure may induce many serious side effects (Juchau et al. 1980; Stirrat 1976). Similarly, drug accumulation in tissues and organs still undergoing development and maturation may have teratogenic effects (Kulvietis et al. 2011).

Placental processing of several types of nanoparticle including liposomes has been examined in pregnant rats and mice, and using human placental lobules perfused ex vivo to mimic in situ conditions, to determine how drug transfer rate is affected by the size, surface charge and composition of the nanoparticle. Findings summarized here will inform the design of a liposome that is capable of targeting the placenta, but will not transfer its contents to the fetus.

1.5.4 Nanoparticle interaction with the placenta

Nanoparticle transfer to the fetus is generally believed to be dependent on the stage of gestation (Kulvietis et al. 2011). In mice, gold nanoparticles intravenously administered before E11.5 (when the placenta is considered fully formed) and left to circulate for 5 hours could be detected in fetal tissues, whereas those administered after E11.5 and left to circulate for the same amount of time were present in fetal tissue at a much lower concentration, if at all (Yang et al. 2012). The group also showed that coating the gold nanoparticles in a layer of poly(ethylene glycol) (PEG) reduced transplacental transfer, whilst maintaining accumulation in extra-embryonic tissues (EET), including the placenta, umbilical cord and membranes. The group monitored the offspring from this experiment for 8 weeks after delivery and did not observe any developmental effects due to treatment and the animals were still able to reproduce normally. Histological samples from the offspring did not reveal tissue damage from nanoparticle exposure. Although it was not observed in this example, nanoparticle exposure is thought to be the most dangerous early in gestation during periods of rapid fetal cell proliferation and organogenesis (Wick et al. 2010; Kulvietis et al. 2011).

Yamashita et al. (Yamashita et al. 2011) examined the size-dependent placental transfer and toxicity of titanium dioxide and silicon dioxide nanoparticles of different sizes after I.V injection in pregnant mice. Smaller silicon dioxide (70 nm) and titanium dioxide (143 nm) nanoparticles caused fetal resorption and FGR, and the particles were observed in placental tissues and in the fetal liver and brain. The larger silicon dioxide particles (300nm and 1000nm) were not found in placental or fetal tissue, indicating

again that nanoparticle placental transfer is size dependent. The toxicity of the smaller silicon dioxide particles was also diminished on coating with carboxyl or amino groups.

Wick et al. (Wick et al. 2010) examined the transfer of polystyrene nanoparticles by the perfused human placenta, with diameters ranging from 50 nm to 500 nm. Smaller nanoparticles were transferred in greater quantities than larger nanoparticles, with the largest ones not being transferred at all. This shows that both the human and mouse placenta transfer nanoparticles in a size-dependent manner.

1.5.5 Liposome interaction with the placenta

There is a positive correlation between liposome size (10nm-1000nm) and their clearance from the circulation in non-pregnant rodents, meaning that larger liposomes are cleared more rapidly (Harashima & Kiwada 1996). However, there is a negative correlation between nanoparticle size and fetal drug transfer (R Bajoria & Contractor 1997), meaning that larger liposomes transfer a lower concentration of drug to the fetus. Therefore a compromise must be sort between liposome clearance and fetal drug exposure when targeting the placenta.

Tuzel Kox et al. (Tuzel Kox et al. 1995) demonstrated that the rat and rabbit placenta efficiently takes up liposomes of varying compositions from maternal plasma, and that accumulation depends on the size, charge and lipid composition. The group report that small negatively charged liposomes comprising soya phosphatidylcholine (a saturated phospholipid; SoyPC) accumulated in the placenta and uterus at the highest concentrations, compared with other compositions examined. They did not examine

placental-fetal transfer, but they did conclude that liposomes are not transferred to the fetus intact, but degrade and release their cargo within the placenta. These findings concur with observations made by Bajoria et al. (Rekha Bajoria et al. 1997) who state that intact liposomes do not cross the human placental barrier.

In several experiments, Bajoria et al. introduced liposomes of varying size, charge and lipid composition to the dual-perfused human placenta lobule (R Bajoria & Contractor 1997). They administered lecithin/cholesterol neutral liposomes of three different diameters (70 nm, 150 nm, 300 nm), each containing the hydrophilic fluorophore carboxyfluorescein (CFS). A negative correlation between the size of the liposomes and the placental transfer of CFS was observed (Figure 1.14).

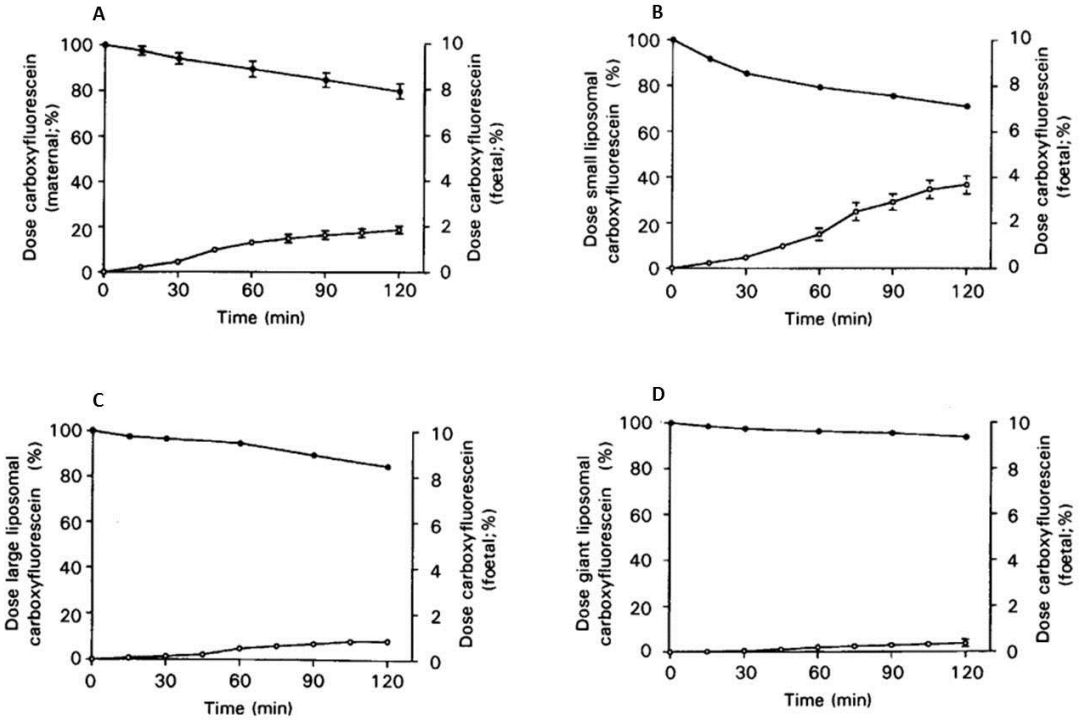

Figure 1.14: The effect of liposome size on transplacental transfer during 2 h of perfusion. Closed circles = maternal concentration, open circles = fetal concentration. A) free CFS, B) CFS from small liposomes, C) CFS from large liposomes, D) CFS from multilamellar liposomes. Reproduced from (R Bajoria & Contractor 1997).

Secondly the group examined how the surface charge of small liposomes affected their drug transfer by synthesizing neutral, anionic and cationic liposomes, again containing CFS, and introducing them to the perfused human placenta (R. Bajoria & Contractor 1997). CFS from the neutral and anionic liposomes passed rapidly into the fetal blood circulation; whereas, when cationic liposomes were used, CFS transfer was significantly decreased, due to either accumulation of cationic liposomes in the placenta or reduced placental uptake and transfer (Figure 1.15).

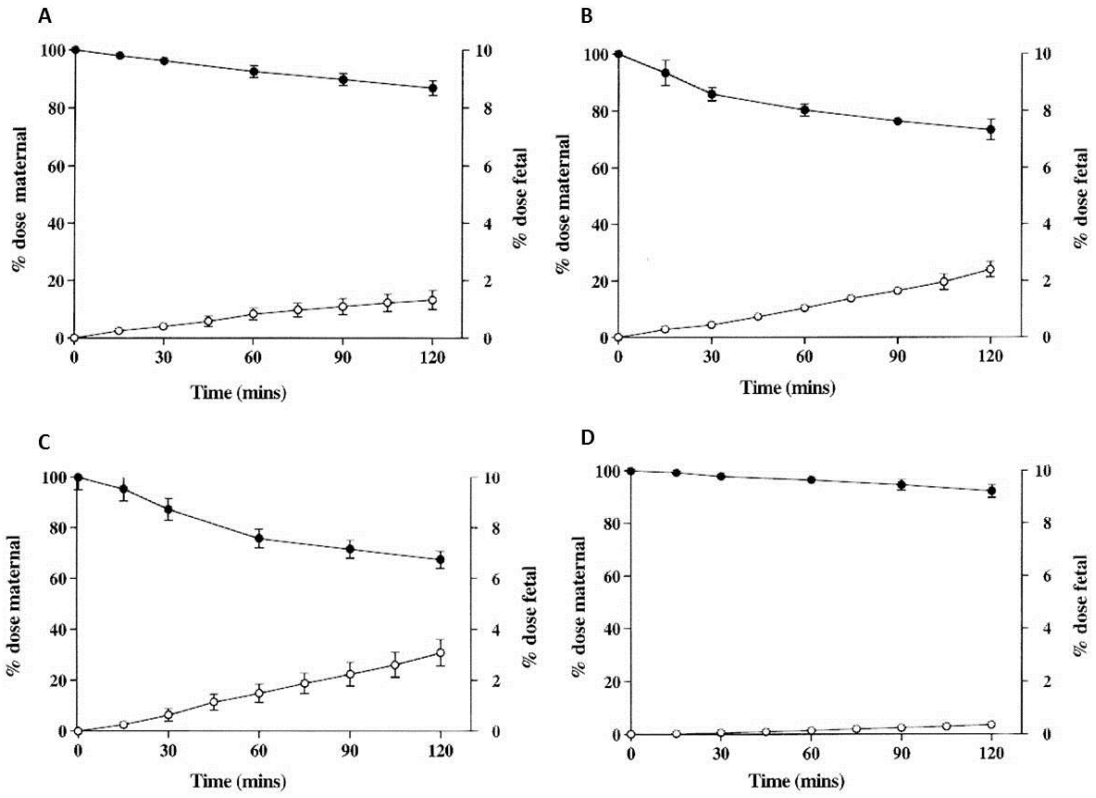

Figure 1.15: The effect of liposome surface charge on transplacental transfer liposomes during 2 h of perfusion. Closed circles = maternal concentration, open circles = fetal concentration. (A) free CFS, (B) CFS from neutral liposomes, (C) CFS from anionic (negative) liposomes, (D) CFS from cationic (positive) liposomes. Adapted from (R. Bajoria & Contractor 1997).

In contrast, Tuzel Kox et al. (Tuzel Kox et al. 1995) found that anionic liposomes accumulated more readily in the rat and rabbit placenta compared with cationic and neutral liposomes. However, in a second study by Bajoria et al. (R Bajoria et al. 1997), cultured term human trophoblast cells took up anionic liposomes more avidly than neutral or cationic liposomes. This suggests that in the previous experiment conducted by Bajoria et al. (R. Bajoria & Contractor 1997), less fetal CFS transfer was observed due to less accumulation of cationic liposomes.

Bajoria et al. also prepared ‘fluid liposomes’ made from unsaturated lecithin and ‘solid liposomes’ made from saturated distearoyl phosphatidylcholine, to examine the dependence of lipid composition on placental transfer of encapsulated thyroxine (Rekha Bajoria et al. 1997) and warfarin (Bajoria et al. 2013). They report that placental uptake and fetal transfer of thyroxine encapsulated by fluid liposomes was higher than that encapsulated by solid liposomes, suggesting, in this case, that fluid liposomes could be used to deliver thyroxine directly to the fetal circulation to treat the fetus in utero (Figure 1.16). The group report the same findings when examining warfarin transfer (Figure 1.17); fluid liposomes transferred a higher concentration of warfarin to the fetus when compared with solid liposomes. Therefore, liposomes made from saturated phospholipids appear to be more appropriate for encapsulation of drugs that require maternal or placental delivery, whereas liposomes made from unsaturated phospholipids are better to encapsulate drugs to be transferred to the fetus.

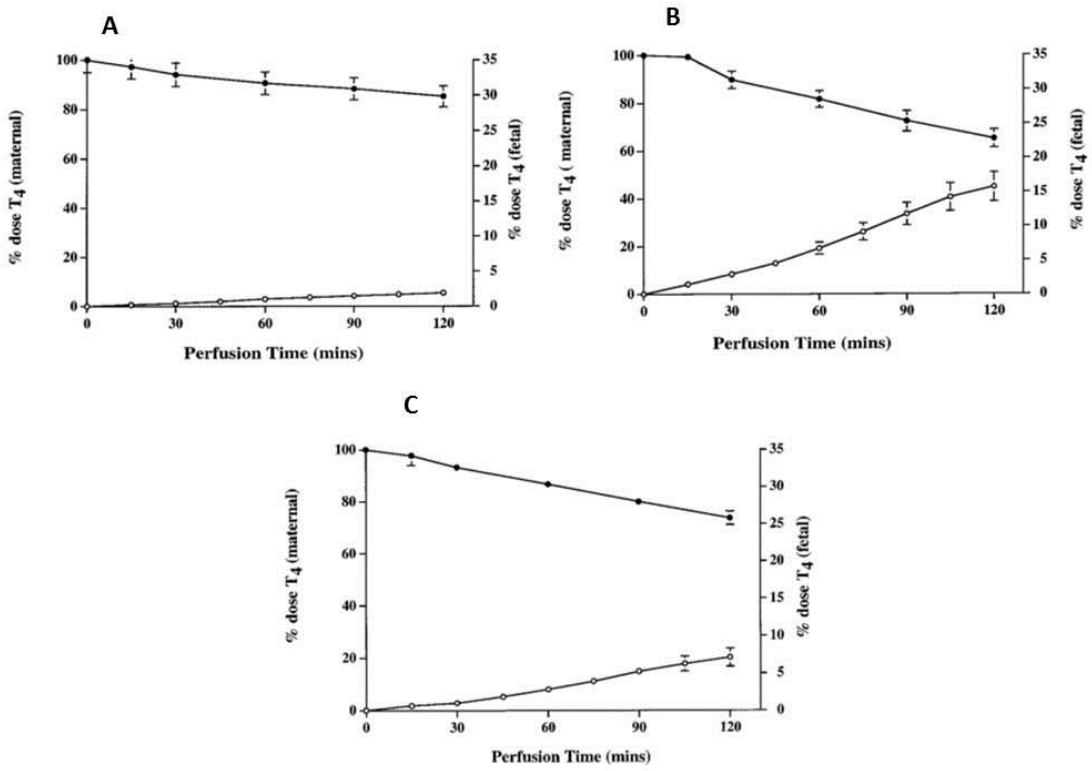

Figure 1.16: Materno-fetal thyroxine transfer is affected by liposome composition during 2 h of perfusion. Closed circles = maternal concentration, open circles = fetal concentration, A) free thyroxine, B) thyroxine from fluid liposomes (unsaturated phospholipids), C) thyroxine from solid liposomes (saturated phospholipids). Reproduced from (Rekha Bajoria et al. 1997).

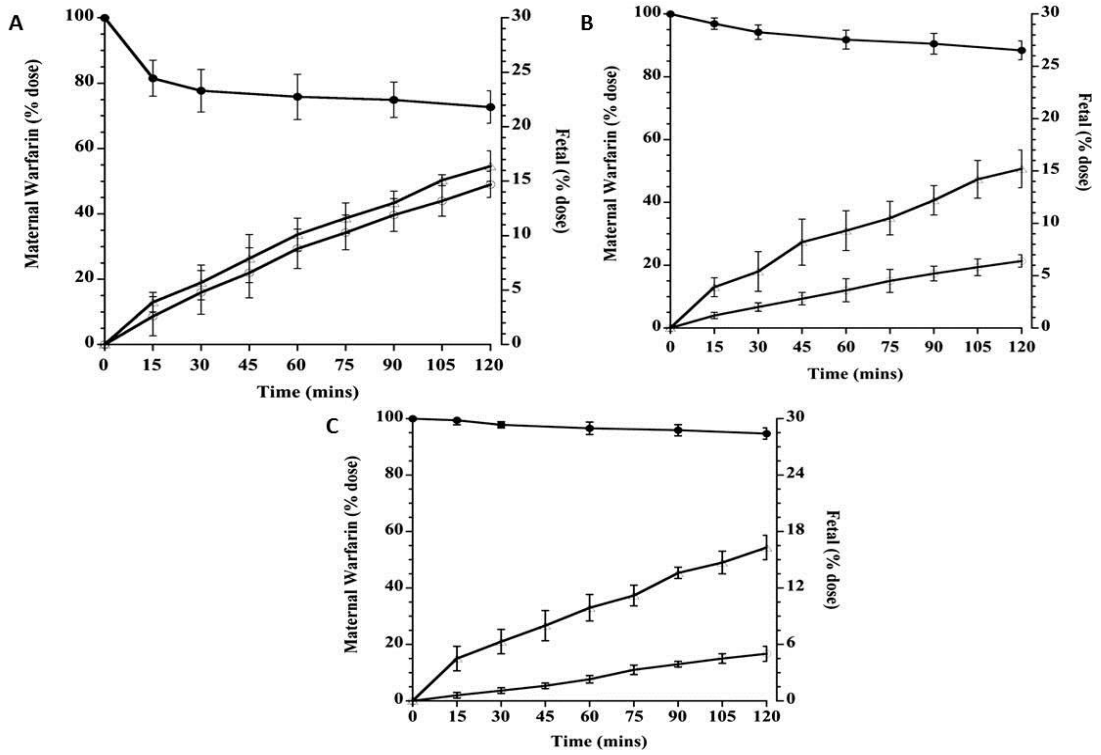

Figure 1.17: Materno-fetal warfarin transfer is affected by the liposome composition during 2h of perfusion. Closed circles = maternal concentration, open circles = fetal concentration, Triangles = fetal concentration of creatinine used as a control marker in all experiments. A) Free warfarin, B) warfarin from fluid liposomes (unsaturated phospholipids), C) warfarin from solid liposomes (saturated phospholipids). Reproduced from (Bajoria et al. 2013).

It is not known whether liposome transfer is governed by the cellular barrier structure (i.e. the intercellular pores present in the placental cell layers) or the charge of the placenta, or is due to the inherent properties of the nanoparticles (i.e. size, surface charge, surface coating, constituent lipids/metals); more likely, it is determined by a combination of all factors. To date, studies have been unable to specify a definitive nanoparticle size, charge or composition that does or does not cross the placenta. It must be noted that due to the differences between rodent and human placental structures (the rat placenta has a pore size of 10-20 nm, whereas the human placenta has a pore size of approximately 6 nm (Refuerzo et al. 2011)), it is difficult to draw comparisons between

species. It will be therefore necessary to make compromises when designing a suitable liposome for placental targeting.

1.5.5.1 Mechanisms of placental cellular uptake of liposomes

Most studies suggest that liposomes and their contents are internalized into cells either by endocytosis or by fusion between liposomal and cell membranes and that uptake is governed by size, charge, composition and surface coating. It is unknown how liposomes are internalised by placental cells. Bajoria et al. (R Bajoria et al. 1997) proposed that this requires an energy-dependent mechanism, possibly endocytosis. Pre-treatment of human primary term cytotrophoblast cells with sodium azide (an inhibitor of cellular respiration) or deoxyglucose (an inhibitor of glycogenolysis) did not alter uptake of cationic liposomes but significantly reduced uptake of anionic and neutral liposomes. The group concluded that endocytosis is predominantly responsible for the uptake of anionic and neutral liposomes.

Homing peptide-cellular interactions are receptor mediated and they undergo endocytosis by a unique mechanism, similar to micropinocytosis (Pang et al. 2014). Studies suggest that molecules conjugated to the homing peptide will be internalised into tumour cells along with the homing peptide (Sugahara et al. 2009), however this hasn’t been fully examined and it is unknown as to whether internalisation of the attached cargo is limited by its characteristics such as size or charge. It is likely that liposomes coated in homing peptides may be endocytosed by placental cells differently from non-decorated liposomes or free homing peptides and this will need to be examined further.

1.5.6 Nanoparticle clearance

Extended nanoparticle circulation is essential for most clinical applications, as such researchers are engineering nanoparticles to try to minimise immune system recognition and clearance. In order to treat placental dysfunction, it is most likely that nanoparticles will be administered systemically to pregnant women. It is therefore important to understand how other organs and the immune system may react to nanoparticle administration. There is some knowledge available, as certain nanoparticles such as liposomes have been studied extensively for cancer treatment. However, for obvious reasons, these treatments have not been trialled in pregnant women and it is not known whether pregnancy alters the way in which the body will react in response to nanoparticles. In the pregnant state there is down-regulation of T helper (Th) 1 cells, which produce the cytokines IFN-γ (interferon-γ) and IL-2 (interleukin-2), and up-regulation of Th2 cells, which produce IL-4 and IL-10 (interleukin-4 and -10) (Reinhard et al. 1998a). This is thought to occur to prevent maternal immune rejection of the semi-allogeneic fetus (Reinhard et al. 1998a). Jones et al. demonstrate that in mice an immune response governed by Th1 cells clear nanoparticles at a slower rate than that governed by Th2 cells (Jones et al. 2013). This finding suggests that nanoparticles may be cleared more rapidly from pregnant mice. There is also a worry that the introduction of a pathogen which activates a Th1 immune response may compromise the pregnancy (Reinhard et al. 1998b), something which will need investigating further.

Foreign bodies in the circulation, such as liposomes are rapidly cleared by the mononuclear phagocyte system (MPS). The MPS is mainly composed of phagocytes; monocytes, granulocytes and dendritic cells circulating in the blood, and macrophages

resident in tissues such as the liver (Kupffer cells) and spleen (red pulp macrophages) (Song et al. 2014). Proteins called opsonins attach themselves to the liposome surface (opsonisation), allowing them to be recognised by the MPS and phagocytosed (Ishida et al. 2002). Opsonic proteins include albumin, immunoglobulins, fibronectin and other extracellular matrix proteins, apolipoproteins, β2-glycoprotein-I and complement related proteins (Semple et al. 1998; Moghimi et al. 2001). The presence of these proteins also changes the size of the liposomes, disrupts their stability and may interfere with their surface coating and targeting ability. They may also cause aggregation which may mean that aggregates get trapped in the lungs, the first capillary bed encountered after I.V administration (Moghimi et al. 2012). Studies have correlated the circulation half-life of nanoparticles directly with their interaction with opsonin proteins (Chonn et al. 1992). To avoid clearance in this way, many liposome formulations include a PEG layer, which sterically hinders opsonisation, thus prolonging circulatory life (Allen et al. 1991).

Liposome administration may also activate the complement system. This is a network of over 30 circulating and bound proteins that act as the first line of defence (Ricklin et al. 2010). Not only is it responsible for clearing particulate materials, such as liposomes (Ishida et al. 2002), but it also can initiate adverse side effects including anaphylaxis and cardiopulmonary disturbances (Moghimi et al. 2012), thus its activation can be very dangerous. The addition of PEG to the surface of nanoparticles does not prevent complement activation completely. Andersen et al. (Andersen et al. 2013) reported that multi-walled carbon nanotubes coated in PEG of different molecular weights activated the complement system in human serum, and the level of activation did not depend on the molecular weight, but on the concentration of nanoparticles the serum was exposed

to. Unfortunately, there is significant variation in the complement system in humans, and even greater interspecies variation, making it difficult to draw comparisons (Moghimi et al. 2012). This is something that will need to be considered in further detail before human administration of liposomes.

The fate of liposomes depends on their size, surface charge, lipid composition and the concentration administered, but due to the differing placental structures between species, different experimental conditions and complement system variation, it is difficult to determine an exact liposome formulation that will circulate in the body without invoking a significant immune response and that will accumulate in the placenta without crossing it. A compromise must be sought when designing a liposome formulation and extensive experimental work must be carried out in both animals and humans. The perfused human placental lobule is a good model to use to monitor nanoparticle uptake, but cannot examine the off target side effects that may occur within the other organs of the mother or fetus. This means that pregnant mice are a better model to use, as they will allow us to examine the fetal transfer of liposomes, as well as the presence of detrimental side effects for the mother or fetus.

1.6 Mouse models of pregnancy

Due to ethical restrictions and experimental limitations, research on the human placenta is limited, so instead animal models are used (Georgiades et al. 2002). Mouse pregnancy is extensively studied due to its short gestational period and because mouse and human placentation share many common features (Carter 2007). Experimental mice are typically inbred, meaning they are a more homogeneous population to study

compared to humans, giving more uniform data and less variation. When studying mouse models of pregnancy complications, it is now commonplace to use the 5th centile of birth weight to define FGR, because of the increased degree of homogeneity compared with the human population (Dilworth et al. 2011). Mice can also be genetically modified to produce gene knockouts or knock-ins, which allows us to study disease pathologies in more detail. Table 1.4 gives a summary of the main comparisons between human and mouse placentation and pregnancy.

Feature	Mouse	Human	Reference
Gestation length	19 – 21 days	37 - 42 weeks	(1), (2)
Offspring number	4-12 fetuses	1-2 fetuses	(1)
Implantation time	4.5 days	6 days	(3), (4)
Trophoblast invasion	Shallow; limited to decidua	Extensive; decidua and myometrial vessels	(5)
Placental perfusion initiated	9.5 days	10-12 weeks	(6)
Placental exchange area	Labyrinth	Villous trees	(6)
Interhaemal barrier	Three trophoblast layers; outer one cellular, inner two syncytial	Single layer of syncytial trophoblast, underlying layer of cytotrophoblast	(7)
Junctional zone (spongiotrophoblast)	Extensive	Absent	(8)
Definitive placental structure formed	12.5 days	21 days	(6), (9)
Placental hormones	mPL, progesterone, estrogen	hCG, hPL, PlGH, IGFs, progesterone, estrogen	(10)

Table 1.4: Comparison of human and mouse placentation and pregnancy. mPL; mouse placental lactogen. Adapted from (Carter 2007), including references: (1) (Murray et al. 2010), (2) (Jukic et al. 2013), (3) (Otis & Brent 1954), (4) (Watson & Cross 2005), (5) (Malassiné et al. 2003), (6) (Georgiades et al. 2002), (7) (Yamashita et al. 2011), (8) (Carter 2007), (9) (Benirschke & Kaufmann 2000), (10) (Wang 2010).

1.6.1 Mouse placentation

In mice, fertilisation occurs at E0.5 post mating and by E3.5 the blastocyst has differentiated into the ICM and outer layers of trophoblast cells (Watson & Cross 2005). Implantation of the blastocyst into the maternal decidua takes place on E4.5, when placentation begins (Watson & Cross 2005). Several fertilised blastocysts implant into the bicornate uterus and it is common for a dam to carry 6-8 live pups, depending on the

strain. The mouse placenta is considered to be fully formed by E12.5 (Georgiades et al. 2002).

Figure 1.18 shows the human and the mouse placental structures at term and the placental barrier of the two species, as well as some of the main cell types (Rossant & Cross 2001). Once formed, both the mouse and human placenta comprises three distinct regions: the maternal facing surface, the fetal facing surface and a central exchange region, facilitating gaseous and nutrient exchange. In both models, the maternal facing surface abuts the decidua basalis, the myometrium, and the basal plate. The mouse placenta has a region adjacent to the decidua called the junctional zone, which contains mainly spongiotrophoblast and glycogen cells (John & Hemberger 2012) and is the main area of hormone secretion (Dilworth & Sibley 2012). The spongiotrophoblast is a source of placental prolactins and pregnancy specific glycoproteins that promote maintenance of the pregnancy and protect the fetus from the maternal immune system (John & Hemberger 2012). Without the junctional zone the pregnancy is unsuccessful (Guillemot et al. 1994).

In humans, the exchange region comprises several villous tree structures extending from the basal fetal surface, surrounded by maternal blood perfusing the intervillous blood space. In mice, this exchange region is called the labyrinth because of its folded maze-like structure. Like human placental villi, the labyrinth provides a large surface area for gaseous and nutrient exchange; maternal blood perfuses fetally-derived trophoblasts lining the maternal blood spaces with the maternal and fetal blood never coming into direct contact (Georgiades et al. 2002). The labyrinth becomes proportionally bigger towards the end of gestation to increase the surface area for diffusion (Coan et al. 2004).

The insets in Figure 1.18 show the placental barrier in both species. The human placental barrier consists of an outer layer of multinucleated syncytiotrophoblast in contact with maternal blood, with an underlying layer of proliferative cytotrophoblast (Yamashita et al. 2011). In mice, there are two layers of syncytiotrophoblast cells, the top one is in direct contact with fetally-derived endothelial cells (Yamashita et al. 2011). The third layer of the mouse placental barrier is made up of trophoblast giant cells and is directly exposed to maternal blood (John & Hemberger 2012). This layer of trophoblast giant cells is highly permeable to most solutes (Dilworth & Sibley 2012) and provides a local endocrine function that maintains the pregnancy (John & Hemberger 2012).

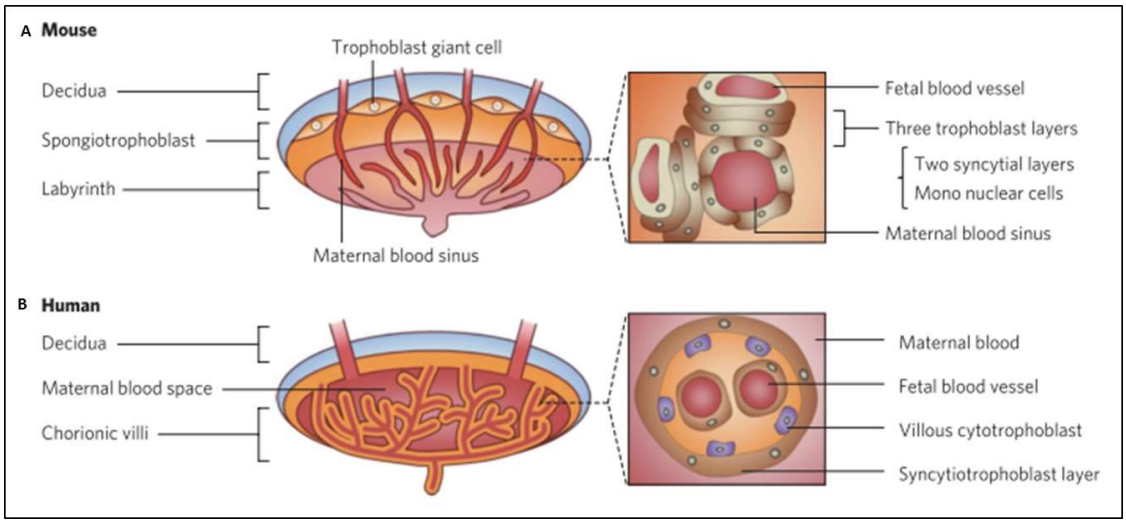

Figure 1.18: Schematic showing a comparison of (A) mouse and (B) human placental anatomy, with inserts showing the maternal-fetal placental interface. Inset (A) shows a cross section of the mouse placental labyrinth and inset (B) shows a cross section of a human placental villus. Reproduced from (Yamashita et al. 2011) .

1.6.2 Mouse placental perfusion

The mouse uterine structure is different when compared with the human uterus; the mouse uterus has two horns converging at the cervix, with each pup having its own

uterine cavity and placenta. Blood flow into the placentas is instigated at approximately E9.5, when glycogen trophoblasts possessing an invasive phenotype invade the mouse decidua and remodel the maternal arteries. Invasion starts later, is shallow compared with humans and does not extend into the myometrium. (Georgiades et al. 2002). Once blood flow is initiated, placentas are perfused in series by blood flowing in opposing directions from two main arteries, the uterine artery and the uterine branch of the ovarian artery. This means that not all fetuses in the horn receive the same access to nutrients, as the blood arriving at the second placenta will have had some of the nutrients removed as it passes through the first placenta (Figure 1.19) (Raz et al. 2012). Often smaller pups are observed in the middle of each horn, possibly due to this reduction in nutrient availability (Raz et al. 2012).

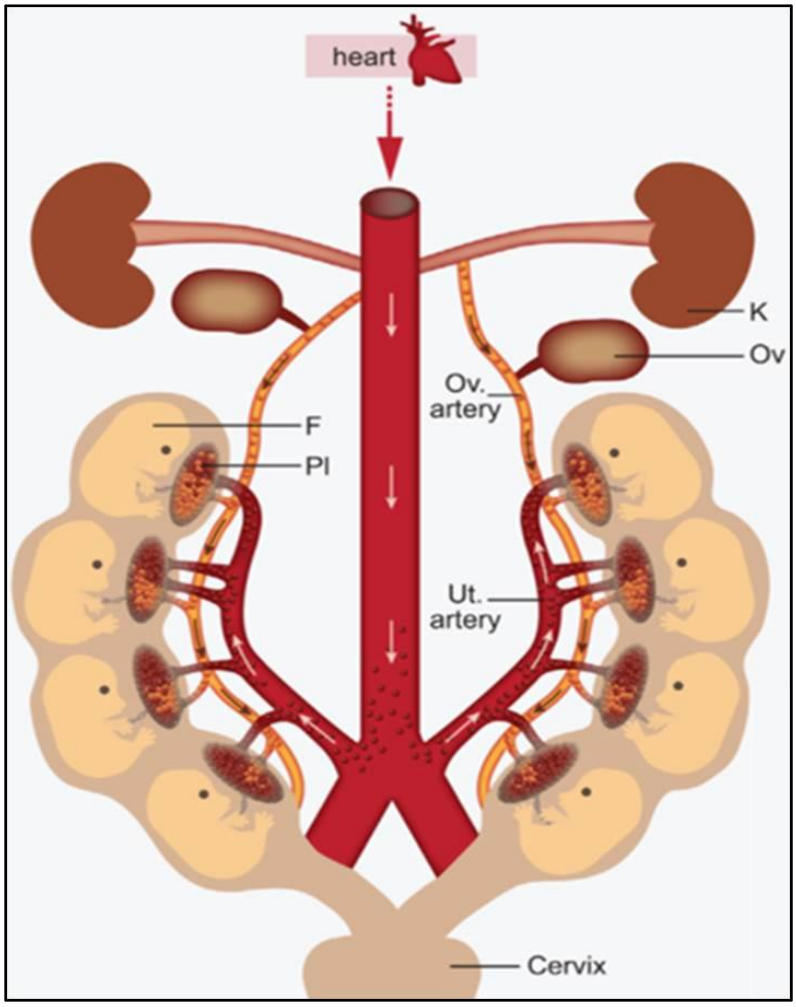

Figure 1.19: Schematic of a pregnant mouse uterus depicting two uterine horns and showing the direction of blood flow. Each placenta is perfused by two arteries; the uterine artery (Ut) and the ovarian artery (Ov), F; fetus, K; Kidney, Pl; placenta. Reproduced from (Raz et al. 2012).

1.6.3 Mouse placental endocrinology

There is a high level of conservation of genes and/or proteins expressed by the human and mouse placenta in analogous regions. Many of these genes, when knocked out, cause pregnancy pathologies similar to those observed in humans, making mice a good model to study (Cox et al. 2009).

Estrogen and progesterone play an important role in maintaining pregnancy in mice and humans (Nayak & Giudice 2003). In humans, these hormones are initially expressed by the corpus luteum and maintained by the expression of hCG from the blastocyst until the placenta takes over production later in gestation. In mice however, the corpus luteum secretes progesterone throughout gestation and this is regulated by twice-daily surges of prolactin and mPL, produced by the pituitary gland. This gland is not needed for the maintenance of pregnancy in humans. (Malassiné et al. 2003).

As in humans, the IGF axis plays an important role in mouse fetal and placental development; the IGFs, their receptors and binding proteins are all expressed by the mouse placenta throughout pregnancy (Sferruzzi-Perri et al. 2011). Figure 1.20 provides a comparison as to where IGF-I, -II and their receptors are expressed in mouse and human placentas (Nayak & Giudice 2003). IGF-II is produced by the spongiotrophoblasts in the junctional zone in early pregnancy, but later on the labyrinth takes over production (Nayak & Giudice 2003).

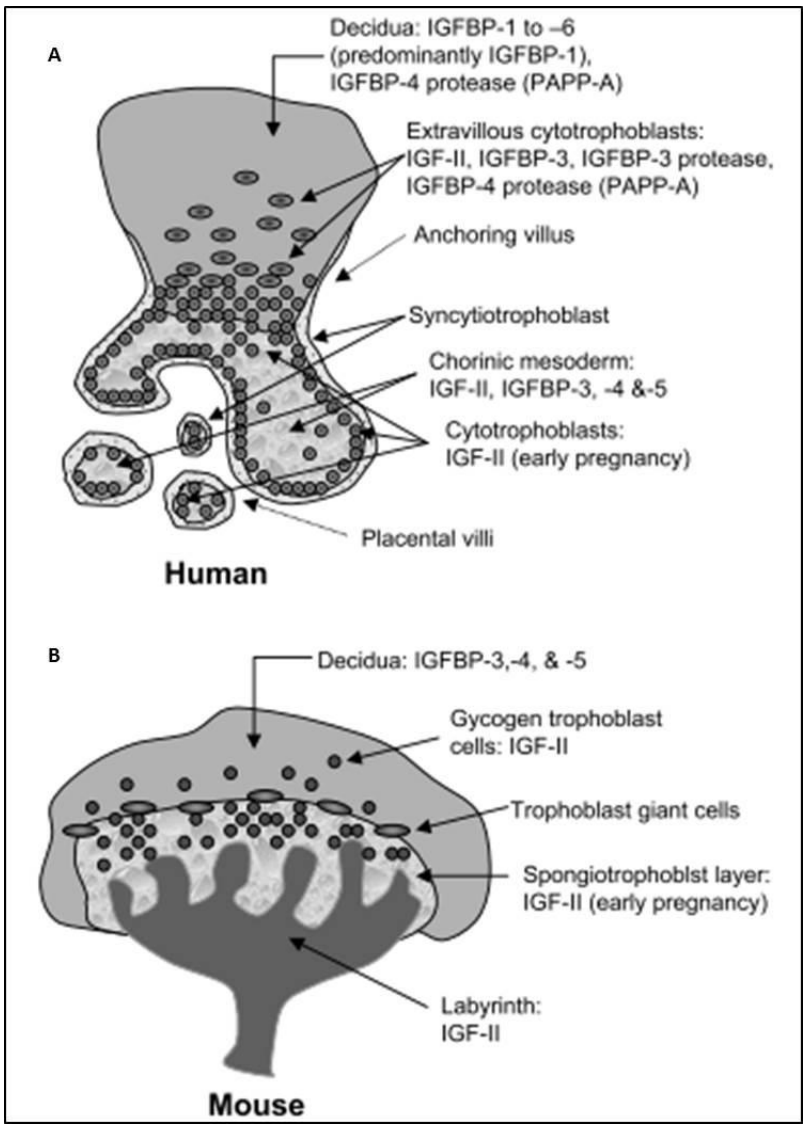

Figure 1.20: Schematic diagram showing the expression of IGF-II and its receptors in the (A) human and (B) mouse placenta in early and late gestation. The spongiotrophoblast found in the JZ of the mouse placenta and the homologous CT in the human placenta strongly express IGF-II in early pregnancy. The mouse placental labyrinth produces IGF-II throughout pregnancy. IGF-II is highly expressed by invading trophoblast cells, namely glycogen cells in the mouse and EVTs in the human placenta. Reproduced from (Nayak & Giudice 2003).

1.6.4 Mouse models of fetal growth restriction

There are several animal models that have been bred to represent aspects of human pregnancy pathologies, including the placental specific IGF-II knock out mouse model ($P0^{-/+}$) which produce mixed litters of healthy wild type (WT) and growth restricted

heterozygous pups (P0) and placentas (Constância et al. 2002), and the eNOS$^{-/-}$ mouse model which produce growth restricted offspring with an increased risk of limb abnormalities (Hefler et al. 2001).

1.6.4.1 Placental specific IGF-II transcript knock out mouse model (P0$^{-/+}$)

Insulin-like growth factor 2 (Igf2) is a paternally imprinted gene (DeChiara et al. 1991) that produces the IGF-II protein. The P0 promoter that codes for the IGF-II transcript (the P0 transcript) is found on mouse chromosome 7 (Coan et al. 2005) and specifically leads to expression of IGF-II in the placental labyrinth trophoblast. Constancia et al. (Constância et al. 2002) abolished this P0 transcript in vivo by deleting a 5-kilobase (kb) region spanning exon u2 of the P0 mRNA. In doing so, *Igf2* transcript activity was selectively reduced in the placental labyrinth, leading to the complete cessation of IGF-II expression in this region. Expression of other fetal and placental *Igf2* gene transcripts was not affected, thus fetal and maternal IGF-II concentrations were similar to WT animals, (Constância et al. 2002).

Fetal growth restriction in this mouse occurs late in gestation. At E12.5 the placentas from P0 fetuses are significantly smaller than the WT placentas, but the fetuses are comparable in size. There is evidence that these smaller placentas increase their nutrient transport capability to maintain the size of the fetus until E15.5. By this time, the mutant placentas can no longer compensate, and the pups become growth restricted. By term, P0 fetuses are 69% the weight of their WT littermates, and their placentas are 68% of the WT size. (Constância et al. 2002)

P0 mutant placentas are unable to transport nutrients and amino acids as effectively regardless of their smaller size. Fetal accumulation of ^{51}Chromium-ethylenediaminetetraacetic acid (^{51}Cr-EDTA; a solute used to measure placental diffusion capacity) per unit weight of placenta drops to 80% of WT levels by E16 and to 60% by E19. Conversely, accumulation of fetal ^{14}C-methyl- aminoisobutyric acid (^{14}C-MeAIB; a solute used to measure amino acid transport via system A) per gram of placenta, increases to 155% of WT by E16, but drops to 116% by E19, showing that the placenta initially tries to compensate for its small size, but is unable to maintain this adaptation. Even with this upregulation, given the small size of the placenta, the P0 fetuses actually receive 74% of the amino acids compared with their WT counterparts. (Constância et al. 2002). Sibley et al. (Sibley et al. 2004) state that this reduction in diffusion capacity of the P0 placentas is due to a smaller surface area for exchange, along with a thicker exchange barrier whereas, Kusinski et al. (Kusinski et al. 2011) report that the reduction in amino acid placental transport is due to a reduction in system A activity, rather than a defect in placental perfusion. However, a recent study has suggested there may be an underlying vascular defect that is also contributing to the phenotype. When P0 mice where administered with the vasodilator sildenafil citrate via drinking water, there was a reduction in the percentage of the smallest fetuses, showing that sildenafil citrate increased fetal growth (Dilworth et al. 2013). This suggests that the P0 mouse either has a previously undetected vascular defect, or that sildenafil citrate has therapeutic effects beyond vasodilation. As umbilical artery Doppler ultrasound did not detect changes in blood flow in treated animals, the latter is more likely to be true.

The P0 mouse shares a number of attributes with human FGR. For example, it is known that in human pregnancies complicated by FGR, fetuses usually have smaller placentas,

with a reduced capability for transporting amino acids, which can sometimes be attributed to an increased barrier thickness or decreased exchange surface area (Desforges & Sibley 2010; Sibley et al. 1997; Sibley et al. 2005). The P0 mouse model has a smaller placenta, with a thickened placental barrier that is unable to transport amino acids as effectively.

An IGF-II-total knock out mouse model also exists. In this mouse model, all four Igf2 transcripts (P0-3) are disrupted, leading to a complete IGF-II knock out in all fetal, maternal and placental tissues. This produces a FGR phenotype, with mutant fetuses 83% of the weight of WT littermates (Murrell et al. 2001). This model is not characterised as thoroughly as the P0 mouse model, and as its deletions are universal, one would conclude that it would have a number of systemic abnormalities rather than those associated solely with placental development and fetal growth. The FGR is less severe with this model too, making the P0 model more favourable to use to develop novel treatments.

1.7 Summary of the literature

Adequate placental function is vital for a successful pregnancy. When the placenta does not function correctly, serious fetal complications can ensue including FGR. There are several therapeutics available that improve placental function in animal models, but to avoid detrimental off-target effects and make them acceptable for administration to humans they need to be delivered selectively to the placenta. In recent years, homing peptides have been identified that bind exclusively to specific surface components of the human and mouse placenta. This project aimed to design a suitable nanoparticle that can

simultaneously incorporate a homing peptide on its surface and encapsulate a range of therapeutics, to allow for the targeted delivery of drugs to the placenta as a possible treatment for FGR. After a careful consideration of the literature, liposomes were chosen as nanoparticles suitable for placental delivery due to their biocompatibility and the fact that previous research has already been conducted into how the placenta processes liposomes. The growth factors IGF-I and IGF-II were selected as candidate therapeutics to target to the placenta as they are crucial for adequate fetal and placental growth and because their receptors are expressed ubiquitously off-target effects could occur if they were administered systemically. Initial studies were conducted in the C57 mouse. The P0 mouse model was selected as a well-characterised model of FGR in which to conduct further treatment studies.

1.8 Aims and objectives of the project

It was hypothesized that targeted placental treatment using homing-peptide decorated nanoparticles would provide a novel treatment route for FGR. To test this hypothesis, the following objectives were put in place:

1. Undertake out an extensive literature review to design and prepared liposomes decorated with the placental homing peptides iRGD and CGKRK. Once prepared, fully characterise these liposomes using dynamic light scattering and laser Doppler micro-electrophoresis.
2. Test the ability homing-peptide decorated liposomes to bind to human placental tissue and release an encapsulated fluorescent cargo, by incubating

term and first trimester explants with fluorescently tagged liposomes and visualising their uptake and drug release using fluorescence microscopy.

3. Test the ability of homing-peptide decorated liposomes to selectively target the murine placenta in vivo. To do this by administering different liposome compositions to pregnant C57 mice at different gestational ages and examine liposome uptake by fluorescence microscopy of the fixed placentas. Along side this, examine off-target accumulation by collecting the main maternal organs and fetal tissues.
4. Investigate techniques to allow for the liposomal encapsulation of IGF-I or IGF-II and quantify the encapsulation efficiency by measuring the IGF-II concentration in the aqueous core and lipid bilayer using an IGF-II ELISA.
5. Examine whether delivery of IGF-I or IGF-II in homing peptide-bearing liposomes:
    a. creates an acceptable therapeutic formulation compatible with maintenance of pregnancy in wild-type mice, ensuring that they do not detrimentally affect litter size, resorption rate, maternal weight gain or behaviour.
    b. can increase fetal and/or placental growth in wild-type mice at E18.5 when delivered throughout later gestation.
    c. can increase fetal and/or placental growth in the P0 mouse model of FGR at E18.5 when delivered throughout later gestation.
    d. elicits any overt off-target side effects in either model by examining maternal organ weight and cell proliferation.

Chapter 2: Methods

2.1 Liposome preparation and characterisation

2.1.1 Liposome preparation

Liposomes were prepared by the thin lipid film extrusion process using a similar lipid composition and preparation method to that used by Nallamothu et al. and Zhang et al. (Nallamothu et al. 2006; Zhang et al. 2010). The constituent lipids were:1,2-distearoyl-sn-glycero-3-phosphocholine (DSPC); 1,2-distearoyl-sn-glycero-3-phosphoethanolamine-N-[amino(polyethylene glycol)-2000] (ammonium salt) (DSPE-PEG); 1,2-distearoyl-sn-glycero-3-phosphoethanolamine-N-[maleimide(polyethylene glycol)-2000] ammonium salt (DSPE-PEG-maleimide), Avanti Polar Lipids, Inc. Instruchemie B. V., The Netherlands); and cholesterol (purity ≥ 99 %, Sigma Aldrich, UK). All liposome compositions could be modified to contain the fluorescent lipid 1,2-distearoyl-sn-glycero-3-phosphoethanolamine-N-(7-nitro-2-1,3-benzoxadiazol-4-yl ammonium salt (NBD-DSPE (0.5 µM;)) to allow for tracking. See Table 2.1 for liposome compositions and Figure 2.1 for lipid structures used.

Liposome	Composition
iRGD-liposomes	DSPC (32.5mM), Cholesterol (15mM), DSPE-PEG (1.875mM), DSPE-PEG-maleimide (0.625mM), Rh-iRGD peptide (0.625mM)
CGKRK-liposomes	DSPC (32.5mM), Cholesterol (15mM), DSPE-PEG (1.875mM), DSPE-PEG-maleimide (0.625mM), TAMRA-CGKRK peptide (0.625mM)
ARA-liposomes	DSPC (32.5mM), Cholesterol (15mM), DSPE-PEG (1.875mM), DSPE-PEG-maleimide (0.625mM), TAMRA-ARA peptide (0.625mM)
Non-coated liposomes	DSPC (32.5mM), Cholesterol (15mM), DSPE-PEG (2.5mM)
iRGD/CFS-liposomes	DSPC (32.5mM), Cholesterol (15mM), DSPE-PEG (1.875mM), DSPE-PEG-maleimide (0.625mM), Rh-iRGD peptide (0.625mM), CFS (2.5mM)
CGKRK/CFS-liposomes	DSPC (32.5mM), Cholesterol (15mM), DSPE-PEG (1.875mM), DSPE-PEG-maleimide (0.625mM), TAMRA-CGKRK peptide (0.625mM), CFS (2.5mM)
ARA/CFS-liposomes	DSPC (32.5mM), Cholesterol (15mM), DSPE-PEG (1.875mM), DSPE-PEG-maleimide (0.625mM), TAMRA-ARA peptide (0.625mM), CFS (2.5mM)
iRGD/IGF-I or IGF-II liposomes	DSPC (32.5mM), Cholesterol (15mM), DSPE-PEG (1.875mM), DSPE-PEG-maleimide (0.625mM), Rh-iRGD peptide (0.625mM), IGF-I or IGF-II (40mM)
ARA/IGF-I or IGF-II liposomes	DSPC (32.5mM), Cholesterol (15mM), DSPE-PEG (1.875mM), DSPE-PEG-maleimide (0.625mM), TAMRA-ARA peptide (0.625mM), IGF-I or IGF-II (40mM)
Non-coated/IGF-I or IGF-II liposomes	DSPC (32.5mM), Cholesterol (15mM), DSPE-PEG (2.5mM), IGF-I or IGF-II (40mM)

Table 2.1: Liposome composition for all formulations prepared.

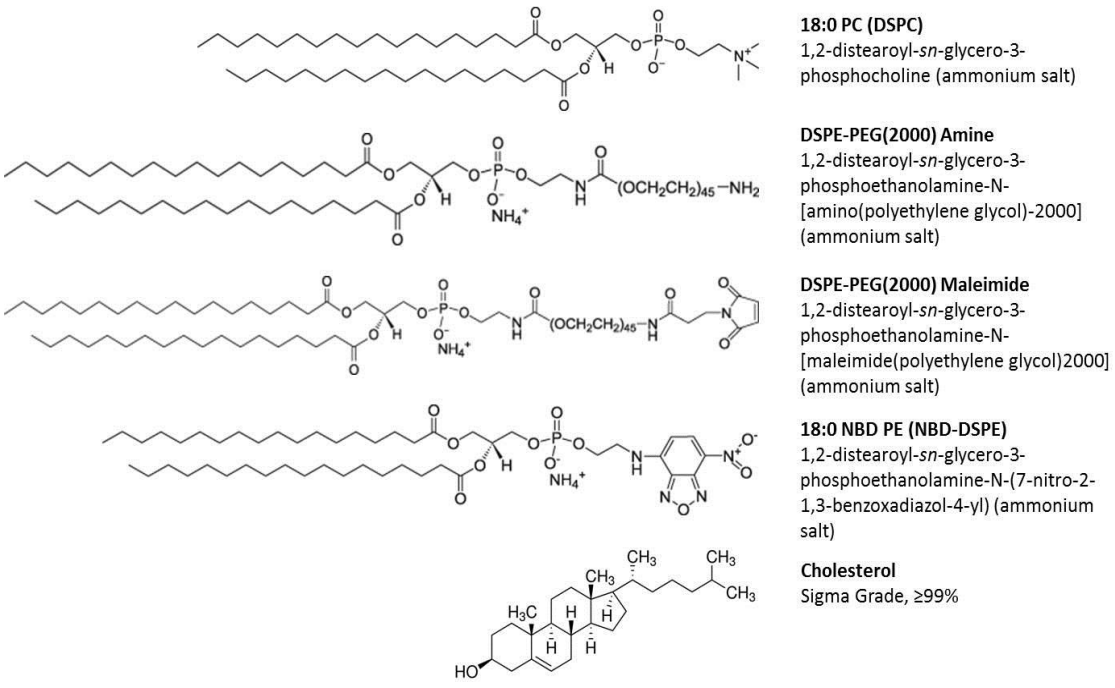

Figure 2.1: Chemical structure of the lipids used to prepare liposomes.

Pre-weighed lipids were dissolved in 10 ml chloroform (CHROMASOLV®, HPLC grade, purity ≥ 99.8 %, Sigma Aldrich, UK) in a 50 ml round bottomed flask. Chloroform was removed by rotary evaporation (40 ˚C; 270 mbar, 20 min) to form a lipid film that was kept in a vacuum oven (Brucker, UK) overnight at room temperature. The film was rehydrated in 1 ml sterile PBS to create unloaded liposomes, or sterile PBS containing 5(6)-carboxyfluorescein (CFS, 2.5 mM, Sigma Aldrich, UK; reconstituted first in 0.1 % (vol/vol) DMSO in PBS) or IGF-I or IGF-II (40 µM; human IGF-I / -II media grade; GroPep Biotechnology, Australia; IGF-I or IGF-II was reconstituted first in 10 mM HCl, 1 mg/ml). The resulting suspension was heated to 45 ˚C (Hybaid, VWR, UK) for 2 h, vortexed (10 min) and extruded through a 1 ml thermobarrel Mini-Extruder (syringes sterilized with 100 % ethanol and pre-wet with sterile PBS before use; 100 nm pore size polycarbonate membranes, Avanti Polar Lipids, Inc., Instruchemie B. V., The Netherlands) 11 times to produce a monodisperse liposome preparation, either unloaded or encapsulating CFS, IGF-I or IGF-II.

To synthesise targeted liposomes, peptides bearing an N-terminal cysteine moiety (TAMRA-CGGGCCGKRK (TAMRA-CGKRK); Rhodamine-CCRGDKGPDC (Rh-iRGD); Insight Biotechnology; dissolved first in 1 mg/ml 95 % vol. PBS: 5% vol. DMSO, and stored at -20 ˚C) were incubated at room temperature with liposomes immediately after synthesis for a minimum of 4 h, with occasional gentle agitation to facilitate conjugation of free thiol groups on the cysteine residues to maleimide groups on the liposomal surface via a Michael-type addition reaction. The non-targeting peptide sequence TAMRA-ARALPSQRSRC (TAMRA-ARA; Insight Biotechnology, UK) was conjugated to the liposome surface in a similar manner to produce control liposomes. Due to the chemical peptide structure, the manufacturer advised the use of two different

fluorophores (TAMRA and rhodamine), but as the fluorophores are a similar molecular weight and are attached to amino acids distal to the targeting region, they should not differentially affect the binding properties of the peptides.

To remove unbound peptide or unencapsulated CFS, liposomes were dialysed against sterile PBS (8 X 500 ml; 24 h) in Slide-A-Lyzer dialysis cassettes with a molecular weight cut off (MWCO) of 3.5 kDa (ThermoFisher Scientific, UK). To remove unencapsulated IGF-I or IGF-II from the preparations, liposomes were dialysed in cassettes with a 10 kDa MWCO. The liposome suspensions were adjusted to pH 7.4 by addition of 1 mM sodium hydroxide (NaOH) or hydrochloric acid (HCl) and stored at 4 ˚C for use within 1 month of preparation.

2.1.2 Size distribution (SD), polydispersity index (PDI), zeta potential (ZP) and stability

The size (hydrodynamic diameter) distribution (SD), the polydispersity index (PDI), and the zeta potential (ZP) of the liposome suspensions were measured by dynamic light scattering (DLS) or laser Doppler micro-electrophoresis (LDE) respectively in PBS at 25 ˚C at a scattering angle of 173 ˚ (Zetasizer Nano ZS, Model ZEN3600, fitted with a 632 nm laser, Malvern Instruments Ltd., UK). To measure SD and PDI, 50 µl of liposome suspension at the prepared concentration was loaded into a disposable semi-micro cell (Model ZEN0040, Malvern Instruments Ltd., UK), the measurement was taken and the Mark Houwink parameter was applied. The ZP was measured by loading 500 µl at the prepared concentration into a disposable folded capillary cell (Model DTS1070, Malvern Instruments Ltd., UK) and the Smoluchowski model was applied to

the measurement. The pH of all suspensions was maintained at 7.4. To ensure that the liposomes were stable and did not flocculate or degrade, the SD and PDI was measured weekly for 4 weeks. Measurements were repeated three times per formulation for a minimum of three independent samples where possible.

2.1.3 Quantification of peptide attachment to liposome surface

Free thiol groups on the N-terminus of the homing peptides iRGD and CGKRK are necessary for peptide-liposome conjugation. To identify the concentration of free thiol groups present, an Ellman's reagent test was conducted. Ellman's reagent (5,5'-dithio-bis-(2-nitrobenzoic acid); (DTNB); Sigma Aldrich, UK) changes colour in the presence of free thiol groups stoichiometrically, so can be used to quantify the concentration of peptides that contain free thiol groups. A standard curve was plotted by carrying out serial dilution of glutathione (GSH; 250 µl in 1 X PBS), a peptide containing a known concentration of free thiol groups (≥ 99.0 %, Sigma Aldrich, UK), with the addition of DTNB (50 µl; concentration matched in 1 X TRIS buffer; 15 min incubation). The absorbance at 412 nm (FLUOstar Omega, BMG Labtech, UK) of two different concentrations of fluorescently tagged homing peptides FAM-iRGD and FAM-CGKRK (250 µl; 50 µM and 100 µM) was measured with and without the addition of DTNB (50 µl; concentration matched in 1 X TRIS buffer; 15 min incubation). After correcting for background, the final absorbance for each sample was then compared with the GSH calibration curve to obtain the thiol concentration for each peptide.

To measure the amount of peptide attached to the liposomal surface, a dialysis was performed to remove unbound peptide from the liposome suspension (8 X 500 ml fresh

PBS) after 4 h of conjugation. Free peptide collected in the dialysate at each time point was quantified fluorescently using spectrophotometry (544/590 nm; 200 µl of sample/well of a 96 well plate; 3 sample repeats, 3 repeats/well; FLUOstar Omega, BMG Labtech, UK). A standard curve was produced by serial dilution of the peptides in PBS, starting at the initial amount of peptide added to the liposomes (0.625 mM), to determine the absolute amount of peptide in each dialysate sample. The amount measured in each dialysate sample from each time point was added together and the total was subtracted from the amount of peptide initially added to the liposome suspensions. By calculating the difference between the initial amount added to the suspension and the concentration of peptide removed by dialysis, the amount of peptide covalently coupled to the liposome surface was calculated.

2.1.4 Quantification of drug encapsulation

To quantify IGF-II encapsulation, the lipid bilayer of the liposomes was disrupted to release the growth factor from the aqueous core (Partearroyo et al. 1992)(Sila et al. 1986). 100 µl of each liposome suspension (iRGD/IGF-II, ARA/IGF-II, non-coated/IGF-II, non-coated empty liposomes) was incubated with 200 µl Triton™ X-100 (0.5 % in dH_2O; Sigma Aldrich, UK) at 37 ˚C for 20 mins, followed by sonication (30 min; max frequency; Ultrawave Ltd., UK) and centrifugation (1 h; 13,000 rpm; Heraeus Pico 21, ThermoScientific, UK). The supernatant was carefully removed and the concentration of free IGF-II in the supernatant and the concentration of bound IGF-II in the lipid pellet were quantified using a human IGF-II ELISA detection kit, according to the manufacturer's instructions (Mediagnostics, Germany). The kit provided a 96 well plate pre-coated with anti-human IGF-II antibody, sample diluent

(SDil), wash buffer (WB), antibody conjugate (ACon; containing biotinylated anti-IGF-II antibody), enzyme conjugate (EC; containing horseradish-peroxidase conjugated to streptavidin), substrate solution (Sub; containing horseradish-peroxidase substrate) and stop solution (SS; 0.2 M sulphuric acid), as well as IGF-II standards at the following concentrations in SDil: 0.45 ng/ml, 1.5 ng/ml, 3 ng/ml, 5.63 ng/ml, 9 ng/ml. ACon (50 µl/well) was first added to the 96 well plate provided before samples were added. Samples (supernatant and pellet) were diluted 1:100 in SDil and added to the plate (50 µl/well, triplicate). Standards were also added to the plate (50 µl/well, triplicate). The plate was covered and incubated with agitation (350 rpm) for 2 h at room temperature, before washing five times with the WB (300 µl/well). After the last wash, EC was added (100 µl/well), the plate was covered and incubated with agitation (350 rpm) for a further 30 min at room temperature. The wells were washed as previously described, before adding Sub (100 µl/well) and incubating in the dark for 30 min at room temperature. After 30 min the reaction was stopped by the addition of SS (100 µl/well) and the absorbance of each well was measured at 450 nm within 30 mins. The absolute concentration of IGF-II was calculated using the standard curve produced. The concentrations of IGF-II in the supernatant and the pellet were added together to calculate the total amount of drug (free and bound) administered in each liposome bolus.

2.2 Human tissue collection and culture

First trimester placenta (5-12 weeks of gestation) was collected following surgical or medical termination of pregnancy. Term placenta (37-42 weeks of gestation) was obtained from uncomplicated pregnancies in women with a body mass index (BMI)

between 18 and 25 within 30 min of vaginal or Caesarean delivery. Written informed consent was obtained from all patients and the tissue was stored in accordance with the following North West Local Research Ethical Committee approval codes: 13/NW/0205, 08/H1010/28 (1st trimester tissue), 08/H1010/55, 08/H1010/55 (+5), 12/NW/0574 and 12/NW/0609 (term tissue).

Villous placental tissue was randomly sampled, and biopsies were washed in serum free culture medium (1:1 ratio of DMEM and Ham's F12 media (Lonza Biosciences) containing glutamine (2 mM), penicillin (100 IU/ml) and streptomycin (100 µg/ml)) and dissected into 3 mm^3 explants under sterile conditions. Explants (1/well) were submerged in 1 ml of serum containing culture medium (as above, but with the addition of 10 % (vol/vol) fetal bovine serum (FBS; Invitrogen)), in 24 well culture plates pre–coated with agarose (1 % (wt/vol) in serum-free culture medium; Sigma Aldrich). Explants were maintained in 20 % O_2, 5 % CO_2 at 37 ˚C for up to 72 h.

2.2.1 Liposome binding assay

Term or first trimester explants were incubated with either non-targeted or targeted unloaded liposomes, or non-targeted or targeted liposomes containing CFS (100 µl / well) for several time points (1, 3, 6, 24, 48, 72 h) and cultured at 20 % O_2, 5 % CO_2 at 37 ˚C in the dark. They were washed in PBS (5 ml, 1 X 5 min), fixed in neutral buffered formalin (NBF; 5 ml, 10 % (vol / vol); pH 7.4; overnight) and embedded in optimal cutting temperature compound (OCT, Cryomatrix, ThermoScientific, UK). Tissue sections were cut (10 µm; CM1850, Leica, UK), fixed on coated slides (poly-L-lysine, 0.1 % (wt / vol) in H_2O; Sigma Aldrich, UK) with paraformaldehyde (PFA; 4 % (wt /

vol; 15 min), washed (PBS; 2 X 5 min), dried and mounted in mounting medium containing DAPI (4′,6-diamidino-2-phenylindole; Vectashield; Vector Laboratories, UK) and examined using a fluorescence microscope (x40 objective; Zeiss Observer Z1, Axiovision, UK). Images were captured at the same exposure (DAPI (blue) = 10-15 ms, peptide (Rh or TAMRA; red) = 1-3 ms, CFS (green) = 1-3 ms) for each channel, using PBS treated tissue to set the exposure, so that comparisons across samples could be made. N = 3 placentas, n = 3 biopsies from each placenta, 5-10 images from each sample were captured and representative images are displayed.

2.3 Animal housing and husbandry

2.3.1 General husbandry

All procedures were performed in accordance with the UK Animals (Scientific Procedures) Act (ASPA) of 1986 at The University of Manchester, under Home Office project licences awarded to Professor Colin Sibley (PPL number 40/3385) and Dr Mark Dilworth (PPL number 70/8504). Mice were housed with no more than 6 animals per cage and were maintained on a 12:12 h light-dark cycle at 21-23 ˚C and 65 % humidity. Animals had free access to food (Beekay Rat and Mouse Diet; Bantin & Kingman; Hull, UK) and water. Females aged 9-16 weeks were mated with a stud male and the presence of a copulation plug after was denoted as E0.5, with term in both mouse strains being E19.5. Females were weighed after mating and again at E11.5 to identify pregnancy by weight gain, before commencement of treatment. Treated females were weighed daily thereafter to confirm normal maternal weight gain and ensure that the treatment was not detrimental to the pregnancy.

Females were euthanized by either cervical dislocation or cardiac perfusion at different gestational time points depending on the experimental requirements. Cardiac perfusion is a well-recognised technique for exsanguination (Gage et al. 2012) and removes any unbound peptide or liposomes from tissues. After euthanasia, a surgical laparotomy was performed to expose the uterine horn and the position of the fetuses in the horn was noted. The horn was removed and placed on ice for 5-10 min to euthanize the fetuses. Thereafter, the horn was carefully dissected and individual placental and fetal weights were recorded; placentas were carefully stripped of all membranes and both placentas and fetuses were blotted to remove excess liquid before weighing. Maternal heart, kidneys, spleen, liver, lungs and brain were dissected free from surrounding tissue, blotted and weighed. For kidneys, the average weight of both kidneys was used in analyses. Placentas, fetuses and maternal organs were either fixed (NBF; 50 ml, 10 % (vol/vol); pH 7.4; overnight before being transferred to PBS for storage), snap frozen by immediate immersion in liquid nitrogen, or placed in RNAlater (Life Technologies; RNAlater removed after 24 h and sample stored at -80 ˚C).

After cervical dislocation, maternal and fetal trunk bloods were collected post-decapitation into heparinized centrifuge tubes, centrifuged (15,000 rpm; 5 min) and the serum supernatant was carefully removed and stored at -80 ˚C until use. Where cardiac perfusion was performed, bloods could not be collected.

2.3.2 Cardiac perfusion

To remove blood containing unbound peptide or liposomes from all mouse tissues, terminal cardiac perfusion was performed. Under general anaesthesia (isoflurane:0_2 mixture, adjusted to maintain an unconscious state) incisions were made to expose the heart. The superior vena cava was cut and PBS was perfused directly into the left ventricle with PBS pressure maintained by a vertical potential. PBS perfusion was continued until the liver and lungs became pale in colour (approximately 10 ml; 5 min) and cessation of life was confirmed. Tissues were collected, processed and stored as described previously.

2.3.3 C57 wild type mouse

The C57 mouse is the most commonly used laboratory wild type mouse due to its short gestational length, its ease of breeding and its genetic robustness. It is also the background strain of the genetically modified P0 mouse, used later in this study.

2.3.4 P0 mouse model

The P0 mouse lacks the placental-specific P0 Igf2 transcript and is derived from the C57 background strain. Males heterozygous for the deletion of the P0 transcript (Igf2 $P0^{+/-}$ (mutant; P0) were mated with 9-16 week old WT females (Igf2 $P0^{+/+}$ (wild type; WT)). Fetal genotyping was conducted retrospectively using fetal tail tips; fetuses were either WT or P0 mutants. Ear-notch tissue was used to determine the genotype of adolescent/adult mice after 4 weeks of age.

2.3.5 Genomic DNA extraction

Genomic DNA was extracted using a DNeasy extraction kit, according to the manufacturer's instructions (Qiagen, UK). The kit contained proteinase K solution to lyse the tissue samples, as well as buffer ATL, buffer AL, wash buffers 1 and 2 and an elution buffer. Briefly, tissue was incubated with buffer ATL (180 µl) and proteinase K (20 µl) overnight at 55 ˚C (Hybaid, VWR, UK). Samples were then vortexed and centrifuged (13,000 rpm; 1 min) and 120 µl of the supernatant transferred to a clean eppendorf tube. Buffer AL was mixed with ethanol (1:1 (vol/vol); 400ul final volume) and added to the supernatant, vortexed, and transferred to a clean DNeasy mini column sitting in a 2 ml collection tube. The sample was centrifuged (8,000 rpm; 1 min) and the flow through discarded. After addition of wash buffer 1 (500 µl), the sample was centrifuged (13,000 rpm, 1 min) and the flow through discarded. The DNeasy mini column was then transferred to a new 2 ml collection tube and wash buffer 2 (500 µl) was added. The DNeasy mini column was then centrifuged (13,000 rpm; 3 min) and the collection tube discarded. The DNeasy mini column was placed in a clean eppendorf tube with elution buffer; (200 µl) and incubated (25 ˚C; 1 min). The eppendorf tube containing the DNeasy mini column was centrifuged (8,000 rpm; 1 min) to elute the extracted genomic DNA. This was stored at -20 ˚C for no longer than 12 weeks before polymerase chain reaction (PCR) was performed.

2.3.6 Polymerase chain reaction (PCR)

Genomic DNA was amplified using Expand High Fidelity PCR reagents (Table 2.2; Roche, UK) and the Techne Prime thermal cycler (Bibby Scientific, UK). A tri-primer

system was used to amplify the 495-base pair (bp) WT fragment and a 740-bp fragment from the 5-kb deletion site (P0 deletion). The primer sequences were as follows:

d-F primer: 5'-TCCTGTACCTCCTAACTACCAC-3'

d-R primer: 5'-GAGCCAGAAGCAAACT-3'

WT primer: 5'-CAATCTGCTCCTGCCTG-3'

Reagent	Volume added (µl)	Final concentration
10 X PCR buffer	2	20 mM Tris-HCl, pH 8.4, 50 mM KCl
2mM dNTPs	2	200 µM
25 mM $MgCl_2$	1.6	2 mM
5 µM d-F primer	1.2	300 nM
5 µM d-R primer	1.2	300 nM
5 µM WT primer	1.2	300 nM
Taq DNA polymerase	1	5 U/µl
gDNA	2	2 µl
PCR H_2O	8.5	Final volume 20 µl

Table 2.2: Polymerase chain reaction reagents.

After the addition of the PCR reagents, the samples were taken through the following steps by the thermal cycler: 1) 4 min at 94 ˚C, 2) 1 min at 94 ˚C, 3) 1 min at 56 ˚C, 4) 1 min at 72 ˚C. Steps 2-4 were repeated for 40 cycles before maintaining 72 ˚C for 10 min.

18µL of PCR product mixed with 2 µl bromophenol blue loading dye was loaded onto a 1.5 % agarose gel. HyperLadder IV molecular weight marker (Bioline, UK) was added to lane 1 and the gel was run at 120 volts for approximately 40 mins. The gel was then visualised using a UV transilluminator (Syngene; Cambridge, UK).

2.4 Administration of liposomes to pregnant mice

2.4.1 Qualitative assessment of liposome homing

Targeted (TAMRA-CGKRK-liposomes; Rh-iRGD-liposomes) or non-targeted (TAMRA-ARA-liposomes; plain-liposomes) liposomes were prepared with either a fluorescent peptide coating (red), a fluorescently tagged lipid film (DSPE-NBD (green)) or the liposomes were loaded with fluorescent CFS (green). Pregnant C57 mice were restrained and the liposomes were administered via tail vein injection (100 µl) at E12.5 and allowed to circulate for 3, 6, 24, 48 or 72 h (n = 3/group). Following terminal cardiac perfusion with PBS, tissues were collected for analysis. Organs were fixed in NBF (10 % (wt/vol) in PBS; 24 h), embedded in OCT and stored at -80 ˚C. Tissue sections (10 µm) were fixed to slides using PFA (4 % (wt/vol) in PBS; 15 min), washed in PBS (2 X 5 min), mounted in mounting medium containing DAPI (Vectashield 4′,6–diamidino–2–phenylindole; Vector Laboratories) and examined on a fluorescence microscope (Zeiss Observer Z1, Axiovision, UK). All images were taken at the same exposure; autofluorescence was corrected for by using PBS-treated animal tissues to set the exposure so that comparisons across samples could be made, 5-10 images of each sample were taken and representative images are shown.

2.4.2 Administration of liposomes to C57 mice

Treatments were administered I.V. via tail vein injection to pregnant C57 mice on E11.5, 13.5, 15.5 and 17.5 of pregnancy (100 µl/dose; equating to approximately 5 µmole/dose of lipids, 15 µg/dose encapsulated IGF-I or –II, 30 µg/dose of free IGF-I or

–II) and the individual treatment groups are outlined in Chapter 5. Mice were weighed daily during treatment to ensure that treatment was not detrimental to the pregnancy. All mice were sacrificed at E18.5 and the following variables measured: i) fetal weight, ii) placental weight, iii) litter size, iv) number of resorptions, v) maternal spleen weight, vi) maternal kidney weight, vii) maternal liver weight, viii) fetal horn position. Placentas and organs were bisected and half fixed in NBF (24 h, before transfer into PBS for storage) while the other half was put into RNAlater (24 h, before removal from RNAlater and storing at -80 ˚C). Maternal and fetal bloods were also collected, processed and stored as previously described.

2.4.3 Administration of liposomes to P0 mice

Pregnant P0 mice were I.V. injected (100 µl/dose; equating to approximately 5 µmole/dose of lipids, 15 µg/dose encapsulated IGF-I or –II, 30 µg/dose of free IGF-I or -II) on E11.5, 13.5, 15.5 and 17.5 of pregnancy and the treatment groups are outlined in Chapter 5. Animals were culled on E18.5 and the same parameters were recorded and tissues stored as outlined in section 2.4.2. Fetal and placental weights of five unhandled P0 animals collected from previous experiments performed by Dr Lewis Renshall and Dr Mark Dilworth were included to reduce the number of animals used in this study. I processed three unhandled animals and compared these with the five collected to ensure fetal and placental weight measurements were not significantly different between investigators. In addition, checks were undertaken throughout to ensure experimental conditions were comparable and data scrutiny confirmed that there was no drift in the phenotype of the P0 mice over the time the experiments were conducted.

2.4.4 Quantification of IGF-II in maternal and fetal serum

Maternal and fetal blood serum was collected after treatment as described above. A human IGF-II ELISA kit (Mediagnostics, Germany) was used to quantify IGF-II in maternal and fetal bloods. Samples were diluted 1:10 using the diluent provided and the ELISA protocol outlined in section 2.1.4 was followed. To ensure that IGF-II could be detected in mouse serum using this kit, serum from an animal that had been administered IGF-II continuously via a subcutaneous osmotic mini pump (from a separate experiment performed by Dr Jayne Charnock) was included as a positive control. The concentration of IGF-II in maternal and fetal serum was quantified using a standard curve.

2.4.5 Examination of placental morphology

Placentas collected from treated C57 or P0 mice were fixed as previously described and paraffin embedded. Three dams from each treatment group were assessed and from each dam, three placentas were randomly selected for histological assessment. Wax sections were cut (5 sections, 10 µm thick, 200 µm apart to produce consistent mid-placental sections) and slides were processed and stained using haematoxylin & eosin. Images of the placentas were obtained (x4 objective; Olympus BH-2 microscope) and tiled (Image-Pro Insight 7 inbuilt tiling software; MediaCy) to produce images of total placental cross sections. The absolute width and height of the tiled placental cross sections were recorded on the microscope (Image-Pro plus measuring software; MediaCy) and used to accurately establish parameters in HistoQuest software

(HistoQuest, TissueGnostics, UK). The percentage of the labyrinthine area as a proportion of the total placental area was calculated.

2.4.6 Quantifying proliferation in harvested placentas and organs

Placentas and maternal organs (brain, heart, lungs, liver, kidney, spleen) were collected from treated mice (C57 and P0, 3 mice / treatment group, 3 placentas / mouse), were fixed and paraffin-embedded. Tissue sections were deparaffinized in Histoclear (3 X 5 min; National Diagnostics, UK) and ethanol (3 X 5 min; Fisher chemicals, UK) and washed (dH_2O; 3 X 5 min). Slides were microwaved (2 X 5 min) in sodium citrate buffer (0.01 M; containing 0.05 % (vol/vol) Tween 20; pH 6.0; Sigma Aldrich, UK) to facilitate antigen unmasking. After cooling, endogenous peroxide activity was blocked by incubating the tissue sections in 3 % (vol/vol) hydrogen peroxide (10 min). Tissue sections were washed in Tris buffered saline (TBS; 0.05 M 3 X 5 min) and non-specific binding sites were blocked (5 % (wt/vol) BSA in TBS; 30 min), before Ki-67 primary antibody (1:1000; anti-Ki-67 rabbit monoclonal [SP6] to Ki-67 antibody; Abcam, UK) was added to the tissue sections, which were then incubated overnight at 4 ˚C in a humidified chamber. Mouse IgG (concentration matched, DAKO, Denmark) was used as a control. Slides were washed (TBS; 3 X 5 min) and the secondary antibody (1:200, polyclonal swine anti-rabbit immunoglobins biotinylated F(ab')2; DAKO) was applied for 30 min at room temperature. Slides were washed again (TBS; 3 X 5 min) and incubated with avidin peroxidase (5 µg/ml in TBS; Sigma Aldrich, UK) for 30 min at room temperature. Slides were washed (TBS; 1 X 5 min) and incubated for 4 min with 0.05 % (wt / vol) diaminobenzidine (DAB) and 0.015 % (vol / vol) hydrogen peroxide (Sigma Aldrich, UK). Slides were washed thoroughly in dH_20, counterstained with

Hematoxylin (Sigma Aldrich, UK), dehydrated in alcohol (3 X 5 min) and Histoclear (3 X 10 min), mounted in DPX (Sigma Aldrich, UK) and left to dry overnight. 10 random images of each organ and placenta were captured, and the area of Ki-67 positive cells was measured as a proportion of the total area of cells per field using HistoQuest (HistoQuest, TissueGnostics, UK). These data were used to determine the mean area of Ki-67 positive cells as a proportion of the total area of cells, within each organ or placenta.

2.4.7 Statistical analysis

All data were analysed using GraphPad Prism statistical software (version 6.0; GraphPad Software, USA). D'Agostino-Pearson omnibus normality testing identified whether datasets were normally distributed. Where data were not normally distributed, medians ± IQR are presented, and the Kruskal-Wallis test followed by a Dunn's multiple comparisons test for significance was performed. Where data were normally distributed, mean ± SD were presented and a one way ANOVA followed by a Tukey's multiple comparisons test for significance was performed.
* = $P < 0.05$, ** = $P < 0.01$, *** = $P < 0.001$, **** = $P < 0.0001$.

The number of animals required to observe a statistically significant following treatment (n = 8-10 mice / group) was estimated using a power calculation performed with an online software (Rollin Brant 2016) (Charan & Kantharia 2013) and using approximate data from previous treatment studies (two tailed test, $\alpha = 0.5$, desired power = 80%, fetal weight mean = 1.15 g, standard deviation = 0.07 g, desired fetal weight mean to give statistical significance = 1.25 g). The population distribution of fetal and placental

weight was plotted as previously described (Dilworth et al. 2011); a histogram of fetal weight was plotted and a non-linear regression performed (Gaussian distribution). The bottom 5th centile and 10th centile of the vehicle control group was calculated using the following equations, where SD is the standard deviation of the control group (EasyCalculation.com 2016) (Zar 1984).

$$Bottom\ 5th\ centile = (-1.6449\ x\ SD) + mean$$

$$Bottom\ 10th\ centile = (-1.2816\ x\ SD) + mean$$

2.5 Standard solutions

2.5.1 Phosphate buffered saline (PBS)

10 X PBS was made by dissolving 80 g NaCl, 2 g KCl, 14.5 g Na_2HPO_4 and 2 g KH_2PO_4 (All Sigma Aldrich, UK) in 1 litre of dH_2O and adjusting the pH to 7.4. A working solution of 1 X PBS was used throughout all experiments and was made by diluting 10 X PBS with dH_2O. PBS was sterilized by autoclave.

2.5.2 Tris-buffered saline (TBS)

1 X TBS was prepared by dissolving 6.05 g Tris and 8.76 g NaCl in (All Sigma Aldrich, UK) in 1 litre of dH_2O and adjusting the pH to 7.5.

2.5.3 Neutral buffered formalin (NBF)

NBF (10 % (wt / vol) in PBS) was prepared by adding 6.5g Na_2HPO_4, 4g NaH_2PO_4, and 100 ml Formaldehyde (40%) (All Sigma Aldrich, UK) in 900 mL dH_2O and adjusting the pH to 7.4.

2.5.4 Paraformaldehyde (PFA)

PFA (4 %) was prepared by warming 800 mL of 1X PBS to 60 ˚C, adding 40 g paraformaldehyde powder (Sigma Aldrich, UK) and stirring. 1 M NaOH was added dropwise until the powder dissolved. Once dissolved, the solution was cooled, filtered and the volume was adjusted to 1 litre and the pH was adjusted to 6.9

Chapter 3: Targeted Nanotherapeutic Design, Development and Characterisation

3.1 Introduction

The homing peptide sequences iRGD and CGKRK have been identified as selectively binding to human and mouse placenta (Harris et al. 2012). By displaying these homing peptides on the surface of a nanoparticle, it was hypothesized that targeted placental delivery of the nanoparticle could be achieved. Chapter 1 acknowledges liposomes as being appropriate nanoparticles to use during pregnancy; they are inherently biocompatible, their surface can be modified to incorporate homing peptides (Dubey et al. 2004; Nallamothu et al. 2006) and drug encapsulation in liposomes can reduce fetal exposure (Bajoria et al. 2013).

The initial aim of this research project was to undertake a literature review to determine the optimal liposome formulation for targeted drug delivery to the placenta. This introduction will summarise my findings and justify the liposome composition used in all subsequent experiments.

3.2 Liposome composition for placental targeting

Figure 3.1 shows a typical liposome composition used for targeted drug delivery. The liposome bilayer can comprise a variety of natural or synthetic phospholipids. Saturated phospholipids are used more often as they oxidise less readily than unsaturated phospholipids and therefore maintain their integrity for longer during storage and in circulation (Grit & Crommelin 1993). Synthetic lipids are favoured for clinical use as they are easier to characterise (Grit & Crommelin 1993) and are less likely to contain contaminants.

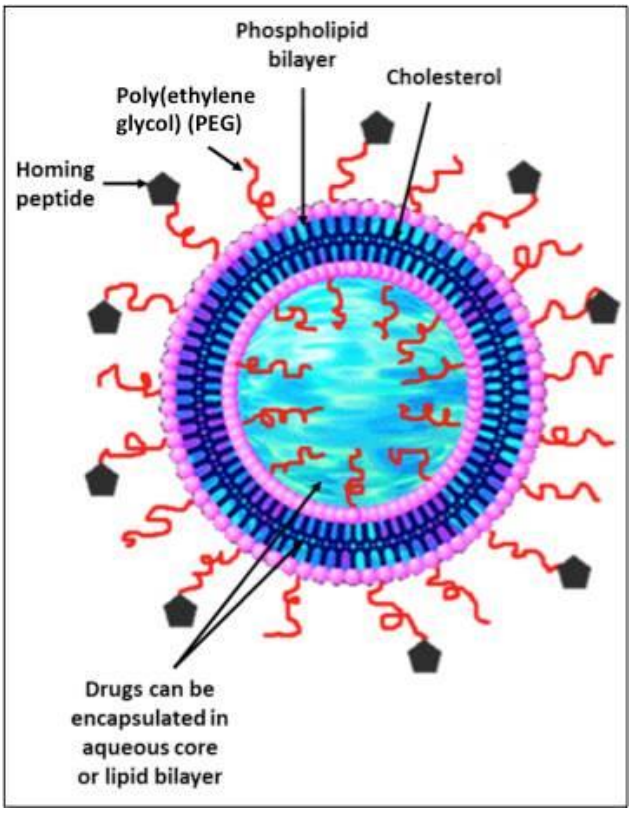

Figure 3.1: Common liposome composition used for targeted drug delivery. Liposome consists of a phospholipid bilayer, often stabilized with cholesterol. PEG is used to coat the liposome to allow it to circulate for longer in vivo. A targeting moiety can be attached to the surface of the liposome, generally through functionalizing the PEG layer. Adapted from (Nallamothu et al. 2006).

The transition temperature of the phospholipid is an important characteristic to consider. It is the temperature at which lipids change from an ordered gel-like phase, where the hydrocarbons are closely packed, into a disordered crystalline phase where the hydrocarbons are randomly ordered (Small 1986). The transition temperature is governed in part by the hydrocarbon chain length (Cevc 1991); as van der Waals forces become stronger they require more energy to disrupt the packing (Cevc 1991). Therefore, long-chain saturated phospholipids such as synthetic distearolphosphatidylcholine (DSPC) (Muppidi et al. 2012), natural hydrogenated soya phosphatidylcholine (SoyHPC) (Nallamothu et al. 2006) and sphingomyelin (SM)

(Webb et al. 1995) are all appropriate for making liposomes suitable for in vivo administration, as they have transition temperatures above that of body temperature, thus won't break down immediately when introduced into the body.

As well as the above considerations, Bajoria et al. (Bajoria et al. 2013; Rekha Bajoria et al. 1997) reported that liposomes made from the saturated, synthetic phospholipid DSPC, transferred less thyroxine, warfarin and CFS into the fetal circulation in a perfused human placental model compared with liposomes made from unsaturated lipids. Similarly, Tuzel Kox et al. (Tuzel Kox et al. 1995) demonstrated that liposomes made from SoyHPC, accumulated in the rat and rabbit placenta at a higher concentration when compared with other formulations examined. Therefore, DSPC was chosen as a suitable phospholipid to construct liposomes for targeted placental delivery. DSPC is a synthetic phospholipid with a hydrocarbon chain length of 18 and a transition temperature of 55 ºC (Avanti Polar Lipids Inc. 2016a), ensuring it will not immediately break down in the body, but can be extruded at a temperature obtainable in the laboratory.

Liposomes composed from DSPC are commonly used to deliver chemotherapeutics to tumours and their surrounding vasculature. Clinically available compositions containing DSPC include: DaunoXome® (liposomally encapsulated daunorubicin, approved to treat Kaposi's sarcoma), Liposomal-Annamycin® (in Phase II clinical trials to treat breast cancer) and DOXIL®/Caelyx®/Myocet® (liposomally-encapsulated doxorubicin approved to treat Kaposi's sarcoma, ovarian and breast cancer) (Immordino et al. 2006). DOXIL®/ Caelyx® is prepared using hydrogenated SoyPC, whereas Myocet® is prepared using egg phosphatidylcholine, both natural phospholipids.

Liposomes are generally stabilised by the addition of cholesterol, which modulates membrane fluidity, elasticity, permeability and affects the rate at which liposomes release their encapsulated drug (Kirby et al. 1980). The ratio of phospholipid to cholesterol can be varied to control the release kinetics of encapsulated drugs. Cholesterol added at concentrations greater than 30 mol% affects phospholipid packing in the bilayer and can reduce the transition temperature of the phospholipid as a result (Ishida et al. 2002). It was decided to use a molar ratio (MR) of 65:30, phospholipid:cholesterol, as MRs similar to this have been shown to be optimal for the release of several chemotherapeutics including the vascular disrupting agent combretastatin-A4 from cyclic RGD-decorated liposomes (65:30 MR, phospholipid:cholesterol) (Nallamothu et al. 2006); the combination of combretastatin-A4 and doxorubicin from RGD-decorated liposomes (65:30 MR, phospholipid:cholesterol) (Y.F. Zhang, Wang, Bian, Zhang, & Zhang, 2010); and the chemotherapeutic 5-fluorouracil from cyclic RGD-decorated liposomes (56:39 MR, phospholipid:cholesterol) (Dubey et al. 2004).

To increase in vivo circulation times, liposomes can be coated with PEG (Immordino et al. 2006), a linear polyether diol that is considered to be biocompatible, inducing minimal immunogenicity and toxicity (Dreborg & Akerblom 1990). PEG sterically hinders biological molecules from binding to the surface of liposomes, reducing detection by the MPS, and in doing so, significantly lengthens the circulation times in the body (Blume & Cevc 1993; Allen et al. 1991). PEGylated liposomes have an extended half-life in circulation in excess of 40 hours, with only 10-15 % of the initial dose administered ending up in the liver, one of the main clearance organs of the MPS (Song et al. 2014), compared with 80-90 % of non-PEGylated liposomes (Weissig

2011). PEG also acts to stabilise liposome formulations in storage by providing strong repulsive forces that can overcome attractive van der Waals forces, reducing liposome aggregation in suspension (Needham et al. 1992).

However, the presence of PEG in clinical formulations has been reported to increase the incidence of a painful condition called palmar-plantar erythrodysesthesia ('hand-foot' syndrome) (Yokomichi et al. 2013). This condition occurs when chemotherapeutics accumulate in the patients' extremities such as the hands and feet. The chemotherapeutic leak out into surrounding tissues causing DNA damage, blisters and open wounds. The condition occurs with the administration of several chemotherapeutics including Docetaxel, Fluorouracil and Paclitaxel (Cancer.Net Editorial Board 2014) but is more common in patients who are administered liposomally encapsulated chemotherapeutics (50-78 % occurrence with DOXIL® administration (Farr & Safwat 2011; Yokomichi et al. 2013)). This is thought to be due to the increased plasma circulation time of the encapsulated chemotherapeutic, caused by the incorporation of PEG (Yokomichi et al. 2013). However, the authors of this study did not state which molecular weight(s) of PEG exacerbated hand-foot syndrome, but say that the severity of the condition is correlated with the concentration and frequency of DOXIL® administration (Yokomichi et al. 2013).

To a point, the higher the molecular weight of PEG used, the longer the liposomes circulate (Allen et al. 1991). Allen et al. demonstrated that coating liposomes with PEG with a molecular weight of 1900 (PEG(1900)), doubled the concentration of lipid remaining in the plasma of mice 24 hours after injection, compared to formulations containing PEG(750) or PEG(120). Coating the liposomes with PEG(5000) did not

further increase the concentration of lipids remaining in circulation. We therefore chose PEG(2000) to coat the liposomes used in this study, as this formulation was more readily available than PEG(1900).

Allen et al. (Allen et al. 1991) report that there was no significant change in the rate of plasma clearance of the liposomes when the concentration of PEG incorporated was varied between 5 and 20 mol%. For this reason, the lowest concentration of PEG possible was used (65:30:5 MR of phospholipid: cholesterol: PEG), to retain its stealth effect, but to reduce the risk of hand-foot syndrome and inhibition of drug release. To facilitate insertion into the phospholipid bilayer, PEG must be conjugated to a charged, cross linked molecule such as 1,2-distearoyl-sn-glycero-3-phosphoethanolamine-N-[methoxy(polyethylene glycol)-2000] (DSPE-PEG(2000)) (Immordino et al. 2006). A fluorophore called nitrobensoxdiazol (NBD, $\lambda_{Ex/Em}$ = 460nm/535nm) may also be incorporated into the lipid bilayer to allow fluorescent tracking to be undertaken (Torchilin et al. 1994). Again the molecule must be attached to the charged phospholipid DSPE, to aid incorporation into the bilayer (NBD-DSPE).

In summary, we formulated control liposomes to be used in this study from DSPC, cholesterol and DSPE-PEG(2000), in the MR 65:30:5. These formulations were chosen to provide maximal circulation and stability in vivo, optimal drug release and minimal transplacental passage. This formulation can also be easily modified to allow for attachment of a targeting moiety to created targeted liposomes.

3.2.1 Homing peptide attachment

It is not known whether the placenta displays the EPR effect, nor is it clear to what extent I.V administered liposomes accumulate in the placenta. To maximise delivery to the placenta and to minimise off-target accumulation, a placental targeting moiety, namely the placental homing peptides iRGD or CGKRK, was added separately to the liposomal surface.

The PEG layer was further functionalised by conjugating a linking molecule to it, to allow for the attachment of the homing peptide to the surface of the liposome. The addition of a maleimide group (DSPE-PEG(2000)-maleimide), allowed for the covalent attachment of peptide to the liposome surface after preparation (Nallamothu et al. 2006; Torchilin 2006). Maleimide has a double bond, which is capable of reacting with a thiol group (S-H bond) to form a covalent bond via a Michael-type addition (Figure 3.2) (Nair et al. 2014). This reaction proceeds rapidly to completion at room temperature and neutral pH (Lutolf & Hubbell 2003). Peptides that contain an amino acid with a thiol group, such as cysteine, can then be attached to the liposome surface (Nair et al. 2014). The placental homing peptides iRGD (**C**CRGDKGPDC) and CGKRK (**C**GGGCGKRK), as well as the scrambled peptide sequence ARA (ARALPSQRSR**C**) used as a control, were synthesised to contain a free cysteine (in bold), allowing for surface attachment via this reaction.

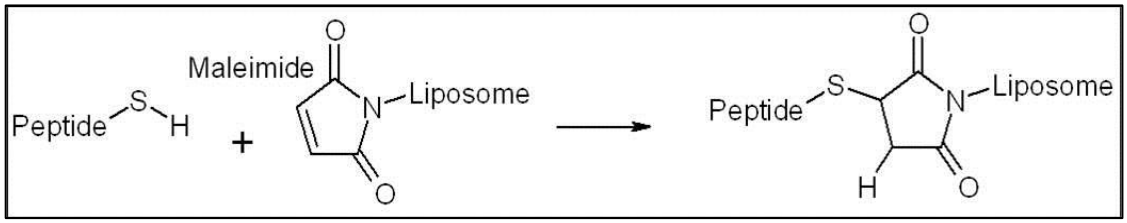

Figure 3.2: Michael-type addition reaction. The peptide contains a free thiol group on the cysteine residue. A covalent bond is formed between the maleimide group and the thiol group. Adapted from (ThermoFisher Scientific 2016).

To develop liposomes capable of targeting the placenta, peptide-decorated liposomes were formulated from DSPC, cholesterol, DSPE-PEG(2000) and DSPE-PEG(2000)-maleimide in the MR 65:30:3.75:1.25. After preparation, the homing peptides iRGD, CGKRK or the control peptide sequence ARA were conjugated to the liposomes and dialysis was performed to remove unbound peptide.

3.2.2 Liposome preparation techniques

There are several methods used to prepare liposomes, and they each produce liposomes with slightly different characteristics (Wagner & Vorauer-Uhl 2011). In general, the constituent lipids are weighed out (Figure 3.3A), dissolved in an organic solvent (usually chloroform) (Figure 3.3B), and then the solvent is removed to produce a lipid film (Figure 3.3C). The lipid film is rehydrated with a buffer solution (Figure 3.3D) and agitated (Figure 3.3E) to create large, self-assembled liposomes (Figure 3.3F). The dispersion is then warmed to its transition temperature and sonication, extrusion or homogenization are used to produce liposomes of a smaller, more homogenous size distribution (Figure 3.3G) (Avanti Polar Lipids Inc. 2016b).

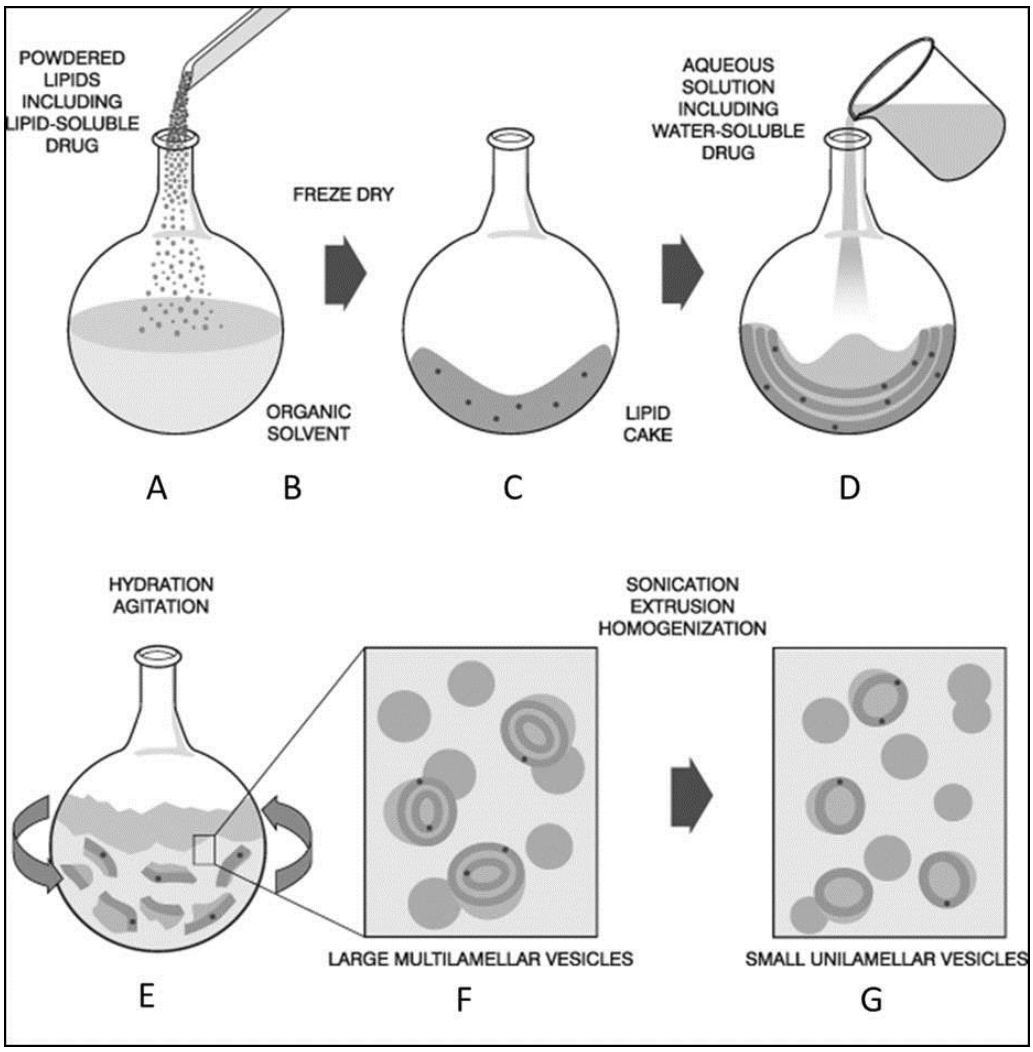

Figure 3.3: The process of liposome preparation via the thin film extrusion method. Adapted from (Avanti Polar Lipids Inc. 2016c)

Sonication is commonly used to reduce the size of large liposomes, typically producing unilamellar liposomes of approximately 15-50 nm in diameter (Avanti Polar Lipids Inc. 2016c). However, their small size results in a high degree of membrane curvature, making them unstable and they spontaneously fuse to form larger vesicles even when stored below their transition temperature (Avanti Polar Lipids Inc. 2016c). It is also nearly impossible to reproduce the exact sonication conditions, meaning that there is large inter-batch variation (Avanti Polar Lipids Inc. 2016c). Therefore, for the purposes of this research, liposomes were prepared using the extrusion method.

Tuzel Kox et al. (Tuzel Kox et al. 1995) showed that smaller liposomes (approximately 30 nm) accumulated in the rat and rabbit placenta in higher concentrations than larger liposomes (approximately 100 nm). However, Bajoria et al.(R Bajoria & Contractor 1997) report an inverse correlation between human placental transfer and liposome size, using liposomes ranging from 70 nm – 300 nm. Since the main purpose of using liposomes is to avoid fetal transfer, it was decided to extrude through a pore size of 100 nm, which generally produces unilamellar liposomes with a mean size distribution slightly larger than 100 nm, to encourage liposome accumulation in the placenta, but reduce fetal exposure risk.

3.2.3 Liposomal drug encapsulation

Liposomes can encapsulate hydrophilic, hydrophobic and amphiphilic drugs (Gulati et al. 1998). Drugs can be loaded into the liposomes during or after preparation depending on the nature and properties of the drug. Figure 3.4 shows how drugs with different properties are incorporated into different liposomal compartments. Hydrophobic molecules interact with the hydrophobic tail group of the phospholipid bilayer and can be incorporated into this layer during formation. If these drugs dissolve in, but are not damaged by, organic solvents, they can be added to the powdered lipids before they are dissolved in organic solvent, then dried to produce a lipid film. In doing this, they are incorporated directly into the lipid bilayer, providing a high encapsulation efficiency, but reducing drug release kinetics (Gulati et al. 1998). Hydrophilic drugs can be added to the buffer used to rehydrate the lipid film during preparation and are therefore incorporated into the aqueous core of the liposomes (Gulati et al. 1998). This generally leads to high encapsulation efficiency, but a high drug leakage (Gulati et al. 1998).

Amphiphilic drugs can be added at either stage of preparation, but often have a lower encapsulation efficiency (Gulati et al. 1998).

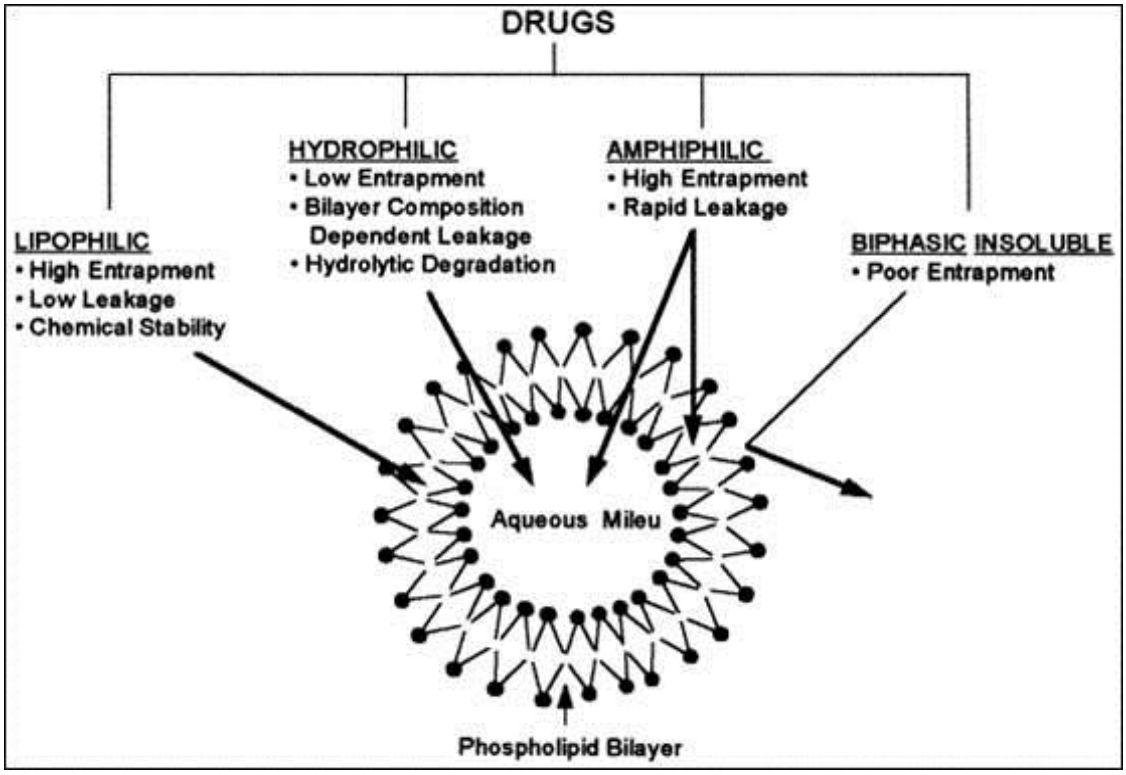

Figure 3.4: Site of drug incorporation into liposomes. Lipophilic drugs are incorporated into the phospholipid bilayer and hydrophilic drugs are encapsulated into the aqueous core. Amphiphilic drugs are encapsulated between the phospholipid bilayer and aqueous core. Reproduced from (Gulati et al. 1998).

It is important to determine whether the bioactivity of the drug will be affected by any stage of preparation. If drugs are incorporated during preparation, they need to be able to withstand higher temperatures necessary to attain the lipid transition temperature prior to extrusion. If a drug is heat-sensitive, it can be loaded after preparation by creating a pH gradient between the inside of the liposome and the surrounding medium, so that drugs move along the pH gradient and into the liposome (Haran et al. 1993; Masashi et al. 2008).

For liposome bio-distribution and functional studies, we encapsulated CFS, IGF-I or IGF-II into our liposomes. CFS is a hydrophilic molecule so can be encapsulated inside the aqueous core of the liposomes, whereas IGF-I and II are mildly amphiphilic molecules so will partition between the aqueous and lipid compartments. CFS is stable at 60 ºC for at least 2 h (Smith & Pretorius 2002) so can be incorporated by rehydrating the lipids with buffer containing CFS and then extruding at the transition temperature of DSPC. IGF-I and II are reported to be stable and bioactive for up to 8 months when stored at 45 ºC (NIBSC 2013). Due to the addition of cholesterol to the liposome formulation, the transition temperature of the lipid film will be reduced, so can be extruded at the lower temperature of 45 ºC. This means that IGF-I and -II can be reconstituted in buffer and then also used to rehydrate the liposome lipid film before extrusion.

3.3 Aims

After determining the liposomal formulation and method of preparation to be used, we aimed to:

1. Prepare liposomes with and without the addition of the homing peptides iRGD, CGKRK or the control sequence ARA
2. Measure the SD, PDI and ZP of all liposome formulations, using dynamic light scattering (DLS) and laser Doppler micro-electrophoresis (LDE)
3. Assess the stability of the liposomes by measuring SD over time.
4. Determine the concentration of peptide that attaches to the liposomal surface
5. Determine the concentration of IGF-II encapsulated.

3.4 Results

3.4.1 Characterisation of liposome size distribution (SD), polydispersity index (PDI), zeta potential (ZP) and stability

Liposomes were prepared using the thin film extrusiofn process outlined in section 2.1.1, with lipid compositions shown by Table 2.1 and Figure 2.1.

In initial experiments, liposomes with and without a PEG layer were prepared and examined. Due to a change in product composition, the liposomes used for preliminary characterisation experiments were prepared using DSPE-PEG(2000) with a carbon chain length of 16 (16:0 PEG-DSPE). Later experiments outlined in Chapters 4 and 5 were conducted using liposomes prepared from DSPE-PEG(2000) with a carbon chain length of 18 (18:0 PEG-DSPE).

The SD, PDI and ZP of all liposomes prepared were measured using the Zetasizer Nano (Malvern Instruments Ltd. 2016) and are shown in Tables 3.1 and 3.2. The SD gives an approximate spread of the diameters of the liposomes in solution. The ZP of any nanoparticle is defined as the electrical potential of a nanoparticle at the slipping plane with respect to the bulk liquid and is an approximate measurement of the surface charge. The PDI determines the spread of the SD, with “0” being a completely monodisperse solution and “1” being a completely polydisperse solution, a cut off of 0.7 is usually applied as it indicates that the solution is very monodisperse and the machine is unlikely to produce an accurate SD measurement (Malvern Instruments Ltd. 2016).

The SD and PDI were measured by DLS, and the ZP was measured using LDE. These techniques provide a quick and accurate way of measuring SD, PDI and ZP with minimal sample preparation required. Using the Zetasizer Nano machine is also more cost effective when compared with other size determination techniques. Unfortunately the ZP could not be measured for every formulation due to the volume needed and the destructive nature of the technique.

(A) DSPC/Cholesterol, mM lipids	Average size, nm	Average PDI, AU	Average zeta potential, mV
50	132 ± 1	0.10 ± 0.02	-0.8 ± 1
25	129 ± 2	0.07 ± 0.02	-1.5 ± 1
12.5	127 ± 2	0.10 ± 0.03	-1.0 ± 1
6.25	127 ± 1	0.07 ± 0.01	-3.0 ± 1
3.125	127 ± 2	0.06 ± 0.01	-6.1 ± 2

(B) DSPC/Cholesterol/PEG, mM lipids	Average size, nm	Average PDI, AU	Average zeta potential, mV
50	160 ± 2	0.28 ± 0.01	-30.3 ± 1
25	151 ± 2	0.16 ± 0.01	-44.1 ± 3
12.5	139 ± 1	0.12 ± 0.03	-36.1 ± 2
6.25	134 ± 1	0.11 ± 0.01	-38.7 ± 2
3.125	141 ± 2	0.10 ± 0.02	-35.7 ± 5

Table 3.1: The SD, PDI and ZP of liposomes measured at different lipid concentrations. (A) DSPC/Cholesterol liposomes and (B) DSPC/Cholesterol/PEG, prepared in water. Results are displayed as means rounded to the nearest whole number or decimal place ± range; n=1 sample with 3 readings recorded per sample. All liposomes were prepared in water and use 16:0 PEG-DSPE.

An initial pilot experiment was performed to examine the reproducibility of the SD, PDI and ZP measurements when liposomes were serially diluted in water (Table 3.1A, B). Changing the concentration of the liposome suspension did not alter the SD (132 ± 1 nm to 127 ± 2 nm) or the PDI (0.10 ± 0.01 to 0.06 ± 0.01), but did alter the ZP (-0.8 ± 1 mV

to -6.1 ± 2 mV) for non-PEGylated liposomes. For PEGylated liposomes, both the SD and ZP were altered (160 ± 2 nm to 141 ± 2 nm; -30.3 ± 1 mV to -44.1 ± 3 mV range).

The addition of PEG increased the average SD by approximately 10-30 nm, increased the PDI and reduced the ZP by approximately 30 mV. For all further experiments, SD, PDI and ZP were measured at the highest lipid concentration. It must be noted that the SD and ZP were increased when comparing DSPC/Chol/PEG made with 16:0 PEG-DSPE (Table 3.2A) and the same composition made with 18:0 PEG-DSPE (Table 3.2B), so these data have been presented separately.

Table 3.2A shows the characteristics of liposomes prepared using 16:0 PEG-DSPE. Non-PEGylated liposomes had an SD of 132 ± 1 nm (measured in water) and this increased to 186 ± 2 nm with the addition of DSPE-PEG. DSPE-PEG-maleimide reduced the SD to 137 ± 2 nm and also made the ZP more neutral (-0.5 ± 1 mV). The addition of the peptides iRGD, CGKRK or ARA increased the SD by approximately 10-20 nm. Inclusion of NBD, the green fluorophore used to label the lipid wall, reduced the SD of the liposomes by approximately 5-10 nm. CFS encapsulation did not alter the SD.

Table 3.2B shows the characteristics of liposomes prepared using 18:0 PEG-DSPE. The liposomes in this table were used for all functional studies so more batches were available for analysis. Non-PEGylated liposomes had an SD of 159 ± 40 nm and this increased to 230 ± 20 nm with the addition of DSPE-PEG. As observed above, the addition of DSPE-PEG-maleimide reduced the SD to 201 ± 35 nm and the addition of the peptides iRGD, CGKRK and ARA altered the SD by 10-20 nm. Inclusion of NBD

reduced the SD slightly, whereas CFS increased the SD. Encapsulating IGF-I or IGF-II increased the SD in a similar manner to that of encapsulating CFS.

(A) Liposome composition (16:0 PEG-DSPE)	Average size, nm (no. of batches)	Average PDI, AU (no. of batches)	Average zeta potential, mV (no. of batches)
DSPC/Chol*	132 ± 1 (1)	0.10 ± 0.02 (1)	-0.8 ± 1 (1)
DSPC/Chol/PEG	186 ± 2 (1)	0.28 ± 0.01 (1)	-3.3 ± 1 (1)
DSPC/Chol/PEG/Mal	137 ± 2 (1)	0.08 ± 0.03 (1)	-0.5 ± 1 (1)
DSPC/Chol/PEG/Mal/CGKRK	156 ± 1 (1)	0.17 ± 0.03 (1)	/
DSPC/Chol/PEG/Mal/iRGD	150 ± 5 (1)	0.16 ± 0.01 (1)	/
DSPC/Chol/PEG/Mal/ARA	142 ± 2 (1)	0.10 ± 0.01 (1)	/
DSPC/Chol/PEG/NBD	130 ± 1 (1)	0.07 ± 0.03 (1)	/
DSPC/Chol/PEG/NBD/Mal/CGKRK	136 ± 2 (1)	0.05 ± 0.03 (1)	/
DSPC/Chol/PEG/NBD/Mal/iRGD	138 ± 2 (1)	0.06 ± 0.03 (1)	/
DSPC/Chol/PEG/NBD/Mal/ARA	146 ± 3 (1)	0.09 ± 0.01 (1)	/
DSPC/Chol/PEG/CFS	152 ± 2 (1)	0.10 ± 0.02 (1)	/
DSPC/Chol/PEG/Mal/CGKRK/CFS	141 ± 2 (1)	0.11 ± 0.09 (1)	/
DSPC/Chol/PEG/Mal/iRGD/CFS	145 ± 2 (1)	0.09 ± 0.03 (1)	/
DSPC/Chol/PEG/Mal/ARA/CFS	157 ± 1 (1)	0.10 ± 0.02 (1)	/

(B) Liposome composition (18:0 PEG-DSPE)	Average size, nm (no. of batches)	Average PDI, AU (no. of batches)	Average zeta potential, mV (no. of batches)
DSPC/Chol	159 ± 40 (3)	0.08 ± 0.1 (3)	1.5 ± 2 (3)
DSPC/Chol/PEG	230 ± 20 (3)	0.21 ± 0.1 (3)	-6.2 ± 4 (3)
DSPC/Chol/PEG/Mal	201 ± 35 (3)	0.11 ± 0.1 (3)	/
DSPC/Chol/PEG/NBD	225 ± 60 (3)	0.22 ± 0.1 (3)	-5.7 ± 4 (3)
DSPC/Chol/PEG/Mal/CGKRK	174 ± 50 (3)	0.09 ± 0.1 (3)	-3.5 ± 2 (3)
DSPC/Chol/PEG/Mal/iRGD	221 ± 65 (4)	0.21 ± 0.1 (4)	-2.7 ± 2 (4)
DSPC/Chol/PEG/Mal/ARA	212 ± 40 (4)	0.24 ± 0.2 (4)	-1.8 ± 2 (4)
DSPC/Chol/PEG/CFS	180 ± 3 (1)	0.07 ± 0.1 (1)	/
DSPC/Chol/PEG/Mal/CGKRK/CFS	224 ± 15 (2)	0.15 ± 0.1 (2)	/
DSPC/Chol/PEG/Mal/iRGD/CFS	282 ± 4 (2)	0.08 ± 0.1 (2)	/
DSPC/Chol/PEG/Mal/ARA/CFS	314 ± 10 (2)	0.30 ± 0.2 (2)	/
DSPC/Chol/PEG/NBD/IGF-II	208 ± 10 (3)	0.10 ± 0.1 (3)	-10.1 ± 4 (3)
DSPC/Chol/PEG/iRGD/IGF-II	303 ± 50 (3)	0.35 ± 0.1 (3)	-8.6 ± 3 (3)
DSPC/Chol/PEG/ARA/IGF-II	320 ± 60 (3)	0.48 ± 0.2 (3)	-7.3 ± 3 (3)
DSPC/Chol/PEG/iRGD/IGF-I	194 ± 25 (3)	0.11 ± 0.1 (3)	-5.6 ± 4 (3)
DSPC/Chol/PEG/ARA/IGF-I	205 ± 45 (3)	0.26 ± 0.3 (3)	-7.0 ± 2 (3)

Table 3.2: The SD, PDI and ZP of all liposome compositions prepared. (A) Liposomes prepared using 16:0 PEG-DSPE, (B) Liposomes prepared using 18:0 PEG-DSPE. Results are displayed as means rounded to the nearest whole number or decimal place ± range; number in brackets are the number of independent batches examined with 3 readings recorded per sample, * indicates that this liposome formulation was prepared in water, whereas all others were in PBS.

The ZP of non-PEGylated liposomes was positive (1.5 ± 2 mV) and this became negative on the addition of DSPE-PEG (-6.2 ± 4 mV). The ZP of the PEGylated liposomes became less negative on the addition of the peptides iRGD, CGKRK or ARA (-2.7 ± 2 mV, -3.5 ± 2 mV, -1.8 ± 2 mV respectively), but became more negative when IGF-I or IGF-II was encapsulated (iRGD/IGF-II = -8.6 ± 3 mV, ARA/IGF-II = -7.3 ± 3 mV, iRGD/IGF-I = -5.6 ± 4 mV, ARA/IGF-I = -7.0 ± 2 mV).

The stability of the liposomes at 4 ºC was examined to determine how long they could be stored after preparation without degradation (Table 3.3). This can be examined by measuring the SD over several weeks (Muppidi et al. 2012). If the liposomes rapidly increase in size, this indicates aggregation is occurring and that they are not stable. The SD of the liposomes was measured every week for 4 weeks and did not change over time, suggesting that neither aggregation nor degradation was occurring and that the liposomes were stable at 4 ºC for up to 4 weeks.

Liposome composition (in PBS) (16:0 PEG-DSPE)	Week 1		Week 2		Week 3		Week 4	
	Average size, nm	Average PDI, AU	Average size, nm	Average PDI, AU	Average size, nm	Average PDI, AU	Average size, nm	Average PDI, AU
DSPC/Chol/PEG	186 ± 2	0.28 ± 0.02	159 ± 3	0.18 ± 0.02	152 ± 3	0.18 ± 0.02	164 ± 4	0.18 ± 0.03
DSPC/Chol/PEG*	121 ± 4	0.09 ± 0.01	116 ± 6	0.08 ± 0.01	130 ± 7	0.13 ± 0.02	119 ± 3	0.08 ± 0.02
DSPC/Chol/PEG/Mal/iRGD	150 ± 4	0.16 ± 0.01	146 ± 1	0.09 ± 0.01	147 ± 1	0.11 ± 0.02	137 ± 4	0.18 ± 0.03
DSPC/Chol/PEG/Mal/CGKRK	156 ± 1	0.17 ± 0.03	160 ± 2	0.12 ± 0.0	160 ± 2	0.11 ± 0.03	160 ± 2	0.11 ± 0.02
DSPC/Chol/PEG/Mal/ARA	142 ± 2	0.08 ± 0.01	144 ± 1	0.09 ± 0.01	142 ± 2	0.08 ± 0.01	144 ± 2	0.09 ± 0.01

Table 3.3: The stability of liposomes of all compositions examined by measuring the SD weekly. All compositions were prepared using 16:0 PEG-DSPE, results are displayed as means rounded to the nearest whole number or decimal place ± range; n=1 sample with 3 readings recorded per sample; * indicates that liposomes were added to culture medium to ensure stability in culture.

3.4.2 Determining the concentration of free thiol groups on iRGD and CGKRK peptides using Ellman's reagent

Ellman's reagent (DTNB) was used to determine the concentration of free thiol groups present on the homing peptides iRGD and CGKRK, necessary for peptide-liposome conjugation. As well as reacting with maleimide, free thiols react with DTNB, cleaving the disulphide bond to generate NTB^{2-} in water. This ion has a yellow colour that can be detected and quantified spectroscopically. The reaction is stoichiometric; 1 mole of thiol produces one mole of NTB^{2-}. Glutathione (GSH) contains 1 thiol group per peptide molecule, so was used to generate a standard curve (Figure 3.5A). This curve was used to quantify the number of free thiol groups that each peptide has, which was then used to optimise the concentration of peptide added to the liposomal formulation.

The absorbance at 412 nm of two different concentrations of fluorescently tagged homing peptides FAM-iRGD and FAM-CGKRK (50 μM and 100 μM, 250 μl) were measured in a spectrophotometer, with and without the addition of DTNB (concentration matched, 50 μl). After correcting for background, the final absorbance for each sample was then compared with the GSH calibration curve to obtain the thiol concentration for each peptide. The concentration of free thiol groups was found to be greater than or equal to one thiol group per peptide at the peptide concentration examined (iRGD (100 μM) = 114.9 ± 7.2μM (mean concentration of thiol ± standard deviation), iRGD (50 μM) = 62.14 ± 15.8 μM, CGKRK (100 μM) = 101.0 ± 4.8 μM, CGKRK (50 μM) = 52.42 ± 0 μM), showing that approximately every peptide had at least one thiol-group available to couple to the liposome surface (Figure 3.5B).

A

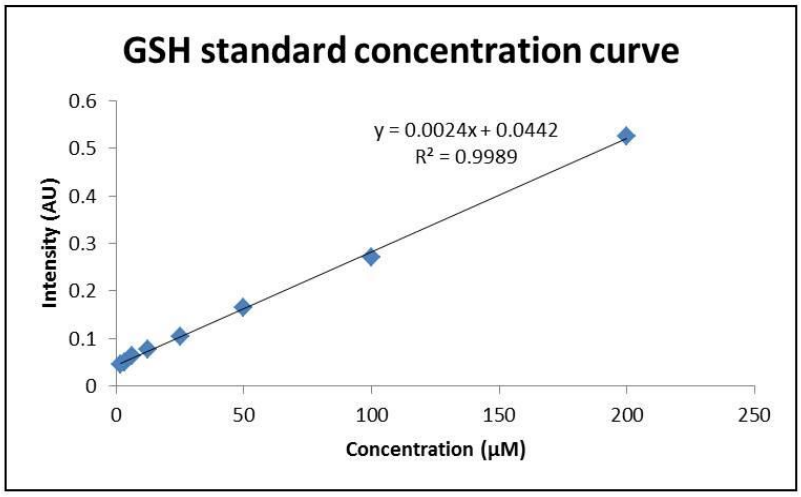

B

Moles of iRGD peptide (µM)	100	100	100	50	50	50
iRGD + DTNB absorbance (AU)	1.22	1.24	1.25	0.88	0.87	0.91
FAM absorbance (AU)	0.92	0.91	0.92	0.73	0.65	0.7
Corrected absorbance (AU)	0.3	0.33	0.33	0.15	0.22	0.21
Thiol concentration (µM)	**106.58**	**119.08**	**119.08**	**44.08**	**73.25**	**69.08**
Moles of CGKRK peptide (µM)	100	100	100	50	50	50
CGKRK + DTNB absorbance (AU)	1.14	1.13	1.14	0.84	0.87	0.86
FAM absorbance (AU)	0.84	0.85	0.86	0.67	0.7	0.69
Corrected absorbance (AU)	0.3	0.28	0.28	0.17	0.17	0.17
Thiol concentration (µM)	**106.58**	**98.25**	**98.25**	**52.42**	**52.42**	**52.42**

Figure 3.5: Calculating the concentration of free thiol groups available on the peptides iRGD and CGKRK.

(A) GSH calibration curve, (B) the concentration of free thiol groups on each peptide examined using (DTNB).

3.4.3 Quantifying peptide-liposome conjugation

One method to quantify peptide-liposome conjugation is to measure the concentration of peptide that is removed from the liposome suspension by dialysis. Dialysis is commonly used to remove non-encapsulated complexes from liposome suspensions (Johnston et al. 2006; Ning et al. 2011; Ruozi et al. 2011; Sur et al. 2014). By subtracting the concentration of peptide in the dialysate from the initial concentration added to the liposomes, one can quantify the concentration of peptide attached to the liposome surface.

After preparation, homing peptide was added to the liposomes at the concentration needed to block all free maleimide groups present on their surface (0.625 mM). After the reaction was complete, liposomes were dialysed against fresh PBS to remove unbound peptide. Spectroscopic analysis of the dialysate allowed quantification of the amount of free peptide remaining in solution; these data indicated that the concentration of peptide conjugated to the liposomes was approximately 100% for all compositions measured (Figure 3.6D). The concentration of peptide conjugated to the surface did not significantly change when the liposomes were encapsulating a drug.

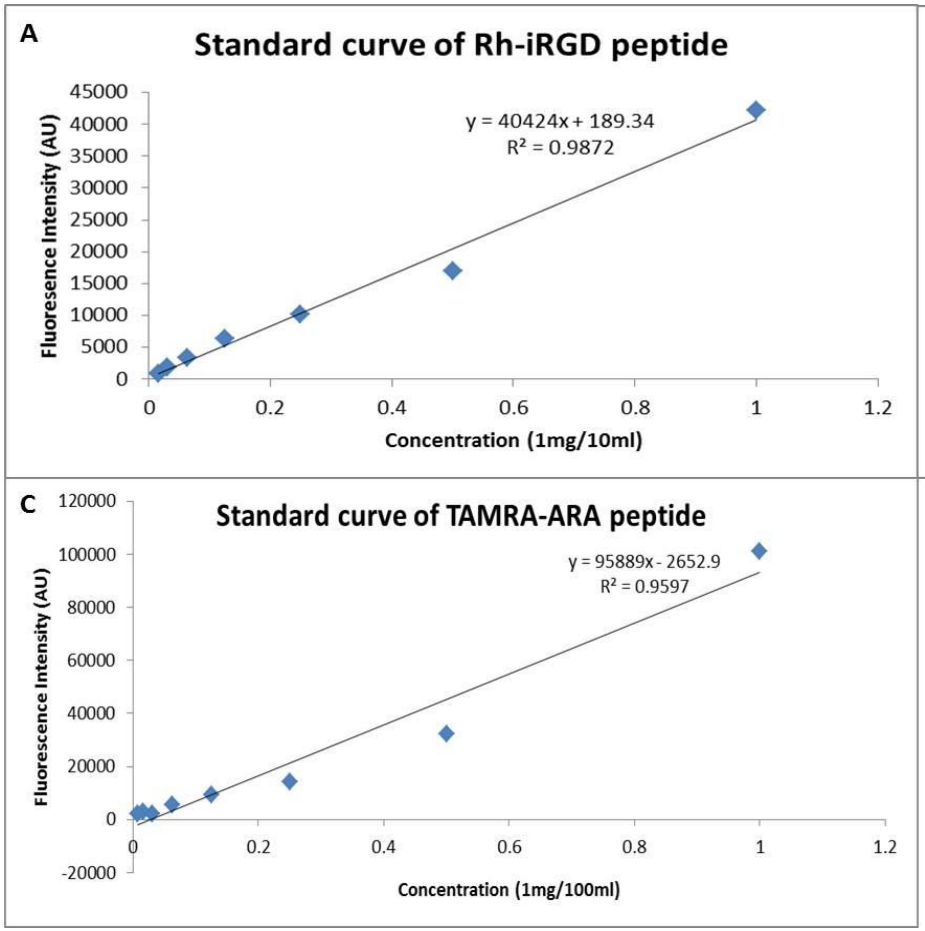

D

Liposome composition	Peptide conjugation efficiency (amount of peptide attached to liposome surface, % (range))
iRGD	96.56 (1.09)
CGKRK	96.26 (5.49)
ARA	99.32 (0.23)
iRGD/IGF-II	97.00 (2.54)
ARA/IGF-II	98.45 (1.52)

Figure 3.6: Quantifying the peptide-liposome conjugation efficiency. Standard curves of A) free Rhodamine-iRGD peptide, B) free TAMRA-CGKRK, C) free TAMRA-ARA, D) conjugation efficiency of peptide conjugated to the liposome surface. N=3-5 independent liposome samples for each composition; all dialysate samples were examined in triplicate.

3.4.4 Determining the encapsulation efficiency of IGF-II

The concentration of IGF-II encapsulated in liposomes was quantified by ELISA after disrupting the liposome bilayer and centrifuging to separate the aqueous and lipid compartments (Partearroyo et al. 1992; Sila et al. 1986). The concentration of IGF-II inside the aqueous core of the liposomes was 14.9% of the initial concentration added for iRGD/IGF-II liposomes and 17.8% of the initial concentration added for ARA/IGF-II liposomes and non-coated/IGF-II liposomes (Figure 3.7B). The concentration of IGF-II in the lipid bilayer was 32.2% of the initial concentration for iRGD/IGF-II liposomes, 31.3% for ARA/IGF-II liposomes and 31.1% for non-coated/IGF-II liposomes. Thus the average concentration of IGF-II incorporated into the liposomes was approximately 50% of the initial concentration added to the suspension for all liposome compositions. The concentration of IGF-II added to the liposomes was based on the intention of delivering 1mg/kg for each 100 µl of liposome suspension injected into the mice, following a similar dosing regimen as that of Sferruzzi-Perri (Sferruzzi-perri et al. 2007). As only 50% was encapsulated, each injected dose of 100 µl contained 0.5 mg/kg, equating to approximately 15 µg/dose.

A

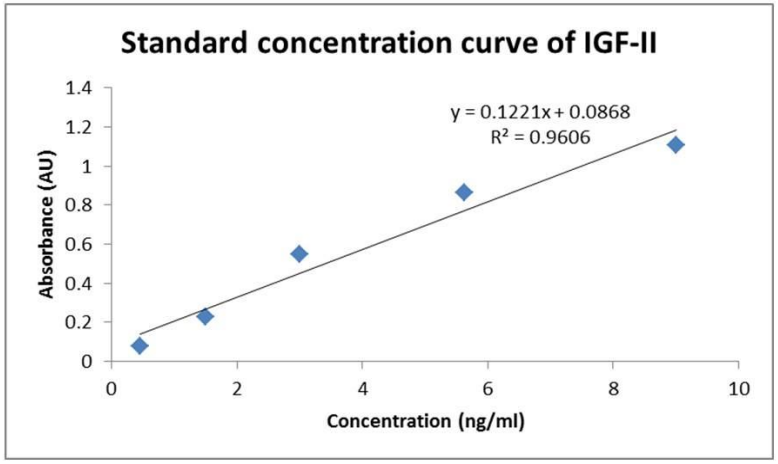

B

Liposome composition	Mean IGF-II concentration in aqueous core (µg)	Mean IGF-II concentration in aqueous core (% of total added)	Mean IGF-II concentration in lipid film (µg)	Mean IGF-II concentration in lipid film (% of total added)	Encapsulation efficiency (% encapsulated of total added)	Amount of IGF-II per injected dose (µg/100µl)
iRGD/IGF-II liposomes	4.46	14.9	9.66	32.2	47.1	14.13
ARA/IGF-II liposomes	5.33	17.8	9.31	31.3	48.1	14.43
Non-coated/IGF-II liposomes	5.34	17.8	10.52	35.1	52.9	15.87

Figure 3.7: Quantifying the concentration of encapsulated IGF-II. (A) IGF-II standard curve, (B) concentration of IGF-II conjugated with the liposomes; n=3 independent batches.

3.5 Discussion

After undertaking an extensive literature review, it was decided to prepare non-targeted liposomes from DSPC:cholesterol:DSPE-PEG(2000) in the MR 65:30:5, and peptide-decorated liposomes from DSPC:cholesterol:DSPE-PEG(2000):DSPE-PEG(2000)-maleimide:peptide in the MR 65:30:3.75:1.25:1.25, using the thin film extrusion method. DSPC is a neutral synthetic phospholipid with an appropriate transition temperature to prevent immediate break down in circulation and cholesterol further controls drug release and reduces the transition temperature of the lipid bilayer. PEG was incorporated as not only does it increase liposome circulation time, but it also decreases fetal transfer of gold nanoparticles (Yang et al. 2012). Post preparation, the homing peptides iRGD and CGKRK or the control scrambled peptide sequence ARA, were covalently coupled to DSPE-PEG(2000)-maleimide inserted in the liposome bilayer and dialysis performed to remove unconjugated peptide from the liposome suspension.

Three different substances (CFS, IGF-I and IGF-II) were encapsulated inside the liposomes by rehydrating the lipid film with the payload reconstituted in PBS. CFS was chosen to allow tracking of the liposomal cargo in vitro and in vivo, and to assess the kinetics of drug release, a process that is further examined in Chapter 4. IGF-I or IGF-II was encapsulated to represent a biological payload to deliver to the placenta; the effects of targeted delivery on mouse pregnancy are further examined in Chapter 5.

3.5.1 Liposome characterisation

The SD and ZP of liposomes are important characteristics to quantify as they govern how the body processes the liposomes, their tissue distribution and clearance profile. The SD gives an approximate spread of the diameters of the liposomes in solution. The ZP of any nanoparticle is defined as the electrical potential of a nanoparticle at the slipping plane with respect to the bulk liquid and is an approximate measurement of the surface charge.

The SD and ZP of the liposomes were engineered to minimise transplacental passage and maximise stability, circulation time and placental drug concentration. Considering the literature, we aimed to prepare liposomes of approximately 100-200 nm in diameter to prevent fetal drug transfer whilst maximising placental accumulation and circulation time of the liposomes. The final size of peptide-coated liposomes containing a payload was between approximately 194 ± 25 nm and 320 ± 60 nm, depending on the encapsulated substance; the final size of non-coated liposomes was between approximately 180 ± 3 nm and 208 ± 10 nm, again depending on the payload.

The SD of our liposomes are similar to those previously reported when liposomes encapsulating doxorubicin and coated in RGDF were prepared (Du et al. 2011). The group report an average SD between 143.9 ± 0.6 nm and 250.2 ± 7.2 nm depending on the lipid composition and the concentration of encapsulated doxorubicin. However, several liposome compositions similar to ours have been reported with a substantially smaller SD. RGD peptide coated liposomes encapsulating combretastatin A4 had an SD of 123.8 ± 41.2 nm (Nallamothu et al. 2006). This could be due to the group using a

slightly different lipid composition and preparation method, as well as combretastatin-A4 having a substantially lower molecular weight than IGF-I or II (316.34 Da compared with 7.5 kDa). A similar lipid composition prepared by reverse phase evaporation resulted in a SD of approximately 105 nm (Dubey et al. 2004).

It is clear that there is a variation in SD between studies and this depends on the lipids used, the preparation methods employed, the cargo encapsulated and any additional surface modifications. The SD measured in our liposome formulations are in the same range as seen in previous reports and are reproducible between batches. We are therefore confident that we have produced non-coated and peptide-decorated liposomes with and without an encapsulated cargo with a monodisperse size distribution using standard and reproducible methods.

As well as the SD, the ZP of nanoparticles also affects processing in vivo. Negatively charged liposomes have a shorter circulation half-life when compared to neutral and positively charged liposomes (Harashima & Kiwada 1996) due to recognition by the MPS (Semple et al. 1998). However, there are several reports that positively charged liposomes are toxic, induce considerable complement activation and are thus quickly removed from circulation (Semple et al. 1998). We therefore concluded that liposomes with an approximately neutral surface charge were better to use to maximise in vivo circulation time.

The ZP also governs how the placenta processes nanoparticles and can affect transplacental drug transfer. Bajoria et al. (R. Bajoria & Contractor 1997) state that positively charged liposomes transfer a lower concentration of drug to the fetus whilst

neutral and anionic liposomes increase fetal drug transfer in a perfused human placenta model. However, Tuzel Kox et al., (Tuzel Kox et al. 1995) report that negatively charged liposomes accumulate more readily in the rabbit and rat placenta, indicating that negatively charged liposomes would transfer a higher concentration of drug to the fetus, although the group did not specifically examine this. Yang et al. (Yang et al. 2012) report that negatively charged (-17 mV) gold nanoparticles injected into pregnant mice were transferred to fetal tissues to a significantly lesser extent when compared with neutral gold nanoparticles.

As we intended to develop liposomes capable of targeting both the mouse and human placenta, which potentially have opposing membrane charges (the human placenta is negatively charged, whereas the rat placenta is positively charged (Refuerzo et al. 2011); the charge of the mouse placenta has not been measured), we concluded that liposomes with a neutral ZP were the most appropriate for this study. This also circumvents the risk of charged lipids interfering with the targeting potential of the placental homing peptides.

The neutral lipids DSPC and cholesterol produced liposomes with an approximately neutral ZP in PBS. The addition of DSPE-PEG decreased the ZP of the liposomes, but the value remained close to neutral. This change in ZP upon the addition of DSPE-PEG is similar to that reported by Li et al (Li et al. 2011), who showed that the ZP changed from 46.2 mV to 39.3 mV with the addition of 7% PEG. The ZP in their study was positive to begin with, due to the addition of the cationic lipid 1,2-doleoyl-3-trimethylammoniumpropane (DOTAP). Therefore, we were confident that we had produced liposomes with an expected ZP using our preparation techniques.

The stability of the liposomes was examined over 4 weeks by measuring the SD weekly. This method has been used when examining liposome stability after encapsulating vinorelbine (Semple et al. 2005), and when examining the stability of PEGylated and non-PEGylated liposomes with a similar formulation to ours (Muppidi et al. 2012). If a change in SD is observed it signifies that the liposomes are flocculating or degrading. Semple et al. (Semple et al. 2005) reported that liposomes comprising sphingomyelin and cholesterol were stable for up to 42 days when stored at 4 ºC, 25 ºC and 40 ºC. In a similar manner, Muppidi et al. (Muppidi et al. 2012) reported that PEGylated DSPC/cholesterol liposomes were stable for 3 months when stored at 4 ºC, but began to aggregate when stored at room or body temperature. For our experiments, liposomes were stored at 4 ºC in between measurements to prolong storage stability, and it was found that all liposomal formulations were stable for at least 4 weeks. The stability of other peptide-decorated liposome formulations has not been reported, so comparisons with the literature cannot be made. However, the stability of non-coated liposomes encapsulating epidermal growth factor (EGF) was investigated by Alemdaroglu et al. (Alemdaroğlu et al. 2007) when stored at 25 ºC and 4 ºC. They report that there was no change in size after 210 days when stored at 4 ºC, but the liposomes increased in size after 90 days when stored at 25 ºC, suggesting that our targeted liposomes encapsulating IGF-II should be stable for several weeks when stored at 4 ºC.

3.5.2 Liposome-peptide conjugation

The homing peptides were conjugated to the liposome surface after preparation, by using a Michael-type addition reaction to covalently couple free thiol groups on cysteine residues of the peptides to the maleimide group of DSPE-PEG-maleimide

displayed on the liposome surface. This is a standard reaction that has been utilised to conjugate RGD-bearing peptide sequences to the surface of liposomes (Nallamothu et al. 2006) and micelles (Sugahara et al. 2009).

Initially, the ability of the peptides to react with the maleimide groups was established using Ellman's reagent, to quantify the concentration of free thiol groups on the peptides. In doing so, it was found that approximately one thiol group per peptide molecule was available to attach to the liposome's surface. An examination of the peptides' structures confirms this result was to be expected; there is at least one cysteine group per peptide available to react with Ellman's reagent.

The efficiency of peptide conjugation to the liposomal surface was quantified using dialysis, followed by spectroscopic analysis of the dialysate; almost 100% conjugation was achieved for all peptides examined. Dubey et al.(Dubey et al. 2004) report a peptide-maleimide conjugation efficiency of 98 ± 0.5%, supporting our results. Several other methods of peptide-liposome quantification are outlined in the literature. Nallamothu et al. (Nallamothu et al. 2006) used HPLC to quantify the concentration of free peptide before and after the conjugation reaction, and in doing so deduced that all of the peptide added to the liposomes became conjugated. We tried this method, but were unable to identify the liposomal fraction using HPLC. Centrifugation could also be used to separate unbound peptide from liposomes which can then be quantified spectroscopically, but the high speeds used can deform the liposomes, causing them to aggregate. Gel filtration column chromatography can also be used to separate and detect unbound peptide or unencapsulated cargo (Dubey et al. 2004). However, this dilutes the sample considerably (Moriya 1998) so was not appropriate for use here.

3.5.3 Drug encapsulation

Liposomes can encapsulate a range of drugs, with an efficiency dependant on the lipid composition, the nature of the drug and the loading technique used. Initially CFS, a water-soluble fluorophore, was encapsulated to monitor drug release kinetics and tissue distribution. It is important to note that CFS will not act in exactly the same way as IGF-I or IGF-II in terms of its release profile and tissue distribution, as it has a different molecular weight and hydrophobicity. However, Harashima et al. (Harashima & Kiwada 1996) state that the lipid composition of the liposomes is one of the most critical factors in determining the release property of encapsulated payloads, thus it can be used to provide an estimate of these parameters in vivo.

For our experiments, IGF-II was encapsulated by rehydrating the lipid bilayer with a buffer containing IGF-II and then extruding the formulation. To quantify the amount of IGF-II stably encapsulated, shortly after preparation the lipid membrane was disrupted and centrifuged and the concentration of IGF-II in the lipid pellet and aqueous supernatant was measured directly using ELISA. This method of encapsulation gave an encapsulation efficiency of approximately 50% for all liposome formulations examined, providing a final concentration of 0.5 mg/kg/dose when injected into mice. This delivers a lower dose than used previously (Sferruzzi-perri et al. 2007) when IGFs were administered subcutaneously to guinea pigs, but as the payload is to be selectively targeted to the placenta, thus less would be released in other tissues, it was hypothesised that a lower encapsulated concentration would still generate a biological response (Gabizon et al. 2002; Ruoslahti 2004).

With a passive encapsulation method such as this, it is to be expected that approximately 50% encapsulation might be achieved at equilibrium between the inside and outside of the lipid bilayer. Several groups reported a similar level of growth factor encapsulation; Alemdaroglu et al. (Alemdaroğlu et al. 2007) reported an encapsulation efficiency of 58.1% determined spectroscopically, when EGF was passively encapsulated; Xie et al. (Xie et al. 2005) reported a 34% encapsulation efficiency of nerve growth factor (NGF) when using lipid film rehydration. However, we observed 15-18% IGF-II encapsulation in the aqueous core of the liposomes and approximately 31-35% of the IGF-II in the pellet of the centrifuged lipids, showing that it associated more readily with the lipid bilayer than the aqueous core. This could alter drug release kinetics, and indicates that IGF-II is an amphiphilic molecule. Other methods could be employed to improve the encapsulation efficiency of IGF-II: a gradient loading method could be used, whereby a pH gradient is created between the inside of the liposome and the surrounding medium, so that the pH gradient drives drug encapsulation (Haran et al. 1993; Masashi et al. 2008). This is a more complicated preparation method and may alter the structure or bioactivity of the drug, but could be trialled for use in future studies.

3.6 Summary

We have shown that the thin lipid film extrusion method produced a monodisperse distribution of liposomes, approximately 200 nm in diameter and of approximately neutral or slightly negative surface charge. Inter-batch reproducibility and stability was acceptable, approximately 100% of the peptides were conjugated to the liposome, and

50% drug encapsulation was achieved. The ability of the liposomes to selectively target the placenta in vitro and in vivo is examined in Chapter 4

Chapter 4: Validation of Liposome Targeting in Mice and Human Tissues

4.1 Introduction

Prior to administering a bioactive payload in our targeted liposomes, it was necessary to confirm selectivity of placental binding in vitro and in vivo, assess liposome bio-distribution and clearance kinetics in vivo, and determine whether the formulation was well tolerated by mice and was compatible with normal pregnancy. It was also important to ensure the liposomes released an encapsulated payload in a timely manner and to examine the tissue distribution of the payload to confirm placental delivery, and examine the extent of fetal transfer and off target release in maternal organs. The fluorescent molecule CFS was encapsulated to represent a drug payload; CFS reportedly crosses the human placenta and enters fetal circulation, so was chosen as an appropriate candidate (R Bajoria & Contractor 1997; Bajoria et al. 2013; R. Bajoria & Contractor 1997). The data generated from these experiments will aid our understanding of liposome biodistribution and clearance in the pregnant mouse, which will inform decisions regarding the suitability of the current formulation, the choice of payload and the design of a treatment study.

4.2 Aims

This chapter aimed to:

1. Investigate whether control and peptide-decorated liposomes could bind to, and accumulate within human placental explants
2. Examine the biodistribution and clearance of control and peptide-decorated liposomes in pregnant mice

3. Examine the biodistribution of a fluorescent liposomal cargo when delivered to pregnant mice using control and peptide-decorated liposomes

4.3 Results

4.3.1 Placental homing peptides accumulate within the syncytiotrophoblast of human placental explants

Free FAM-iRGD and FAM-CGKRK were incubated with first trimester or term placental explants for up to 3 h. Accumulation of both peptides in the outer syncytiotrophoblast layer was evident after 30 min (Figure 4.1 A, D, G, J), and the fluorescent signal increased in intensity from 1 h (Figure 4.1 B, E, H, K) to 3 h (Figure 4.1 C, F, I, L), suggesting continued uptake of the peptides in the syncytiotrophoblast. The fluorescent signal from the FAM-iRGD peptide appeared to be weaker in first trimester tissue after 1 h (figure 4.1B) when compared with term tissue of the same time point (figure 4.1E), but after 3 h, the intensity appeared to be similar (figure 4.1C and F). Both placental homing peptides remained in the syncytiotrophoblast for 3 h and did not appear to enter the underlying cytotrophoblast or villous stroma in significant amounts.

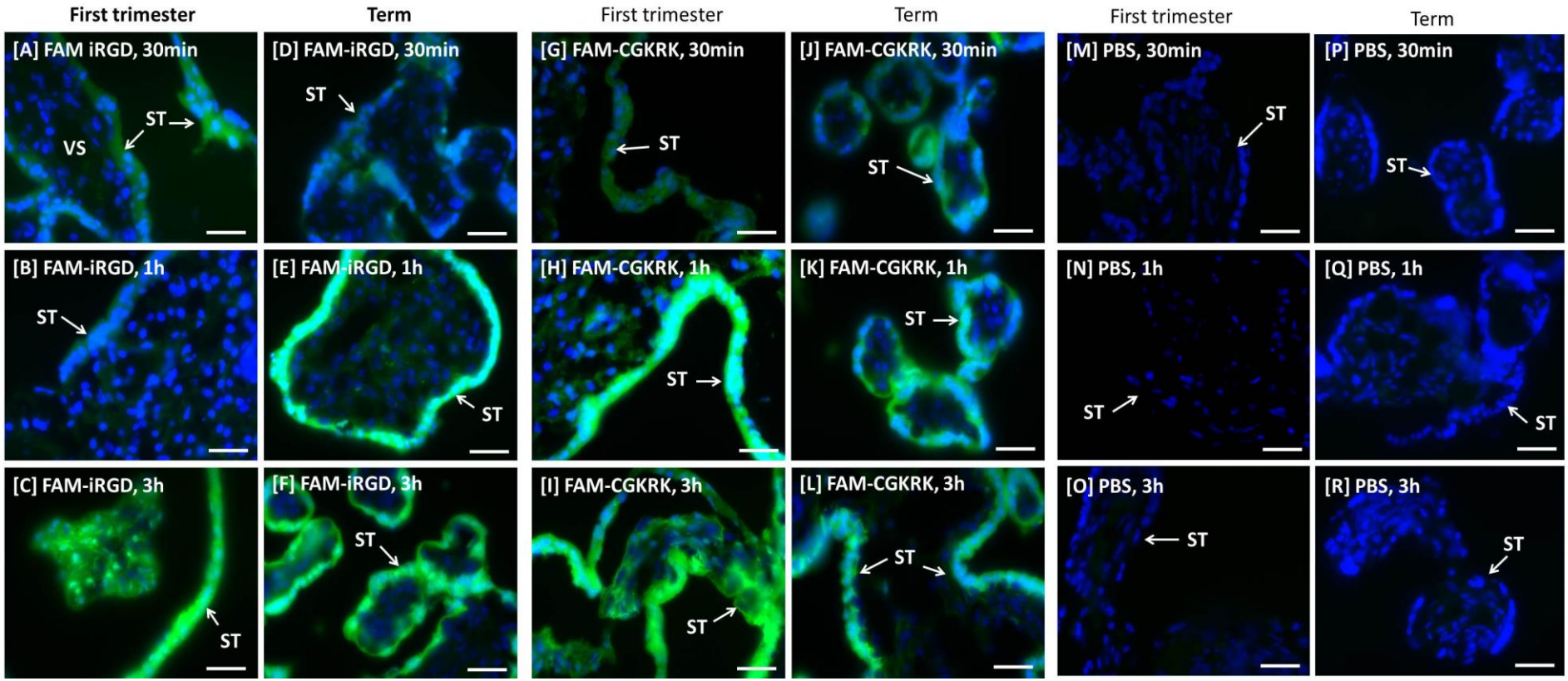

Figure 4.1: Homing peptide binding to human placental explants. The placental homing peptides (A-F) FAM-iRGD (green) and (G-L) FAM-CGKRK (green) accumulated in the ST of both human first trimester and term placental explants and did not significantly penetrate into the VS. All images were taken at the same exposure; autofluoresence was corrected for by using PBS-treated tissue sections to set the exposure (M-R). Nuclei were stained with DAPI (blue), N=3 placentas, n=3 biopsies from each placenta were examined, 10 images were taken of each sample, representative images are shown (Scale bar = 50µm).

4.3.2 Homing peptide-decorated liposomes bind to the syncytiotrophoblast of human placental explants.

To assess whether liposomes decorated with homing peptides accumulated in placental explants in a similar manner to free homing peptide, term human explants were incubated with liposomes decorated with FAM-iRGD (FAM-iRGD-liposomes; targeted liposomes; green), FAM-CGKRK (FAM-CGKRK-liposomes; targeted liposomes; green), rhodamine-iRGD (Rh-iRGD-liposomes; targeted liposomes; red), TAMRA-CGGGCGKRK (TAMRA-CGKRK-liposomes; targeted liposomes; red) or the control peptide sequence, TAMRA-ARA (TAMRA-ARA-liposomes; non-targeted liposomes; red). Liposomes not coated in peptide, but synthesised using lipids labelled with the fluorophore NBD (Non-coated liposomes; non-targeted liposomes; green) were also tested as an additional control. Liposomes were incubated with the explants for several time points ranging from 3 h – 48 h. With the exception of non-coated liposomes, it was the peptide moiety that was fluorescently tagged, thus any fluorescent signal observed could originate from peptide-coupled lipids or from peptide liberated from the liposomal surface.

Targeted liposomes accumulated in the syncytiotrophoblast of human term placental explants to a similar extent to free peptide, confirming that the peptides were still functional after conjugation to the liposome surface. However kinetics were slower: whereas the free peptides were visible in the syncytiotrophoblast of term placental explants within 30 min (figure 4.1 D & J), targeted liposomes were only visible after 3 h (figure 4.2 A, B, I, J, Q, R). The fluorescence intensity increased over 48 h, suggesting that the targeted liposomes continued to accumulate over this time. Based on

fluorescence intensity, liposomes accumulated in a concentration-dependent manner over all time periods examined.

TAMRA-ARA-liposomes also accumulated in the placental syncytiotrophoblast, but were not visible until 24 h of incubation (figure 4.2 KK & LL), and were no longer visible at 48 h (figure 4.2 MM & NN). Non-coated liposomes labelled with NBD were not visible accumulating in the syncytiotrophoblast, but diffuse areas of green fluorescence were observed in the villous stroma at 6 h (figure 4.2 RR) and 24 h (figure 4.2 SS & TT); the signal intensity was stronger when the higher concentration was used (figure 4.2 TT). In a similar manner to TAMRA-ARA-liposomes, fluorescence attributed to the non-coated liposomes was not observed at 48 h (figure 4.2 QQ & RR).

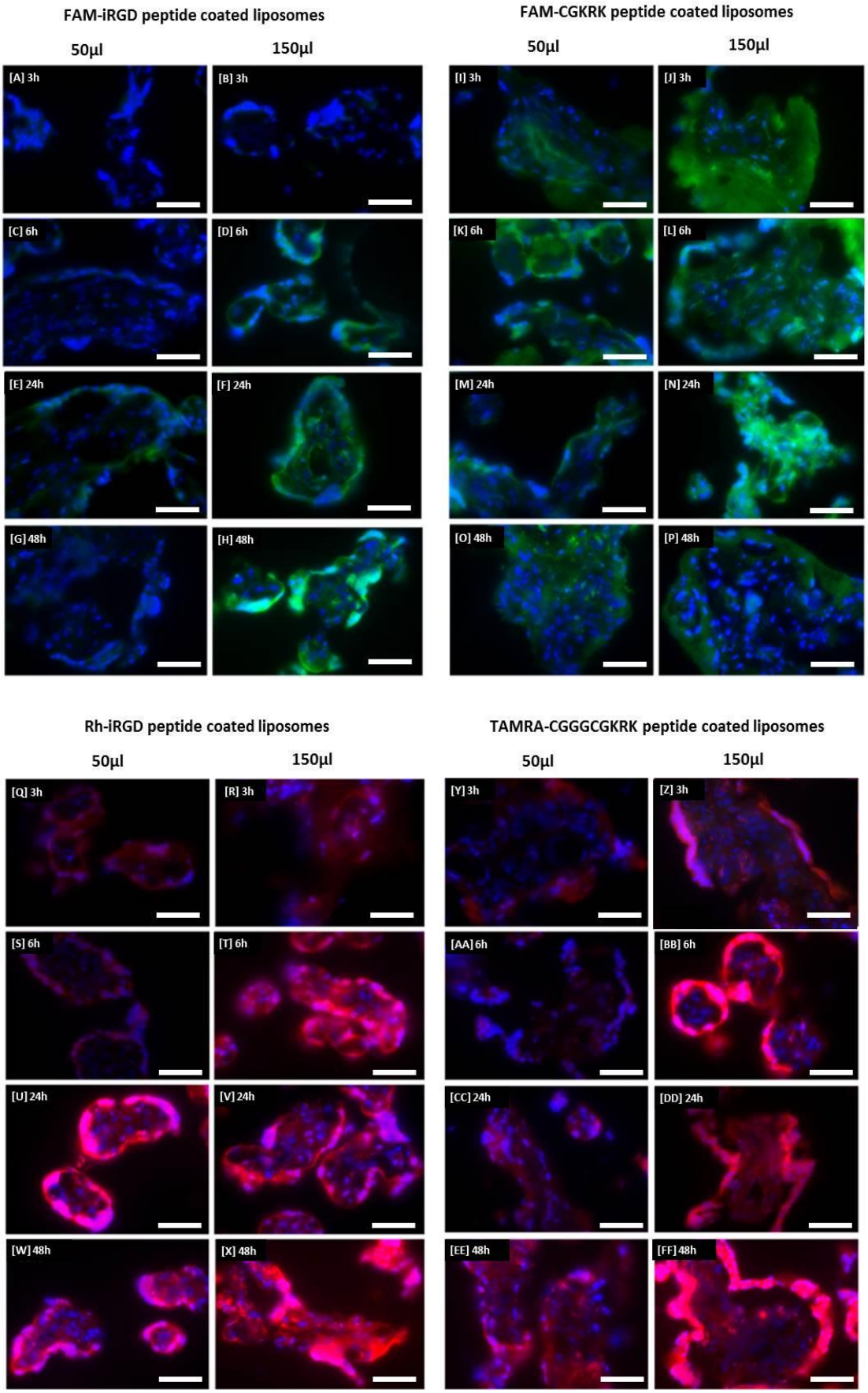
FAM-iRGD peptide coated liposomes
50µl
150µl
[A] 3h
[B] 3h
[C] 6h
[D] 6h
[E] 24h
[F] 24h
[G] 48h
[H] 48h
FAM-CGKRK peptide coated liposomes
50µl
150µl
[I] 3h
[J] 3h
[K] 6h
[L] 6h
[M] 24h
[N] 24h
[O] 48h
[P] 48h
Rh-iRGD peptide coated liposomes
50µl
150µl
[Q] 3h
[R] 3h
[S] 6h
[T] 6h
[U] 24h
[V] 24h
[W] 48h
[X] 48h
TAMRA-CGGGCGKRK peptide coated liposomes
50µl
150µl
[Y] 3h
[Z] 3h
[AA] 6h
[BB] 6h
[CC] 24h
[DD] 24h
[EE] 48h
[FF] 48h

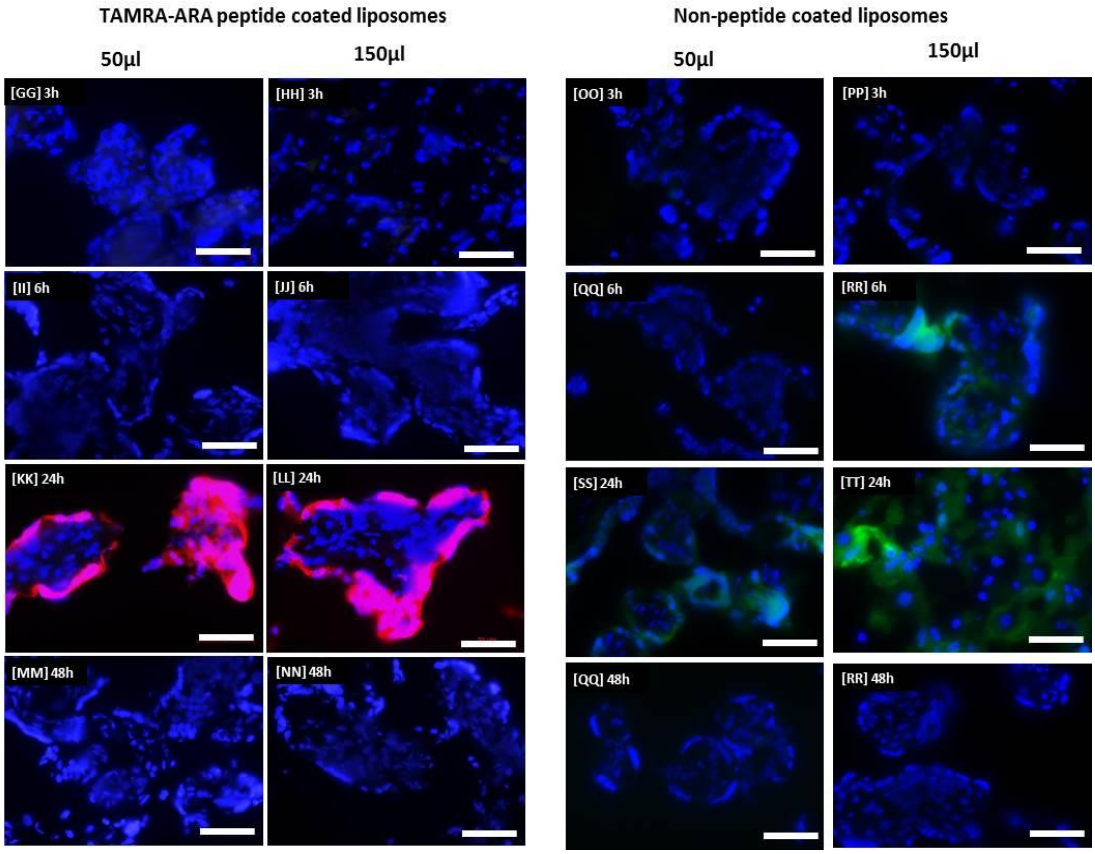

Figure 4.2: Liposome binding to human term placental explants. Liposomes decorated with the placental homing peptides (A-H) FAM-iRGD (green), (I-P) FAM-CGKRK (green), (Q-X) Rh-iRGD (red), (Y-FF) TAMRA-CGGGCGKRK (red) accumulated in the ST of human term placental explants; a low concentration was observed in the VS. Liposomes coated with (GG-NN) TAMRA-ARA also accumulated in the ST at 24h; (OO-RR) uncoated liposomes (green) accumulated to a less extent. Nuclei were stained with DAPI (blue), N=3 placentas, n=3 biopsies from each placenta were examined, 10 images were taken of each sample, representative images are shown (Scale bar = 50µm).

4.3.3 Homing peptide-decorated liposomes bind to the mouse placental labyrinth and spiral arteries throughout gestation

To examine whether homing peptide-decorated liposomes selectively accumulated in the mouse placenta and to assess liposome biodistribution, pregnant C57 mice were injected I.V. at E12.5 with liposomes, which were allowed to circulate for several time points before the mice were subjected to terminal cardiac perfusion.

After 6 h, a fluorescent signal was visible within the placental labyrinth, but not in the junctional zone following injection of iRGD-liposomes and CGKRK-liposomes; this pattern of targeting was observed at all subsequent time points examined (figure 4.3 B, C, E and G). The fluorescent signal persisted up to 48 h (figure 4.3 C & G), but was markedly decreased at 72 h, implying that liposomes were being cleared from, or metabolised by the placental tissue (figure 4.3 D & H). ARA-liposomes modestly accumulated in the labyrinth and junctional zone within 6 h (figure 4.3 I) and persisted for 48 h, with a reduction at 72 h (figure 4.3 L). Non-coated liposomes were observed in the labyrinth and junctional zone, but not until 48 h post-injection (figure 4.3 O) and were still present, but at a lower intensity, at 72 h (figure 4.3 P).

Targeted liposomes were not observed in the major maternal organs or the fetal tissues at any time point studied (figures 4.4-7 A-D and H-K), with the exception of the liver, spleen and kidney (figures 4.4-7 E-G and L-N), which take up all nanoparticles non-selectively (Agemy et al. 2011). Intense red fluorescence was observed in the kidney, liver and spleen at 6 h (figures 4.4 E-G and L-N), which gradually decreased over time. Urine collected from mice 3 h after injection with targeted liposomes was pink in

colour, suggesting that the liposomes and/or peptides were, at least in part, cleared by the kidneys (figure 4.8). iRGD-liposomes were not observed in the liver or spleen after 72 h (figure 4.7 F & G), but a low level of signal was observed in the kidney (figure 4.7 E). CGKRK-liposomes were still present after 72 h in the kidney, liver and spleen at a low concentration (figure 4.7 L-N).

ARA-liposomes were also present in the maternal clearance organs within 6 h (figure 4.4 S-U) and were visible at a lower concentration at 24, 48 and 72 h (figure 4.5-7 S-U). They appeared to accumulate in the clearance organs at a lower concentration than the targeted liposomes. Signal from ARA-liposomes was also detected at low levels in the maternal heart at 24, 48 and 72 h (figure 4.5-7 O) reaching a maximum at 72 h (figure 4.7 O). Non-coated liposomes were not observed in any maternal organs at any time points examined (figure 4.4-7 V-X, Z, BB), except a small amount of green fluorescence in the spleen at 24h and the liver at 48h and 72 h (figure 4.7 AA).

ARA-liposomes and non-coated liposomes were observed in fetal tissues, in particular near the cord insertion point and abdominal region at 48 h (figure 4.6 R & Y), indicating placental transfer of liposomes (or liposomal components) to the fetal circulation.

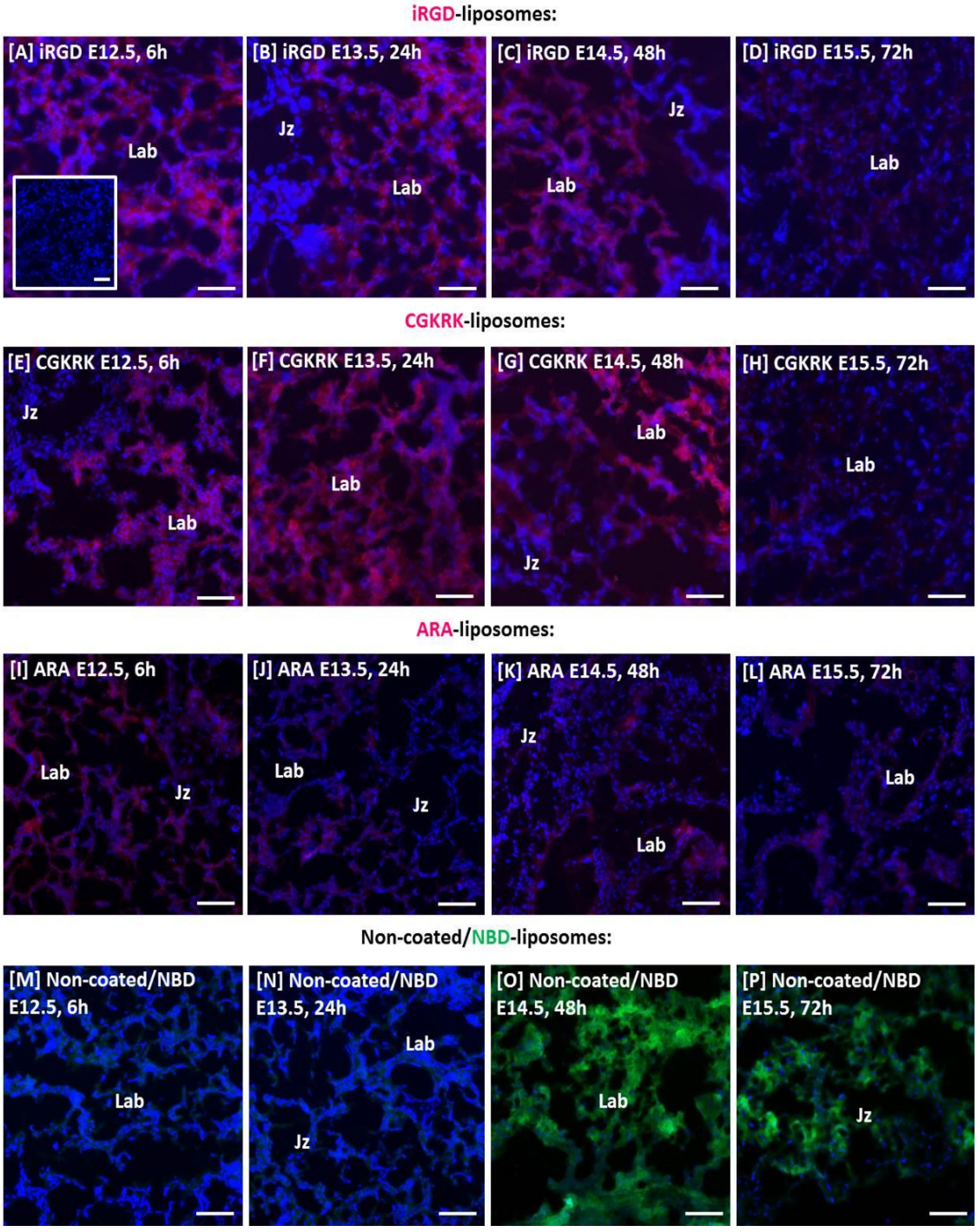

Figure 4.3: Liposome accumulation in the mouse placenta. A-D) Rh-iRGD liposomes (inset shows control tissue), E-H) TAMRA-CGKRK liposomes, I-K) TAMRA-ARA liposomes, M-P) Non-decorated/NBD liposome accumulation in the placental labyrinth (Lab), junctional zone (Jz) and maternal spiral arteries (SA) after I.V (tail vein) injection to pregnant mice at E12.5, collected after 6, 24, 48 and 72 h of circulation and cardiac perfusion. Peptide (red); nuclei stained with DAPI (blue); NBD lipid (green). (scale bar = 100µm).

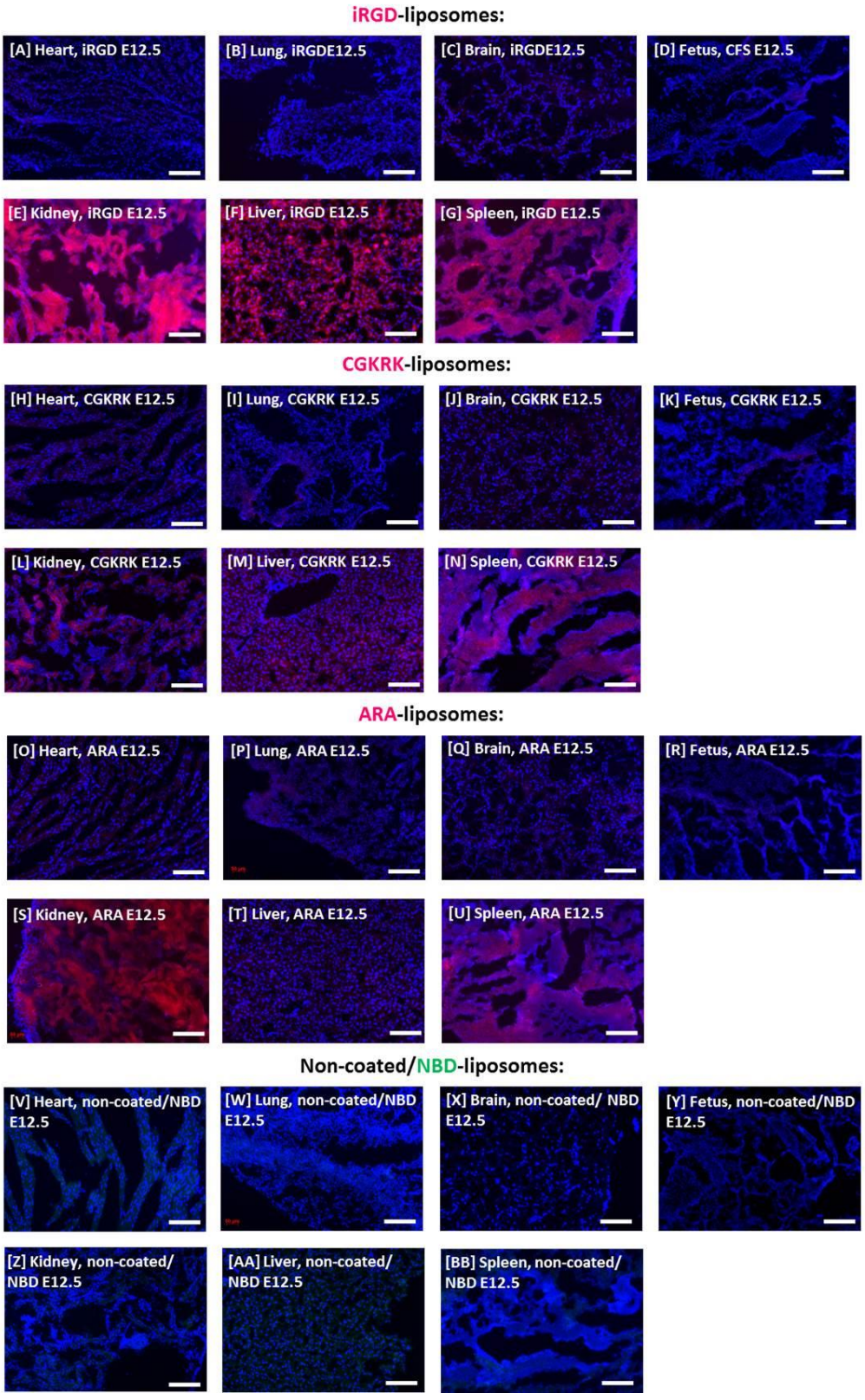

Figure 4.4: Liposome distribution in mouse organs after 6 h circulation. (A-G) Rh-iRGD-liposomes, (H-N) TAMRA-CGKRK-liposomes, (O-U) TAMRA-ARA-liposomes and (V-BB) non-coated/NBD liposome distribution in maternal organs and fetal tissue after I.V injection into pregnant mice at E12.5, collected after 6 h of circulation. Peptide (red); nuclei stained with DAPI (blue); NBD lipid (green), (scale bar = 100µm).

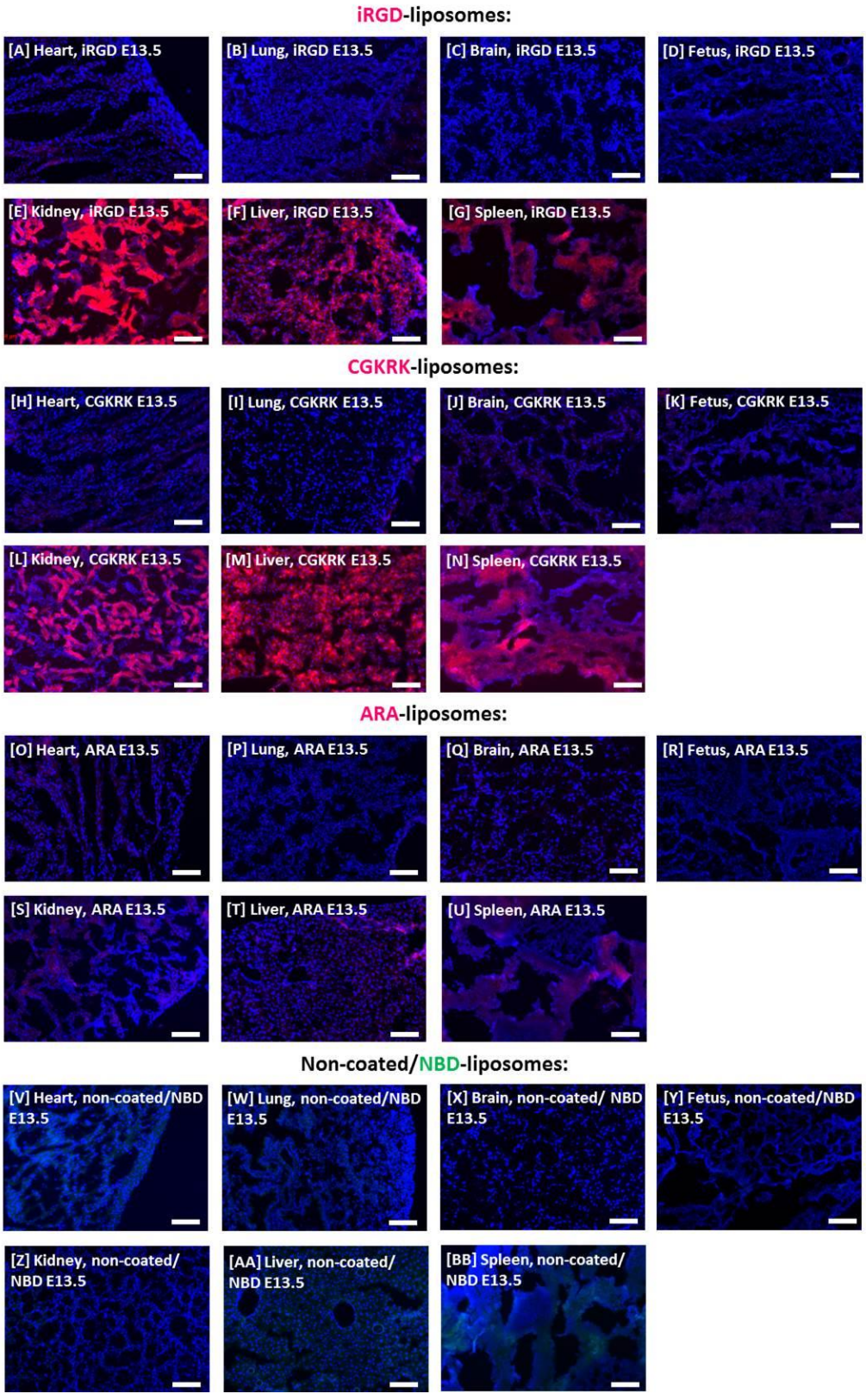

Figure 4.5: Liposome distribution in mouse organs after 24 h circulation. (A-G) Rh-iRGD-liposome, (H-N) TAMRA-CGKRK-liposome, (O-U) TAMRA-ARA-liposome and (V-BB) non-coated/NBD liposome distribution in maternal organs and fetal tissue after I.V injection into pregnant mice at E12.5, collected after 24 h of circulation.. Peptide (red); nuclei stained with DAPI (blue); NBD lipid (green). (scale bar = 100µm).

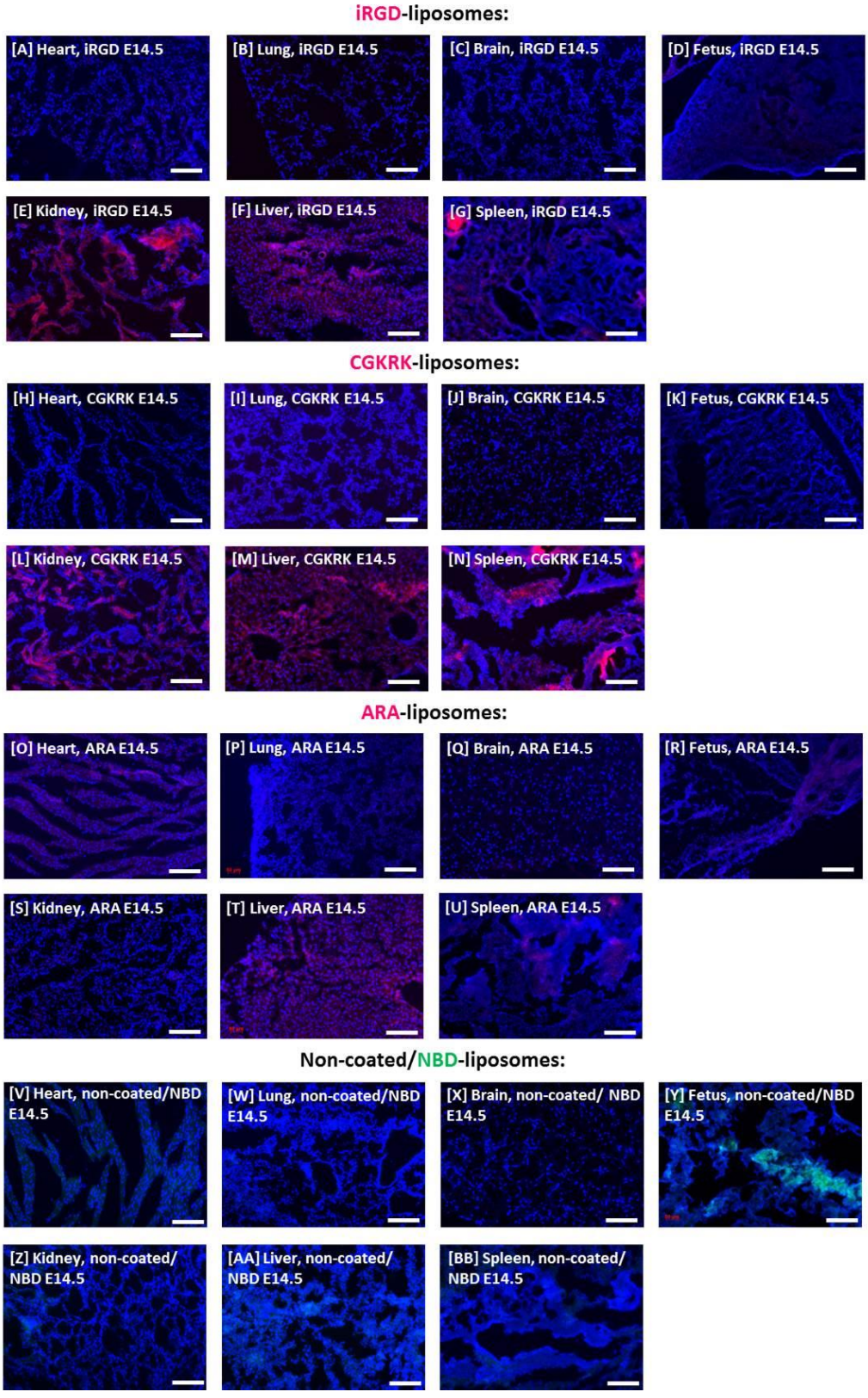

Figure 4.6: Liposome distribution in mouse organs after 48 h circulation. (A-G) Rh-iRGD-liposome, (H-N) TAMRA-CGKRK-liposome, (O-U) TAMRA-ARA-liposome and (V-BB) non-coated/NBD liposome distribution in maternal organs and fetal tissue after I.V injection into pregnant mice at E12.5, collected after 48 h of circulation. Peptide (red); nuclei stained with DAPI (blue); NBD lipid (green). (scale bar = 100µm).

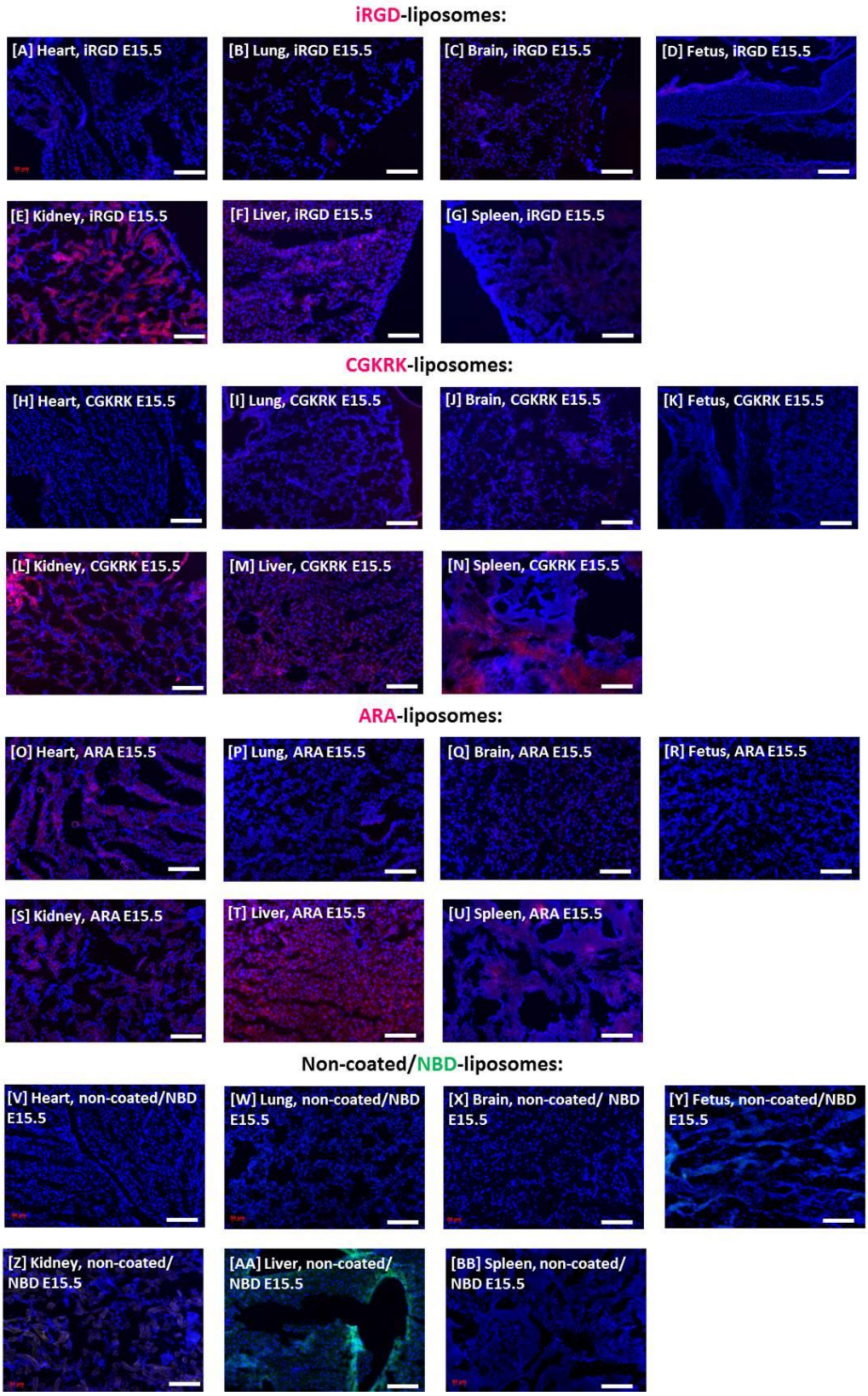

Figure 4.7: Liposome distribution in mouse organs after 72 h circulation. (A-G) Rh-iRGD-liposome, (H-N) TAMRA-CGKRK-liposome, (O-U) TAMRA-ARA-liposome and (V-BB) non-coated/NBD liposome distribution in maternal organs and fetal tissue after I.V injection into pregnant mice at E12.5, collected after 72 h of circulation. Peptide (red); nuclei stained with DAPI (blue); NBD lipid (green). (scale bar = 100µm).

Figure 4.8: Mouse urine collected 3h after I.V. administration of iRGD-liposomes.

4.3.4 Repeated dosing of homing peptide-decorated liposomes highlights different clearance kinetics

As a potential drug treatment study would involve multiple injections of liposomes throughout pregnancy, the biodistribution of liposomes was investigated on E18.5 following intravenous injections on E11.5, 13.5, 15.5, 17.5 with either iRGD-liposomes, CGKRK-liposomes, ARA-liposomes or non-coated-liposomes. This experiment was undertaken to examine the phenomenon of "accelerated blood clearance" (Ishida et al. 2002), whereby a second dose of liposomes is cleared more rapidly than the first dose, as it is recognised more readily by the immune system. As the final dose of liposomes was administered 24 h before the animal was culled, the tissue distribution should be comparable to that observed after one dose administered 24 h previously.

iRGD-liposomes and CGKRK-liposomes were still observed in the placenta at E18.5 (figure 4.9, H & P), suggesting that the final dose administered to the animal remained in the placenta for at least 24 h, and the signal was comparable to that observed after a single dose was administered and allowed to circulate for 24 h. There was lower

fluorescence intensity in the placenta of those animals treated with ARA-liposomes and non-coated/NBD-liposomes (figure 4.9 X & FF) compared to the targeted liposomes, but signal was comparable to that observed after a single administration.

Fluorescence was not observed in any of the maternal organs or fetal tissues of the animal treated with iRGD-liposomes (figure 4.9 A-G), suggesting that the liposomes are cleared rapidly from all organs except the placenta. A fluorescent signal was observed in the clearance organs of the animal treated with CGKRK-liposomes (figure 4.9 M-Q), but was not detected in any other maternal or fetal tissues (figure 4.9 I-L).

A strong fluorescent signal was visible in the spleen of ARA-liposome-treated animals (figure 4.9 W), with a lesser amount present in the liver and kidney (figure 4.9 U & V). Fluorescence was not present in any other maternal organs examined (figure 4.9 Q-S), but was observed in the fetal tissues (figure 4.9 T). Green fluorescence attributed to the NBD fluorophore used to track non-coated liposomes was not observed in any maternal organs examined (figure 4.9 Y-AA & CC-DD), except for the spleen (figure 4.9 EE). A strong fluorescent signal was also observed in the fetal tissues (figure 4.9 BB), particularly near the fetal abdomen, showing placental transfer of the fluorescent lipids.

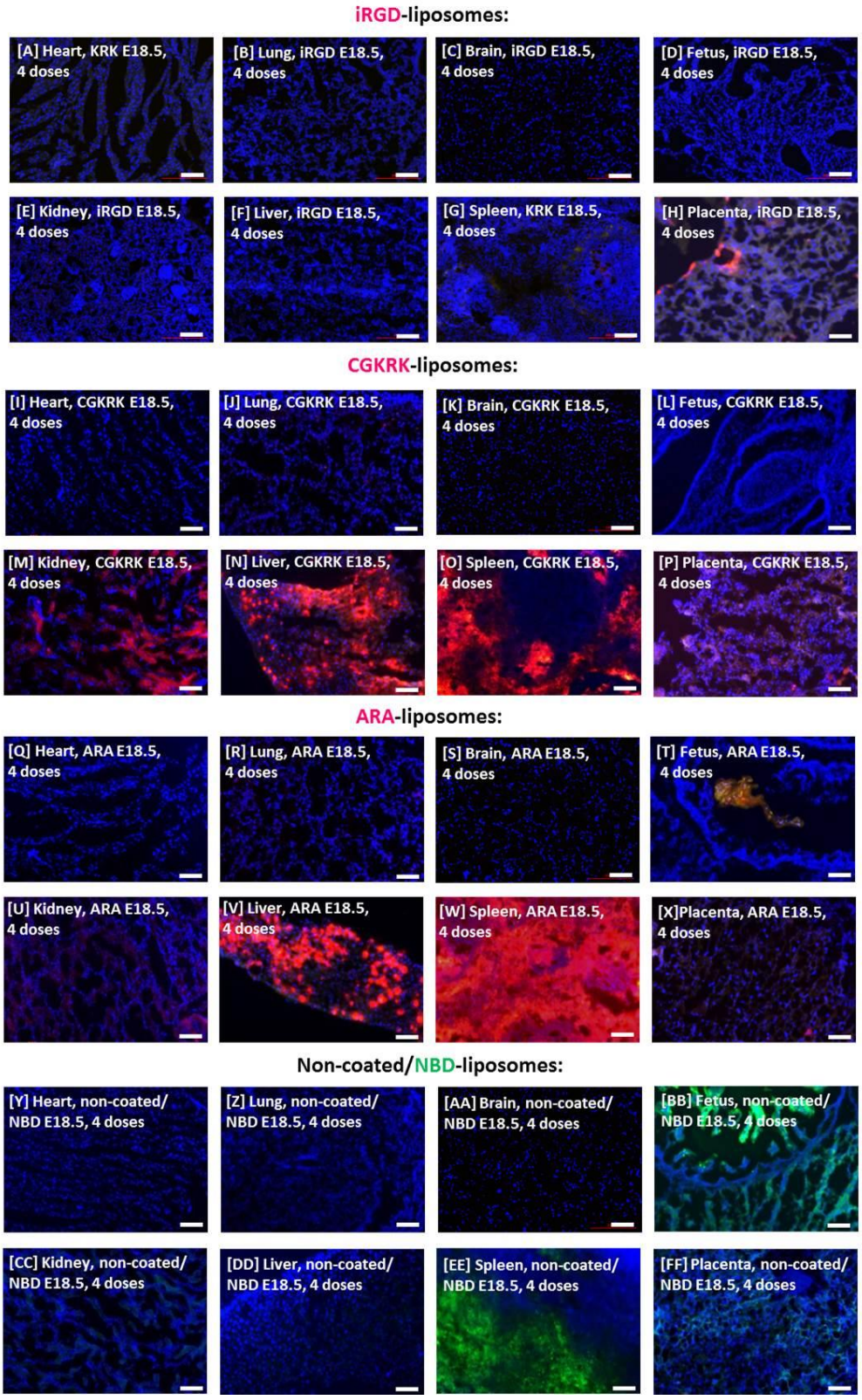

Figure 4.9: Liposome accumulation in the mouse placenta after multiple injections. (A-H) Rh-iRGD-liposome, (I-P) TAMRA-CGKRK-liposome, (Q-X) TAMRA-ARA-liposome, (Y-FF) non-coated/NBD liposome distribution in maternal organs and fetal tissue after four I.V injections into pregnant mice starting at E11.5 and finishing on E17.5, with culling taking place on E18.5. Peptide (red); CFS cargo (green); nuclei stained with DAPI (blue).

4.3.5 Homing peptide-decorated liposomes bind to the syncytiotrophoblast of human placental explants and can deliver an encapsulated cargo.

To assess whether liposomes decorated with homing peptides can deliver an encapsulated cargo to the trophoblast bilayer, human term placental explants were incubated with Rh-iRGD (iRGD/CFS-liposomes) or TAMRA-CGKRK (CGKRK/CFS-liposomes) coated liposomes encapsulating the water-soluble fluorophore CFS (green) for several time points up to 48h. Liposomes coated in the non-targeting sequence Rh-ARA (ARA/CFS-liposomes), and non-coated liposomes both encapsulating CFS (non-coated/CFS liposomes) were used as controls. CFS self-quenches at the concentration encapsulated inside of the liposomes, but fluoresces as it becomes more dilute, thus any green signal observed was due to the release of CFS into the tissue. Non-coated liposomes were not fluorescently tagged with NBD for the purposes of this experiment.

iRGD/CFS-liposomes and CGKRK/CFS-liposomes showed similar accumulation kinetics as those described in section 4.3.2. They began to accumulate in the syncytiotrophoblast within 3 h and remained there for at least 48 h (figure 4.10 A-H). Co-localisation of the homing peptides and CFS was observed after 3 h, indicating liposomal release of the cargo (figure 4.10 A, E); the fluorescence intensity increased with time (figure 4.10 A-D, E-H) suggesting sustained delivery. After 24 h, CFS fluorescence was detected in stromal tissue, showing that the fluorophore was able to penetrate the trophoblast bilayer (figure 4.10 C, G). This accumulation of CFS in the stroma was still observed after 48 h (figure 4.10 D, H).

ARA/CFS-liposomes also accumulated in the syncytiotrophoblast, but at a much slower rate and they did not release CFS (figure 4.10 I-L). They were still visible in the syncytiotrophoblast at 48 h, which is different from what was observed when ARA-liposomes were incubated with placental explants in section 4.1.2, and were only visible in the syncytiotrophoblast at 24 h. Non-coated liposomes were not detected and green fluorescence was not observed, indicating that the non-coated liposomes did not release CFS (figure 4.10 M-P).

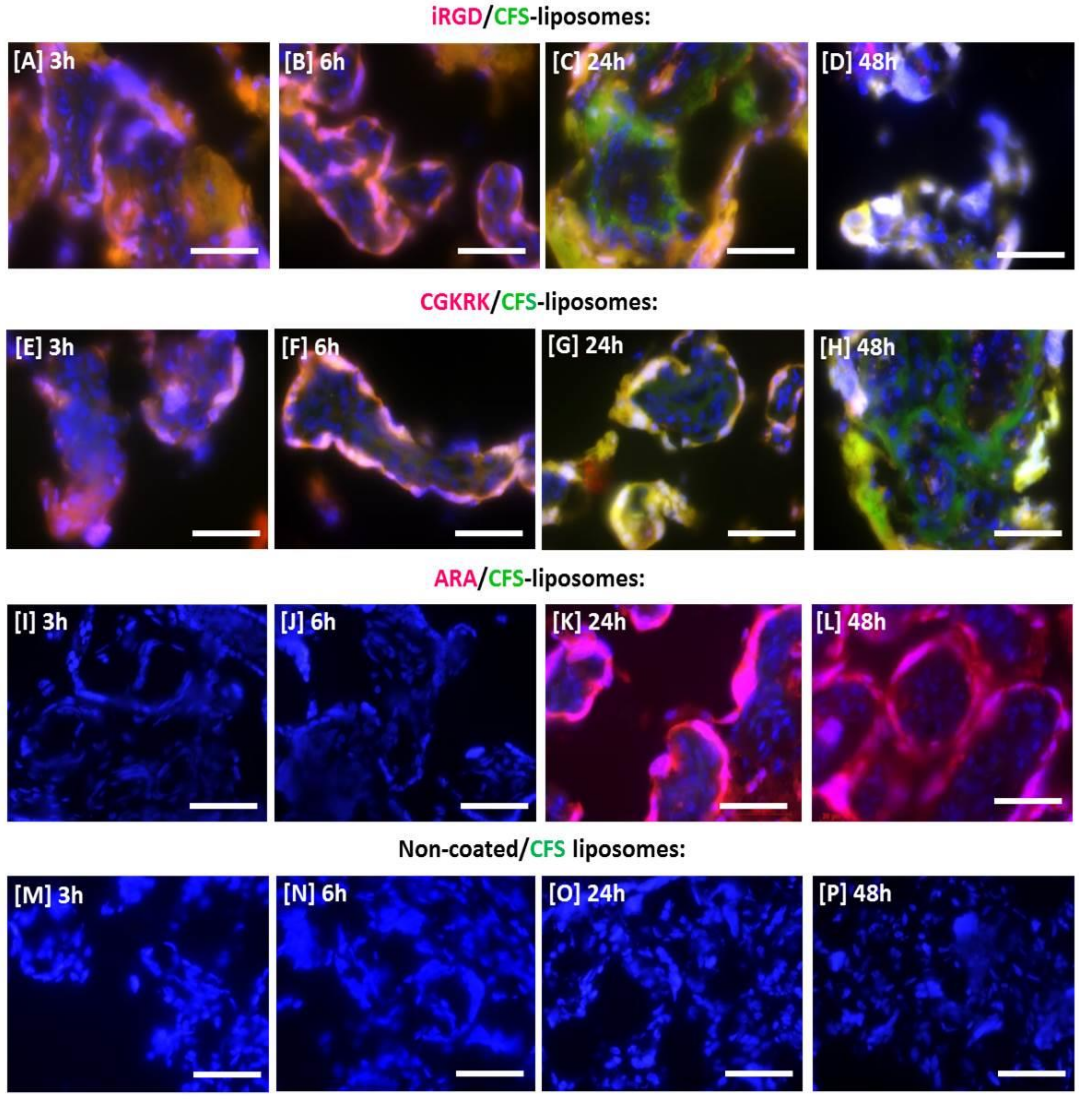

Figure 4.10: Liposome accumulation and cargo distribution in term human placental explants. (A-D) Rh-iRGD/CFS liposomes, (E-H) TAMRA-CGKRK/CFS liposomes, (I-K) TAMRA-ARA/CFS liposomes, (M-P) Non-coated/CFS liposome accumulation in human term placental explants, after incubation for 3, 6, 24 and 48 h. Peptide (red); CFS cargo (green); nuclei stained with DAPI (blue). (Scale bar = 50μm).

4.3.6 Homing peptide-decorated liposomes encapsulating a fluorescent drug analogue bind to the mouse placental labyrinth and release their contents

To examine the capability of liposomes decorated in placental homing peptides to selectively deliver a cargo to the placenta in vivo, CFS was encapsulated inside of the liposomes and injected into pregnant C57 mice. The mice were injected intravenously on E12.5 with iRGD/CFS-liposomes, CGKRK/CFS-liposomes, ARA/CFS liposomes or non-coated/CFS liposomes. In a similar manner to that reported in section 4.3.3, targeted liposomes encapsulating CFS were observed in the placental labyrinth within 6 h (figure 4.11 A), with CGKRK/CFS-liposomes also detectable within the endothelium of maternal spiral arteries (figure 4.11 E) as previously described (Harris et al. 2012) (Harris, 2012). The appearance of a yellow colour on the image shows co-localisation of the red fluorescently tagged homing peptide and the green CFS, indicating that CFS is released from the iRGD/CFS-liposomes (figure 4.11 A) and the CGKRK/CFS-liposomes (figure 4.11 E) within 6 h. Accumulation of the targeted liposomes and release of CFS occurred within the labyrinth and spiral arteries and was not observed in the junctional zone for all time points examined (figure 4.11 A-H). Fluorescence attributed to the homing peptide was evident until 72 h (figure 4.11 D, H), and the fluorescence intensity of the green CFS cargo diminished over time, indicating drug clearance. In particular, iRGD/CFS-liposomes accumulated in the spiral arteries and released CFS at all time points examined, with figure 4.11 D showing an example of accumulation within the epithelium and the surrounding perivascular area.

ARA/CFS-liposomes modestly accumulated in the labyrinth, spiral arteries and to a lesser extent in the junctional zone (figure 4.11 I-L), in a distribution similar to that

described in section 4.3.3. A small amount of CFS release was observed from 24-72 h (figure 4.11 J-L), but not to the same extent as that seen with the targeted liposomes. Non-coated/CFS liposomes appeared to release CFS in the labyrinth within 24 h (figure 4.11 N). The highest intensity signal from CFS release was observed at 48 h (figure 4.11 O) and this diminished by 72 h (figure 4.11 P)

Targeted liposomes were observed in the clearance organs at high concentrations within 6 h (figure 4.12 E-G, L-N), in a distribution similar to that described in section 4.3.3. Small amounts of green fluorescence were observed in the liver of CGKRK/CFS-liposome treated animals after 6 h (figure 4.12 M), and the spleen after 24 h (figure 4.13 M) indicating that some free CFS was present; however the majority of the signal observed in the clearance organs at 24h and beyond was that of the red, peptide-coupled fluorophore and not the CFS cargo. The intensity of fluorescence of iRGD/CFS-liposomes in the maternal clearance organs diminished over time, showing that the peptide/liposome conjugate was cleared over 72 h, however a low intensity signal was still observed in the kidney at 72 h (figure 4.15 L). Targeted liposomes and CFS were not observed in any other maternal or fetal tissues (figure 4.12-4.15 A-D & H-K).

ARA/CFS-liposomes were also observed in the maternal clearance organs within 6 h (figure 4.12 S-U), but at a lower concentration when compared with iRGD/CFS- or CGKRK/CFS-liposomes. Again the predominant signal observed came from the red peptide; signal decreased over time and a small amount was visible in the liver at 72 h (figure 4.15 T). Liposomes were not observed in any other maternal organs (figure 4.12-15 O-R), but were present in fetal tissues within 24 h (figure 4.13 R) and persisted for

72 h (figure 4.15 R), indicating placental transfer of both the liposome and the payload into the fetal circulation.

Non-coated/CFS liposomes were not fluorescently tagged, but CFS release was observed in the maternal liver at 24 h (figure 4.13 AA); a higher intensity was observed in the liver at 48 h (figure 4.14AA), but this was absent at 72 h (figure 4.15AA), suggesting more rapid clearance of non-coated liposomes than ARA-decorated liposomes. CFS from non-coated liposomes was not observed in any other maternal organs (figure 4.12-15 V-Y), but was present in fetal tissues at 24 h and 48 h (figure 4.13-14 Y).

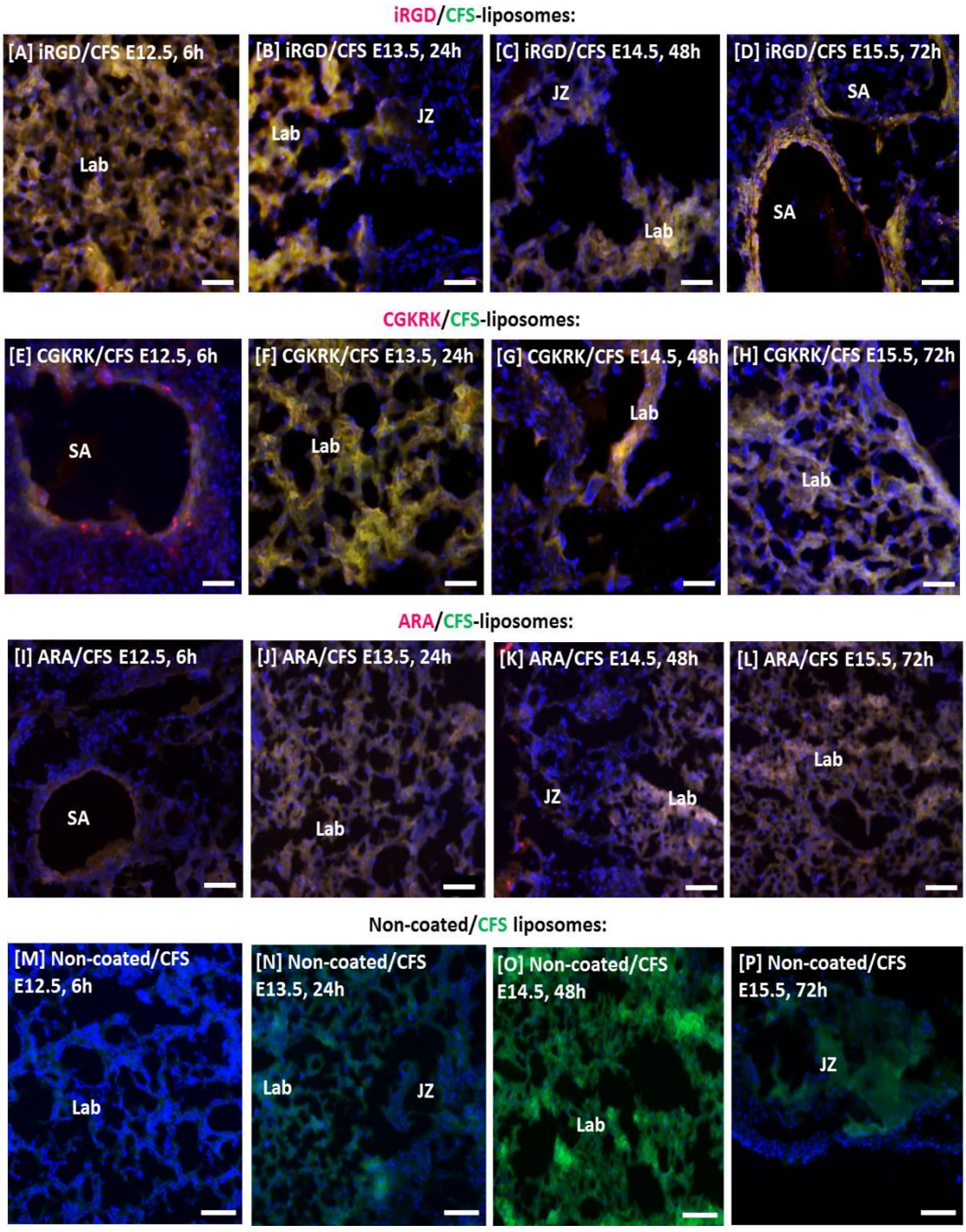

Figure 4.11: Liposome accumulation and cargo distribution in the mouse placenta. (A-D) Rh-iRGD/CFS liposomes, (E-H) TAMRA-CGKRK/CFS liposomes, (I-K) TAMRA-ARA/CFS liposomes, (M-P) Non-coated/CFS liposome accumulation in the placental labyrinth (Lab), junctional zone (JZ) and maternal spiral arteries (SA) after I.V injection to pregnant mice at E12.5, collected after 6, 24, 48 and 72 h of circulation and cardiac perfusion. Peptide (red); CFS cargo (green); nuclei stained with DAPI (blue). (scale bar = 100µm).

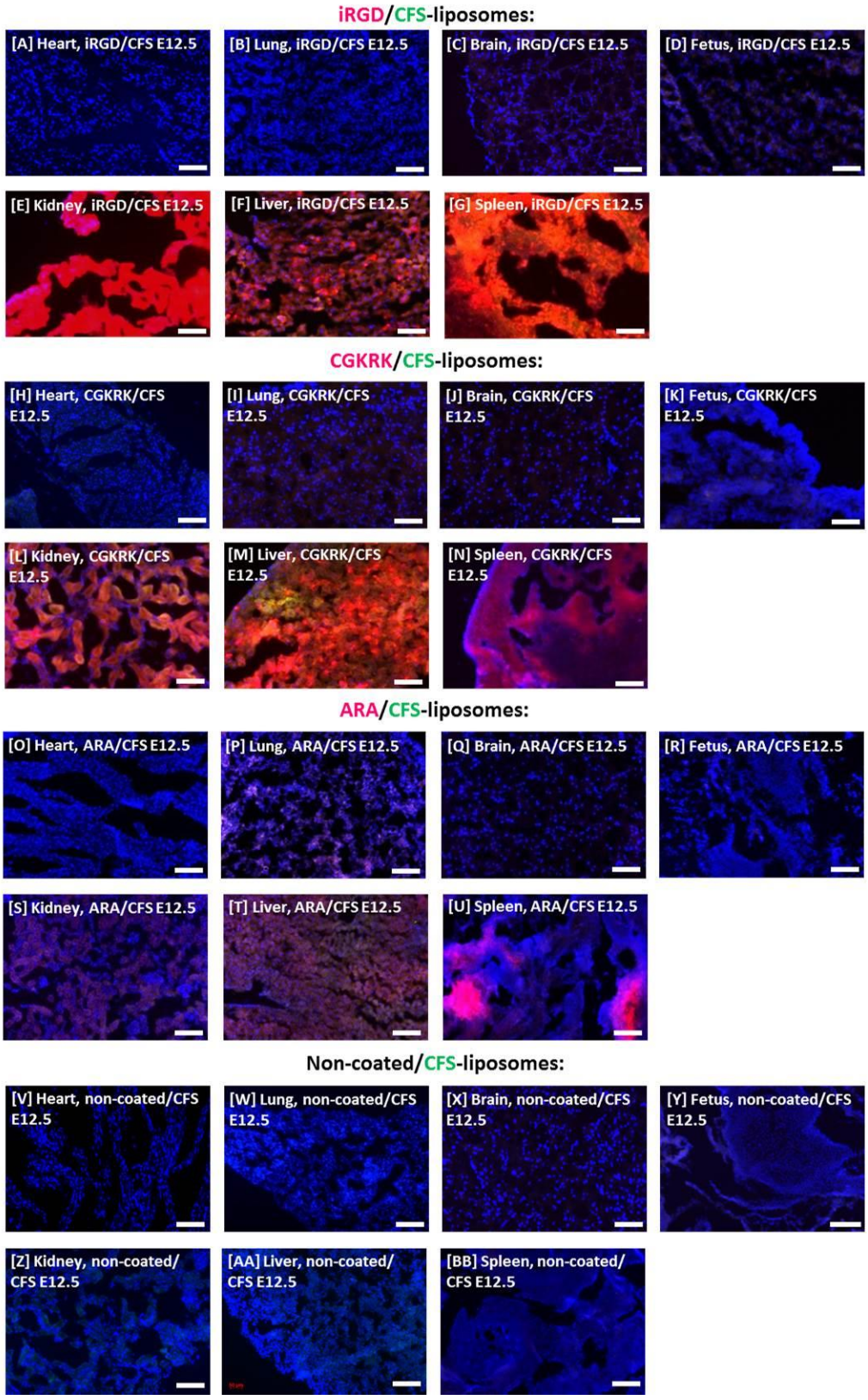

Figure 4.12: Liposome and cargo distribution in mouse organs after 6 h circulation. (A-G) Rh-iRGD/CFS-liposome, (H-N) TAMRA-CGKRK/CFS-liposome, (O-U) TAMRA-ARA/CFS-liposome, (V-BB) non-coated/CFS-liposome distribution in maternal organs and fetal tissue after I.V injection into pregnant mice at E12.5, collected after 6 h of circulation. Peptide (red); CFS cargo (green); nuclei stained with DAPI (blue). (scale bar = 100µm).

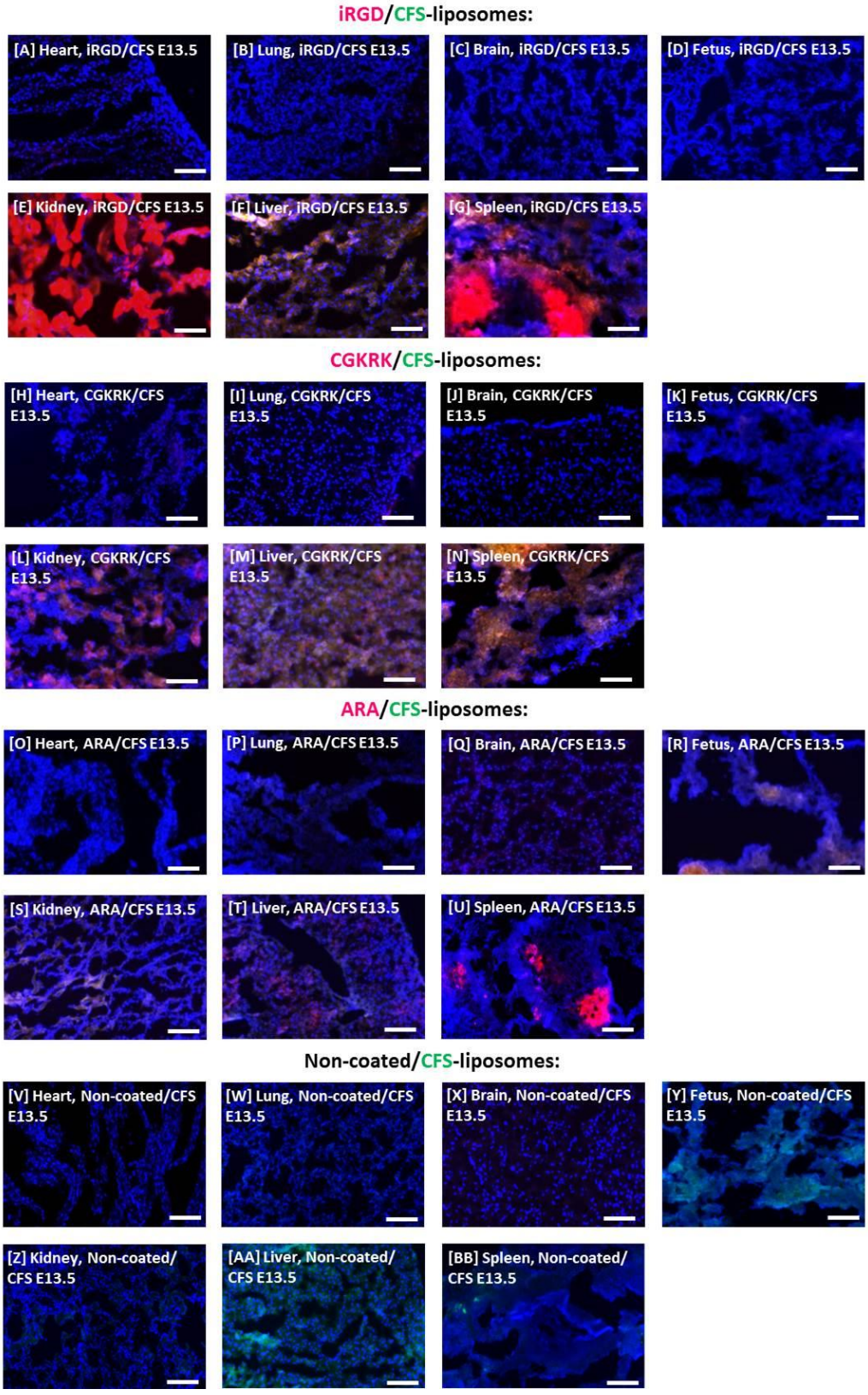

Figure 4.13: Liposome and cargo distribution in mouse organs after 24 h circulation. (A-G) Rh-iRGD/CFS-liposome, (H-N) TAMRA-CGKRK/CFS-liposome, (O-U) TAMRA-ARA/CFS-liposome, (V-BB) non-coated/CFS-liposome distribution in maternal organs and fetal tissue after I.V injection into pregnant mice at E12.5, collected after 24 h of circulation. Peptide (red); CFS cargo (green); nuclei stained with DAPI (blue). (scale bar = 100µm).

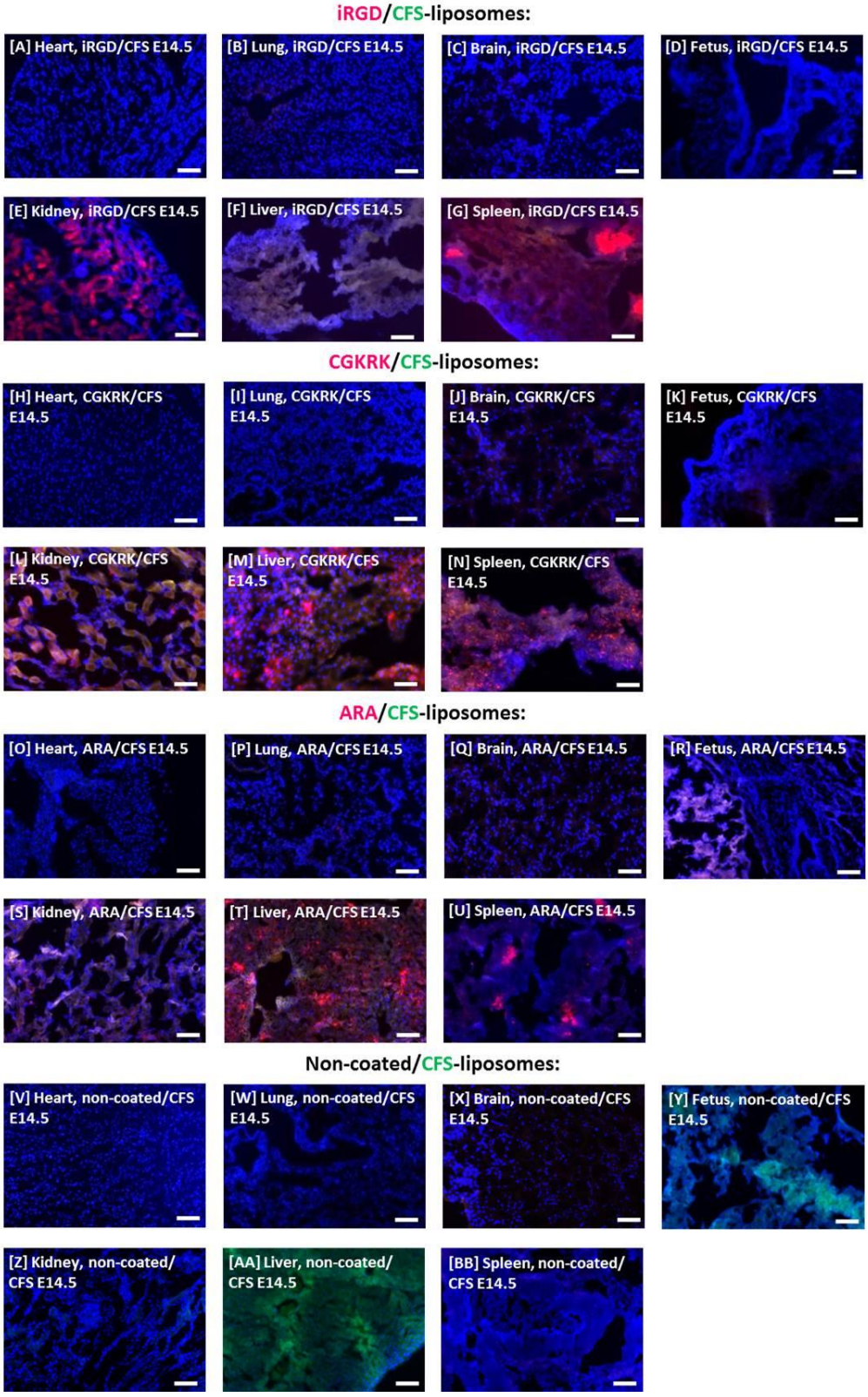

Figure 4.14: Liposome and cargo distribution in mouse organs after 48 h circulation. (A-G) Rh-iRGD/CFS-liposome, (H-N) TAMRA-CGKRK/CFS-liposome, (O-U) TAMRA-ARA/CFS-liposome, (V-BB) non-coated/CFS-liposome distribution in maternal organs and fetal tissue after I.V injection into pregnant mice at E12.5, collected after 48 h of circulation. Peptide (red); CFS cargo (green); nuclei stained with DAPI (blue). (scale bar = 100µm).

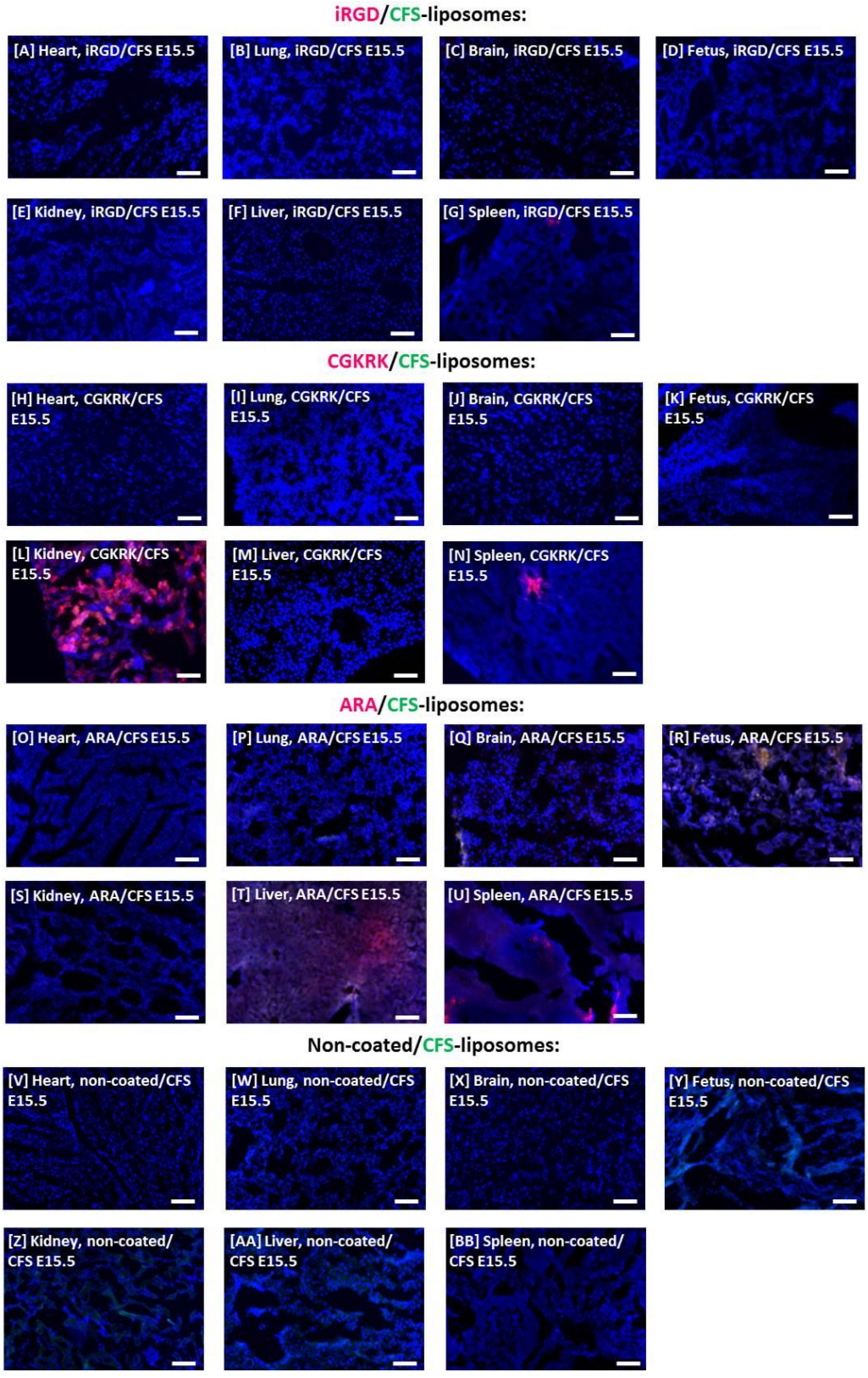

Figure 4.15: Liposome and cargo distribution in mouse organs after 72 h circulation. (A-G) Rh-iRGD/CFS-liposome, (H-N) TAMRA-CGKRK/CFS-liposome, (O-U) TAMRA-ARA/CFS-liposome, (V-BB) non-coated/CFS-liposome distribution in maternal organs and fetal tissue after I.V injection into pregnant mice at E12.5, collected after 72 h of circulation. Peptide (red); CFS cargo (green); nuclei stained with DAPI (blue). (scale bar = 100µm).

4.4 Discussion

The uptake kinetics and tissue distribution of peptides, lipids and CFS after targeted liposome exposure were tracked in human placental tissue ex vivo and in mice in vivo using fluorescence microscopy. Table 4.1 provides a summary of the localisation and biodistribution data for each liposomal formulation.

Our initial experiments demonstrated that we were able to replicate the findings of King et al (King et al. 2016), confirming that the homing peptides iRGD and CGKRK accumulated in the placental syncytiotrophoblast of first trimester and term placental explants. This allowed us to conjugate the homing peptides to liposomes to produce targeted liposomes that were examined for their ability to target the human and mouse placenta. CFS was encapsulated into targeted and non-targeted liposomes to track drug release and biodistribution over time. It is considered as a good candidate because it is self-quenching at high concentrations when encapsulated inside liposomes, but fluoresces upon release, (Weinstein et al. 1977), it doesn't become incorporated into the liposomal lipid bilayer (R Bajoria et al. 1997), it can be quantified by spectroscopy, it is non-toxic to mice, cells and tissues, and has previously been used to examine liposomal drug transfer from maternal circulation to fetal circulation in the ex vivo dual perfused human placenta model (R Bajoria & Contractor 1997; Bajoria et al. 2013; R. Bajoria & Contractor 1997).

(A)	Human placental tissue				Mouse tissues																	
					Placental Labyrinth		Placental Junctional zone		Maternal brain		Maternal heart		Maternal lung		Maternal liver		Maternal kidney		Maternal spleen		Fetal tissues	
Liposome composition	Time (h)	Pep	CFS	Time (h)	Pep	CFS	Pep	CFS	Pep	CFS	Pep	CFS	Pep	CFS	Pep	CFS	Pep	CFS	Pep	CFS	Pep	CFS
iRGD-liposomes	3	+	/	6	++	/	-	/	-	/	-	/	-	/	++	/	++	/	++	/	-	/
	6	+	/	24	+++	/	-	/	-	/	-	/	-	/	+	/	+++	/	+	/	-	/
	24	++	/	48	++	/	-	/	-	/	-	/	-	/	+	/	+	/	+	/	-	/
	48	+++	/	72	+	/	-	/	-	/	-	/	-	/	-	/	+	/	-	/	-	/
CGKRK- liposomes	3	+	/	6	++	/	-	/	-	/	-	/	-	/	+	/	+	/	+	/	-	/
	6	+	/	24	+++	/	-	/	-	/	-	/	-	/	++	/	++	/	++	/	-	/
	24	++	/	48	+++	/	-	/	-	/	-	/	-	/	+	/	+	/	+	/	-	/
	48	+++	/	72	+	/	-	/	-	/	-	/	-	/	+	/	+	/	+	/	-	/
ARA- liposomes	3	-	/	6	+	/	+	/	-	/	-	/	-	/	-	/	++	/	+	/	-	/
	6	-	/	24	+	/	+	/	-	/	+	/	-	/	+	/	+	/	+	/	-	/
	24	++	/	48	+	/	+	/	-	/	+	/	-	/	+	/	+	/	-	/	+	/
	48	-	/	72	+	/	+	/	-	/	+	/	-	/	+	/	+	/	+	/	-	/
Non-coated liposomes	3	-	/	6	-	/	-	/	-	/	-	/	-	/	-	/	-	/	-	/	-	/
	6	+	/	24	-	/	-	/	-	/	-	/	-	/	-	/	-	/	+	/	-	/
	24	+	/	48	++	/	++	/	-	/	-	/	-	/	-	/	-	/	-	/	+	/
	48	-	/	72	+	/	+	/	-	/	-	/	-	/	+	/	-	/	-	/	-	/

(B)	Human placental tissue				Mouse tissues																	
					Placental Labyrinth		Placental Junctional zone		Maternal brain		Maternal heart		Maternal lung		Maternal liver		Maternal kidney		Maternal spleen		Fetal tissues	
Liposome composition	Time (h)	Pep	CFS	Time (h)	Pep	CFS	Pep	CFS	Pep	CFS	Pep	CFS	Pep	CFS	Pep	CFS	Pep	CFS	Pep	CFS	Pep	CFS
iRGD/CFS-liposomes	3	+	+	6	++	++	-	-	-	-	-	-	-	-	++	-	+++	-	+++	-	-	-
	6	+	+	24	++	++	-	-	-	-	-	-	-	-	+	+	+++	-	++	+	-	-
	24	++	++	48	++	++	-	-	-	-	-	-	-	-	+	+	+	-	+	-	-	-
	48	++	++	72	+	+	-	-	-	-	-	-	-	-	-	-	-	-	-	-	-	-
CGKRK/CFS-liposomes	3	+	-	6	++	++	-	-	-	-	-	-	-	-	++	+	++	+	+	-	-	-
	6	+	+	24	++	++	-	-	-	-	-	-	-	-	+	+	+	+	+	+	-	-
	24	++	++	48	++	++	-	-	-	-	-	-	-	-	+	+	+	+	+	-	-	-
	48	++	++	72	+	+	-	-	-	-	-	-	-	-	-	-	+	-	+	-	-	-
ARA/CFS-liposomes	3	-	-	6	+	-	+	-	-	-	-	-	+	-	+	+	+	-	+	-	-	-
	6	-	-	24	+	+	+	+	-	-	-	-	-	-	+	-	+	+	+	-	+	+
	24	++	-	48	+	+	+	+	-	-	-	-	-	-	+	+	+	+	+	-	+	+
	48	++	-	72	+	+	+	+	-	-	-	-	-	-	+	-	-	-	-	-	+	+
Non-coated/CFS liposomes	3	-	-	6	/	-	/	-	/	-	/	-	/	-	/	-	/	-	/	-	/	-
	6	-	-	24	/	+	/	+	/	-	/	-	/	-	/	+	/	+	/	+	/	+
	24	-	-	48	/	++	/	++	/	-	/	-	/	-	/	++	/	-	/	-	/	++
	48	-	-	72	/	+	/	+	/	-	/	-	/	-	/	-	/	-	/	-	/	+

Table 4.1: Summary of localisation and biodistribution data in human placental explants and mice. (A) Liposome distribution, (B) liposome and CFS cargo distribution.

4.4.1 Homing peptide-decorated liposomes accumulate in the human placental syncytiotrophoblast and can release their cargo there

Empty homing peptide-decorated liposomes and those encapsulating CFS accumulated in the syncytiotrophoblast of the human placental explants in a similar manner to free peptides, but with slower kinetics. Once internalised, co-localisation of the homing peptides and CFS was observed, with the fluorescence intensity increasing over time, suggestive of sustained release and uptake of the cargo. It has previously been reported that free peptides and peptide-decorated micelles accumulate to a similar extent in the tumor parenchyma in vivo, but do not accumulate in normal tissues (Sugahara et al. 2009). Therefore our hypothesis that homing peptide-decorated liposomes would show similar localisation in human placental explants as that of free homing peptides was proven to be correct.

Non-targeted empty and CFS encapsulating liposomes also accumulated in the syncytiotrophoblast, but at a much slower rate. A reason for this uptake by placental explants could be due to the presence of choline in the phospholipid bilayer. Choline, a catabolic product of phosphatidylcholine (Li & Vance 2008) (a constituent of DSPC), is necessary to support fetal development throughout pregnancy. Choline transporters are expressed on the placental surface to ensure transport of choline to the fetus to support cell membrane lipid synthesis (Baumgartner et al. 2015); liposomes containing choline may be internalised into the syncytiotrophoblast in part via these receptors.

It is important to note that after 24 h in culture, a proportion of the CFS entered the villous stroma underlying the trophoblast bilayer, indicating the possibility of drug

transfer into fetal circulation when administered in vivo. This phenomenon would need to be investigated in more detail with additional preclinical testing to ensure fetal safety; the ex vivo dual perfused human placenta would be an ideal model to undertake these studies in.

Although ARA-liposomes and non-coated liposomes were taken up by the placental explants, there was no evidence of CFS release from these liposomes. Lack of CFS release suggests that these control formulations are not internalised and degraded by placental explants in the same way as targeted liposomes, possibly due to the lack of cell-penetrating peptide. It has previously been reported that the uptake and drug release from non-coated anionic liposomes containing CFS by isolated primary term human cytotrophoblast cells was much greater than that from neutral or cationic liposomes over a 3 h period (R Bajoria et al. 1997). Our non-coated liposomes are slightly anionic (approximate ZP = -6mV), which suggests that they, along with the CFS cargo should be internalised by placental explants. However, it is likely that the cell membrane of primary cytotrophoblasts does not express the same repertoire of receptors as the overlying syncytiotrophoblast layer (which is exposed to the maternal circulation); thus rates of binding and cannot be directly compared in these two different models.

The uptake kinetics of peptide-decorated liposomes was much slower than that of free homing peptides and there may be for several reasons for this. Conjugation of free peptide to the liposomal surface causes it to be held in a rigid conformation, so it is not free to orientate itself to optimally bind to its target ligand, making binding less likely to occur. Also, it has been reported that multivalent display of the homing peptides on the liposome surface increases the avidity of the homing peptides binding to cell surface

epitopes (Ruoslahti et al. 2010). However, this effect depends on the distribution of the epitopes across the plasma membrane (Ruoslahti et al. 2010). If the distance between peptide receptors is too great, multivalency will not improve uptake. The addition of a surface PEG layer can also shield the distal end of the peptide, preventing it from actively targeting the tissue as quickly (Sawant & Torchilin 2012); however, as we still observed selective targeting with homing peptide-decorated liposomes compared to controls, this doesn't stop our liposomes from binding to the tissue, but may be a limiting factor.

It is clear that the presence of homing peptides on the liposome surface improves liposome uptake and promotes drug release in the human explant model. This is to be expected as both the iRGD and CGKRK sequences have proven cell penetrating properties, that improve cellular uptake of attached cargo (Sugahara et al. 2009). Several studies suggest that undecorated liposomes and their contents are internalized into cells either by fusion with the cell membrane or by endocytosis (Papahadjopoulos et al. 1973; Poste & Papahadjopoulos 1976; Düzgüneş & Nir 1999), with endocytosis being the more likely mechanism in the placenta (R Bajoria et al. 1997). However, the iRGD and CGKRK homing peptide sequences are known to be internalised into cancer cells by receptor-mediated uptake; following binding to integrin α_v as described in Section 1.5.1 (Sugahara et al. 2009) and it is believed that CGKRK is internalised by a similar, but unknown receptor-mediated mechanism. The change in kinetics observed between free peptide and peptide-decorated liposomes could be due to a difference in uptake mechanisms induced by (i) multivalent display of the homing peptide and (ii) the size, charge and/or properties of the liposome itself. The exact uptake mechanism needs

to be examined in further detail, possibly by using receptor blocking antibodies and endocytotic pathway inhibitors.

Currently, both free homing peptide and peptide-decorated liposomes predominantly remain confined to the outer syncytiotrophoblast layer of the placental explants. This syncytial confinement is different from what has been observed using peptide-decorated quantum dots (QD) (M. Bayatti; personal communication): after incubation for 24 h with first trimester explants, non-coated QDs were present in the syncytiotrophoblast only, whereas iRGD-decorated QD penetrated the syncytiotrophoblast and were present in the underlying cytotrophoblasts. Again, these results show that the route and mechanism of peptide binding and uptake differs depending on the attached cargo.

Although uptake of targeted liposomes by human placental tissue has not been examined before, our results support those of several other studies performed in a variety of cell lines. Liposomes decorated with iRGD peptide accumulated in HUVECs to a greater extent than non-coated liposomes after 4 h of incubation, (Nallamothu et al. 2006) accumulating over a similar time course to our targeted liposomes. Liposomes decorated with the homing peptide HAIYPRH, which selectively binds to the transferrin receptor, were incubated with the human ovarian carcinoma cell line A2780, which overexpresses the transferrin receptor. As observed in our experiments, non-targeted liposomes were taken up by the cells, but not to the same extent as targeted liposomes, which reached 3.7 fold higher levels than uptake of non-targeted liposomes (Wu et al. 2015). Finally, liposomes encapsulating VEGF siRNA to limit angiogenesis in tumour vasculature, and docetaxel, a chemotherapeutic, were decorated in two receptor-specific peptides: Angiopep-2, which targets the low-density lipoprotein receptor-related protein

overexpressed on the blood brain barrier and glioblastoma cells, and the neuropilin-1 receptor tLyP-1, which will mediate tissue penetration in a similar way to the iRGD peptide. The liposomes were incubated with four different cell lines; the human glioblastoma cell line U87 MG, bovine brain microvascular endothelial cells (a model of the blood brain barrier), the rat glial tumor cell line C6 and the human glial tumor cell line U251 MG. Again, similar results to ours were observed: all liposome formulations were taken up by all cell lines, but liposomes decorated with both homing peptides showed the greatest up take (Yang et al. 2014).

Our results are also supported by several other studies that have examined drug release from peptide decorated-liposomes. Combretastatin A-4, which has a similar molecular weight to CFS encapsulated in a similar liposome formulation to ours, was completely released from RGD-decorated liposomes within 10 h of incubation in saline at 37 ºC (Zhang et al. 2010). Liposomes decorated in RGD peptide and encapsulating doxorubicin were incubated with the melanoma cell line B16F10 or HUVECs for up to 3 h (Zhang et al. 2010). Significantly higher concentrations of doxorubicin were observed in both cell lines when incubated with targeted-liposomes, compared to incubation with non-targeted liposomes, showing that RGD improved cellular uptake of the drug. The efficacy of the doxorubicin was also improved, with more of the cells dying as a result of exposure to the RGD/doxorubicin liposomes. The same liposomes were administered to mice bearing B16F10 tumours (Du et al. 2011); treatment with targeted liposomes significantly reduced the tumour size and increased the mouse survival rates when compared with non-targeted liposome treatment. Similar results have been reported when mice bearing S^{180} sarcoma were administered RGDF-targeted liposomes encapsulating doxorubicin (Du et al. 2011); treatment reduced tumour size

and increased survival rates when compared with non-targeted liposomes encapsulating doxorubicin, again demonstrating enhanced efficacy. These findings support our observations that targeted-liposomes release their encapsulated drug more effectively than non-targeted liposomes and that a greater concentration of drug release occurs at the target site.

4.4.2 Homing peptide-decorated liposomes accumulate in the mouse placental labyrinth and can release their cargo there

Human placental explants represent a good model to examine liposome binding and uptake, as they are a physiologically relevant model used to study placental growth and function (Forbes et al. 2008). If liposomes were injected intravenously into a pregnant woman, they would enter the intervillous space via the spiral arteries and encounter the syncytiotrophoblast of the placental villi; the same region liposomes encounter when they are incubated with human placental explants in vitro. However, it is only possible to assess the targeting ability of homing-peptide decorated liposomes in vivo. Thus, the use of pregnant mice permitted assessment of tissue distribution of the targeted and non-targeted liposomes and allowed us to investigate whether fetal transfer of the liposomes or liposomally encapsulated cargo occurred.

As the premise of this study was to develop a means of selectively targeting the placenta, whilst maintaining its barrier function, we purposely restricted liposome administration until after E11.5, when the placental barrier is considered to be fully formed and can limit the transfer of nanoparticles and drugs to the fetus (Yang et al. 2012). We believe that fetal transfer would occur prior to this time point and wanted to

actively avoid this. For these reasons, pregnant C57 mice at E11.5 were used to examine the tissue distribution and drug delivery capabilities of the liposomes in vivo.

Table 4.1 shows that homing peptide- decorated liposomes accumulated in the mouse placental labyrinth, but not in the junctional zone at any time point examined; similar to the observations of King et al (King et al. 2016) when free peptides were injected intravenously into pregnant mice, but with slower uptake kinetics. Within the placenta, the homing peptide-decorated liposomes were able to release their cargo in the labyrinth, recapitulating what was observed when homing-peptide decorated liposomes were incubated with human placental explants. ARA-liposomes accumulated to a much lower extent in the placental labyrinth and also accumulated in the junctional zone and released CFS. Non-coated liposomes accumulated in both the placental labyrinth and junctional zone and were able to release CFS.

It has been reported that the rabbit and rat placenta takes up liposomes very efficiently, almost as efficiently as the liver and spleen (Tuzel Kox et al. 1995), which could explain why all liposome compositions were present in the mouse placenta within 48 h of injection. Also, as described previously, liposomes are a good source of choline and fatty lipids so may be transported via choline receptors. The non-targeted liposome compositions accumulated to a lesser extent than the targeted liposomes in the placenta and accumulated non-specifically in both the labyrinth and the junctional zone. This confirms that the addition of a homing peptide enables targeted delivery of a potentially higher liposome concentration to the labyrinth, which may ultimately result in a higher concentration of drug at this exchange region. One key reason for using targeted liposomes to treat placental dysfunction is to reduce fetal drug exposure. Non-targeted

liposomes accumulated in fetal tissues, in particular near the cord insertion point and abdominal region, indicating, a high risk of fetal exposure to any payload they may carry. This observation is similar to what has previously been reported when liposomes were tested in the dual-perfused human placenta model. Although targeted liposomes have not previously been examined, small liposomes with a neutral or negative surface charge, (similar to ours) were able to transfer more encapsulated CFS to the fetal circulation, when compared with free CFS and positively charged liposomes containing CFS (R. Bajoria & Contractor 1997). These findings demonstrate why non-targeted liposomes are not appropriate for placental delivery, and further support targeted drug delivery strategies.

4.4.3 Off-target accumulation of liposomes

When maternal organs were examined, targeted and non-targeted liposomes were transiently observed in the liver, kidney and spleen at high concentrations as previously reported (Ishida et al. 2002), but not in the other major maternal organs or fetal tissues. There was a limited amount of CFS observed in these organs, suggesting that liposomes were cleared from these organs before drug release occurred, which should limit the off target side effects of the drug. CFS release was more readily observed in the placenta, likely due to internalisation of the liposomes aided by the presence of the cell penetrating homing peptides. The clearance route and kinetics of these two peptides or peptide-liposome conjugates have not been properly examined previously, so we are unable to draw comparisons from the literature. iRGD-liposomes were not observed in the liver or spleen at 72 h, but a small amount of fluorescent signal was noted in the kidney. CGKRK-liposomes were still present in all clearance organs at 72 h, exhibiting

a slower rate of clearance or degradation compared to iRGD liposomes. After 72 h, targeted liposomes were still observed at a low concentration within the placental labyrinth, but fluorescent signal within the maternal clearance organs was dramatically reduced. This indicates selective liposome retention within the placenta and clearance of the liposomes from the maternal organs. The fluorescent signal from the targeted liposomes observed in the clearance organs was higher than that observed in the placenta for all time points examined, possibly suggesting that the dose of liposome administered was too high, placental receptors were saturated and the excess of liposomes was rapidly cleared, as described previously (Ruoslahti et al. 2010).

4.5 Summary

Data presented in this chapter show that biocompatible liposomes decorated in the placental homing peptides iRGD or CGKRK are capable of selectively accumulating in the syncytiotrophoblast of human placental tissue and can also target and bind to the placental labyrinth and spiral arteries of pregnant mice in vivo. CFS, a fluorescent drug analogue, was used to track drug release from these targeted liposomes and showed placental delivery of an encapsulated cargo. All liposome formulations were transiently observed within the maternal clearance organs. Importantly, targeted liposomes were not transferred to fetal tissues, whereas non-targeted liposomes and their encapsulated CFS were present in fetal tissues.

Chapter 5: Targeted Placental Delivery of IGF-I and IGF-II in C57 and P0 Mice

5.1 Introduction

Once placental targeting and drug release in vivo was confirmed, a review of the literature was undertaken to decide on a candidate drug to encapsulate that would benefit from placental delivery. Several candidate drugs, outlined in section 1.3.3, improve placental function and increase fetal weight and survival when administered systemically to pregnant mice, but have concerning off-target side effects (Renshall et al. 2014).

As our targeted liposomes accumulate in the human placental syncytiotrophoblast and the mouse placental labyrinth, it was therefore important to choose a therapeutic that would enhance ST or CT function and in doing so would improve placental function. The growth factors IGF-I and -II, discussed in section 1.3.3.5, were selected as candidate therapies for placental-specific delivery. IGF-1R is expressed on the human ST and CT, and is expressed throughout the mouse labyrinth trophoblast (Charnock et al. 2015), meaning that the appropriate receptors are present to bind to targeted IGFs. Incubation with IGFs increase CT proliferation and decrease apoptosis (Forbes et al. 2008), whilst administering exogenous IGF-I or IGF-II to healthy pregnant animals enhances placental function and increases in fetal growth and viability (Sferruzzi-perri et al. 2007). However, these growth factors cannot safely be administered systemically to humans as a potential therapy for FGR, because their receptors are ubiquitously expressed (Jones & Clemmons 2013) and there is a risk of inducing detrimental off-target pathology, including breast cancer (Osborne et al. 1989) and retinal angiogenesis (Lofqvist et al. 2009). Therefore IGFs are the ideal biological payload to encapsulate and administer to pregnant mice, with the aim of enhancing placental function. IGF-II is

of particular interest as it has been shown to act directly on the placenta, increasing placental growth and nutrient transfer to indirectly promote fetal growth (Sferruzzi-Perri et al. 2008; Sferruzzi-perri et al. 2007).

Healthy C57 mice were treated with targeted liposomes containing IGF-I or IGF-II to examine whether treatment significantly enhanced normal placental and/or fetal development. Maternal body weight and organ weights were examined to assess evidence of potential off target effects. Secondly, the P0 mouse model was treated to assess whether targeted delivery of IGF-II could rescue impaired placental and/or fetal growth. As our approach involves targeting exogenous IGF-II to the placental labyrinth, the P0 mouse, which lacks expression of IGF-II in this area, was considered to be a suitable model for proof of principle experiments.

5.2 Aims

This chapter aimed to:

1. Examine the safety profile of targeted nanoparticles encapsulating IGFs following administration to pregnant C57 mice
2. Examine whether targeted delivery of IGFs alters fetal and/or placental weight when administered to pregnant C57 or P0 mice
3. Examine whether targeted delivery of IGF-II alters gross placental morphology and/or basal cell proliferation rate within the placenta
4. Examine whether excretion of liposomal components via the maternal clearance organs results in altered gross morphology or induced abnormal cell proliferation in these tissues, indicative of off-target cargo release.

5.3 Results

5.3.1 Experimental details

Treatment was administered I.V to pregnant C57 or P0 mice on E11.5, 13.5, 15.5 and 17.5 of pregnancy. C57 treatment groups were as follows, N = number of dams treated, n = number of fetuses collected:

(a) Non-treated (N = 14, n = 99)

(b) Vehicle (PBS) (N = 8, n = 59)

(c) Free IGF-I (N = 9, n = 62)

(d) Free IGF-II (N = 8, n = 43)

(e) Non-coated liposomes (N = 8, n = 49)

(f) ARA-liposomes (N = 8, n = 53)

(g) iRGD-liposomes (N = 8, n = 56)

(h) CGKRK-liposomes (N = 9, n = 62)

(i) iRGD/IGF-I liposomes (N = 8, n = 86),

(j) Non-coated/IGF-II liposomes (N = 9, n = 68),

(k) ARA/IGF-II liposomes (N = 8, n = 45) and

(l) iRGD/IGF-II liposomes (N = 8, n = 43).

P0 treatment groups were as follows, (n(total) = total number of fetuses collected, n(WT) = total number of wild type fetuses collected, n(P0) = total number of mutant P0 fetuses collected):

(m) Free IGF-II (N=8, n(total) = 53, n(WT) = 21, n(P0) = 32)

(n) iRGD/IGF-II (N=8, n(total) = 60, n(WT) = 32, n(P0) = 28)

(o) iRGD liposomes (N=3, n(total) = 20, n(WT) = 13, n(P0) = 7)

(p) Non-treated group (N=5, n(total) = 41, n(WT) = 20, n(P0) = 21)

(q) Non-treated group (N=3, n(total) =16, n(WT) = 10, n(P0) = 6)

Free IGFs were administered systemically to compare the effect of non-targeted treatment; recombinant human IGFs were used to allow their plasma concentration to be measured using an anti-human IGF ELISA. IGFs were administered at 1mg/kg/dose, reflecting the concentration delivered by subcutaneous osmotic mini-pump to pregnant guinea pigs (Sferruzzi-perri et al. 2007). IGFs encapsulated inside liposomes were administered at a final concentration of 0.5mg/kg, half of the concentration of freely administered IGF. The non-treated animals (a, p, q) and those injected with vehicle (PBS; b) were included to control for the stress of restraint and repeated injections. I processed three unhandled animals (group q) and compared these with five collected previously by my colleagues (group p) to reduce the number of animals used. Data from (p) and (q) were combined because the mean from each group was not significantly different.

5.3.2 Repeated liposome administration was not detrimental to pregnancy outcome in C57 mice

No treatment was detrimental to pregnancy outcome, as the number of live fetuses per litter (figure 5.1A), the number of resorptions per litter (figure 5.1B) and the median

maternal weight gain from onset of treatment (E11.5 to E18.5) were not significantly altered (figure 5.1C) compared to non-treated animals and those injected with PBS. There were no behavioural changes or evidence of pathology in the dams, nor were there any gross fetal or placental pathology after multiple injections. This suggests that the chosen liposome formulation and dosing regimen was well tolerated during pregnancy in the mouse.

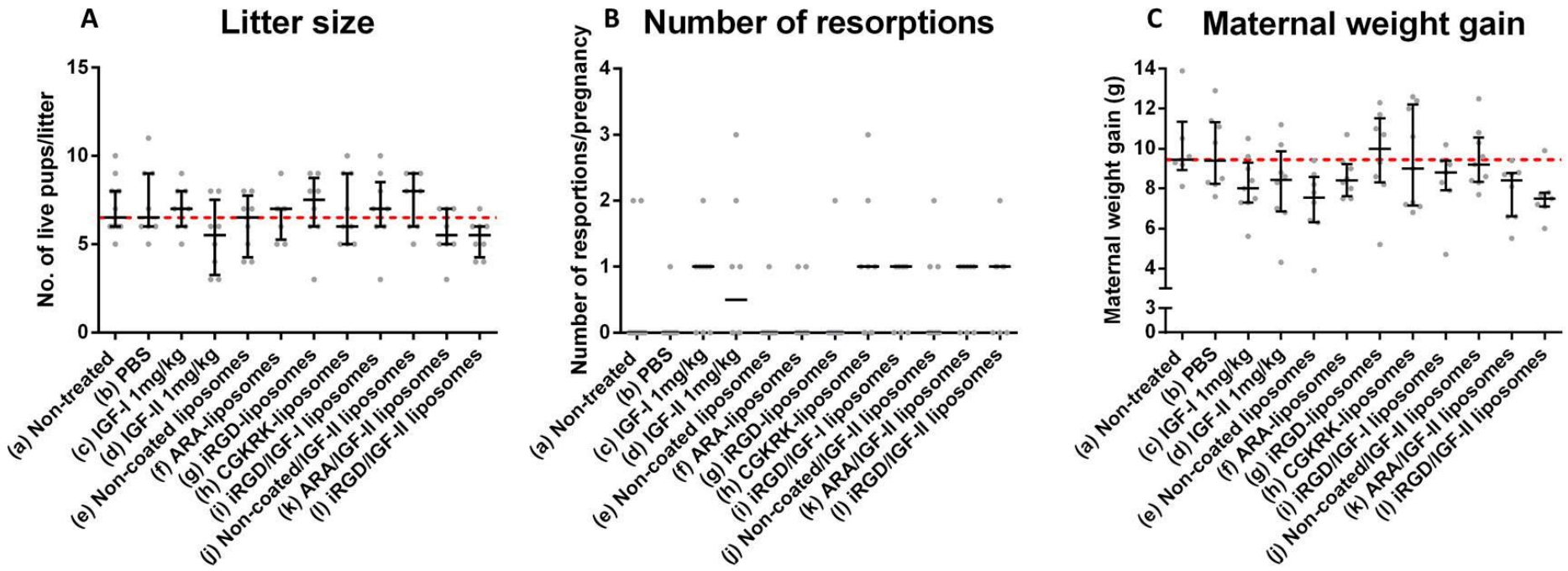

Figure 5.1: Repeated administration of liposomes to pregnant C57 mice did not detrimentally affect pregnancy outcome. There were no significant alterations in (A) number of live pups per litter, (B) number of resorptions per litter, (C) maternal weight gain from E11.5 - E18.5. N = 8/9 dams per group, with the exception of non-treated animals where N=14. Median ± IQR are plotted, dotted red line shows median of non-treated group.

5.3.3 Targeted delivery of IGF-II to C57 mice increased placental weight

As IGFs are essential for optimal placental growth and function, it was hypothesized that targeted delivery of IGFs to the placenta would enhance placental growth, translating to an increase in placental weight at E18.5, with a concomitant increase in fetal weight.

Administration of free IGF-I or IGF-II did not significantly increase median fetal or placental weight at E18.5 (Figures 5.2A & B, (c), (d)), but did alter the fetal weight distribution, with the percentage of fetal weights sitting above the 95th centile increasing with IGF treatment; 1.01% (1/99) of fetuses from non-treated dams and no (0/59) fetuses from PBS treated dams were above the 95th centile, whereas 9.68% (6/62) of fetuses from IGF-I treated dams and 6.98% (3/43) of fetuses from IGF-II treated dams were above the 95th centile (Figure 5.3A, IGF-I green curve; IGF-II dark blue curve).

Treatment with empty liposomes (non-coated liposomes, ARA-liposomes, iRGD-liposomes and CGKRK-liposomes) had differing effects on fetal and placental weights (Figure 5.2A & B (e), (f), (g), (h)). The only treatment that increased fetal weight was empty, non-coated liposomes (Figure 5.2B (e)), (+6.4%, $p < 0.001$ compared to non-treated (a); +7.2%, $p < 0.01$ compared to PBS-treated (b)); this formulation also uniformly increased the fetal weight distribution (Figure 5.3B, orange curve), but had no significant effect on placental weight (Figure 5.2A (e)). In contrast, non-coated/IGF-II liposome treatment significantly decreased fetal weight compared with non-coated liposomes (-10.7%, $p < 0.0001$ (e) (Figure 5.2B) and shifted the fetal weight distribution curve leftwards (Figure 5.3C, light blue curve). Empty CGKRK-liposomes significantly

reduced fetal weight (-6.7%, $p < 0.0001$ compared to non-treated (a), -6.1% $p < 0.01$ compared to-PBS treated (b)) (Figure 5.2B (h)), so this liposome formulation was not used for IGF–II delivery.

Targeted IGF-I treatment using iRGD/IGF-I liposomes did not alter median fetal or placental weights (Figure 5.2A & B (i)), or the fetal weight distribution when compared with non-treated or PBS-treated animals (Figure 5.3D, yellow curve). However, targeted delivery of IGF-II using iRGD/IGF-II liposomes significantly increased the median placental weight at E18.5 (Figure 5.2A (l)) when compared with non-treated mice (+8.9%, $p < 0.001$ (a)), or mice treated with PBS (+7.5%, $p < 0.01$ (b)), or with empty ARA-liposomes (+11.7% $p < 0.0001$ (f)), empty iRGD-liposomes (+5.5% $p < 0.05$ (g)), iRGD/IGF-I liposomes (+6.8% $p < 0.01$ (i)) and non-coated/IGF-II liposomes (+6.8% $p < 0.05$ (j)). The increase in placental weight observed when iRGD/IGF-II liposomes were administered did not result in an increase in fetal weight, when compared with appropriate controls (Figure 5.2B (l)) and the fetal weight population distribution was also unaffected (Figure 5.3E, purple curve).

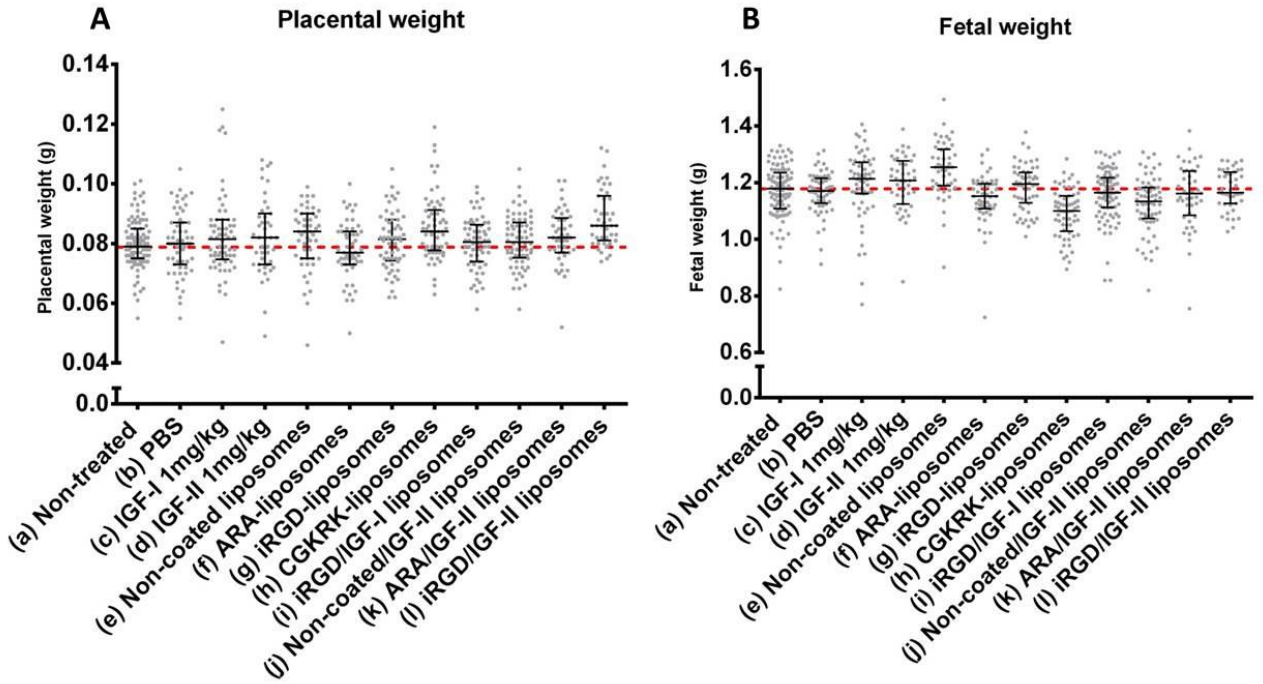

Figure 5.2: Effect of targeted delivery of IGF-II on placental and fetal weights in C57 mice. Fetal and placental weights were measured at E18.5 after repeated administration of liposomes to pregnant C57 mice: (A) Targeted delivery of IGF-II to pregnant C57 mice significantly increased placental weight; (l) is significantly different from (a) $p < 0.001$, (b) $p < 0.01$, (f) $p < 0.0001$, (g) $p < 0.05$, (i) $p < 0.001$, (j) $p < 0.05$; (h) is significantly different when compared with (f) $p < 0.05$, (B) Targeted delivery of IGF-II to pregnant C57 mice did not affect fetal weights; (e) Is significantly different from (a) $p < 0.001$, (b) $p < 0.01$, (f) $p < 0.0001$, (h) $p < 0.0001$, (j) $p < 0.0001$; (h) Is significantly different from (a) $p < 0.0001$, (b) $p < 0.01$, (c) $p < 0.0001$, (d) $p < 0.0001$, (g) $p < 0.0001$; (j) Is significantly different from (d) $p < 0.01$**.** Median ± IQR are shown; N = 8/9 dams per group, with the exception of non-treated animals where N=14; Kruskall-Wallis and Dunn's multiple comparisons test for significance were performed

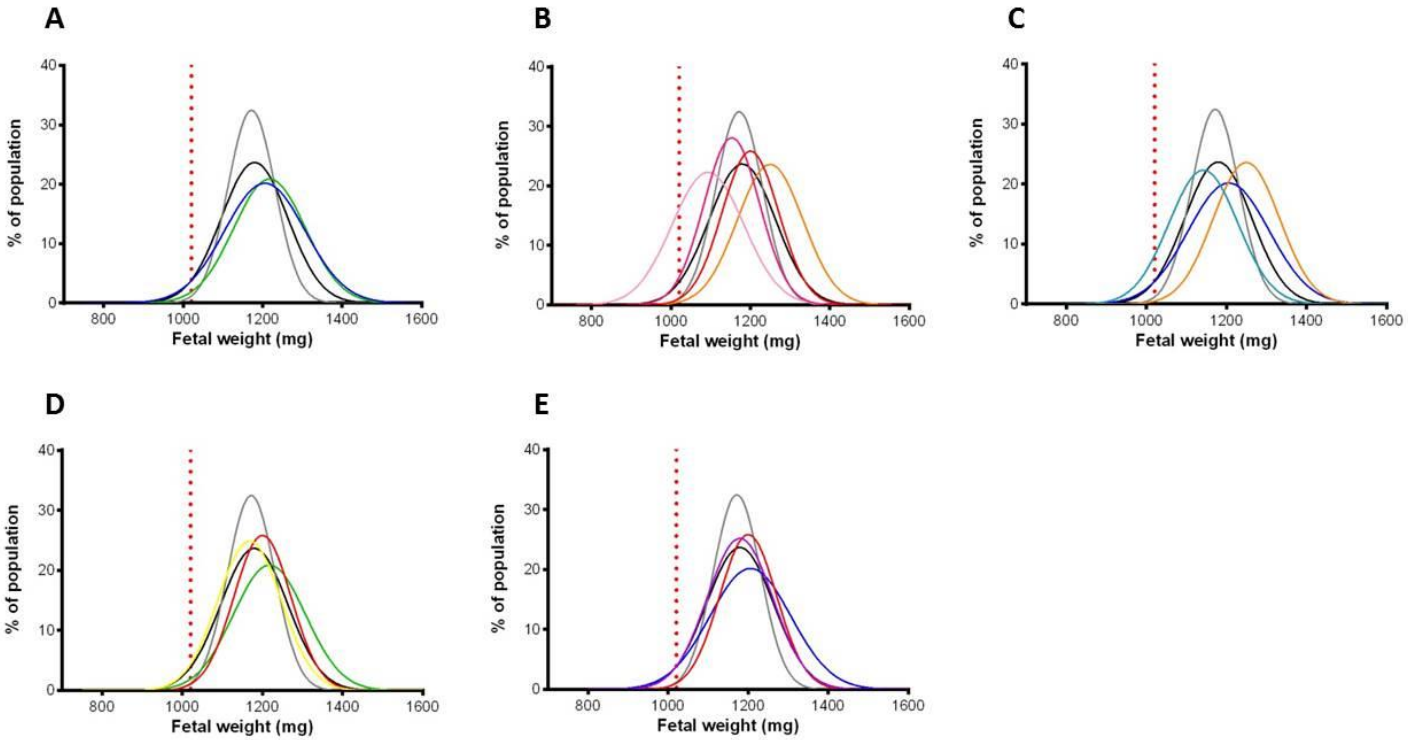

Figure 5.3: Population fetal weight curves collected after repeated administration of liposomes to C57 mice. (A) non-treated, PBS, IGF-I and IGF-II treated dams, (B) non-treated, PBS, iRGD-liposomes, CGKRK-liposomes, ARA-liposomes, Non-coated-liposomes treated, (C) non-treated, PBS, IGF-II, non-coated liposomes, non-coated/IGF-II liposomes treated, (D) Non-treated, PBS, IGF-I, iRGD-liposomes, iRGD/IGF-I liposomes treated, (E) non-treated, PBS, IGF-II, iRGD-liposomes, iRGD/IGF-II liposomes treated. Red line represents the 5th centile of fetal weights collected from non-treated animals. Black = (a) untreated, Grey = (b) PBS, Green = (c) IGF-I, Dark blue = (d) IGF-II, Orange = (e) Non-coated liposomes, Dark pink = (f) ARA-liposome, Red = (g) iRGD-liposomes, Light pink = (h) CGKRK-liposomes, Yellow = (i) iRGD/IGF-I liposomes , (j) Light blue = Non-coated/IGF-II liposomes, (k) Brown = ARA/IGF-II liposomes, (l) Purple = iRGD/IGF-II liposome.

5.3.4 IGF-II was not detected in fetal or maternal plasma

24 h after administration of the final dose of free IGF-II or liposomes encapsulating IGF-II, animals were culled, maternal and fetal plasma were collected and the concentration of circulating recombinant human IGF-II was measured by ELISA (Figure 5.4B). IGF-II was not present at detectable levels in maternal or fetal circulation 24 h after IV administration of PBS, free IGF-II, iRGD/IGF-II liposomes or ARA/IGF-II liposomes, but was detected in maternal plasma at a concentration of 164.7 ± 29.6 ng/ml plasma when administered in non-coated liposomes. Plasma collected from one mouse continuously administered IGF-II (1mg/kg/day) via a subcutaneous osmotic mini pump was included as a positive control; 29.8 ng/ml IGF-II was detected in the maternal plasma of this mouse, but no IGF-II was detected in the fetal plasma.

A

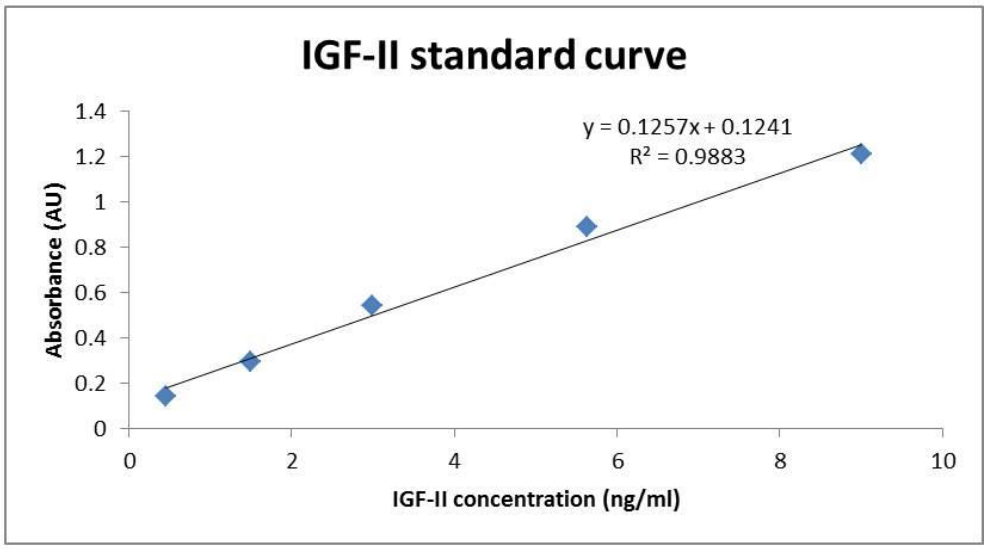

B

Average IGF-II concentration in maternal and fetal plasma		
Injected with:	**Maternal plasma (ng/ml)**	**Fetal plasma (ng/ml)**
PBS	0	0
IGF-II (IV)	0	0
IGF-II (SC)*	29.8	0
iRGD/IGF-II liposomes	0	0
ARA/IGF-II liposomes	0	0
Plain/IGF-II liposomes	164.7 ± 29.6	0

Figure 5.4: IGF-II concentration in maternal and fetal plasma of treated mice. Recombinant human IGF-II was quantified in maternal and fetal plasma 24 hours after I.V injection. (A) Standard curve of IGF-II, (B) Concentration of human IGF-II detected in mouse plasma, displayed as mean ± SEM. Plasma from mice continuously administered IGF-II via subcutaneous osmotic mini-pumps (SC)* was included as a positive control. N=3 plasma samples from each treatment (*N=1 plasma sample). Fetal plasma was pooled for each litter; samples were examined in duplicate.

5.3.5 Liposome formulations affected gross placental morphology

Subcutaneous administration of IGF-II to guinea pigs increased the area of the placental labyrinth as a percentage of the total placental cross sectional area by 9% (Sferruzzi-Perri et al. 2006). Placental morphology was therefore examined in mice treated with

free IGF-II, iRGD-liposomes or iRGD/IGF-II liposomes, alongside a non-treated control group. The labyrinth cross sectional area as a percentage of the total placental cross sectional area at the midline (excluding obvious membranes) (Figure 5.5A) was quantified using the image analysis program HistoQuest (Figure 5.5B). Targeted IGF-II treatment did not significantly increase the labyrinth cross sectional area as a percentage of the total placental cross sectional area compared to controls, although the area was increased by 6.2% compared to placentas from non-treated mice, and by 7.2% compared to placentas from IGF-II treated mice (Figure 5.5B). However, empty iRGD-liposomes significantly increased the labyrinth cross sectional area as a percentage of the total placental area by 10.3%, compared with both non-treated and free IGF-II treated (Figure 5.5B).

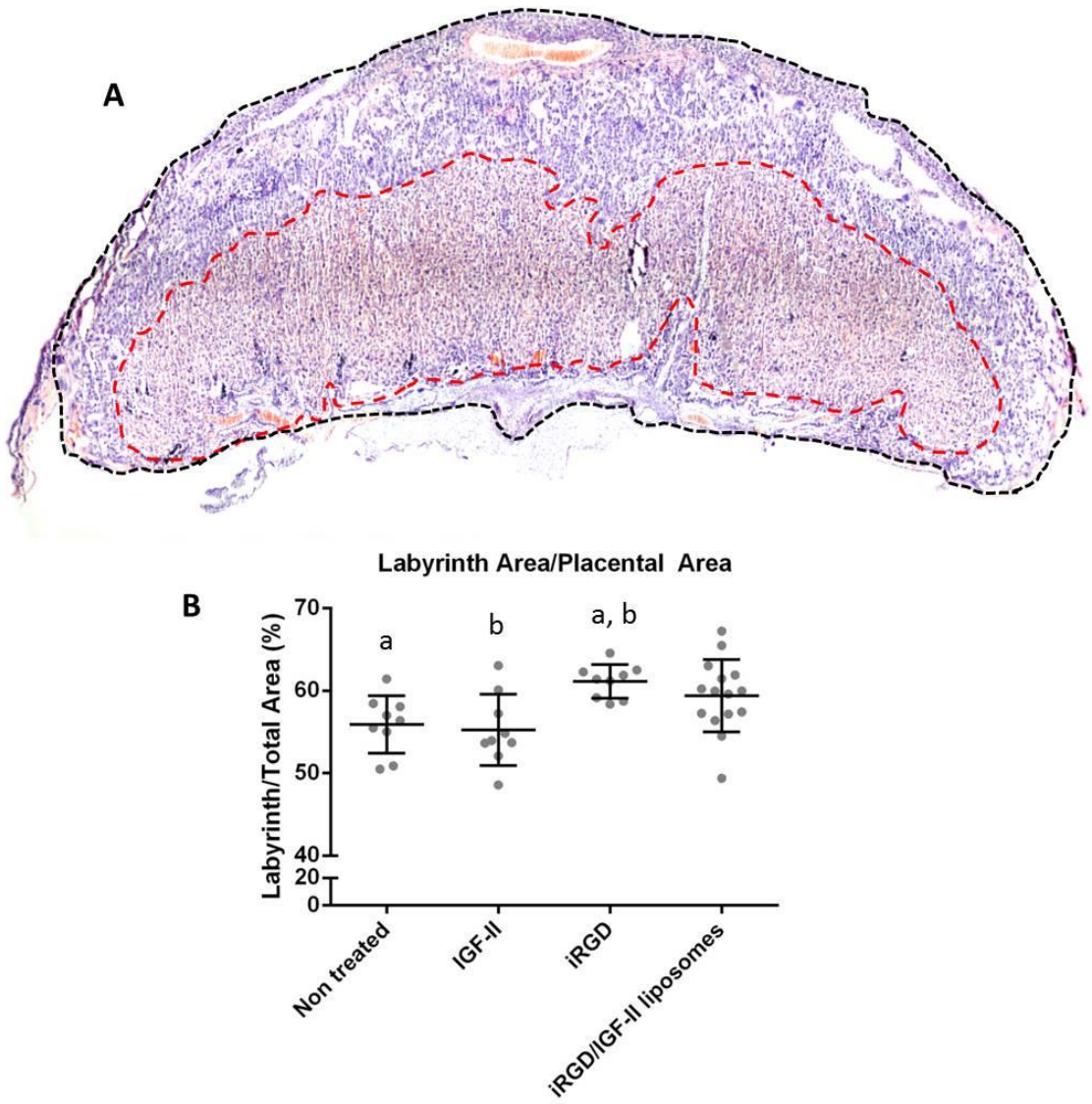

Figure 5.5: Effect of IGF-II treatment on gross placental morphology. (A) Gross placental morphology was assessed using HistoQuest image analysis software. Red dotted line denotes placental labyrinth area. Black dotted line denotes total placental area (excluding membranes). (B) Quantification of the labyrinth area as a percentage of the total placental area. a, b = $p < 0.05$; one way ANOVA and Turkey's multiple comparisons test. Mean ± SD shown. N=3 mice from each treatment group (except for iRGD/IGF-II liposomes where N=5), n=3 placentas from each mouse, 5 cross sectional images from each placenta were imaged.

5.3.6 iRGD/IGF-II liposomes did not alter placental cell proliferation in the labyrinth, junctional zone or total placenta.

As IGF-II is a mitogenic growth factor, it was hypothesized that the increase in placental weight observed when IGF-II was targeted to the placenta using iRGD/IGF-II liposomes could be due to an increase in cell proliferation. Also, the increase in labyrinth cross sectional area observed after treatment with iRGD liposomes may be due to increased proliferation within the labyrinth as we have previously observed that free iRGD peptide has a modest mitogenic effect (King et al. 2016). Figure 5.6 shows that treatment with IGF-II, iRGD-liposomes or iRGD/IGF-II liposomes did not affect the area of in-cycle Ki-67 positive cells as a proportion of the total area of cells in the labyrinth (Figure 5.6A), the junctional zone (Figure 5.6B) or the total placenta (Figure 5.6C), suggesting that treatment did not affect basal proliferation rate 24 h after administration.

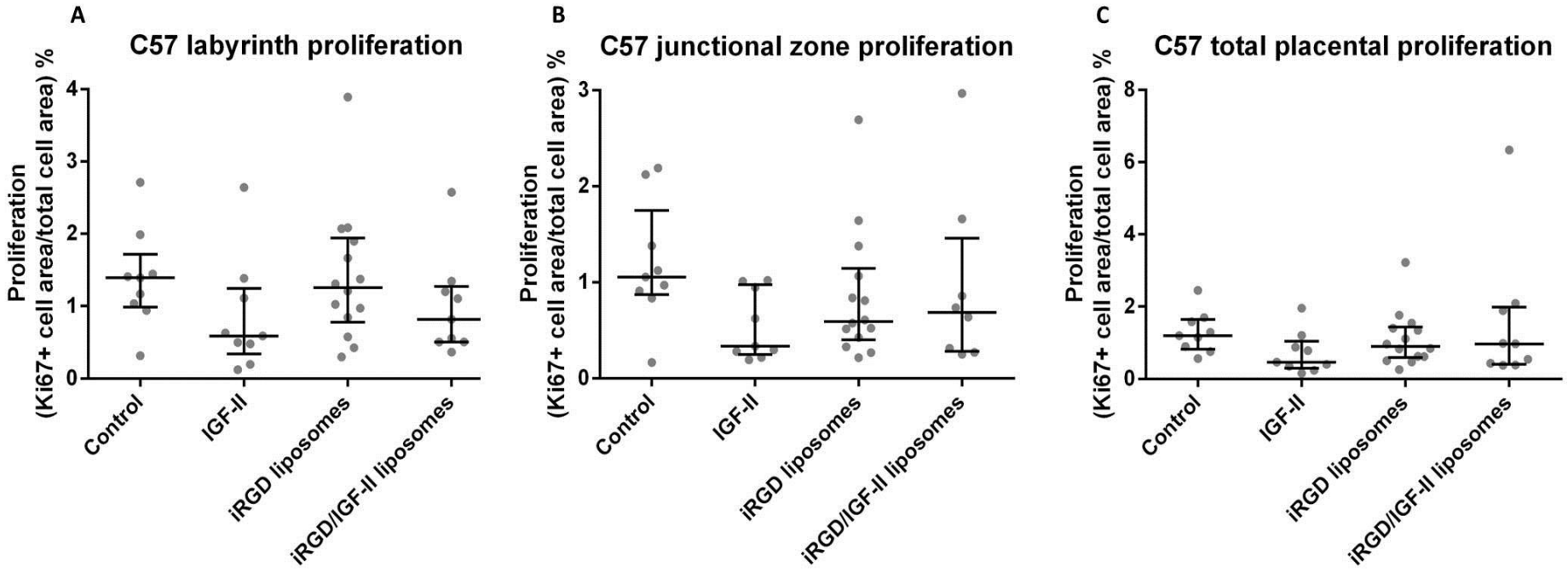

Figure 5.6: Effect of targeted delivery of IGF-II on basal proliferation rate in placentas from C57 mice. Treatment with IGF-II, iRGD liposomes or iRGD/IGF-II liposomes did not significantly alter the area of Ki-67 positive cells as a proportion of the total area of cells in (A) the labyrinth, (B) the junctional zone, or (C) the total placenta. N=3 mice, n=3/4 placentas taken from each mouse, 10 images from each placental zone were analysed. No significance observed when Kruskall-Wallis and Dunn's multiple comparisons test for significance were performed; median ± IQR are shown.

5.3.7 Liposome administration did not affect weight or basal rate of proliferation in the maternal clearance organs

Although the main aim of this project was to improve fetal growth by targeting treatment to the placenta, a secondary aim was to examine possible maternal and fetal side effects associated with treatment. To ensure that empty liposomes did not cause undesirable maternal side effects and that liposomes containing IGF-I or -II did not cause off-target mitogenic effects, the weights of maternal clearance organs through which liposomes are degraded and/or excreted were recorded in the various treatment groups. Figure 5.7 shows that there was no significant change in maternal kidney or spleen weight after any treatment and Figure 5.8 shows that the area of Ki-67 positive cells in the maternal heart (Figure 5.8A), lung (Figure 5.8B), liver (Figure 5.8C), kidney (Figure 5.8D) and spleen (Figure 5.8E) as a proportional of the total cell area was not significantly increased by any treatment, suggesting that treatment did not induce any gross pathology in these organs.

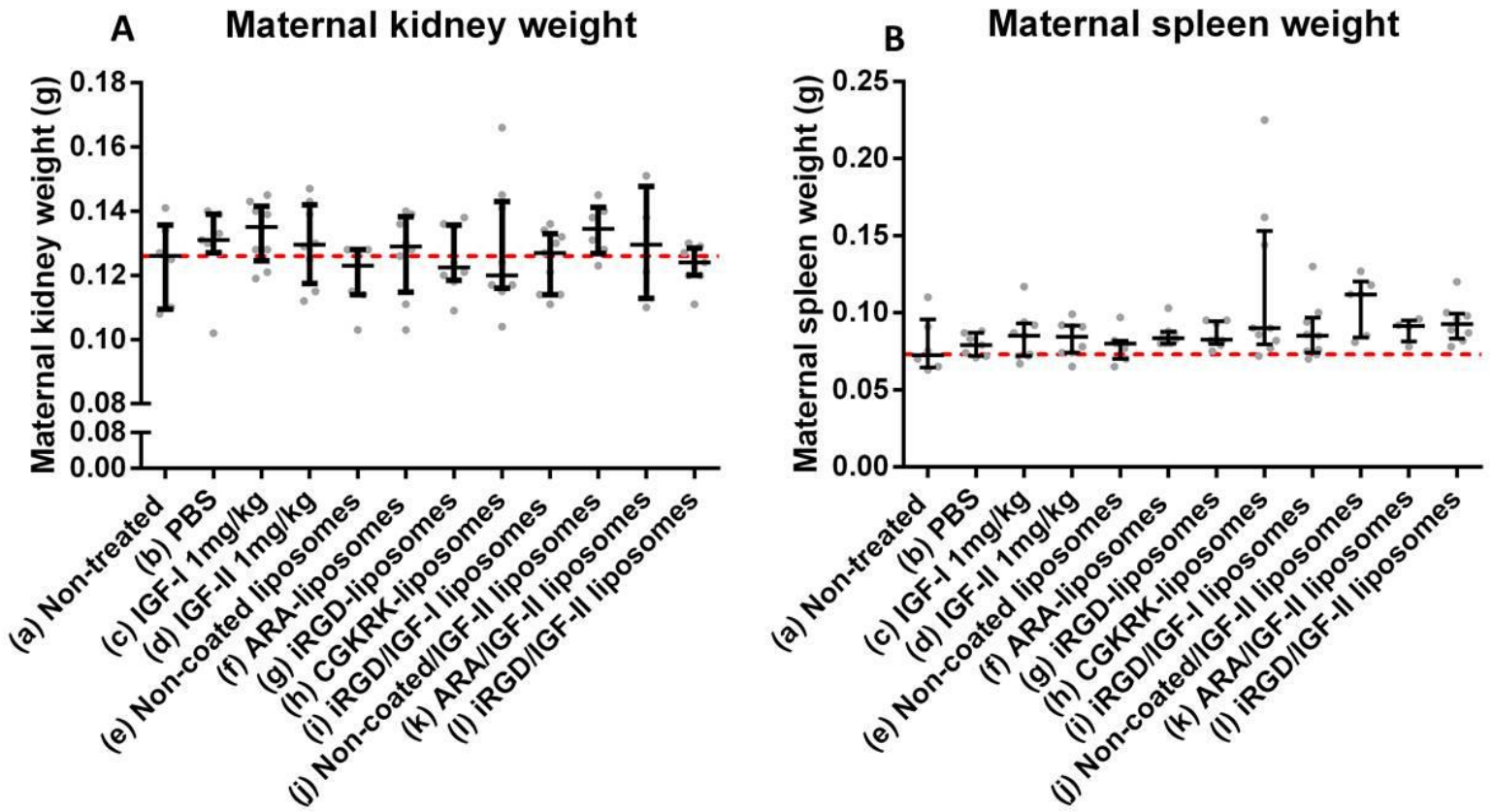

Figure 5.7: Effect of treatment on maternal clearance organ weights. Administration of free IGF-II or different liposome formulations did not alter (A) maternal left kidney weight or (B) spleen weight. Median ± IQR are shown, dotted red line represents median weight. N=4-9 for all groups

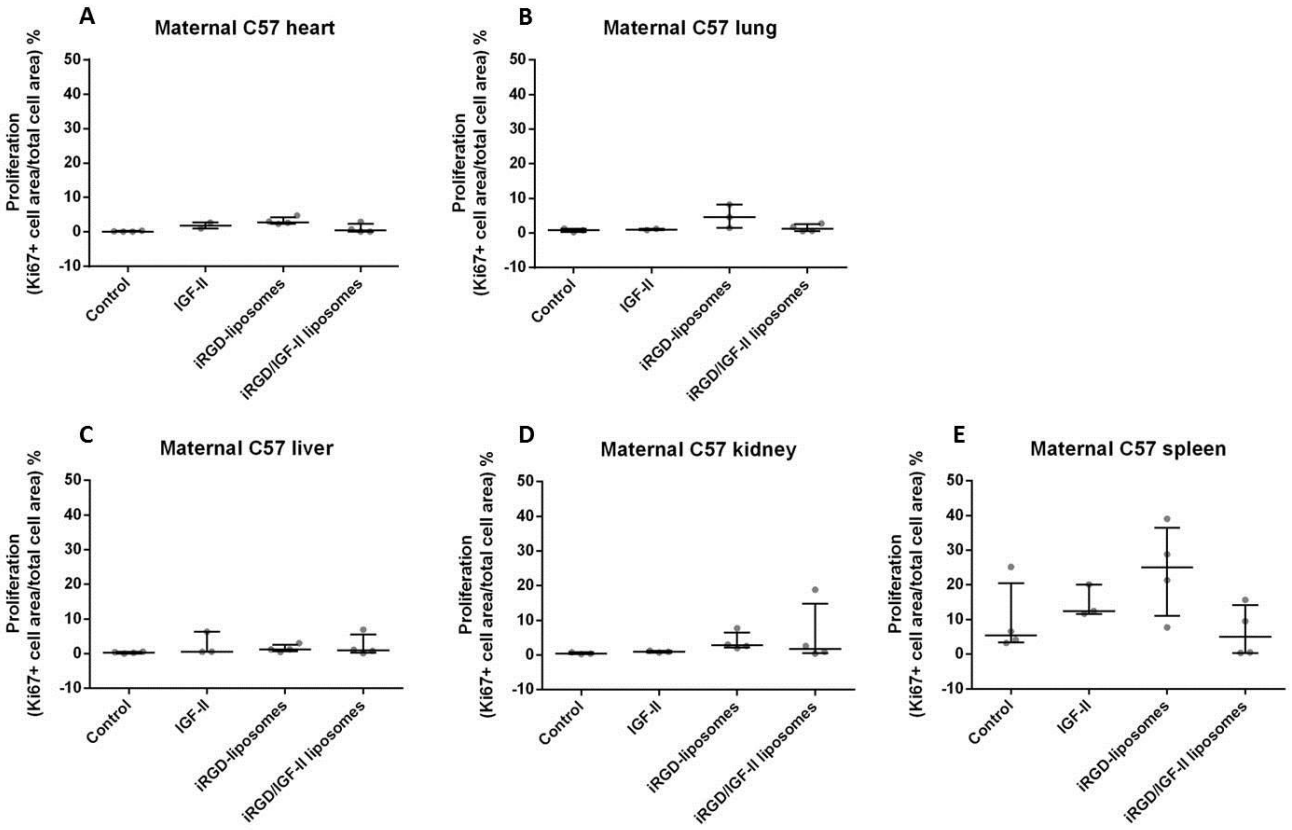

Figure 5.8: Effect of treatment on basal rate of proliferation in major maternal organs. Treatment of C57 mice did not significantly alter the area of proliferating cells as a proportion of the total area of cells in the maternal (A) heart, (B) lung, (C) liver, (D) kidney, (E) spleen. N=3 mice, 10 images of each organ were analysed. All graphs are displayed using the same y-axis scale so comparisons between organs can be made. No significance was observed when Kruskall-Wallis and Dunn's multiple comparisons test for significance were performed; median ± IQR are shown

5.3.8 Repeated liposome administration was not detrimental to pregnancy outcome in P0 mice

As observed in C57 mice, no treatment was detrimental to pregnancy outcome in the P0 mouse model; there was no significant difference in the number of live fetuses per litter (Figure 5.9A), the number of resorptions (Figure 5.9B) or maternal weight gain from E11.5-E18.5 (Figure 5.9C).

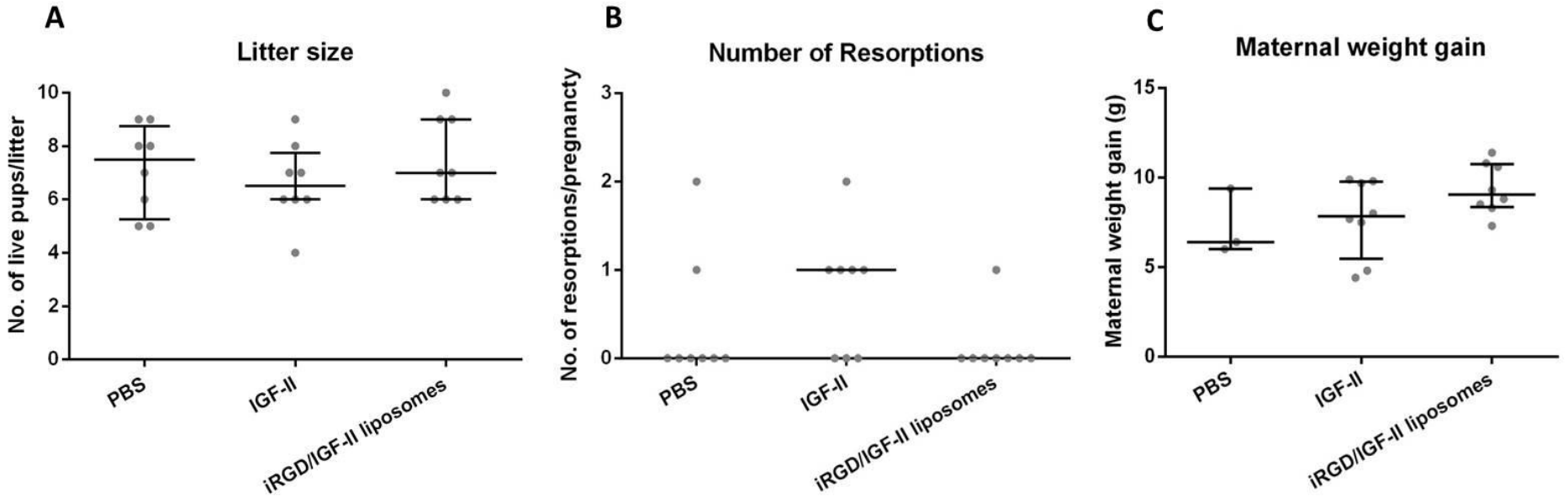

Figure 5.9: Repeated administration of liposomes to pregnant P0 mice did not detrimentally affect pregnancy outcome. (A) Number of live pups per litter (B) number of resorptions per litter (C) maternal weight gain from E11.5-E18.5. N=8 dams/ group. No significance was observed when Kruskall-Wallis and Dunn's multiple comparisons test for significance were performed; median ± IQR are shown.

5.3.9 Targeted delivery of IGF–II altered the P0 fetal weight distribution

The expected P0 phenotype was maintained for all treatment groups; P0 fetuses were approximately 69% of the weight of the WT fetuses as previously described (Constância et al. 2002); PBS-treated P0 = 76.8% median WT weight; IGF-II-treated P0 = 77.1% median WT weight; iRGD/IGF-II liposome-treated P0 = 79.8% median WT weight (Figure 5.10B). The P0 placentas were approximately 68% of the weight of the WT placentas also as previously reported (Constância et al. 2002); PBS-treated P0 = 72.9% median WT weight; IGF-II-treated P0 = 69.4% median WT weight; iRGD/IGF-II liposome-treated P0 = 66.8% median WT weight (Figure 5.10A). Treatment with free IGF-II or iRGD/IGF-II liposomes did not significantly increase the median fetal or placental weight compared with PBS-treated animals (Figure 5.10A & B). However, treatment with iRGD/IGF-II liposomes significantly increased the median P0 fetal weight (+5.2%, $p < 0.05$), but not the median placental weight of P0 or WT compared with PBS treated animals (Figure 5.10B). This treatment also altered fetal weight distribution with fewer of the lightest P0 fetuses observed. Figures 5.11 B & C show the 5^{th} and 10^{th} centiles of fetal weights from untreated dams; 7.4% (2/27) of P0 fetuses from untreated dams and 15.6% (5/32) of P0 fetuses from IGF-II treated dams fell below the 10^{th} centile of the P0 weight distribution. In contrast, no (0/28) P0 fetuses from iRGD/IGF-II treated dams fell below the 10^{th} centile of this distribution. Overlapping the WT and P0 fetal weight distribution curves (Figure 5.11C) shows that the increase in P0 fetal weight observed when the dams were treated with iRGD/IGF-II did not restore the P0 fetal weight distribution to that of the WT fetal weight, but did shift it closer toward the 5^{th} centile of the WT fetal weight distribution. The same effect

was not observed in WT fetuses, whose weight distribution curves were unaltered with treatment (Figure 5.11A).

As an additional control, empty iRGD-liposomes were administered to P0 mice. Unfortunately, due to time constraints only 3 animals could be treated, and one litter was composed entirely of WT fetuses, so fetal and placental weights are not shown here. The tissues collected were used for further experiments included below.

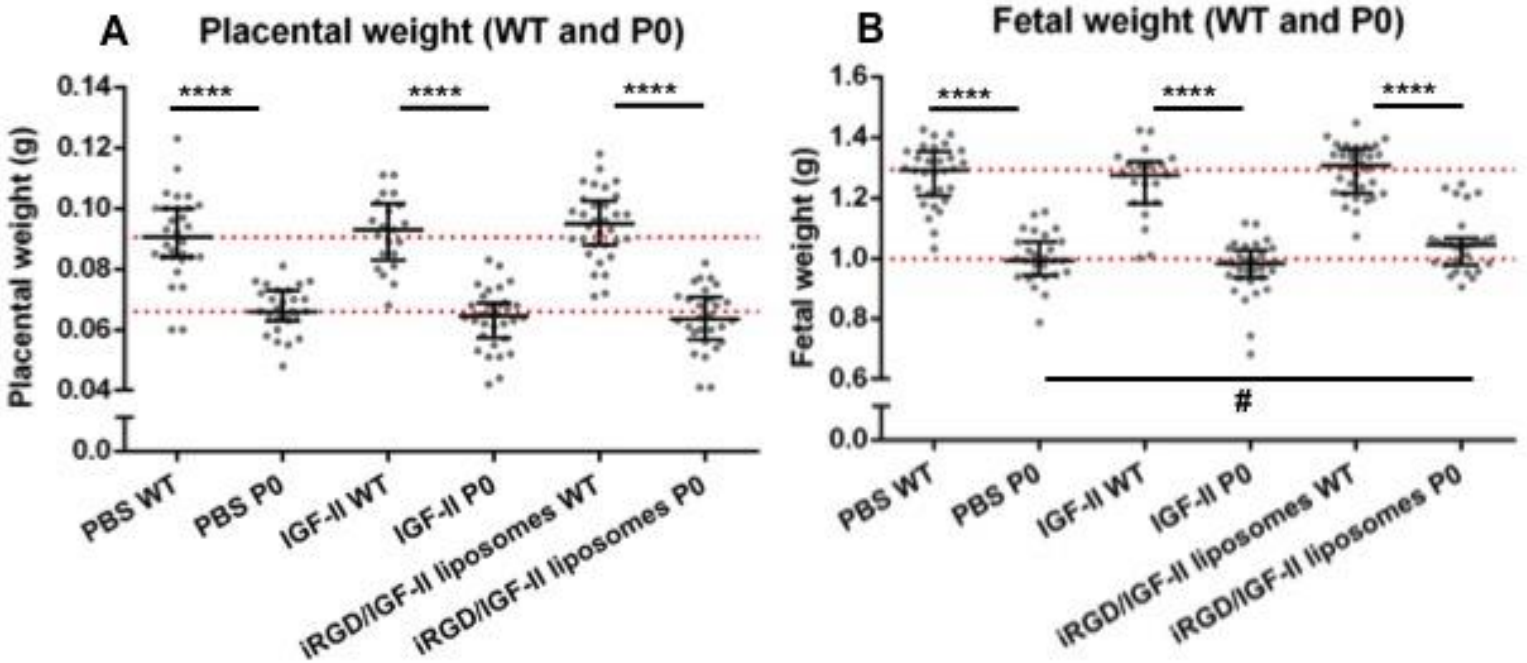

Figure 5.10: Effect of targeted delivery of IGF-II on placental and fetal weights in P0 mice. (A) P0 and WT placental weights, (B) P0 and WT fetal weights. Median ± IQR are shown ****= $p < 0.0001$. Kruskall-Wallis test and Dunns post hoc test, # = $p < 0.05$, Mann-Whitney test between P0 PBS fetuses and P0 iRGD/IGF-II liposome fetuses. N=8 dams/group; red dotted lines show median weights of WT and P0 pups from PBS treated dams.

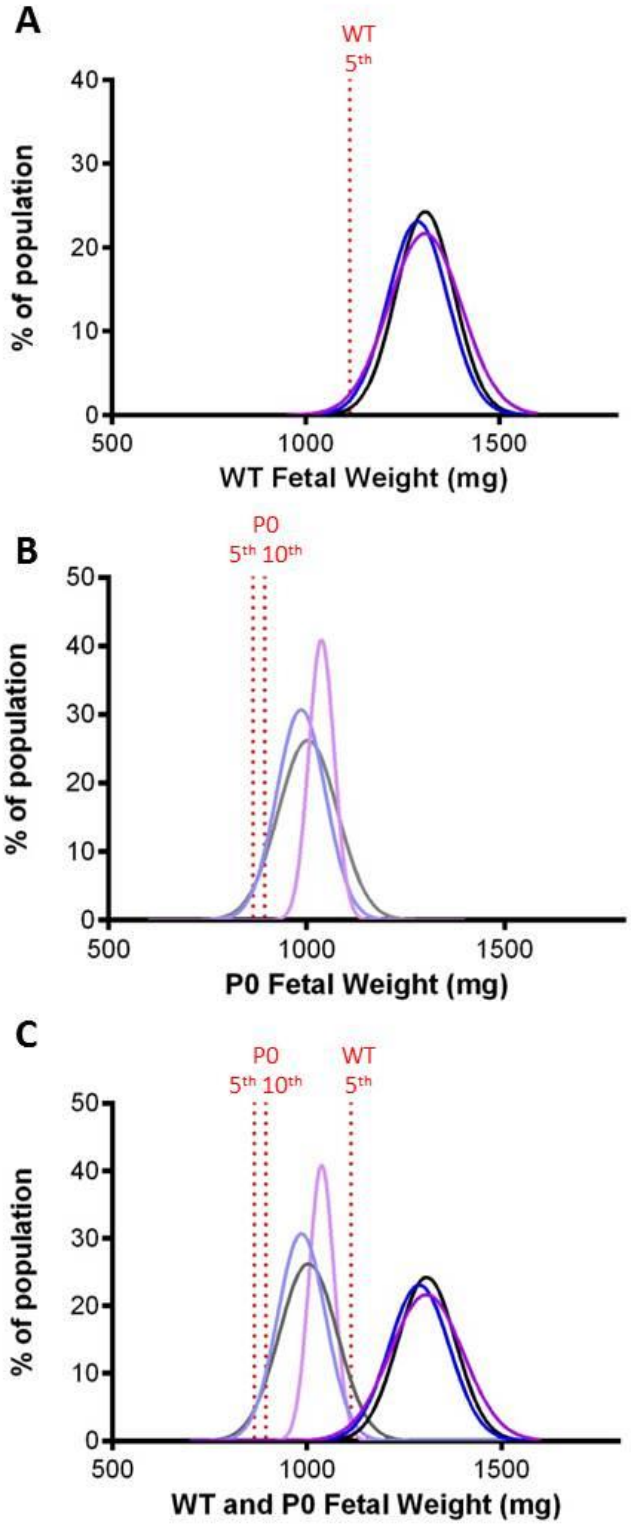

Figure 5.11: Targeted delivery of IGF-II alters fetal weight distribution of P0 fetuses. Black = WT fetuses/placentas from untreated dams, Dark blue = WT fetuses/placentas from IGF-II treated dams, Purple = WT fetuses/placentas from iRGD/IGF-II liposome treated dams, Grey = P0 fetuses/placentas from untreated dams, Faded blue = P0 fetuses/placentas from IGF-II treated dams, Faded purple = P0 fetuses/placentas from iRGD/IGF-II liposome treated dams. N=8 dams/group.

5.3.10 Liposomes encapsulating IGF-II decreased proliferation in the placenta of the P0 mouse

Although iRGD/IGF-II liposome treatment of P0 mice did not significantly affect placental weight, altered placental cell proliferation might be associated with an increase in surface area, translating into the observed increase in fetal weight. Figure 5.12 shows that when P0 animals were treated with iRGD/IGF-II liposomes, placentas collected from P0 fetuses exhibited a decreased area of Ki-67 positive cells as a percentage of the total area of cells in the labyrinth (Figure 5.12A), the junctional zone (Figure 5.12B) and the placenta as a whole (Figure 5.12C). There was no effect of treatment on the area of Ki-67 positive cells in placentas collected from WT fetuses (Figure 5.12D-F).

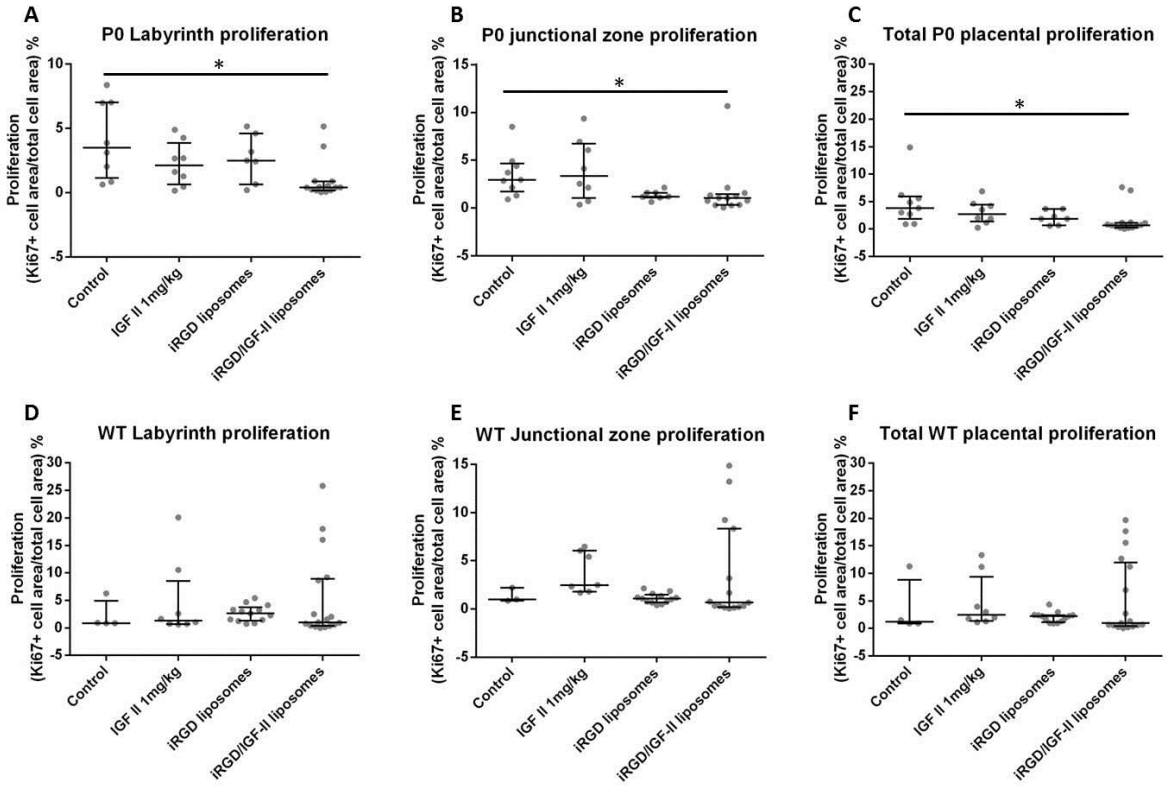

Figure 5.12: Effect of targeted delivery of IGF-II on basal proliferation rate in placentas from P0 mice. Treatment of P0 mice with IGF-II, iRGD liposomes and iRGD/IGF-II liposomes, significantly decreased proliferation in (A) the labyrinth, (B) the junctional zone, and (C) the total placenta, collected from P0 fetuses. Treatment did not significantly affect proliferation in (D) the labyrinth, (E) the junctional zone, or (F) the total placenta collected from WT fetuses. N=3 mice, n=6 placentas from each mouse (3 P0 and 3 WT placentas), 10 images from each placental zone were analysed. Significance observed when Kruskall-Wallis and Dunn's multiple comparisons test for significance were performed; *= $p < 0.05$; Median ± IQR plotted.

5.3.11 iRGD/IGF-II liposomes did not affect maternal organ weight or basal rate of proliferation

Following treatment, maternal organ weights were collected and area of Ki-67 positive cells was examined. There was no significant alteration in proliferation rate in the maternal kidney (Figure 5.13 A), spleen (Figure 5.13 B) or liver (Figure 5.13 C). The area of Ki-67 positive cells as a proportional of the total area of cells in the maternal brain, heart and lung was also unaltered (Figure 5.14A-F).

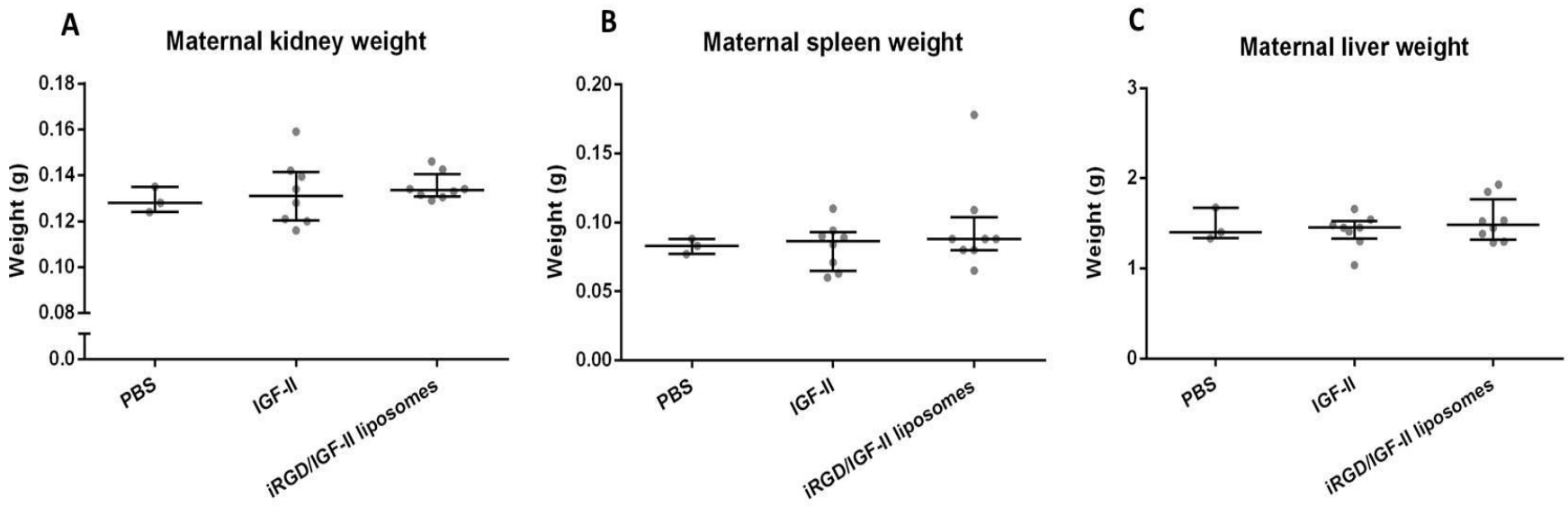

Figure 5.13: Effect of treatment on maternal clearance organ weights. Administration of free IGF-II or iRGD/IGF-II liposomes did not alter maternal (A) mean kidney weight, (B) spleen weight or (C) liver weight. N=8 for IGF-II and iRGD/IGF-II treated animals and N=3 for PBS-treated animals. No significance was observed when Kruskall-Wallis and Dunn's multiple comparisons test for significance were performed; median ± IQR plotted.

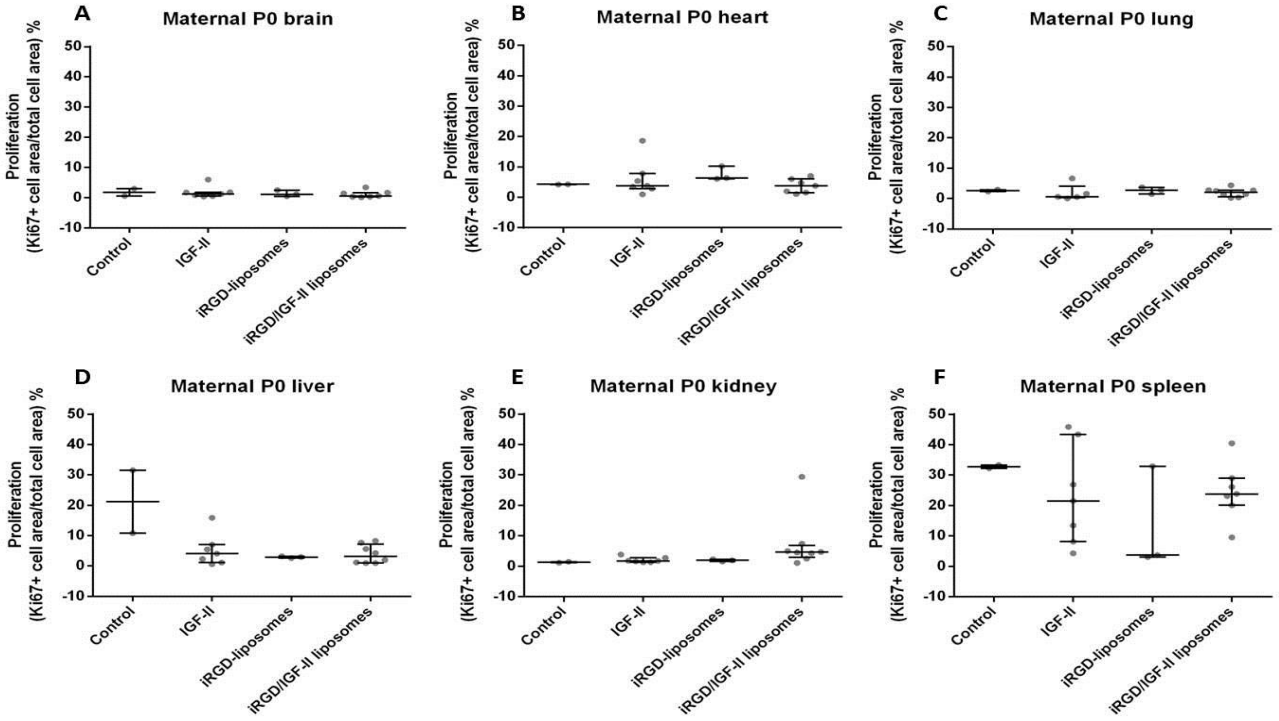

Figure 5.14: Effect of targeted delivery of IGF-II on basal proliferation rate in major maternal organs. Treatment of P0 mice with IGF-II, iRGD liposomes and iRGD/IGF-II liposomes did not significantly affect the area of proliferating cells as a proportion of the total area of cells in the maternal (A) brain, (B) heart, (C) lung, (D) liver, (E) kidney, (F) spleen. N=3/8 mice, 10 images of each organ were analysed. All graphs are displayed on the same axis, so comparisons between organs can be made. No significance was observed when Kruskall-Wallis and Dunn's multiple comparisons test for significance were performed; median ± IQR plotted.

5.4 Discussion

Here we report that IGF-II can be delivered selectively to the placenta by encapsulation in iRGD-liposomes and can elicit a biological response in both the C57 and P0 mouse strains. Table 5.1 gives a summary of the effects of treatment on fetal and placental weights, placental morphology and proliferation rate.

It was first important to assess the safety of treatment. Liposomes are inherently biocompatible, but few studies have been undertaken to investigate the effects of their administration during pregnancy, thus it was important to determine whether their repeated administration detrimentally affected pregnancy outcome. Free IGF-I or II have also not previously been administered I.V. to pregnant mice, so it was important to assess their effects on the pregnancy.

No treatment (free IGFs or liposomally encapsulated IGFs) administered to C57 or P0 mice significantly altered the number of resorptions, the number of live pups per litter, or maternal weight gain during the latter half of pregnancy, with the exception of CGKRK-liposomes which decreased fetal weight significantly; this outcome will need to be examined further in due course. There was also no gross fetal or maternal pathology or any alterations in maternal behaviour suggestive of discomfort. Liposomes were therefore considered acceptable to use during pregnancy.

Mouse strain	Treatment	Fetal weight (median)	Placental weight (median)	Placental morphology	Placental proliferation
C57	(c) Free IGF-I	↔	↔	NA	NA
C57	(d) Free IGF-II	↔	↔	↔	↔
C57	(e) Non-coated liposomes	↑ (+6.4% (a))	↔	NA	NA
C57	(f) ARA-liposomes	↔	↔	NA	NA
C57	(g) iRGD-liposomes	↔	↔	↑ (+10.3% (a))	↔
C57	(h) CGKRK-liposomes	↓ (-6.7% (a))	↔	NA	NA
C57	(i) iRGD/IGF-I liposomes	↔	↔	NA	NA
C57	(j) Non-coated/IGF-II liposomes	↓ (-10.7% (e))	↔	NA	NA
C57	(k) ARA/IGF-II liposomes	↔	↔	NA	NA
C57	(l) iRGD/IGF-II liposomes	↔	↑ (+8.9% (a))	↔	↔
P0 (WT fetuses)	(m) Free IGF-II	↔	↔	NA	↔
P0 (P0 fetuses)	(m) Free IGF-II	↔	↔	NA	↔
P0 (WT fetuses)	(o) iRGD liposomes	↔	↔	NA	↔
P0 (P0 fetuses)	(o) iRGD liposomes	↔	↔	NA	↔
P0 (WT fetuses)	(n) iRGD/IGF-II liposomes	↔	↔	NA	↔
P0 (P0 fetuses)	(n) iRGD/IGF-II liposomes	↑(+5.2% (p/q))	↔	NA	↓ (p/q)

Table 5.1: Treatment summary of C57 and P0 animals showing the differences in fetal weight, placental weight, placental morphology and placental cell proliferation.

↑ = treatment significantly increased variable, ↓ = treatment significantly decreased variable, when compared with group displayed in brackets, ↔ = treatment had no effect on variable when compared with untreated animals (a).

5.4.1 Liposome administration to C57 mice

Within a normal C57 litter a range of fetal weights is observed, including a proportion that are defined as growth restricted (<5th centile). It was therefore hypothesized that targeted placental delivery of the mitogens IGF-I and -II in this mouse strain would enhance placental function, improve fetal growth and increase fetal weights at term.

Free IGF-I or IGF-II did not affect litter size, nor the number of resorptions per litter, possibly because they were administered from E11.5, thus could not influence implantation success, as previously reported (Tian et al. 2002; Pinto et al. 2002). Our findings for IGF-I treatment contradict those reported by Sferruzzi-perri et al., (Sferruzzi-perri et al. 2007) who state that continuous subcutaneous administration of IGF-I to guinea pigs reduced the number of resorptions compared with control litters and reduced maternal adipose stores late in pregnancy; we observed no change in maternal weight gain with treatment following 4 bolus injections. Sferruzzi-perri also reported that IGF-II treatment did not alter maternal body weight (Sferruzzi-Perri et al. 2008), supportive of our findings.

Table 5.1 shows that IV administration of free IGF-I or -II to C57 or P0 mice did not significantly alter fetal or placental weights. This opposes previous reports (Sferruzzi-Perri et al. 2008) whereby IGFs enhanced fetal growth (IGF-I = +17% , IGF-II = +11%) and viability near term in guinea pigs by promoting placental nutrient transport to the fetus. The group report that although IGFs did not affect placental weight, IGF-II treatment did increase the cross sectional labyrinth as a percentage of the whole placental area by 9% when compared with controls (Sferruzzi-Perri et al. 2006).

Here, in contradiction to Sferruzzi-perri et al (Sferruzzi-Perri et al. 2006), we report that targeted administration of IGF-II using iRGD/IGF-II liposomes significantly increased placental weight in C57 mice, but this did not increase fetal weight, and targeted IGF-I treatment did not alter fetal or placental weight. As well as this, targeted IGF-II treatment did not significantly increase the placental labyrinth surface area as a proportion of total placental area, but the mean area was increased by 6.2% compared to placentas from non-treated mice, and by 7.2% compared to placentas from IGF-II treated mice. Although these findings were not significant, they are similar to what was reported in guinea pigs (+9%) (Sferruzzi-Perri et al. 2006).

Empty iRGD-liposomes did significantly increase the labyrinth area by 10.3%, compared with both non-treated and free IGF-II treated animals. The rate of cell proliferation was unaffected by treatment at E18.5, suggesting that the observed weight increase may be a result of enhanced proliferation at earlier time points in gestation, or may be due to a decrease in trophoblast apoptosis; the iRGD peptide has been shown to modestly reduce the number of M30 positive cytotrophoblasts when incubated with first trimester human explants (King et al. 2016).

There may be several reasons for the disparities between our data and IGF treatment in pregnant guinea pigs. Firstly, IGFs may be processed differently by mice and guinea pigs; Figure 1.7 shows that there is a high level of variation in the maternal concentration of IGF between species, and Table 1.1 shows that there are different biological responses observed between species when exposed to increased IGF levels. This shows that comparisons between species cannot be easily made. The route of administration (I.V bolus verses subcutaneous infusion) and the timing of

administration (every other day via liposomal delivery verses continuous delivery via osmotic mini-pump) may also affect the results observed. IGFs when administered I.V are likely to have a much shorter half-life than when administered subcutaneously; it has been reported that the half-life of IGF-I/-II is approximately 4 h when administered I.V to male rats (Zapf et al. 1986), but is 21 h when administered subcutaneously to human adolescents (Camacho-Hübner et al. 2006).

It has been hypothesized that IGFs may have a growth regulatory function (Charnock et al. 2015); the hormones don't uniformly increase fetal weight, but normalise fetal weight to within optimal range, so that the fetus doesn't under- or overgrow. This could be a reason as to why we didn't observe an increase in fetal weight following targeted IGF-I or IGF-II treatment in healthy C57 mice, where fetal growth is already following an optimal trajectory. One way to examine this theory was to treat animals with an FGR phenotype such as the P0 mouse.

5.4.2 Liposome administration to P0 mice

We report that targeted IGF-II treatment improved the fetal weight distribution of P0 mice, but did not increase placental weight. In particular, the median P0 fetal weights increased significantly when compared with untreated animals, but the weights of the heavier WT fetuses were unaltered, supporting the normalising theory (Charnock et al. 2015). As litter size and resorption rate was unaffected, this suggests that the growth of the smallest P0 fetuses was enhanced, rather than pregnancy losses occurring earlier in gestation. This finding is clinically relevant as a treatment that increases the weight of the smallest babies, but does not cause overgrowth of appropriately grown babies fulfils

a currently unmet clinical need. Although the P0 phenotype is not rectified to the extent that P0 fetuses are a similar weight to WT fetuses, the relevance of improving the fetal weight distribution, even marginally, has a significant impact on fetal survival and neonatal health; a growth restricted fetus with a birth weight < 10^{th} centile is at a significantly increased risk of fetal death, fetal respiratory distress syndrome and necrotizing enterocolitis (where portions of the bowel undergo necrosis) (Bernstein et al. 2000). It also influences longer-term adult health with FGR babies more likely to develop a range of metabolic and cardiovascular diseases as adults (Ozanne et al. 2004). A pertinent example of which is seen in a cohort of 64-year-old men; those with birthweights less than 2.95 kg (6.5 pounds) were 10 times more likely to have type-2 diabetes than those with birthweights more than 4.31 kg (9.5 pounds) (Barker, Hales, et al. 1993). Therefore a small increase in fetal weight could have a dramatic influence on short and longer term health and even influence future generations (Fernandez-Twinn et al. 2015).

Similar results have been reported when Leu^{27}IGF-II, a human IGF-II analogue that binds to the IGF clearance receptor IGF-2R and in doing so increases the concentration of endogenous IGF-II, was administered subcutaneously to the $eNOS^{-/-}$ mouse model of FGR (Charnock et al. 2015); the mean fetal weights were not significantly increased, nor restored to WT levels, but the fetal weight distribution curve was shifted to the right and a higher proportion of fetuses with weights closer to the mean were observed.

Targeted IGF-II treatment increased placental weight in C57 animals, but did not affect placental weight when administered to P0 animals. This was an unexpected finding, but may be because IGF-II expression is almost eliminated from the labyrinth of P0 animals

so that targeted IGF-II administration is only replacing a small amount of that lost, whereas targeting IGF-II to the placenta of C57 animals is increasing the concentration of IGF-II above optimal levels, potentially saturating available receptors. This excess could have additional functions, including enhancing nutrient transfer to the fetus to promote fetal growth or altering the placental structure, in particular increasing the placental labyrinth cross sectional area (Sferruzzi-Perri et al. 2006), something which we have not yet investigated in the P0 mouse. Although treatment did not increase placental weight, it did alter the basal rate of cell proliferation, but only in the placentas collected from P0 fetuses: the area of Ki-67 positive cells as a proportion of the total area of cells was significantly reduced in the labyrinth, junctional zone and the total placenta. This could mean that proliferation has decreased due to treatment, or that resources have been directed towards fetal growth, rather than placental proliferation. Also, there may have been an initial increase in proliferation when treatment was administered, which increased the total area of cells, meaning that following a return to the basal proliferation rate, the number of proliferating cells as a proportion of total cell area would appear to be decreased.

To fully rescue the P0 mouse model, it may be necessary to treat with a higher dose of IGF-II from a much earlier time point. In this mouse model, the reduction of IGF-II expression in the placental labyrinth has not been quantified (Constância et al. 2002), so we cannot estimate an adequate dose to administer to achieve a physiologically normal concentration, comparable to that expressed by the WT placenta. This is something that could be tried in the future. As well as this, earlier dosing may be necessary. In humans and many other species, IGF-II is expressed in fetal and placental tissues from pre-implantation until just before birth (Nayak & Giudice 2003). The gross placental

structure has already been laid down by E11.5, meaning that treatment from this point may not be able to fully rescue the phenotype due to the abnormal placental pathology already present. Administering targeted IGF-II from shortly after conception may enhance fetal and placental growth to a greater extent than what was observed when treating from E11.5. However, earlier treatment is not yet clinically translatable, as FGR is not usually detected until the second trimester (Papageorghiou et al. 2004).

A benefit of using targeted liposomes is that the therapeutic is selectively delivered to the placenta with minimal drug accumulation in other tissues; thus a lower dose can be administered to achieve the same response (Wang et al. 2010). Due to the passive encapsulation technique used, a concentration of 0.5 mg/kg/dose of IGFs was encapsulated in the liposomes; half of the dose of freely administered IGFs. Encapsulation inside of liposomes increases the drug circulation half-life when compared with the administration of free drug, meaning that dosing was limited to every second day; a regime adjusted to provide a similar concentration of IGFs to that administered previously (Sferruzzi-perri et al. 2007) without stressing the animal with daily injections. By altering the formulation in the future, liposomes could be engineered to release their contents over a much longer time period to provide a sustained dose similar to continuous infusion administration (El-Kareh & Secomb 2000). We observed a biological response of administering targeted IGF-II to both mouse strains, supporting our statement that targeted delivery is more efficient. By this reasoning we can also assume that IGF-II is released from the liposomes when injected in vivo and is capable of interacting with IGF-1R, expressed throughout the labyrinth trophoblast and the junctional zone giant cells, trophoblast and glycogen cells (Charnock et al. 2015), to elicit a biological response. When the concentration of IGF-II

in maternal and fetal blood plasma was quantified, IGF-II was only detectable in maternal plasma when administered in non-coated liposomes. This may be because the undecorated liposomes circulate in the plasma for longer, as they do not display the homing peptide necessary for placental cell binding and internalisation. IGF-II was not detected in pooled fetal bloods when administered freely or using non-targeted or targeted-liposomes, suggesting either that placental drug transfer is minimal, or more likely, given the observation of non-targeted liposomes in the fetal abdomen, that IGF-II is cleared from fetal circulation within 24 hours of maternal administration or is present at an undetectable concentration.

We have previously demonstrated that liposomes are observed in the maternal clearance organs and although release of their CFS payload was not observed in large quantities, IGF release may still occur in the maternal kidney, liver and spleen and cause unwanted side effects. As IGFs are mitogenic hormones, an increase in the weight of these clearance organs could be an indication that abnormal proliferation and therefore IGF-II release had occurred. There was no significant change in the weight of the maternal clearance organs, suggesting that this was not the case. Furthermore, there was no significant increase in the area of Ki-67 positive cells in these organs following any treatment in either mouse model. Off target effects such as these are not normally examined in other drug targeting studies, even though it is accepted that liposomes accumulate in these organs; we believed it was necessary to undertake these experiments. However, we did not observe an alteration in placental weight in the P0 mice, or an increase in proliferation in the C57 mice, but still observed a biological effect, showing that we need to examine the clearance organs more closely to ensure no detrimental side effects. There is also concern that IGF administration or high levels of

endogenous IGFs can cause breast cancer (Sachdev & Yee 2001), retinal damage caused by pathological angiogenesis (Lofqvist et al. 2009), and neural alterations (Lopes et al. 2014), meaning that more detailed histopathological analysis of these tissues will be required in due course.

5.5 Summary

We have shown that targeted IGF-I or IGF-II treatment does not affect fetal weight when administered to healthy C57 pregnant mice, but targeted IGF-II treatment does increase placental weight when compared to controls. Thus it appears that the targeted liposomes can successfully deliver a growth stimulus to the placenta. The lack of effect on the fetus could be due to its growth already being optimal; an increase in fetal weight above its pre-determined optimum could be detrimental to the pregnancy. However in the P0 mouse, where growth restriction is present, targeted IGF-II treatment improved the fetal weight distribution to produce fewer of the lightest and therefore most vulnerable fetuses, without causing overgrowth in their normally growing littermates. As well as this, absence of side effects in maternal clearance organs is encouraging. To conclude, we have developed a method of selectively delivering a payload to the placenta and in doing so have induced a pharmacological effect on the placenta or fetuses; further work needs to be undertaken to fully capitalise on the use of such a targeted system.

Chapter 6: General Discussion and Future Work

6.1.1 Introduction

FGR, defined as the inability of the fetus to reach its maximum growth potential (Chiswick 1985) is associated with a poorly functioning placenta (Chiswick 1985), for which there is no adequate treatment except to deliver the fetus prematurely (Fisk & Atun 2008). Several drugs have been investigated with the aim of improving placental function, increasing nutrient transfer and/or blood perfusion with the hope of increasing fetal growth and viability (Ganzevoort et al. 2014; Alers et al. 2013). However, given the reluctance to administer drugs to pregnant women, the availability of suitable treatment options for FGR is still lacking (Fisk & Atun 2008). Here we demonstrate a targeted strategy that can deliver IGF-II selectively to the mouse placenta, enhancing growth of the smallest, most vulnerable fetuses. This may make treating FGR safer, addressing an important and unmet clinical need.

6.1.2 Development of a targeted nanoparticle for placental drug delivery

To develop a targeted nanoparticle suitable for placental drug delivery, we prepared liposomes displaying the placental homing peptides iRGD or CGKRK on their surface. Scrutinising previous studies in which targeted liposomes have been used to enhance the efficacy of chemotherapeutics (Hoffman et al. 2003; Agemy et al. 2011), as well as examining nanoparticle interactions with human (R. Bajoria & Contractor 1997; Bajoria et al. 2013; R Bajoria et al. 1997; Rekha Bajoria et al. 1997; R Bajoria & Contractor 1997; Barzago et al. 1996) and rodent placentas (Refuerzo et al. 2015; Kaga et al. 2012), informed our decision to synthesise non-targeted liposomes from DSPC:cholesterol:DSPE-PEG(2000) in the MR 65:30:5, and targeted liposomes from

DSPC:cholesterol:DSPE-PEG(2000):DSPE-PEG(2000)-maleimide:peptide in the MR 65:30:3.75:1.25:1.25. This formulation was considered appropriate to deliver and release encapsulated cargo at the placenta, whilst limiting fetal and maternal tissue exposure.

The composition, size and surface charge of the liposomes are important characteristics to control and assess, as they dictate stability and govern how the body and the placenta process the liposomes. The final SD of peptide-coated liposomes containing a payload was between 194 ± 25 nm and 320 ± 60 nm, depending on the encapsulated substance and the final SD of non-coated liposomes was between 180 ± 3 nm and 208 ± 10 nm, again depending on the cargo. All formulations had an approximately neutral or slightly negative ZP in PBS. These measurements are similar to those observed previously (Dubey et al. 2004), (Du et al. 2011), (Nallamothu et al. 2006), (Li et al. 2011), showed good reproducibility and were appropriate for placental delivery. All liposome compositions were stable when stored at 4 ºC for up to 4 weeks, as determined by SD measurements. Good stability is necessary to ensure extended shelf life and reduce manufacturing costs if used clinically.

6.1.3 Targeted liposomes accumulated in the human and mouse placenta

Liposomes coated in CGKRK or iRGD homing peptides selectively bound to human placental tissue; specifically, the targeted liposomes bound to and accumulated within the placental syncytiotrophoblast and remained there for several days. Release and uptake of CFS was observed and, after 48 hours a proportion appeared to have penetrated the trophoblast bilayer and was present within the villous stroma. This

suggests a potential risk of placental transfer into fetal circulation, which will need to be investigated in more detail, either by using the dual perfused human placenta or in Phase 0/I trials in human pregnancies by examining fetal cord blood and/or plasma. Although CFS was used as a tracer to study drug release and tissue distribution, it is unlikely that IGF-I/-II or any other encapsulated payload will behave in exactly the same way, due to differences in structure, size, charge and uptake mechanism. Indeed, CFS was observed in the mouse placental labyrinth within 6 h of targeted liposome administration and remained there for 72 h, but IGF-II was not detected in fetal plasma 24 h after targeted administration of liposomally encapsulated IGF-II. Once internalised, CFS remains within the cytoplasm for a prolonged period of time (R Bajoria et al. 1997). The same may not be true for IGF-II: the growth hormone interacts with its receptors, is broken down and cleared rapidly, with a half-life of approximately 4 hours when administered I.V. to rodents (Zapf et al. 1986); this would explain why they were not detected in maternal or fetal plasma.

Targeted and non-targeted liposomes were both taken up by human placental explants cultured in vivo, perhaps because the liposomes are comprised of fatty lipids, a good nutrient source, and choline; there are choline transporters present on the ST of human placental explants throughout gestation (Baumgartner et al. 2015). Liposomes can be internalised into cells by either fusion (Düzgüneş & Nir 1999; Poste & Papahadjopoulos 1976; Huth et al. 2006) or endocytosis (Huth et al. 2006). There is evidence that they are predominantly endocytosed by isolated term human placental cytotrophoblasts (R Bajoria et al. 1997). However, the syncytiotrophoblast of intact explants differs in many ways from the underlying cytotrophoblast layer, and the presence of surface homing peptides increased the kinetics of liposome uptake, suggesting that targeted liposomes

may be internalised by a different mechanism. iRGD is an example of a CendR protein sequence as it contains an R/KXXR/K motif at its C-terminus (Sugahara et al. 2009). This peptide sequence associates with integrin α_v on tumour vasculature, after which it is cleaved and internalised via neuropilin-1 (Sugahara et al. 2009), often appearing in endosomes or multivesicular bodies after entry (Pang et al. 2014). This process is similar to pinocytosis, but is nutrient-dependent, cannot be suppressed by standard inhibitors of pinocytosis and does not depend on any known components of the endocytosis machinery (Pang et al. 2014). King et al (King et al. 2016) report that iRGD co-localises with α_v expressed on the syncytiotrophoblast of placental explants, suggesting that it is also internalised via neuropilin-1. Agemy et al. (Agemy et al. 2013) report that CGKRK is internalised by a similar mechanism, mediated by interactions with p32, a protein expressed on the surface of angiogenic vascular endothelium and tumour cells, but they do not elucidate further on the mechanism of internalisation. King et al. (King et al. 2016) report that CGKRK interacts with calrecticulin expressed on the placental syncytiotrophoblast; the mechanism of internalisation is unknown and will need to be examined further. As CGKRK and iRGD are cell-penetrating peptides that aid internalisation of attached cargo (Pang et al. 2014; Agemy et al. 2011; Sugahara et al. 2009), it is likely that they are responsible for internalization of our targeted liposomes by the syncytiotrophoblast, where they are degraded by lysosomes, releasing their encapsulated drug. This might explain why uptake of targeted liposomes is quicker than uptake of non-targeted liposomes as observed here and previously reported by Nallamouthu et al. (Nallamothu et al. 2006), and why drug release is only observed from targeted liposomes, as previously reported (Zhang et al. 2010) in support of our findings.

For in vivo studies, C57 mice were intravenously injected with liposomes at different stages of gestation. To reduce the risk of fetal exposure, animals were only treated after E11.5 when the placental barrier is fully formed (Georgiades et al. 2002). The targeted liposomes selectively accumulated in the placental labyrinth and spiral arteries and once there, were able to deliver CFS to the materno-fetal interface. There was no evidence of drug transfer to the fetus when using targeted liposomes, but non-targeted liposomes and CFS were observed in fetal tissues after 24 h, suggesting fetal liposome transfer and CFS uptake, as previously observed with the perfused human placenta (R. Bajoria & Contractor 1997; R Bajoria & Contractor 1997). This further supports the use of targeted liposomes for placental delivery to minimise the risk of fetal drug exposure.

With the exception of transient accumulation in the maternal clearance organs, as previously reported (Agemy et al. 2011), peptide decorated-liposomes were not detected in any other maternal organs, demonstrating selectivity of placental targeting. Liposomes were not detected in the clearance organs 72 hours after administration, whereas they were still present in the placenta, suggestive of selective retention. The liposomes prepared here were too large to be rapidly excreted by glomerular filtration through the kidneys (Andresen et al. 2005), suggesting that the pink urine collected 3 h after liposome administration contained degraded fluorophore, fluorophore-labelled peptide and/or fluorophore-peptide-lipid conjugates, rather than intact liposomes.

6.1.4 The effect of targeted IGF treatment on pregnant C57 and P0 mice

The specificity of liposome accumulation within the labyrinth of the mouse placenta provided us with the opportunity to deliver a therapeutic to this region that could

improve placental growth, cell survival and/or enhance nutrient exchange. We decided to encapsulate IGF-I or IGF-II in the targeted liposomes as their receptors are expressed by the placental labyrinth (Charnock et al. 2015) and they enhance healthy placental function in both human tissue (Forbes et al. 2008) and animals (Sferruzzi-perri et al. 2007). We therefore hypothesized that targeted IGF administration would enhance placental function, increase fetal growth, which would translate into a heavier fetus at term.

The effect of IGF-I or -II administration to pathological human placental tissue or mouse models of FGR has not been examined. However, administration of Leu^{27}(IGF-II), which increases the concentration of endogenous IGF-II, did increase fetal weight in the $eNOS^{-/-}$ mouse model and reduced the number of fetuses falling below the 5^{th} centile in weight (Charnock et al. 2015). Also, mouse models of FGR and/or PE such as the P0, $eNOS^{-/-}$ or the catechol-O-methyl transferase knockout ($COMT^{-/-}$) mouse, can be rescued by the administration of vasodilators (Stanley, Andersson, Poudel, et al. 2012; Dilworth et al. 2013) or antioxidants (Stanley, Andersson, Hirt, et al. 2012), which help to ameliorate maternal symptoms, enhance placental function and improve fetal growth and viability.

Our study showed that multiple doses of liposomes were well tolerated during the latter half of mouse pregnancy in C57 and P0 mice; treatment did not affect litter size, resorption rate or normal maternal weight gain and no overt maternal or fetal pathology was observed. Repeated liposome administration has not been undertaken before and the results were promising, suggesting that liposomes have therapeutic potential in pregnancy and may be clinically useful for safer administration of drugs to pregnant

women, such as indomethacin, warfarin and valproic acid (Refuerzo et al. 2015; Bajoria et al. 2013; Barzago et al. 1996).

We report that administering iRGD/IGF-liposomes to C57 mice significantly increased placental weight, but this increase did not translate into an increase in fetal weight. We can conclude that the targeted liposomes successfully delivered IGF-II to the placental surface eliciting a biological response, but an alteration in placental cell proliferation was not observed at the time of tissue collection, nor was the surface area of the labyrinth increased as a proportion of the total placental area, as previously reported with subcutaneous IGF-II administration in guinea pigs (Sferruzzi-Perri et al. 2008). The fact that fetal weight did not increase suggests that although the placenta is larger, it had not subsequently become more efficient (Coan et al. 2008); the mass of fetus produced per unit mass of placenta had actually decreased. Parallel experiments undertaken with targeted IGF-I showed that placental growth-promoting effect was IGF-II specific, confirming that IGF-II has a bigger influence on placental development than IGF-I, as previously reported (Baker et al. 1993; Sferruzzi-Perri et al. 2011).

IGF-II has recently been hypothesized to have a growth normalising effect in pregnancy (Charnock et al. 2015); an increase in fetal weight was not observed when Leu^{27}(IGF-II) was administered via subcutaneous mini-pump to C57 mice, but treatment did increase fetal weight in the $eNOS^{-/-}$ mouse, which exhibits FGR. Our findings in healthy C57 mice also support the notion that there are regulatory mechanisms in place to prevent detrimental fetal overgrowth, as is observed in human macrosomia (Stotland et al. 2004). To examine this effect further, we decided to administer IGF-II treatment to the P0 mouse: targeted IGF-II treatment significantly increased the median fetal weight of

the P0 fetuses, but did not affect the WT fetuses. It also altered the fetal weight distribution curves, with no fetuses from treated dams falling below the 5th and 10th weight centiles of P0 fetuses from untreated dams. The treatment had no effect on median placental weight in either P0 or WT fetuses and did not increase the fetal:placental weight ratio, suggesting that it must have increased fetal weight by enhancing one or more aspects of placental function, rather than just increasing its weight. Assessment of rates of placental cell proliferation showed that targeted IGF-II treatment decreased the area of Ki-67 positive cells as a proportion of total cells in the placental labyrinth, junctional zone and the whole placenta collected from P0 fetuses, but did not alter proliferation in placentas from WT fetuses. Targeted IGF-II treatment may have diverted resources from placental cell growth to fetal growth. Or it may be that treatment initially increased proliferation, increasing the total number of cells in the placenta, so that when the proportion of Ki-67 positive cells were examined 24 hours after the cessation of treatment, there appeared to be a reduction. Targeted IGF-II treatment only affected proliferation in the placentas from the smallest, most vulnerable fetuses, supporting the hypothesis that a growth normalising mechanism may have been stimulated.

Empty, non-coated liposomes increased fetal weight when administered to C57 animals, but non-coated liposomes encapsulating IGF-II decreased fetal weight significantly. As we have shown non-specific placental uptake of liposomes in human tissue, and accumulation of non-coated liposomes in fetal tissues, we believe that this increase may be due to the metabolism of the lipids that make up the liposomes by the fetus (Baumgartner et al. 2015). By itself, this appears to be a potential treatment for FGR, but increasing fetal weight solely by metabolism of fat, rather than promoting healthy

fetal growth by appropriate nutrient delivery from the placenta, is not ideal. It may be that this is equivalent to a high fat maternal diet, which has already been shown to cause fetal macrosomia (Hardy 1999), and future adult metabolic and cardiovascular diseases (Newbern & Freemark 2011; Ozanne et al. 2004; Aiken et al. 2013). Further experiments to assess the health of the offspring from treated animals could be done to confirm this and are described in section 6.1.5

In contrast, fetal weight was reduced when the fetus received IGF-II via non-coated liposomes, suggesting that exposure to high concentrations of IGF-II are detrimental to fetal growth and development, possibly by inducing downregulation of endogenous IGF-II production, downregulation of IGF-II receptor expression, or activation of an unknown regulatory mechanism to limit overgrowth. This hypothesis can be investigated further by undertaking immunohistochemistry on archived fetal tissue at a later date. This evidence of fetal drug exposure when using non-coated liposomes further supports our use of targeted liposomes to limit drug delivery to the placenta.

Treatment of C57 animals with iRGD-liposomes and ARA-liposomes did not significantly alter fetal or placental weight compared with the non-treated group. It must therefore be assumed that the placenta handles peptide-decorated liposomes differently. As discussed previously when examining uptake of liposomes by human explants, the presence of the surface homing peptide may induce internalisation by a pinocytosis-like receptor mediated mechanism, as opposed to fusion/endocytosis of non-coated liposomes. We have shown that iRGD-liposomes were retained within the placenta and were not transferred to the fetus, whereas ARA-liposomes were transferred to the fetus. As an increase in fetal weight was not observed, it could be hypothesised that ARA-

liposomes do not enter the fetal tissue to the same extent as the non-coated liposomes, that ARA-liposomes release their cargo prior to fetal transfer, or that once inside the fetus, they are metabolised differently to undecorated liposomes. It is also possible that the peptide coating inhibits lipid breakdown and utilisation by the fetus.

Finally, intravenous injections of free IGF-I or IGF-II to C57 animals did not increase fetal or placental weight significantly when compared with the non-handled group. IV injection of free IGF-II to P0 animals also had no effect on fetal or placental weight. These findings differ from those previously reported, whereby subcutaneous continuous administration of IGF-I or IGF-II to guinea pigs at a similar concentration to that used in our study, increased fetal weight and viability by increasing the placenta's ability to transport nutrients to the fetus (Sferruzzi-Perri et al. 2006). This may suggest that the route of administration of growth factors determine their physiological effect; however, differences in species and dosing regimen (continuous versus bolus) and route of administration may also influence outcome.

The biological consequences of administering liposomes and homing peptides to healthy organs and tissues have not previously been investigated. We believed that this was important to assess, as we observed transient passage of liposome through the maternal clearance organs, and it is possible that if IGF-II is released from the liposomes at this point, unwanted biological effects such as altered proliferation may be induced. Our study did not detect an increase in the weight of the maternal kidney, spleen or liver in C57 or P0 mice, nor was the basal rate of proliferation altered in these organs at the time of tissue collection, providing evidence that there was no significant drug release. However, there was also no effect of free IGF-II treatment on maternal

organs, possibly due to the short half-life associated with I.V. administration (Zapf et al. 1986). It will therefore be necessary to assess the morphology and function of the organs in more detail in due course, to ensure that targeted placental treatment truly reduces the risk of off-target side effects.

To summarise, by targeting IGF-II to the placenta using homing peptide decorated liposomes, we have enhanced placental growth in healthy mice and improved fetal growth in mice exhibiting FGR. We have demonstrated that multiple doses of targeted liposomes are well tolerated and can elicit tissue specific effects in pregnancy, showing that IGF-II encapsulated inside liposomes remains bioactive. The liposomes also accumulated in the human placental syncytiotrophoblast ex vivo, and released their encapsulated payload. This suggests that targeted treatment has the potential be translated into humans, with the aim of administering a drug that can enhance placental function and increase fetal weight; a novel approach to the treatment of FGR.

6.1.5 Future work

6.1.5.1 Immediate experiments

To support some of the findings of this project, it will be necessary to conduct further experiments. Firstly, it would be informative to obtain morphological images of targeted liposomes using cryo-tranmission electron microscopy (cryo-TEM) (Almgren et al. 2000) to validate current data regarding homing peptide-liposomes conjugation, cargo encapsulation and size distribution. The encapsulation efficiency of IGF-I by ELISA should be quantified, and the release profiles of IGF-I and -II from liposomes in vitro

should be characterised by performing dialysis in culture medium, allowing us to better estimate drug release rates in vivo. It may be necessary to take into account the actions of tissue-derived enzymes such as placental lipases (Barrett et al. 2015) released from human placental explants as they may enhance release in vivo, so could be incorporated into the assay. Targeted liposomes could also be tracked in real time in vivo, using techniques such as positron emission tomography (PET) (Seo et al. 2008) or MRI (Kamaly & Miller 2010), to further assess tissue distribution and pharmacokinetics of the liposomes and encapsulated drug. Together, these findings may inform our choice of dosing regime and drug concentration to be used for future experiments.

Additionally, it would be useful to examine whether targeted IGF-II treatment increases placental nutrient transport in C57 and/or P0 mice, as reported in guinea pigs (Sferruzzi-Perri et al. 2008). This can be quantified by administering radiolabelled analogues of glucose ([3H]-methyl-D-glucose) and amino acids (methyl [14C]-amino-isobutyric acid) to the mother, then detecting radionucleide accumulation in the placenta and transfer into the fetal plasma (Dilworth et al. 2010).

6.1.5.2 Long term studies

To achieve translation into a clinical setting, it will be necessary to examine the safety and efficacy of our liposome-drug formulation and to undertake toxicity studies in appropriate large animal models. To do this, the liposome formulation may need to be modified to further optimise efficacy, stability and drug release. Different surface peptide concentrations and different lipid formulations could be tested, and liposomes could be synthesised from pH-sensitive lipids that break down in a hypoxic

environment (Andresen et al. 2005), such as a poorly perfused placenta to optimise drug release at the placental surface. Different methods of IGF-II encapsulation such as incorporating IGF-II in the lipid film before rehydration or using the pH-gradient loading method (Fritze et al. 2006) could also be utilised to achieve higher encapsulation concentration, translating to a higher delivered dose. Different drugs or a combination of drugs could be examined to further enhance placental function. Combining a vasodilator with a growth factor may enhance placental blood flow, and therefore the nutrient and oxygen supply required to support growth factor-induced enhancement of proliferation. Delivering a combination of drugs to diseased tissues has previously been reported to increase the efficacy of chemotherapeutics (Hare et al. 2013). IGF-I and IGF-II could also be co-encapsulated and administered in combination, as they are both essential for adequate fetal and placental growth and may need to be present together to induce optimal growth. We could also examine the use of the antioxidant melatonin, which is currently undergoing clinical trials as treatment for PE and FGR, with the hope of simultaneously decreasing oxidative stress and improving placental function (Hobson et al. 2013). Findings from the literature combined with our data indicate that targeted IGF-II delivery could be combined with an enhanced maternal dietary regime, providing optimal resources to facilitate enhanced placental nutrient partitioning in favour of the fetus, without detrimentally affecting the mother (Sferruzzi-Perri et al. 2008).

The effectiveness of different dosing regimens and the consequences of administering therapies earlier in pregnancy will also need to be examined. This will become particularly important as diagnostic testing allows for earlier detection of pathology and earlier implementation of treatment. Appropriate nutrient availability and fetal growth

early in pregnancy affects fetal outcome and long-term adult health (Fleming et al. 2012), hence early treatment of suboptimal growth could be particularly effective. It will be important to determine whether administering treatment every other day is appropriate in humans or whether daily dosing or weekly infusion may be needed; it has been shown that bolus liposomal administration of encapsulated drug provides a similar plasma dose to continuous infusion of free drug (El-Kareh & Secomb 2000), our formulation of targeted liposomes could provide a more selective treatment option that is quicker to administer.

To facilitate translation into clinical trials, initially, safety and tissue distribution studies will need to be conducted in larger animal models, such as the ovine model (David et al. 2011) or non-human primates (Liu et al. 2013). The potential for off target side effects of treatment on fetal development and long-term health will need to be examined by conducting longitudinal studies of the offspring of treated females. Several parameters will need to be studied including; examining alterations in glucose metabolism by performing glucose tolerance tests (Andrikopoulos et al. 2008); assessing evidence of cardiovascular disorders, altered vascular responses and/or hypertension using tail cuff or radiotelemetry techniques (Whitesall et al. 2004), and ensuring there is not postnatal overgrowth or adult obesity by monitoring weight gain; all of which are associated with excessive IGF-II exposure in utero and postnatally (Livingstone & Borai 2014). It will also be important to examine the effects of treatment on reproductive capability and epigenetic modifications (Fernandez-Twinn et al. 2015), ensuring that future generations are unaffected by treatment. Beyond this, initial safety testing, liposome tissue distribution and drug release kinetics could be examined in women requiring a pregnancy termination. Eventually, the treatment could be tested in a small clinical trial

recruiting pregnant women with severe early-onset FGR with dismal prognosis, to see if treatment improves fetal viability and/or placental function, as is current practice with other studies (von Dadelszen et al. 2011; Hobson et al. 2013). This stage may be easier to conduct using liposomes encapsulating sildenafil citrate or melatonin, both of which have already been approved for administration to pregnant women for clinical studies.

Finally, it may be possible to expand studies by administering targeted treatment to mouse models of other pregnancy complications such as pre-eclampsia, miscarriage and premature labour. Indomethacin has already been encapsulated inside liposomes with the aim of stopping early onset contractions whilst limiting fetal drug exposure, and has been shown to be effective in rats/mice (Refuerzo et al. 2015); targeted liposomes may improve safety and efficacy of this approach.

Chapter 7: References

Abheiden, C. et al., 2015. Does low-molecular-weight heparin influence fetal growth or uterine and umbilical arterial Doppler in women with a history of early-onset uteroplacental insufficiency and an inheritable thrombophilia? Secondary randomised controlled trial results. *BJOG*. Available at: http://doi.wiley.com/10.1111/1471-0528.13421.

Agemy, L. et al., 2013. Proapoptotic peptide-mediated cancer therapy targeted to cell surface p32. *Molecular Therapy*, 21(12), pp.2195–2204. Available at: http://www.ncbi.nlm.nih.gov/pubmed/23959073.

Agemy, L. et al., 2011. Targeted nanoparticle enhanced proapoptotic peptide as potential therapy for glioblastoma. *PNAS*, 108(42), pp.17450–17455. Available at: http://www.pnas.org/content/108/42/17450.short.

Aiken, C.E., Tarry-Adkins, J.L. & Ozanne, S.E., 2013. Suboptimal nutrition in utero causes DNA damage and accelerated aging of the female reproductive tract. *FASEB Journal*, 27(10), pp.3959–3965.

Aiken, C.E., Tarry-Adkins, J.L. & Ozanne, S.E., 2015. Transgenerational developmental programming of ovarian reserve. *Scientific reports*, 5. Available at: http://www.pubmedcentral.nih.gov/articlerender.fcgi?artid=4630792&tool=pmcentrez&rendertype=abstract.

Alemdaroğlu, C. et al., 2007. Investigation of epidermal growth factor containing liposome formulation effects on burn wound healing. *Journal of biomedical materials research. Part A*, 85(1), pp.271–83. Available at: http://www.ncbi.nlm.nih.gov/pubmed/17937411.

Alers, N.O. et al., 2013. Antenatal melatonin as an antioxidant in human pregnancies complicated by fetal growth restriction - a phase I pilot clinical trial: study protocol. *BMJ Open*, 3(12), p.004141. Available at: http://bmjopen.bmj.com/cgi/doi/10.1136/bmjopen-2013-004141.

Allen, T.M. et al., 1991. Liposomes containing synthetic lipid derivatives of poly(ethylene glycol) show prolonged circulation half-lives in vivo. *Biochimica et Biophysica Acta*, 1066, pp.29–36. Available at: http://www.sciencedirect.com/science/article/pii/0005273691902465 [Accessed August 29, 2012].

Almgren, M., Edwards, K. & Karlsson, G., 2000. Cryo transmission electron microscopy of liposomes and related structures. *Colloids and Surfaces A: Physicochemical and Engineering Aspects*, 174, pp.3–21.

Andersen, A.J. et al., 2013. Complement activation by PEG-functionalized multi-walled carbon nanotubes is independent of PEG molecular mass and surface density. *Nanomedicine: Nanotechnology, Biology, and Medicine*, 9(4), pp.469–473. Available at: http://dx.doi.org/10.1016/j.nano.2013.01.011.

Andresen, T.L., Jensen, S.S. & Jørgensen, K., 2005. Advanced strategies in liposomal cancer therapy: problems and prospects of active and tumor specific drug release.

Progress in lipid research, 44(1), pp.68–97. Available at: http://www.ncbi.nlm.nih.gov/pubmed/15748655 [Accessed March 6, 2013].

Andrikopoulos, S. et al., 2008. Evaluating the glucose tolerance test in mice. *American Journal of Physiology: Endocrinology And Metabolism*, 295, pp.1323–1332.

Aplin, J.D., 2000. The cell biological basis of human implantation. *Baillière's best practice & research. Clinical obstetrics & gynaecology*, 14(5), pp.757–764. Available at: http://www.ncbi.nlm.nih.gov/pubmed/11023797 [Accessed August 20, 2012].

Aris, A. et al., 2008. Detrimental effects of high levels of antioxidant vitamins C and E on placental function: Considerations for the Vitamins in Preeclampsia (VIP) trial. *Journal of Obstetrics and Gynaecology Research*, 34(4), pp.504–511. Available at: http://doi.wiley.com/10.1111/j.1447-0756.2008.00722.x.

Avanti Polar Lipids Inc., 2016a. Lipids for liposome formation. Available at: http://avantilipids.com/tech-support/liposome-preparation/lipids-for-liposome-formation/ [Accessed January 1, 2015].

Avanti Polar Lipids Inc., 2016b. Liposome preparation. Available at: http://avantilipids.com/tech-support/liposome-preparation/.

Avanti Polar Lipids Inc., 2016c. Preparing large, unilamellar vesicles by extrusion. Available at: http://avantilipids.com/index.php?option=com_content&view=article&id=1600&Itemid=381 [Accessed January 1, 2012].

Bajoria, R. & Contractor, S.F., 1997. Effect of surface charge of small unilamellar liposomes on uptake and transfer of carboxyfluorescein across the perfused human term placenta. *Pediatric Research,*, 42(2), pp.520–527.

Bajoria, R. & Contractor, S.F., 1997. Effect of the size of liposomes on the transfer and uptake of carboxyfluorescein by the perfused human term placenta. *The Journal of pharmacy and pharmacology*, 49(7), pp.675–81. Available at: http://www.ncbi.nlm.nih.gov/pubmed/9255710.

Bajoria, R., Fisk, N.M. & Contractor, S.F., 1997. Liposomal thyroxine: a noninvasive model for transplacental fetal therapy. *Journal of Clinical Endocrinology and Metabolism*, 82(10), pp.3271–3277.

Bajoria, R., Sooranna, S. & Chatterjee, R., 2013. Effect of lipid composition of cationic SUV liposomes on materno-fetal transfer of warfarin across the perfused human term placenta. *Placenta*, 34(12), pp.1216–22. Available at: http://www.ncbi.nlm.nih.gov/pubmed/24183755.

Bajoria, R., Sooranna, S.R. & Contractor, S.F., 1997. Endocytotic uptake of small unilamellar liposomes by human trophoblast cells in culture. *Human reproduction*, 12(6), pp.1343–8. Available at: http://www.ncbi.nlm.nih.gov/pubmed/9222028.

Baker, J. et al., 1993. Role of insulin-like growth factors in embryonic and postnatal growth. *Cell*, 75(1), pp.73–82. Available at: http://www.ncbi.nlm.nih.gov/pubmed/8402902.

Barker, D.J.P., Godfrey, K.M., et al., 1993. Fetal nutrition and cardiovascular disease in adult life. *The Lancet*, 341, pp.938–941.

Barker, D.J.P. et al., 1989. Growth in utero, blood pressure in childhood and adult life, and mortality from cardiovascular disease. *BMJ*, 298, pp.564–567.

Barker, D.J.P., Hales, C.N., et al., 1993. Type 2 (non-insulin-dependent) diabetes mellitus, hypertension and hyperlipidaemia (syndrome X): relation to reduced fetal growth. *Diabetologia*, 36(1), pp.62–67.

Barrett, H.L. et al., 2015. Placental lipase expression in pregnancies complicated by preeclampsia: a case-control study. *Reproductive biology and endocrinology*, 13(100), pp.1–9. Available at: http://www.rbej.com/content/13/1/100.

Barzago, M.M. et al., 1996. Placental transfer of vaiproic acid after liposome encapsulation during in vitro human placenta perfusion. *The journal of Pharmacology and Experimental Therapeutics*, 277, pp.79–86.

Bates, D.O. & Harper, S.J., 2003. Regulation of vascular permeability by vascular endothelial growth factors. *Vascular Pharmacology*, 39, pp.225–237.

Baumgartner, H. et al., 2015. Characterization of choline transporters in the human placenta over gestation. *Placenta*, 36, pp.1362–1369.

Becker, P.M. et al., 2005. Neuropilin-1 regulates vascular endothelial growth factor-mediated endothelial permeability. *Circulation Research*, 96(12), pp.1257–1265.

Benirschke, K. & Kaufmann, P., 2000. Pathology of the human placenta.

Bernstein, I.M. et al., 2000. Morbidity and mortality among very-low-birth-weight neonates with intrauterine growth restriction. *American Journal of Obstetrics and Gynecology*, 182(1), pp.198–206.

Biswas, S. & Ghosh, S.K., 2008. Gross morphological changes of placentas associated with intrauterine growth restriction of fetuses: a case control study. *Early Human Development*, 84(6), pp.357–362.

Biswas, S., Ghosh, S.K. & Chhabra, S., 2008. Surface area of chorionic villi of placentas: an index of intrauterine growth restriction of fetuses. *Journal of Obstetrics and Gynaecology Research*, 34(4), pp.487–493.

Blume, G. & Cevc, G., 1993. Molecular mechanism of the lipid vesicle longevity in vivo. *Biochim Biophys Acta.*, 1146, pp.157–168.

Bowen, J.A. & Hunt, J.S., 1999. Expression of cell adhesion molecules in murine placentas and a placental cell line. *Biology of reproduction*, 60, pp.428–434.

Brosens, I., Robertson, W. & Dixon, H., 1972. The role of the spiral arteries in the pathogenesis of preeclampsia. *Obstet Gynecol Annu.*, 1, pp.177–91.

Bujold, E., Roberge, S. & Nicolaides, K.H., 2014. Low-dose aspirin for prevention of adverse outcomes related to abnormal placentation. *Prenatal Diagnosis*, 34, pp.642–648.

Burton, G.J. et al., 2009. Rheological and physiological consequences of conversion of the maternal spiral arteries for uteroplacental blood flow during human pregnancy. *Placenta*, 30(6), pp.473–482. Available at: http://linkinghub.elsevier.com/retrieve/pii/S0143400409000666.

Calvert, S.J. et al., 2013. Analysis of syncytial nuclear aggregates in preeclampsia shows increased sectioning artefacts and decreased inter-villous bridges compared to healthy placentas. *Placenta*, 34(12), pp.1251–1254. Available at: http://dx.doi.org/10.1016/j.placenta.2013.10.001.

Camacho-Hübner, C. et al., 2006. Pharmacokinetic studies of recombinant human insulin-like growth factor I (rhIGF-I)/rhIGF-binding protein-3 complex administered to patients with growth hormone insensitivity syndrome. *J Clin Endocrinol Metab.*, 91(4), pp.1246–1253.

Cancer.Net Editorial Board, 2014. Hand-Foot Syndrome or Palmar-Plantar Erythrodysesthesia. Available at: http://www.cancer.net/navigating-cancer-care/side-effects/hand-foot-syndrome-or-palmar-plantar-erythrodysesthesia.

Carter, A.M., 2007. Animal models of human placentation - a review. *Placenta*, 21, pp.S41–S47. Available at: http://dx.doi.org/10.1016/j.placenta.2006.11.002.

Cetin, I. et al., 1988. Umbilical amino acid concentrations in appropriate and small for gestational age infants: a biochemical difference present in utero. *Am J Obstet Gynecol*, 158(1), pp.120–126.

Cevc, G., 1991. How membrane chain-melting phase-transition temperature is affected by the lipid chain asymmetry and degree of unsaturation: an effective chain-length model. *Biochemistry*, 30(29), pp.7186–93. Available at: http://www.ncbi.nlm.nih.gov/pubmed/1854729.

Chan, W.S. & Ray, J.G., 1999. Low molecular weight heparin use during pregnancy: issues of safety and practicality. *Obstet Gynecol Surv.*, 54(10), pp.649–54.

Charan, J. & Kantharia, N.D., 2013. How to calculate sample size in animal studies? *J Pharmacol Pharmacother*, 4, pp.303–306.

Charnock, J.C. et al., 2015. The impact of a human IGF-II analogue ([Leu 27]IGF-II) on fetal growth in a mouse model of fetal growth restriction. *American Journal of Physiology - Endocrinology And Metabolism*, (4), pp.E24–E31. Available at: http://ajpendo.physiology.org/lookup/doi/10.1152/ajpendo.00379.2015.

Chiswick, M.L., 1985. Intrauterine growth retardation. *British medical journal*, 291, pp.845–848.

Chonn, A., Semple, S.C. & Cullis, P.R., 1992. Association of blood proteins with large unilamellar liposomes in vivo: relation to circulation lifetimes. *Journal of Biological Chemistry*, 267(26), pp.18759–18765.

Christians, J.K. & Gruslin, A., 2010. Altered levels of insulin-like growth factor binding protein proteases in preeclampsia and intrauterine growth restriction. *Prenatal diagnosis*, 30, pp.815–820.

Coan, P.M. et al., 2008. Adaptations in placental nutrient transfer capacity to meet fetal growth demands depend on placental size in mice. *The Journal of physiology*, 586(Pt 18), pp.4567–4576.

Coan, P.M., Burton, G.J. & Ferguson-Smith, A.C., 2005. Imprinted genes in the placenta - a review. *Placenta*, 26, pp.10–20.

Coan, P.M., Ferguson-Smith, A.C. & Burton, G.J., 2004. Developmental dynamics of the definitive mouse placenta assessed by stereology. *Biology of reproduction*, 70(6), pp.1806–13. Available at: http://www.ncbi.nlm.nih.gov/pubmed/14973263 [Accessed May 11, 2015].

Constância, M. et al., 2002. Placental-specific IGF-II is a major modulator of placental and fetal growth. *Nature*, 417, pp.945–948. Available at: http://www.ncbi.nlm.nih.gov/pubmed/12087403.

Cooley, S.M. et al., 2010. Maternal insulin-like growth factors 1 and 2 (IGF-1, IGF-2) and IGF BP-3 and the hypertensive disorders of pregnancy. *The journal of maternal-fetal & neonatal medicine*, 23(7), pp.658–61. Available at: http://www.ncbi.nlm.nih.gov/pubmed/20540659 [Accessed August 2, 2012].

Cox, B. et al., 2009. Comparative systems biology of human and mouse as a tool to guide the modeling of human placental pathology. *Molecular systems biology*, 5(279). Available at: http://www.pubmedcentral.nih.gov/articlerender.fcgi?artid=2710868&tool=pmcentrez&rendertype=abstract [Accessed January 29, 2013].

Von Dadelszen, P. et al., 2011. Sildenafil citrate therapy for severe early-onset intrauterine growth restriction. *BJOG*, 118(5), pp.624–628. Available at: http://www.ncbi.nlm.nih.gov/pubmed/21392225 [Accessed August 20, 2012].

Daraghmeh, N. et al., 2001. Determinaton of sildenafil citrate and related substances in the commercial products and tablet dosage form using HPLC. *Journal of Pharmaceutical and Biomedical Analysis*, 25, pp.483–492. Available at: http://linkinghub.elsevier.com/retrieve/pii/S0731708500005124.

David, A.L. et al., 2011. Recombinant adeno-associated virus-mediated in utero gene transfer gives therapeutic transgene expression in the sheep. *Human Gene Therapy*,

22(4), pp.419–426. Available at: http://www.liebertonline.com/doi/abs/10.1089/hum.2010.007.

Davidge, S.T. et al., 1992. Sera antioxidant activity in uncomplicated and preeclamptic pregnancies. *Am J Obstet Gynecol*, 79(6), pp.897–901.

DeChiara, T.M., Robertson, E.J. & Efstratiadis, a, 1991. Parental imprinting of the mouse insulin-like growth factor II gene. *Cell*, 64(4), pp.849–859.

Denley, A. et al., 2005. Molecular interactions of the IGF system. *Cytokine & Growth Factor Reviews*, 16, pp.421–439. Available at: http://linkinghub.elsevier.com/retrieve/pii/S1359610105000559.

Desforges, M. & Sibley, C.P., 2010. Placental nutrient supply and fetal growth. *The International journal of developmental biology*, 54, pp.377–90. Available at: http://www.ncbi.nlm.nih.gov/pubmed/19876836 [Accessed August 20, 2012].

Dilworth, M.R. et al., 2011. Defining fetal growth restriction in mice: a standardized and clinically relevant approach. *Placenta*, 32(11), pp.914–916. Available at: http://www.ncbi.nlm.nih.gov/pubmed/21889207 [Accessed May 11, 2015].

Dilworth, M.R. et al., 2010. Placental-specific Igf2 knockout mice exhibit hypocalcemia and adaptive changes in placental calcium transport. *PNAS*, 107(8), pp.3894–3899.

Dilworth, M.R. et al., 2013. Sildenafil citrate increases fetal weight in a mouse model of fetal growth restriction with a normal vascular phenotype. *PLoS ONE*, 8(10), p.e77748. Available at: http://dx.plos.org/10.1371/journal.pone.0077748.

Dilworth, M.R. & Sibley, C.P., 2012. Review: Transport across the placenta of mice and women. *Placenta*, 44, pp.1–6. Available at: http://www.ncbi.nlm.nih.gov/pubmed/23153501 [Accessed January 29, 2013].

DOHaD, 2015. International society for Developmental Origins of Health and Disease (DOHaD). Available at: http://www.mrc-leu.soton.ac.uk/dohad/index.asp [Accessed March 18, 2016].

Dou, Z. et al., 2012. Synthesis of PEGylated fullerene-5-fluorouracil conjugates to enhance the antitumor effect of 5-fluorouracil. *Nanoscale*, 4, pp.4624–4630. Available at: http://www.ncbi.nlm.nih.gov/pubmed/22706520 [Accessed March 4, 2013].

Dreborg, S. & Akerblom, E., 1990. Immunotherapy with monomethoxypolyethylene glycol modified allergens. *Crit Rev Ther Drug Carrier Syst.*, 6(4), pp.315–365.

Du, H. et al., 2011. Novel tetrapeptide, RGDF, mediated tumor specific liposomal doxorubicin (DOX) preparations. *Molecular pharmaceutics*, 8(4), pp.1224–1232. Available at: http://www.ncbi.nlm.nih.gov/pubmed/21630705.

Dubey, P.K. et al., 2004. Liposomes modified with cyclic RGD peptide for tumor targeting. *Journal of drug targeting*, 12(5), pp.257–264. Available at: http://www.ncbi.nlm.nih.gov/pubmed/15512776 [Accessed August 13, 2012].

Düzgüneş, N. & Nir, S., 1999. Mechanisms and kinetics of liposome-cell interactions. *Advanced Drug Delivery Reviews*, 40, pp.3–18.

EasyCalculation.com, 2016. Percentile to Z score calculation. Available at: https://www.easycalculation.com/statistics/percentile-to-z-score.php.

El-Kareh, A.W. & Secomb, T.W., 2000. A mathematical model for comparison of bolus injection, continuous infusion, and liposomal delivery of doxorubicin to tumor cells. *Neoplasia*, 2(4), pp.325–338.

Ellis, L.M., 2006. The role of neuropilins in cancer. *Molecular cancer therapeutics*, 5(5), pp.1099–1107.

Farquharson, R. & Stephenson, M.D., 2010. *Early pregnancy*, Cambridge University Press.

Farr, K.P. & Safwat, A., 2011. Palmar-plantar erythrodysesthesia associated with chemotherapy and its treatment. *Case reports in oncology*, 4(1), pp.229–235. Available at: http://www.pubmedcentral.nih.gov/articlerender.fcgi?artid=3085037&tool=pmcentrez&rendertype=abstract.

Fernandez-Twinn, D.S., Constância, M. & Ozanne, S.E., 2015. Intergenerational epigenetic inheritance in models of developmental programming of adult disease. *Seminars in Cell and Developmental Biology*, 43, pp.85–95. Available at: http://dx.doi.org/10.1016/j.semcdb.2015.06.006.

Filant, J. & Spencer, T.E., 2014. Uterine glands: biological roles in conceptus implantation, uterine receptivity and decidualization. *International Journal of Developmental Biology*, 58, pp.107–116. Available at: http://www.intjdevbiol.com/paper.php?doi=130344ts.

Fisk, N.M. & Atun, R., 2008. Market failure and the poverty of new drugs in maternal health. *PLoS medicine*, 5(1), p.e22. Available at: http://www.pubmedcentral.nih.gov/articlerender.fcgi?artid=2211556&tool=pmcentrez&rendertype=abstract [Accessed January 29, 2013].

Fleming, T.P. et al., 2012. Nutrition of females during the peri-conceptional period and effects on foetal programming and health of offspring. *Animal Reproduction Science*, 130(3-4), pp.193–197. Available at: http://dx.doi.org/10.1016/j.anireprosci.2012.01.015.

Forbes, K. et al., 2008. Insulin-like growth factor I and II regulate the life cycle of trophoblast in the developing human placenta. *American journal of physiology. Cell physiology*, 294(6), pp.C1313–C1322. Available at: http://www.ncbi.nlm.nih.gov/pubmed/18400990 [Accessed August 20, 2012].

Fowden, A.L., 2003. The insulin-like growth factors and feto-placental growth. *Placenta*, 24, pp.803–812.

Friedman, A.D., Claypool, S.E. & Liu, R., 2013. The smart targeting of nanoparticles. *Curr Pharm Des*, 19(35), pp.6315–6329.

Fritze, A. et al., 2006. Remote loading of doxorubicin into liposomes driven by a transmembrane phosphate gradient. *Biochimica et biophysica acta*, 1758(10), pp.1633–1640. Available at: http://www.ncbi.nlm.nih.gov/pubmed/16887094 [Accessed January 29, 2013].

Gabizon, A. et al., 2002. Dose dependency of pharmacokinetics and therapeutic efficacy of pegylated liposomal doxorubicin (DOXIL) in murine models. *Journal of drug targeting*, 10(7), pp.539–548. Available at: http://www.ncbi.nlm.nih.gov/pubmed/12683721 [Accessed January 29, 2013].

Gabizon, A. & Martin, F., 1997. Polyethylene glycol-coated (pegylated) liposomal doxorubicin. Rationale for use in solid tumours. *Drugs*, 54(4), pp.15–21.

Gage, G.J., Kipke, D.R. & Shain, W., 2012. Whole animal perfusion fixation for rodents. *Journal of visualized experiments*, 65, p.e3564.

Ganzevoort, W. et al., 2014. STRIDER: Sildenafil therapy in dismal prognosis early-onset intrauterine growth restriction - a protocol for a systematic review with individual participant data and aggregate data meta-analysis and trial sequential analysis. *Systematic Reviews*, 3(1), p.23. Available at: http://www.systematicreviewsjournal.com/content/3/1/23.

Gardosi, J. et al., 2005. Classification of stillbirth by relevant condition at death (ReCoDe): population based cohort study. *BMJ*, 331, pp.1113–1117. Available at: http://www.pubmedcentral.nih.gov/articlerender.fcgi?artid=1283272&tool=pmcentrez&rendertype=abstract [Accessed August 20, 2012].

Gargosky, S. et al., 1991. Administration of insulin-like growth factor-I, but not growth hormone, increases maternal weight gain in late pregnancy without affecting fetal or placental growth. *Journal Endocrinol.*, 130(3), pp.395–400.

Garovic, V.D. et al., 2007. Urinary podocyte excretion as a marker for preeclampsia. *American journal of obstetrics and gynecology*, 196(4), pp.320.e1–7. Available at: http://www.ncbi.nlm.nih.gov/pubmed/17403404 [Accessed July 23, 2012].

Georgiades, P., Ferguson-Smith, A.C. & Burton, G.J., 2002. Comparative developmental anatomy of the murine and human definitive placentae. *Placenta*, 23(1), pp.3–19. Available at: http://www.ncbi.nlm.nih.gov/pubmed/11869088 [Accessed July 17, 2012].

Ghidini, A., 2014. Overview of low molecular weight heparin for preventative treatment of adverse obstetric outcomes related to abnormal placentation. *Prenatal diagnosis*, 34, pp.649–654. Available at: http://www.ncbi.nlm.nih.gov/pubmed/24752745.

Giudice, L.C. et al., 2013. Insulin-like growth factors and their binding proteins in the term and preterm human fetus and neonate with normal and extremes of intrauterine growth. *The Journal of Clinical Endocrinology & Metabolism*, 80(5).

Glazier, J.D. et al., 1997. Association between the activity of the system A amino acid transporter in the microvillous plasma membrane of the human placenta and severity of fetal compromise in intrauterine growth restriction. *Pediatric research*, 42, pp.514–519.

Gluckman, P.D. et al., 1992. Elevating maternal insulin-like growth factor-I in mice and rats alters the pattern of fetal growth by removing maternal constraint. *Journal of Endocrinology*, 134(1).

Gourvas, V. et al., 2012. Angiogenic factors in placentas from pregnancies complicated by fetal growth restriction (review). *Molecular medicine reports*, 6(1), pp.23–27. Available at: http://www.ncbi.nlm.nih.gov/pubmed/22552373 [Accessed August 20, 2012].

Grit, M. & Crommelin, D.J.A., 1993. Chemical stability of liposomes: implications for their physical stability. *Chemistry and physics of lipids*, 64, pp.3–18.

Guillemot, F. et al., 1994. Essential role of Mash-2 in extraembryonic development. *Nature*, 371, pp.333–336.

Gulati, M. et al., 1998. Lipophilic drug derivatives in liposomes. *International Journal of Pharmaceutics*, 165(2), pp.129–168. Available at: http://linkinghub.elsevier.com/retrieve/pii/S0378517398000064.

Gupta, B. & Torchilin, V.P., 2007. Monoclonal antibody 2C5-modified doxorubicin-loaded liposomes with significantly enhanced therapeutic activity against intracranial human brain U-87 MG tumor xenografts in nude mice. *Cancer immunology, immunotherapy*, 56(8), pp.1215–23. Available at: http://www.ncbi.nlm.nih.gov/pubmed/17219149 [Accessed March 8, 2013].

Hadidi, N. et al., 2013. PEGylated single-walled carbon nanotubes as nanocarriers for Cyclosporin A delivery. *AAPS PharmSciTech*. Available at: http://www.ncbi.nlm.nih.gov/pubmed/23479049 [Accessed March 26, 2013].

Han, V.K. & Carter, a M., 2000. Spatial and temporal patterns of expression of messenger RNA for insulin-like growth factors and their binding proteins in the placenta of man and laboratory animals. *Placenta*, 21(4), pp.289–305.

Haran, G. et al., 1993. Transmembrane ammonium sulfate gradients in liposomes produce efficient and stable entrapment of amphipathic weak bases. *Biochimica et biophysica acta*, 1151(2), pp.201–215. Available at: http://www.ncbi.nlm.nih.gov/pubmed/8373796.

Harashima, H. & Kiwada, H., 1996. Liposomal targeting and drug delivery: kinetic consideration. *Advanced Drug Delivery Reviews*, 19(3), pp.425–444.

Hardy, D.S., 1999. A multiethnic study of the predictors of macrosomia. *The Diabetes Educator*, 25(6), pp.925–933.

Hare, J.I., Moase, E.H. & Allen, T.M., 2013. Targeting combinations of liposomal drugs to both tumor vasculature cells and tumor cells for the treatment of HER2-positive breast cancer. *Journal of drug targeting*, 21(1), pp.87–96. Available at: http://www.ncbi.nlm.nih.gov/pubmed/23039213.

Harris, L. et al., 2012. Tumour homing peptides as tools for targeted delivery to the placenta. *Placenta*, 33(9), p.A43.

Harris, L.K. & Aplin, J.D., 2007. Vascular remodeling and extracellular matrix breakdown in the uterine spiral arteries during pregnancy. *Reproductive Sciences*, 14(8), pp.28–34.

Hefler, L.A. et al., 2001. Perinatal development of endothelial nitric oxide synthase-deficient mice. *Biology of reproduction*, 64(2), pp.666–673. Available at: http://www.ncbi.nlm.nih.gov/pubmed/11159371.

Hobson, S.R. et al., 2013. Phase I pilot clinical trial of antenatal maternally administered melatonin to decrease the level of oxidative stress in human pregnancies affected by pre-eclampsia (PAMPR): study protocol. *BMJ open*, 3(9), p.e003788. Available at: http://www.pubmedcentral.nih.gov/articlerender.fcgi?artid=3780337&tool=pmcentrez&rendertype=abstract.

Hoffman, J.A. et al., 2003. Progressive vascular changes in a transgenic mouse model of squamous cell carcinoma. *Cancer cell*, 4(5), pp.383–391. Available at: http://www.ncbi.nlm.nih.gov/pubmed/14667505.

Hoffmann, D.S. et al., 2008. Chronic tempol prevents hypertension, proteinuria, and poor feto-placental outcomes in BPH/5 mouse model of preeclampsia. *Hypertension*, 51(4), pp.1058–1065. Available at: http://www.ncbi.nlm.nih.gov/pubmed/18259014 [Accessed August 20, 2012].

Holmes, R. et al., 1997. Fetal and maternal plasma insulin-like growth factors and binding proteins in pregnancies with appropriate or retarded fetal growth. *Early Human Development*, 49, pp.7–17.

Holtan, S.G. et al., 2009. Cancer and pregnancy: parallels in growth, invasion, and immune modulation and implications for cancer therapeutic agents. *Mayo Clinic Proceedings*, 84(11), pp.985–1000.

Hung, T.H., Skepper, J.N. & Burton, G.J., 2001. In vitro ischemia-reperfusion injury in term human placenta as a model for oxidative stress in pathological pregnancies. *The American journal of pathology*, 159(3), pp.1031–1043. Available at: http://www.sciencedirect.com/science/article/pii/S0002944010617786 [Accessed July 11, 2015].

Huppertz, B., 2008. The anatomy of the normal placenta. *Journal of clinical pathology*, 61(12), pp.1296–1302. Available at: http://www.ncbi.nlm.nih.gov/pubmed/18755720 [Accessed August 20, 2012].

Huth, U.S., Schubert, R. & Peschka-Süss, R., 2006. Investigating the uptake and intracellular fate of pH-sensitive liposomes by flow cytometry and spectral bio-imaging. *Journal of controlled release*, 110(3), pp.490–504. Available at: http://www.ncbi.nlm.nih.gov/pubmed/16387383 [Accessed March 25, 2013].

Immordino, M.L., Dosio, F. & Cattel, L., 2006. Stealth liposomes: review of the basic science, rationale, and clinical applications, existing and potential. *International journal of nanomedicine*, 1(3), pp.297–315. Available at: http://www.pubmedcentral.nih.gov/articlerender.fcgi?artid=2426795&tool=pmcentrez&rendertype=abstract.

Ishida, T., Harashima, H. & Kiwada, H., 2002. Liposome clearance. *Bioscience Reports*, 22(2), pp.197–224.

Ishihara, N. et al., 2002. Increased apoptosis in the syncytiotrophoblast in human term placentas complicated by either preeclampsia or intrauterine growth retardation. *American Journal of Obstetrics and Gynecology*, 186(1), pp.158–166.

Jansson, T., 2001. Amino Acid Transporters in the Human Placenta. *Pediatric Research*, 49(2), pp.141–147.

John, R. & Hemberger, M., 2012. A placenta for life. *Reproductive biomedicine online*, 25(1), pp.5–11. Available at: http://www.ncbi.nlm.nih.gov/pubmed/22578825 [Accessed August 20, 2012].

Johnston, M.J.W. et al., 2006. Therapeutically optimized rates of drug release can be achieved by varying the drug-to-lipid ratio in liposomal vincristine formulations. *Biochimica et biophysica acta*, 1758(1), pp.55–64. Available at: http://www.ncbi.nlm.nih.gov/pubmed/16487476 [Accessed August 20, 2012].

Jones, B., Mohan, A. & Bennett, P., 2004. The drugs we deserve. *BJOG : an international journal of obstetrics and gynaecology*, 111(4), pp.392–3; author reply 393. Available at: http://www.ncbi.nlm.nih.gov/pubmed/19336489.

Jones, C.J.P., Choudhury, R.H. & Aplin, J.D., 2015. Tracking nutrient transfer at the human maternofetal interface from 4 weeks to term. *Placenta*, 36(4), pp.372–380. Available at: http://linkinghub.elsevier.com/retrieve/pii/S0143400415000326.

Jones, C.J.P. & Fox, H., 1991. Ultrastructure of the normal human placenta. *Electron Microscopy Reviews*, 4(1), pp.129–178. Available at: http://www.sciencedirect.com/science/article/pii/0892035491900199\nhttp://dx.doi.org/10.1016/0892-0354(91)90019-9.

Jones, J.I. & Clemmons, D.R., 2013. Insulin-Like Growth Factors and Their Binding Proteins: Biological Actions. *Endocrine Reviews*, 16(1).

Jones, S.W. et al., 2013. Nanoparticle clearance is governed by Th1/Th2 immunity and strain background. *The Journal of clinical investigation*, 123(7), pp.3061–3073.

Jordan, A. et al., 2006. The effect of thermotherapy using magnetic nanoparticles on rat malignant glioma. *Journal of Neuro-Oncology*, 78(1), pp.7–14.

Juchau, M., Chao, S. & Omencinski, C., 1980. Drug metabolism by the human fetus. *Clinical Pharmacokinetics*, 5(4), pp.320–339.

Jukic, A.M. et al., 2013. Length of human pregnancy and contributors to its natural variation. *Human reproduction (Oxford, England)*, 28(10), pp.2848–2855. Available at: http://www.ncbi.nlm.nih.gov/pubmed/23922246 [Accessed February 5, 2014].

Kaga, M. et al., 2012. Liposome-encapsulated hemoglobin (hemoglobin-vesicle) is not transferred from mother to fetus at the late stage of pregnancy in the rat model. *Life sciences*, 91, pp.420–428. Available at: http://www.ncbi.nlm.nih.gov/pubmed/22935405 [Accessed January 29, 2013].

Kaitu'u-Lino, T.J. et al., 2013. Targeted nanoparticle delivery of Doxorubicin into placental tissues to treat ectopic pregnancies. *Endocrinology*, 154(2), pp.911–919. Available at: http://www.ncbi.nlm.nih.gov/pubmed/23288908 [Accessed January 29, 2013].

Kamaly, N. & Miller, A.D., 2010. Paramagnetic liposome nanoparticles for cellular and tumour imaging. *International journal of molecular sciences*, 11(4), pp.1759–1776. Available at: http://www.pubmedcentral.nih.gov/articlerender.fcgi?artid=2871136&tool=pmcentrez&rendertype=abstract [Accessed August 20, 2012].

Karl, P.I., 1995. Insulin-like growth factor-1 stimulates amino acid uptake by the cultured human placental trophoblast. *J Cell Physiol*, 165(1), pp.83–88.

King, A. et al., 2016. Tumour homing peptides as tools for targeted delivery of payloads to the placenta. *Science Advances*.

Kirby, C., Clarke, J. & Gregoriadis, G., 1980. Effect of the cholesterol content of small unilamellar liposomes on their stability in vivo and in vitro. *The Biochemical journal*, 186(2), pp.591–598. Available at: http://www.pubmedcentral.nih.gov/articlerender.fcgi?artid=1161612&tool=pmcentrez&rendertype=abstract.

Kniss, D. et al., 1994. Insulin-like growth factors. Their regulation of glucose and amino acid transport in placental trophoblasts isolated from first-trimester chorionic villi. *J. Reprod. Med.*, 39(4), pp.249–256.

Kolodkin, A.L. et al., 1997. Neuropilin is a semaphorin III receptor. *Cell*, 90(4), pp.753–762.

Koutsaki, M. et al., 2011. Decreased placental expression of hPGH, IGF-I and IGFBP-1 in pregnancies complicated by fetal growth restriction. *Growth hormone & IGF research*, 21(1), pp.31–36. Available at: http://www.ncbi.nlm.nih.gov/pubmed/21212012.

Kulvietis, V. et al., 2011. Transport of Nanoparticles through the Placental Barrier. *The Tohoku Journal of Experimental Medicine*, 225, pp.225–234.

Kusinski, L.C. et al., 2011. System A activity and vascular function in the placental-specific Igf2 knockout mouse. *Placenta*, 32(11), pp.871–876. Available at: http://www.ncbi.nlm.nih.gov/pubmed/21851977 [Accessed January 29, 2013].

Lassarre, C. et al., 1991. Serum insulin-like growth factors and insulin-like growth factor binding proteins in the human fetus. Relationships with growth in normal subjects and in subjects with intrauterine growth retardation. *Pediatric research*, 29(3), pp.219–225.

Laviola, L. et al., 2005. Intrauterine growth restriction in humans is associated with abnormalities in placental insulin-like growth factor signaling. *Endocrinology*, 146(3), pp.1498–1505.

Leitich, H. et al., 1997. A meta-analysis of low dose aspirin for the prevention of intrauterine growth retardation. *Br J Obstet Gynaecol.*, 104(4), pp.450–459.

Lemley, C.O. et al., 2012. Melatonin supplementation alters uteroplacental hemodynamics and fetal development in an ovine model of intrauterine growth restriction. *AJP: Regulatory, Integrative and Comparative Physiology*, 302(4), pp.R454–R467.

Levine, R.J. et al., 2004. Circulating angiogenic factors and the risk of preeclampsia. *The New England journal of medicine*, 350(7), pp.672–683. Available at: http://www.ncbi.nlm.nih.gov/pubmed/22753210.

Li, Y. et al., 2011. Relationships between liposome properties, cell membrane binding, intracellular processing, and intracellular bioavailability. *The AAPS journal*, 13(4), pp.585–597. Available at: http://www.pubmedcentral.nih.gov/articlerender.fcgi?artid=3231863&tool=pmcentrez&rendertype=abstract [Accessed January 29, 2013].

Li, Z. & Vance, D.E., 2008. Thematic review series: glycerolipids. Phosphatidylcholine and choline homeostasis. *The Journal of Lipid Research*, 49(6), pp.1187–1194. Available at: http://www.jlr.org/cgi/doi/10.1194/jlr.R700019-JLR200.

Linzer, D.I. & Fisher, S.J., 1999. The placenta and the prolactin family of hormones: regulation of the physiology of pregnancy. *Molecular endocrinology*, 13(6), pp.837–840.

Liu, J. et al., 2013. Assessing clinical prospects of silicon quantum dots: studies in mice and monkeys. *ACS Nano*, 7(8), pp.7303–7310.

Livingstone, C. & Borai, A., 2014. Insulin-like growth factor-II: its role in metabolic and endocrine disease. *Clin Endocrinology*, 80(6), pp.773–781.

Lof, M. et al., 2005. Changes in basal metabolic rate during pregnancy in relation to changes in body weight and composition, cardiac output, insulin- like growth factor I, and thyroid hormones and in relation to fetal growth. *The American journal of clinical nutrition*, 81, pp.678–685.

Lofqvist, C. et al., 2009. Quantification and localization of the IGF/insulin system expression in retinal blood vessels and neurons during oxygen-induced retinopathy in mice. *Investigative Ophthalmology and Visual Science*, 50(4), pp.1831–1837.

Lopes, C. et al., 2014. IGF-1 Intranasal Administration Rescues Huntington's Disease Phenotypes in YAC128 Mice. *Molecular Neurobiology*, 49(3), pp.1126–1142. Available at: http://link.springer.com/10.1007/s12035-013-8585-5.

Lutolf, M.P. & Hubbell, J.A., 2003. Synthesis and physicochemical characterization of end-linked poly(ethylene glycol)-co-peptide hydrogels formed by Michael-type addition. *Biomacromolecules*, 4(3), pp.713–722. Available at: http://www.ncbi.nlm.nih.gov/pubmed/12741789.

Maeda, H. et al., 2000. Tumor vascular permeability and the EPR effect in macromolecular therapeutics: a review. *Journal of controlled release*, 65, pp.271–284. Available at: http://www.ncbi.nlm.nih.gov/pubmed/10699287.

Maglione, D. et al., 1991. Isolation of a human placenta cDNA coding for a protein related to the vascular permeability factor. *PNAS*, 88(20), pp.9267–9271.

Malassiné, A., Frendo, J.L. & Evain-Brion, D., 2003. A comparison of placental development and endocrine functions between the human and mouse model. *Human Reproduction Update*, 9(6), pp.531–539.

Malvern Instruments Ltd., 2016. Zeta sizer. *Zeta sizer*. Available at: http://www.malvern.com/en/products/product-range/zetasizer-range/default.aspx.

Many, A. et al., 2001. Pathologic features of the placenta in women with severe pregnancy complications and thrombophilia. *Obstet Gynecol.*, 98(6), pp.1041–1044.

Masashi, I. et al., 2008. Liposome preparation. , p.Patent US 2008/0279916 A1.

Matsubara, K. et al., 2015. Nitric oxide and reactive oxygen species in the pathogenesis of preeclampsia. *International Journal of Molecular Sciences*, 16(3), pp.4600–4614. Available at: http://www.mdpi.com/1422-0067/16/3/4600/.

McIntyre, D.D. et al., 1999. Birth weight in relation to morbidity and mortality among newborn infants. *The New England journal of medicine*, pp.1234–1238.

Van Mieghem, T. et al., 2009. Insulin-like growth factor-II regulates maternal hemodynamic adaptation to pregnancy in rats. *American journal of physiology. Regulatory, integrative and comparative physiology*, 297(5), pp.R1615–21.

Miller, A.G., Aplin, J.D. & Westwood, M., 2005. Adenovirally mediated expression of insulin-like growth factors enhances the function of first trimester placental fibroblasts. *Journal of Clinical Endocrinology and Metabolism*, 90(1), pp.379–385.

Miller, S.L., Wallace, E.M. & Walker, D.W., 2012. Antioxidant therapies: a potential role in perinatal medicine. *Neuroendocrinology*, 96(1), pp.13–23.

Moghimi, S.M., Hunter, A.C. & Andresen, T.L., 2012. Factors controlling nanoparticle pharmacokinetics: an integrated analysis and perspective. *Annual Review of Pharmacology and Toxicology*, 52(1), pp.481–503. Available at: http://www.annualreviews.org/doi/abs/10.1146/annurev-pharmtox-010611-134623.

Moghimi, S.M., Hunter, A.C. & Murray, J.C., 2001. Long-circulating and target-specific nanoparticles: theory to practice. *Pharmacological Reviews*, 53(2), pp.283–318.

Moll, S.J. et al., 2007. Epidermal growth factor rescues trophoblast apoptosis induced by reactive oxygen species. *Apoptosis*, 12(9), pp.1611–1622. Available at: http://link.springer.com/10.1007/s10495-007-0092-6.

Montet, X. et al., 2006. Multivalent effects of RGD peptides obtained by nanoparticle display. *Journal of Medicinal Chemistry*, 49(20), pp.6087–6093.

Moriya, H., 1998. *Gel filtration: principles and methods*,

Muppidi, K. et al., 2012. Development and stability studies of novel liposomal vancomycin formulations. *ISRN pharmaceutics*, pp.636743–636751. Available at: http://www.pubmedcentral.nih.gov/articlerender.fcgi?artid=3302012&tool=pmcentrez&rendertype=abstract [Accessed August 20, 2012].

Murray, S.A. et al., 2010. Mouse gestation length is genetically determined. *PloS one*, 5(8), p.e12418. Available at: http://www.pubmedcentral.nih.gov/articlerender.fcgi?artid=2928290&tool=pmcentrez&rendertype=abstract [Accessed July 27, 2012].

Murrell, A. et al., 2001. An intragenic methylated region in the imprinted Igf2 gene augments transcription. *EMBO Reports*, 2(12), pp.1101–1106.

Nair, D.P. et al., 2014. The thiol-Michael addition click reaction: a powerful and widely used tool in materials chemistry. *Chemistry of Materials*, 26(1), pp.724–744.

Nallamothu, R. et al., 2006. A tumor vasculature targeted liposome delivery system for combretastatin A4: design, characterization, and in vitro evaluation. *AAPS PharmSciTech*, 7(2), pp.E1–10. Available at: http://www.ncbi.nlm.nih.gov/pubmed/16796350.

Nayak, N.R. & Giudice, L.C., 2003. Comparative biology of the IGF system in endometrium, decidua, and placenta, and clinical implications for foetal growth and implantation disorders. *Placenta*, 24(4), pp.281–296.

Needham, D., McIntosh, T.J. & Lasic, D.D., 1992. Repulsive interactions and mechanical stability of polymer-grafted lipid membranes. *Biochimica et biophysica acta*, 1108(1), pp.40–48.

Newbern, D. & Freemark, M., 2011. Placental hormones and the control of maternal metabolism and fetal growth. *Current opinion in endocrinology, diabetes, and obesity*, 18(6), pp.409–416. Available at: http://www.ncbi.nlm.nih.gov/pubmed/21986512.

Newnham, J.P. et al., 1995. Low dose aspirin for the treatment of fetal growth restriction: a randomized controlled trial. *Australian and New Zealand Journal of Obstetrics and Gynaecology*, 35(4), pp.370–374.

NIBSC, 2013. WHO reference reagent: Insulin-like growth factor-II (human recombinant). *Journal of Chemical Information and Modeling*, 53(9), pp.1689–1699.

Ning, S. et al., 2011. Functionalized dextran-coated liposomes for doxorubicin loading. *Journal of controlled release*, 152, pp.e49–51. Available at: http://www.ncbi.nlm.nih.gov/pubmed/22195919 [Accessed January 29, 2013].

Norwitz, E., Schust, D. & Fisher, S., 2001. Implantation and the survival of early pregnancy. *New England Journal of Medicine*, 345(19), pp.1400–1408. Available at: http://www.nejm.org/doi/full/10.1056/NEJMra000763 [Accessed August 29, 2012].

O'Dell, S.D. & Day, I.N.M., 1998. Molecules in focus Insulin-like growth factor II (IGF-II). *The International Journal of Biochemistry & Cell Biology*, 30(7), pp.767–771. Available at: http://linkinghub.elsevier.com/retrieve/pii/S135727259800048X.

Osborne, C.K. et al., 1989. Insulin-like growth factor-ll (IGF-II): a potential autocrine/paracrine growth factor for human breast cancer acting via the IGF-I receptor. *Molcular Endocrinology*, 3(11), pp.1701–1709.

Otis, E.M. & Brent, R., 1954. Equivalent ages in mouse and human embryos. *The Anatomical record*, 120(1), pp.33–63. Available at: http://www.ncbi.nlm.nih.gov/pubmed/13207763.

Ozanne, S.E., Fernandez-Twinn, D. & Hales, C.N., 2004. Fetal growth and adult diseases. *Seminars in Perinatology*, 28(1), pp.81–87. Available at: http://linkinghub.elsevier.com/retrieve/pii/S0146000503001113 [Accessed March 25, 2013].

Pang, H.-B. et al., 2014. An endocytosis pathway initiated through neuropilin-1 and regulated by nutrient availability. *Nature communications*, 5, p.4904. Available at:

http://www.pubmedcentral.nih.gov/articlerender.fcgi?artid=4185402&tool=pmcentrez&rendertype=abstract.

Papageorghiou, A.T., Yu, C.K.H. & Nicolaides, K.H., 2004. The role of uterine artery Doppler in predicting adverse pregnancy outcome. *Best practice & research. Clinical obstetrics & gynaecology*, 18(3), pp.383–396. Available at: http://www.ncbi.nlm.nih.gov/pubmed/15183134 [Accessed July 12, 2012].

Papahadjopoulos, D., Poste, G. & Schaeffer, B., 1973. Fusion of mammalian cells by unilamellar lipid vesicles: inflluence of lipid surface charge, fluidity and cholesterol. *Biochim Biophys Acta.*, 323(1), pp.23–42.

Partearroyo, A., Urbaneja, A. & Gofii, F., 1992. Effective detergent/lipid ratios in the solubilization of phosphotidylcholine vesicles by Triton X- 100. *Federation of European Biochemical Societies*, 302(2), pp.138–140.

Pasqualini, R. & Ruoslahti, E., 1996. Organ targeting in vivo using phage display peptide libraries. *Nature*, 380, pp.364–366.

Philipps, A. et al., 1978. Tissue concentrations of free amino acids in term human placentas. *Am J Obstet Gynecol.*, 131(8), pp.881–887.

Pinto, A.B., Schlein, A.L. & Moley, K.H., 2002. Preimplantation exposure to high insulin-like growth factor I concentrations results in increased resorption rates in vivo. *Human reproduction*, 17(2), pp.457–462.

Poste, G. & Papahadjopoulos, D., 1976. Lipid vesicles as carriers for introducing materials into cultured cells: influence of vesicle lipid composition on mechanism(s) of vesicle incorporation into cells. *PNAS*, 73(5), pp.1603–1607.

Poston, L. et al., 2006. Vitamin C and vitamin E in pregnant women at risk for pre-eclampsia (VIP trial): randomised placebo-controlled trial. *Lancet*, 367, pp.1145–1154.

Protein Atlas, 2016. Calreticulin expression. Available at: http://www.proteinatlas.org/ENSG00000179218-CALR/tissue.

Raz, T. et al., 2012. The hemodynamic basis for positional- and inter-fetal dependent effects in dual arterial supply of mouse pregnancies. *PloS one*, 7(12), p.e52273. Available at: http://www.pubmedcentral.nih.gov/articlerender.fcgi?artid=3527527&tool=pmcentrez&rendertype=abstract [Accessed February 12, 2013].

RCOG contributors, 2013. The Investigation and Management of the Small for Gestational Age Fetus. *Royal College of Obstetricians and Gynaecologists*, (31).

Refuerzo, J.S. et al., 2015. Liposomes: a nanoscale drug carrying system to prevent indomethacin passage to the fetus in a pregnant mouse model. *American journal of obstetrics and gynecology*, 212(508), pp.e1–7. Available at: http://www.ncbi.nlm.nih.gov/pubmed/25683966 [Accessed May 11, 2015].

Refuerzo, J.S. et al., 2011. Size of the nanovectors determines the transplacental passage in pregnancy: study in rats. *American journal of obstetrics and gynecology*, 204(546), pp.e5–9. Available at: http://www.pubmedcentral.nih.gov/articlerender.fcgi?artid=3135739&tool=pmcentrez&rendertype=abstract [Accessed August 20, 2012].

Reinhard, G. et al., 1998a. Shifts in the TH1/TH2 balance during human pregnancy correlate with apoptotic changes. *Biochemical and Biophysical Research Communications*, 245(3), pp.933–938. Available at: http://www.sciencedirect.com/science/article/pii/S0006291X98985497.

Reinhard, G. et al., 1998b. Shifts in the TH1/TH2 balance during human pregnancy correlate with apoptotic changes. *Biochemical and Biophysical Research Communications*, 245(3), pp.933–938.

Reis, F.M., D'Antona, D. & Petraglia, F., 2002. Predictive value of hormone measurements in maternal and fetal complications of pregnancy. *Endocrine Reviews*, 23(2), pp.230–257.

Renshall, L.J. et al., 2014. In vitro assessment of mouse fetal abdominal aortic vascular function. *AJP: Regulatory, Integrative and Comparative Physiology*, 307(6), pp.R746–R754. Available at: http://ajpregu.physiology.org/cgi/doi/10.1152/ajpregu.00058.2014.

Richter, H.G. et al., 2009. Melatonin improves placental efficiency and birth weight and increases the placental expression of antioxidant enzymes in undernourished pregnancy. *Journal of Pineal Research*, 46(4), pp.357–364. Available at: http://doi.wiley.com/10.1111/j.1600-079X.2009.00671.x.

Ricklin, D. et al., 2010. Complement: a key system for immune surveillance and homeostasis. *Nature immunology*, 11(9), pp.785–797. Available at: http://dx.doi.org/10.1038/ni.1923.

Riyazi, N. et al., 1998. Low-molecular-weight heparin combined with aspirin in pregnant women with thrombophilia and a history of preeclampsia or fetal growth restriction: a preliminary study. *Eur J Obstet Gynecol Reprod Biol.*, 80(1), pp.49–54.

Roggensack, A.M., Zhang, Y. & Davidge, S.T., 1999. Evidence for peroxynitrite formation in the vasculature of women with preeclampsia. *Hypertension*, 33(1), pp.83–89.

Roje, D. et al., 2011. Trophoblast apoptosis in human term placentas from pregnancies complicated with idiopathic intrauterine growth retardation. *The journal of maternal-fetal & neonatal medicine*, 24(5), pp.745–751.

Rollin Brant, 2016. Inference for Means: Comparing two independent samples. Available at: http://www.stat.ubc.ca/~rollin/stats/ssize/n2a.html.

Roos, S. et al., 2009. Regulation of amino acid transporters by glucose and growth factors in cultured primary human trophoblast cells is mediated by mTOR signaling. *American journal of physiology. Cell physiology*, 297, pp.723–731.

Rossant, J. & Cross, J.C., 2001. Placental development: lessons from mouse mutants. *Nature reviews. Genetics*, 2(7), pp.538–548. Available at: http://www.ncbi.nlm.nih.gov/pubmed/11433360.

Ruoslahti, E., 2002. Drug targeting to specific vascular sites. *Drug discovery today*, 7(22), pp.1138–1143. Available at: http://www.ncbi.nlm.nih.gov/pubmed/12546857.

Ruoslahti, E., 1996. RGD and other recognition sequences for integrins. *Annual review of cell and developmental biology*, 12, pp.697–715. Available at: http://www.ncbi.nlm.nih.gov/pubmed/8970741.

Ruoslahti, E., 2004. Vascular zip codes in angiogenesis and metastasis. *Biochemical Society transactions*, 32, pp.397–402. Available at: http://www.ncbi.nlm.nih.gov/pubmed/15157146.

Ruoslahti, E., Bhatia, S.N. & Sailor, M.J., 2010. Targeting of drugs and nanoparticles to tumors. *The Journal of cell biology*, 188(6), pp.759–768. Available at: http://www.pubmedcentral.nih.gov/articlerender.fcgi?artid=2845077&tool=pmcentrez&rendertype=abstract [Accessed July 31, 2012].

Ruozi, B. et al., 2011. AFM, ESEM, TEM, and CLSM in liposomal characterization: a comparative study. *International journal of nanomedicine*, 6, pp.557–563. Available at: http://www.pubmedcentral.nih.gov/articlerender.fcgi?artid=3065801&tool=pmcentrez&rendertype=abstract.

Sachdev, D. & Yee, D., 2001. The IGF system and breast cancer. *Endocrine-Related Cancer*, 8(3), pp.197–209.

Sawant, R.R. & Torchilin, V.P., 2012. Challenges in development of targeted liposomal therapeutics. *The AAPS journal*, 14(2), pp.303–315. Available at: http://www.ncbi.nlm.nih.gov/pubmed/22415612 [Accessed August 20, 2012].

Semple, S.C. et al., 2005. Optimization and characterization of a sphingomyelin/cholesterol liposome formulation of vinorelbine with promising antitumor activity. *Journal of pharmaceutical sciences*, 94(5), pp.1024–1038. Available at: http://www.ncbi.nlm.nih.gov/pubmed/15793796 [Accessed August 20, 2012].

Semple, S.C., Chonn, A. & Cullis, P.R., 1998. Interactions of liposomes and lipid-based carrier systems with blood proteins: relation to clearance behaviour in vivo. *Advanced Drug Delivery Reviews*, 32, pp.3–17.

Seo, J.W. et al., 2008. A novel method to label preformed liposomes with 64Cu for positron emission tomography (PET) imaging. *Bioconjugate Chemistry*, 19(12), pp.2577–2584.

Sferruzzi-perri, A.N. et al., 2007. Early treatment of the pregnant guinea pig with IGFs promotes placental transport and nutrient partitioning near term. *Am J Physiol Endocrinol Metab*, 292, pp.668–676.

Sferruzzi-Perri, A.N. et al., 2008. Maternal insulin-like growth factor-II promotes placental functional development via the type 2 IGF receptor in the guinea pig. *Placenta*, 29(4), pp.347–355. Available at: http://www.ncbi.nlm.nih.gov/pubmed/18339421 [Accessed August 20, 2012].

Sferruzzi-Perri, A.N. et al., 2006. Maternal insulin-like growth factors-I and -II act via different pathways to promote fetal growth. *Endocrinology*, 147(7), pp.3344–3355. Available at: http://www.ncbi.nlm.nih.gov/pubmed/16556757 [Accessed May 11, 2015].

Sferruzzi-Perri, A.N. et al., 2011. The neglected role of insulin-like growth factors in the maternal circulation regulating fetal growth. *The Journal of physiology*, 589, pp.7–20. Available at: http://www.pubmedcentral.nih.gov/articlerender.fcgi?artid=3021777&tool=pmcentrez&rendertype=abstract.

Sibley, C., Glazier, J. & D'Souza, S., 1997. Placental transporter activity and expression in relation to fetal growth. *Experimental physiology*, 82, pp.389–402. Available at: http://ep.physoc.org/content/82/2/389.short [Accessed August 29, 2012].

Sibley, C.P. et al., 2005. Placental phenotypes of intrauterine growth. *Pediatric Research*, 58(5), pp.827–832.

Sibley, C.P. et al., 2004. Placental-specific insulin-like growth factor 2 (Igf2) regulates the diffusional exchange characteristics of the mouse placenta. *PNAS*, 101(21), pp.8204–8208.

Sila, M., Au, S. & Weiner, N., 1986. Effects of Triton X-100 concentration and incubation temperature on carboxyfluorescein release from multilamellar liposomes. *Biochimica et Biophysica Acta*, 859(2), pp.165–170.

Siler-Khodr, T.M., Forman, T. & Sorem, K.A., 1995. Dose-related effect of IGF-I on placental prostanoid release. *Prostaglandins*, 49, pp.1–14.

Small, D.M., 1986. *Handbook of lipid research: the physical chemistry of lipids, from alkanes to phospholipids*,

Smith, S. a. & Pretorius, W. a., 2002. The conservative behaviour of fluorescein. *Water SA*, 28(4), pp.403–406.

Smith, S.C., Baker, P.N. & M, S.E., 1997. Increased placental apoptosis in intrauterine growth restriction. *American Journal of Obstetrics and Gynecology*, 177(6), pp.1395–1401.

Sohlström, A. et al., 2001. Maternal nutrition affects the ability of treatment with IGF-I and IGF-II to increase growth of the placenta and fetus, in guinea pigs. *Growth hormone & IGF research : official journal of the Growth Hormone Research Society and the International IGF Research Society*, 11(6), pp.392–398. Available at: http://www.ncbi.nlm.nih.gov/pubmed/11914027.

Song, G. et al., 2014. Nanoparticles and the mononuclear phagocyte system: pharmacokinetics and applications for inflammatory diseases. *Current Rheumatology Reviews*, 10(1), pp.22–34. Available at: http://www.eurekaselect.com/openurl/content.php?genre=article&issn=1573-3971&volume=10&issue=1&spage=22.

Stanley, J.L., Andersson, I.J., Hirt, C.J., et al., 2012. Effect of the anti-oxidant tempol on fetal growth in a mouse model of fetal growth restriction. *Biology of reproduction*, 87(1), p.25. Available at: http://www.ncbi.nlm.nih.gov/pubmed/22423051 [Accessed August 20, 2012].

Stanley, J.L., Andersson, I.J., Poudel, R., et al., 2012. Sildenafil citrate rescues fetal growth in the catechol-O-methyl transferase knockout mouse model. *Hypertension*, 59(5), pp.1021–1028. Available at: http://www.ncbi.nlm.nih.gov/pubmed/22392899 [Accessed August 2, 2012].

Stirrat, G., 1976. Prescribing problems in the second half of pregnancy and during lactation. *Obstet Gynecol Surv.*, 31(1), pp.1–7.

Stotland, N.E. et al., 2004. Risk factors and obstetric complications associated with macrosomia. *International journal of gynaecology and obstetrics*, 87(3), pp.220–226.

Sugahara, K.N. et al., 2010. Coadministration of a tumor-penetrating peptide enhances the efficacy of cancer drugs. *Science*, 328(5981), pp.1031–1035. Available at: http://www.pubmedcentral.nih.gov/articlerender.fcgi?artid=2881692&tool=pmcentrez&rendertype=abstract [Accessed July 15, 2012].

Sugahara, K.N. et al., 2009. Tissue-penetrating delivery of compounds and nanoparticles into tumors. *Cancer cell*, 16(6), pp.510–520. Available at: http://www.pubmedcentral.nih.gov/articlerender.fcgi?artid=2791543&tool=pmcentrez&rendertype=abstract [Accessed July 20, 2012].

Sur, S. et al., 2014. Remote loading of preencapsulated drugs into stealth liposomes. *PNAS*, 111(6), pp.2283–2288. Available at: http://www.ncbi.nlm.nih.gov/pubmed/24474802 [Accessed February 9, 2014].

Sutherland, A.E., Calarco, P.G. & Damsky, C.H., 1993. Developmental regulation of integrin expression at the time of implantation in the mouse embryo. *Development*, 119(4), pp.1175–1186.

Teesalu, T. et al., 2009. C-end rule peptides mediate neuropilin-1-dependent cell, vascular, and tissue penetration. *PNAS*, 106(38), pp.16157–16162.

ThermoFisher Scientific, 2016. Sulfhydryl-reactive Crosslinker Chemistry. Available at: https://www.thermofisher.com/uk/en/home/life-science/protein-biology/protein-biology-learning-center/protein-biology-resource-library/pierce-protein-methods/sulfhydryl-reactive-crosslinker-chemistry.html#.

Tian, Y. et al., 2002. IGF-II and IGFBP-1 reversely regulate blastocyst implantation in mouse. *Science Bulletin*, 47(21), pp.1816–1820. Available at: http://link.springer.com/10.1007/BF03183849.

Torchilin, V.P., 2006. Multifunctional nanocarriers. *Advanced drug delivery reviews*, 58(14), pp.1532–1555. Available at: http://www.ncbi.nlm.nih.gov/pubmed/17092599 [Accessed July 12, 2012].

Torchilin, V.P. et al., 1994. Poly(ethylene glycol) on the liposome surface: on the mechanism of polymer-coated liposome longevity. *Biochimica et Biophysica Acta: Biomembranes*, 1195(1), pp.11–20.

Tortora, G. & Derrickson, B., 2009. *Principles of Anatomy and Physiology* 12th ed.,

Tuzel Kox, S.N., Patel, H.M. & Kox, W.J., 1995. Uptake of drug-carrier liposomes by the placenta: transplacental delivery of drugs and nutrients. *The journal of Pharmacology and Experimental Therapeutics*, 274(1), pp.104–109.

Vanderpuye, O.A., Labarrere, C.A. & McIntyre, J.A., 1991. A vitronectin-receptor-related molecule in human placental brush border membranes. *Biochem J*, 280, pp.9–17. Available at: http://www.ncbi.nlm.nih.gov/entrez/query.fcgi?cmd=Retrieve&db=PubMed&dopt=Citation&list_uids=1720617.

Vatten, L.J. et al., 2008. Changes in circulating level of IGF-I and IGF-binding protein-1 from the first to second trimester as predictors of preeclampsia. *European journal of endocrinology*, 158(1), pp.101–105. Available at: http://www.ncbi.nlm.nih.gov/pubmed/18166823 [Accessed August 20, 2012].

Wagner, A. & Vorauer-Uhl, K., 2011. Liposome technology for industrial purposes. *Journal of drug delivery*, p.591325. Available at: http://www.pubmedcentral.nih.gov/articlerender.fcgi?artid=3065896&tool=pmcentrez&rendertype=abstract [Accessed January 29, 2013].

Wallace, A.E., Fraser, R. & Cartwright, J.E., 2012. Extravillous trophoblast and decidual natural killer cells: a remodelling partnership. *Human reproduction update*, 18(4), pp.458–471. Available at: http://www.ncbi.nlm.nih.gov/pubmed/22523109 [Accessed August 20, 2012].

Wallace, J.M. et al., 1997. Maternal endocrine status in relation to pregnancy outcome in rapidly growing adolescent sheep. *The Journal of endocrinology*, 155, pp.359–368.

Wallace, J.M., Aitken, R.P. & Cheyne, M.A., 1996. Nutrient partitioning and fetal growth in rapidly growing adolescent ewes. *Journal of reproduction and fertility*, 107, pp.183–190.

Wang, Y., 2010. *Vascular Biology of the Placenta*,

Wang, Z. et al., 2013. Fabrication and characterization of a triple functionalization of graphene oxide with Fe3O4, folic acid and doxorubicin as dual-targeted drug nanocarrier. *Colloids and surfaces B: Biointerfaces*, 106, pp.60–65. Available at: http://www.ncbi.nlm.nih.gov/pubmed/23434692 [Accessed March 26, 2013].

Wang, Z., Chui, W.-K. & Ho, P.C., 2010. Integrin targeted drug and gene delivery. *Expert opinion on drug delivery*, 7(2), pp.159–171. Available at: http://www.ncbi.nlm.nih.gov/pubmed/20095940.

Wareing, M. et al., 2005. Sildenafil citrate (Viagra) enhances vasodilatation in fetal growth restriction. *The Journal of clinical endocrinology and metabolism*, 90(5), pp.2550–2555. Available at: http://www.ncbi.nlm.nih.gov/pubmed/15713717 [Accessed August 20, 2012].

Watson, E.D. & Cross, J.C., 2005. Development of structures and transport functions in the mouse placenta. *Physiology*, 20, pp.180–193. Available at: http://www.ncbi.nlm.nih.gov/pubmed/15888575 [Accessed July 17, 2012].

Webb, M.S. et al., 1995. Sphingomyelin-cholesterol liposomes significantly enhance the pharmacokinetic and therapeutic properties of vincristine in murine and human tumour models. *British journal of cancer*, 72(4), pp.896–904. Available at: http://www.pubmedcentral.nih.gov/articlerender.fcgi?artid=2034038&tool=pmcentrez&rendertype=abstract.

Weinstein, J.N. et al., 1977. Liposome-cell interaction: transfer and intracellular release of a trapped fluorescent marker. , 3, pp.489–492.

Weissig, V., 2011. *Liposomes Methods and Protocols*, Springer Protocols.

Whitesall, S.E. et al., 2004. Comparison of simultaneous measurement of mouse systolic arterial blood pressure by radiotelemetry and tail-cuff methods. *American journal of physiology. Heart and circulatory physiology*, 286, pp.H2408–H2415.

Wick, P. et al., 2010. Barrier capacity of human placenta for nanosized materials. *Environmental health perspectives*, 118(3), pp.432–436. Available at: http://www.pubmedcentral.nih.gov/articlerender.fcgi?artid=2854775&tool=pmcentrez&rendertype=abstract [Accessed August 1, 2012].

Working, P. & Dayan, A., 1996. Pharmacological-toxicological expert report. CAELYX. (Stealth liposomal doxorubicin HCl). *Hum Exp Toxicol*, 15(9), pp.751–85.

Wu, H. et al., 2015. Development of synthetic of peptide-functionalized liposome for enhanced targeted ovarian carcinoma therapy. *International journal of clinical and*

experimental pathology, 8(1), pp.207–216. Available at: http://www.ncbi.nlm.nih.gov/pubmed/25663977.

Xie, Y. et al., 2005. Transport of nerve growth factor encapsulated into liposomes across the blood-brain barrier: In vitro and in vivo studies. *Journal of Controlled Release*, 105, pp.106–119.

Yamashita, K. et al., 2011. Silica and titanium dioxide nanoparticles cause pregnancy complications in mice. *Nature nanotechnology*, 6(5), pp.321–328. Available at: http://www.ncbi.nlm.nih.gov/pubmed/21460826 [Accessed July 23, 2012].

Yang, H. et al., 2012. Effects of gestational age and surface modification on materno-fetal transfer of nanoparticles in murine pregnancy. *Scientific reports*, 2, p.847. Available at: http://www.pubmedcentral.nih.gov/articlerender.fcgi?artid=3496197&tool=pmcentrez&rendertype=abstract [Accessed January 29, 2013].

Yang, Z.Z. et al., 2014. Tumor-targeting dual peptides-modified cationic liposomes for delivery of siRNA and docetaxel to gliomas. *Biomaterials*, 35(19), pp.5226–5239. Available at: http://dx.doi.org/10.1016/j.biomaterials.2014.03.017.

Yokomichi, N. et al., 2013. Pathogenesis of hand-foot syndrome induced by PEG-modified liposomal doxorubicin. *Human Cell*, 26, pp.8–18.

Yu, C.K.H. et al., 2003. Randomized controlled trial using low-dose aspirin in the prevention of pre-eclampsia in women with abnormal uterine artery Doppler at 23 weeks' gestation. *Ultrasound in obstetrics & gynecology*, 22(3), pp.233–239. Available at: http://www.ncbi.nlm.nih.gov/pubmed/12942493 [Accessed July 12, 2012].

Zapf, J. et al., 1986. Acute metabolic effects and half-lives of intravenously administered Insulin like growth factors I and II in normal and hypophysectomized rats. *Journal of clinical investigation*, 77, pp.1768–1775.

Zar, J., 1984. Proportions of a normal distribution. In editor. Kurtz B, ed. *Biostatistical Analysis. 2nd edition*. pp. 83–86.

Zhang, L. et al., 2008. Nanoparticles in Medicine: Therapeutic Applications and Developments. *Nature Translational Medicine*, 83(5), pp.761–769.

Zhang, Y.-F. et al., 2010. Targeted delivery of RGD-modified liposomes encapsulating both combretastatin A-4 and doxorubicin for tumor therapy: in vitro and in vivo studies. *European journal of pharmaceutics and biopharmaceutics*, 74(3), pp.467–473. Available at: http://www.ncbi.nlm.nih.gov/pubmed/20064608 [Accessed January 29, 2013].

Chapter 8: Appendix

8.1 Publications

Publications of work contained in this thesis:

A. King, C. Ndifon, S. Lui, K. Widdows, V. R. Kotamraju, L. Agemy, T. Teesalu, J. D. Glazier, F. Cellesi, N. Tirelli, J. D. Aplin, E. Ruoslahti, L. K. Harris, 2016, "Tumour homing peptides as tools for targeted delivery of payloads to the placenta", *Science Advances* (in press at time of printing)

8.2 Presentations

2013 A. King, N. Tirelli, F. Cellesi, J. D. Aplin, L. K. Harris, "Development of novel nanocarriers displaying tumour homing peptides for targeted delivery of drugs to the placenta", *International Federation of Placenta Associations (IFPA) Whistler, Vancouver, Canada,* poster presentation.

2014 A. King, N. Tirelli, J. D. Aplin, L. K. Harris, "Targeted delivery of Insulin-like growth factor-II to the placenta using homing peptide-decorated liposomes increases placental weight", *IFPA, Paris, France*, oral presentation.

A. King, N. Tirelli, J. D. Aplin, L. K. Harris, "Development of Targeted Nanocarriers to Treat Impaired Placental Function", *Society for Reproductive Investigation (SRI), Florence, Italy,* oral presentation.

A. King, N. Tirelli, J. D. Aplin, L. K. Harris, "Targeted delivery of Insulin-like growth factor-II to the placenta using homing peptide-decorated liposomes increases murine placental weight", *Liposome research days (LRD), Copenhagen, Denmark,* poster presentation.

2015 A. King, N. Tirelli, J. D. Aplin, L. K. Harris, “Targeted placental delivery of insulin-like growth factor-II increases fetal weight in P0 mice”, *IFPA, Brisbane Australia,* oral presentation.